The regulation of the hepcidin by modulators of the bone morphogenetic protein (BMP) pathway

Patel, Neeta

Awarding institution:
King's College London

Title: The regulation of the hepcidin by modulators of the bone morphogenetic protein (BMP) pathway

Author: Neeta Patel

THE REGULATION OF HEPCIDIN BY MODULATORS OF THE BONE MORPHOGENETIC PROTEIN (BMP) PATHWAY

Neeta Patel

A thesis submitted in partial fulfilment of the requirements for the degree of Doctor of Philosophy in King's College London

Diabetes & Nutritional Sciences Research Division

The School of Medicine

King's College London

Franklin-Wilkins Building

150 Stamford Street

London

SE1 9NH

October 2012

Abstract

Hepcidin, the iron regulatory peptide, has emerged as the master regulator of systemic iron homeostasis. Under normal circumstances, hepcidin expression is upregulated by excess iron and inflammation; and downregulated by iron deficiency, anaemia and hypoxia. Insights gained into the pathogenesis of iron-storage disorders such as hereditary haemochromatosis (HH) and hypotransferrinaemia (HPX), have contributed to the identification of the molecular mechanisms governing hepcidin expression. In these disorders, hepcidin expression is inappropriately low, causing increased absorption of iron by the gut thus leading to iron overload. The precise mechanism by which hepcidin is suppressed in these disorders is unclear.

The regulation of hepcidin is principally transcriptional, where the Bone Morphogenetic Protein (BMP) pathway has been shown to be a major network governing hepcidin expression. The current study utilised the HPX mouse model to identify potential regulators of hepcidin that are produced locally in liver with a focus on the regulation of hepcidin by the BMP signalling pathway.

A known regulator of the BMP pathway, bone morphogenetic protein [BMP]-binding endothelial cell precursor-derived regulator (BMPER), was found to be overexpressed in the HPX mouse liver. Soluble BMPER peptide in excess strongly inhibited BMP-dependent hepcidin promoter activity in both HepG2 and Huh7, cells abolishing the effects of BMP2 and attenuating the effects of BMP6. These effects correlated with reduced cellular pSMAD levels. Addition of recombinant BMPER peptide to primary human hepatocytes strongly downregulated hepcidin mRNA levels and abolished the effects of BMP2. These effects were reflected *in vivo* where the injection of mice with recombinant BMPER peptide significantly reduced hepcidin mRNA expression which correlated with increased serum iron levels. Thus, the protein may play an important

role in suppressing hepcidin production to increase iron availability under conditions of chronic anaemia.

Using the same HPX model, several other genes related to the BMP pathway also demonstrated differential gene expression. Atonal Homologue 8 (ATOH8), a basic helix-loop helix (bHLH) transcription factor, was previously shown to be regulated by iron loading however its precise role in iron metabolism was unknown. The studies presented in this thesis identified hepatic ATOH8 mRNA and protein expression to be robustly downregulated in various mouse models of altered iron metabolism where increased erythropoietic activity was shown to suppress hepcidin. Further investigations demonstrated that ATOH8 expression in HEK-293 cells directly regulated the hepcidin promoter and increased cellular pSMAD levels, thereby establishing a hitherto missing link between the regulation of hepcidin, erythropoietic activity and the BMP/SMAD pathway.

Finally, the little known BMP, BMP8b, and the clotting factor, von Willebrand Factor which were also found to be significantly increased in the liver of the HPX mouse, were investigated as potential regulators of hepcidin. BMP8b has the potential to form heterodimeric complexes with other BMP members and therefore could be important in modulating BMP signalling and thus in turn hepcidin promoter activity. Whereas von Willebrand factor contains BMP binding sites and therefore may sequester BMPs, thus inhibiting BMP signalling. However the present study was unable to show consistent effects of either molecule on hepcidin promoter activity and so the roles of BMP8b and von Willebrand Factor in iron metabolism, if any, remains unclear.

In conclusion, the analyses presented in this thesis demonstrate the novel molecular interactions governing hepcidin regulation by the BMP pathway. The new knowledge generated will be useful in the development of therapeutic strategies to diagnose, prevent, or mitigate disorders of iron homeostasis.

Acknowledgements

I would like to express my gratitude to all those who have supported me throughout my PhD studies. Without the help of the following people, this study would not have been complete.

First and foremost I owe sincere thankfulness to my primary supervisor, Professor Andrew McKie, whose support and guidance from the beginning to the end has enabled me to develop an understanding of the subject. I appreciate all his contributions of time, ideas, and funding to make my PhD experience productive and stimulating. I am also very grateful to my second supervisor Dr. Robert Simpson for his advice and encouragement on both practical and theoretical aspects throughout my PhD studies. I am deeply indebted to all the members of the iron metabolism group (both past and present) for their stimulating suggestions and scientific discussions. I would especially like to thank to Dr. Patarabutr Masaratana whose guidance has helped me navigate the world of science and has been invaluable on both an academic and a personal level, for which I am extremely grateful. I also thank Dr. Yemisi Latunde-dada for her generous assistance with *in vivo* studies and motivation over the past four years.

I would like to acknowledge my friend and colleague Nisha Hirani, for helping me get through the difficult times and for all the emotional support she has provided. I would also like to thank my parents and siblings who have taught me strength and persistence throughout my studies. A special thanks to my sister, Poonam Patel, for her practical support and encouragement. I am eternally obliged to my Fiancé, Amit Bhudia, for making me laugh even when experiments were failing and whose support and reassurance is deeply appreciated.

Table of contents

List of figures

List of tables

Abbreviations

Abbreviation	Full word
A	Absorbance
Actb	Beta-actin
AGM	aorta-gonad-mesonephros
ANOVA	Analysis of variance
ALK	Activin receptor-like kinase
ATCC	American type culture collection
ATOH8	Atonal homologue 8
bHLH	Basic Helix-loop-helix
BMPER	Bone morphogenetic protein [BMP]-binding endothelial cell precursor-derived regulator
BMP	Bone morphogenetic protein
bp	Base pairs
BSA	Bovine serum albumin
cDNA	Complementary deoxyribonucleic acid
C/EBPα	CCAAT/enhancer-binding protein α
Co-SMAD	common-mediator Mothers against decapentaplegic homologue
CR	Cysteine rich
CV-2	Crossveinless-2
Dcytb	Duodenal cytochrome b
DFO	Desferrioxamine
DMEM	Dulbecco's Modified Eagle Medium
DMT1	Divalent metal transporter 1
DNA	Deoxyribonucleic acid
dNTP	Deoxynucleotide triphosphate
DPP	Decapentaplegic
DTT	Dithiothreitol
EDTA	Ethylenediaminetetraacetic acid
E Box 1,2	Enhancer box 1,2
EPO	Erythropoietin
EPOR	Erythropoietin receptor
ERK1/2	Extracellular signal-regulated kinase ½
FAC	Ferric ammonium citrate
FBS	Fetal bovine serum
FCS	Fetal calf serum
Fe^{2+}	Ferrous
Fe^{3+}	Ferric
$FeCl_3$	Ferric chloride
FITC	Fluorescein isothiocyanate
FLK-1	Fetal liver kinase 1
FPN1	Ferroportin
g	G-force (force)
GDF15	Growth differentiation factor 15

Abbreviation	Full word
GFP	Green fluorescent protein
Gp130	Glycoprotein 130
H_2O_2	Hydrogen peroxide
HCl	Hydrochloric acid
HCP1	Haem carrier protein 1
HEPES	4-(2-hydroxyethyl)-1-piperazineethanesulfonic acid
Het	Heterozygote
Hamp1$^{-/-}$	Hepcidin1 knockout
H-ferritin	Ferritin heavy chain
HH	Hereditary haemochromatosis
HIF-1α	Hypoxia inducible factor-1α
HIF-2α	Hypoxia inducible factor-2α
HJV	Hemojuvelin
HPX	Hypotransferrinaemic
HRE	Hypoxia-response element
HRP	Horseradish peroxidase
HUVEC	Human Umbilical Vein Endothelial Cells
Il-1	Interleukin-1
Il-6	Interleukin-6
IRE	Iron responsive element
IREG1	Iron regulated gene 1
IRP	Iron responsive protein
IRIDA	Iron refractory iron deficiency anaemia
I-SMAD	Inhibitor Mothers against decapentaplegic homologue
JAK	Janus kinase
JH	Juvenile haemochromatosis
kDa	Kilodalton
KO	Knockout
LEAP-1	Liver expressed antimicrobial peptide 1
L-Ferritin	Ferritin light chain
LIC	Liver iron content
LIP	Labile iron pool
LPS	Lipopolysaccharide
MATH6	Mouse atonal homologue 6
MT-2	Matriptase-2
MHC	Major histocompatibility complex
m-HJV	Membrane hemojuvelin
MOPS	3-(N-morpholino) propanesulfonic acid
mRNA	Messenger ribonucleic acid
MTP1	Metal transporter protein-1
MUT	Mutant
NTBI	Nontransferrin-bound iron
$O_2^{\cdot-}$	Superoxide ion
$OH^{\cdot}$	Hydroxyl radical
OH^-	Hydroxide ion
PBS	Phosphate buffered saline
PBST	Phosphate buffered saline – Tween

Abbreviation	Full word
PCR	Polymerase chain reaction
PGC	Primordial germ cells
PHZ	Phenylhydrazine
PI3K	Phosphoinositide 3-kinase
PLB	Passive lysis buffer
PNS	Peripheral nervous system
ppm	Part per million
PVDF	Polyvinylidene fluoride
RDA	Recommended dietary allowance
RGM	Repulsive guidance molecule
RIPA	Radioimmunoprecipitation assay buffer
RM1	Rodent maintenance diet
RNA	Ribonucleic acid
ROS	Reactive oxygen species
RT-PCR	Reverse transcription polymerase chain reaction
R-SMAD	receptor-regulated Mothers against decapentaplegic homologue
SD	Standard deviation
SDS	Sodium dodecyl sulphate
SDS-PAGE	sodium dodecyl sulphate polyacrylamide gel electrophoresis
sHJV	Soluble hemojuvelin
SLA	Sex-linked anaemia
SMAD	Mothers against decapentaplegic homologue
STAT3	Signal transducer and activator of transcription 3
TBE	Tris/Borate/EDTA
TCA	Trichloroacetic acid
TEMED	N,N,N′,N′-tetramethylethylenediamine
TfR1	Transferrin receptor 1
TfR2	Transferrin receptor 2
TGF-β	Transforming growth factor beta
TIBC	Total iron binding capacity
TLR4	Toll-like receptor 4
TMPRSS6	Matriptase-2
TNF-α	Tumour necrosis factor alpha
TSS	Transcriptional start site
TWSG1	Twisted gastrulation 1
UIBC	Unsaturated iron binding capacity
USF1	Upstream stimulatory factor 1
USF2	Upstream stimulatory factor 2
UTR	Untranslated region
VEGF	Vascular endothelial growth factor
VWC	von Willebrand factor C
VWF	von Willebrand factor
WT	Wild type
β2m	Beta-2 microglobulin
%TS	Transferrin saturation
$^{+/-}$	Heterozygote
$^{-/-}$	Knockout

Chapter 1 .

General introduction

1.1 Importance of iron in mammalian physiology

1.1.1 Maintaining iron balance

Iron is a key element in the metabolism of almost all living organisms. Iron is a functional component of the oxygen carrying unit, haemoglobin; additionally it is important in numerous other biological processes including electron transfer and DNA synthesis (Lieu et al., 2001). The biological importance of iron can be determined by its chemistry. Iron can switch between the ferrous form (Fe^{2+}) and the ferric (Fe^{3+}) forms making it a useful component of cytochromes, oxygen binding molecules and a variety of enzymes (Andrews, 2000). Its ability to accept and donate electrons also renders iron as a toxic metal where it is able to participate in the Fenton reaction, converting hydrogen peroxide (H_2O_2) into dangerous free radicals, which cause damage to fatty acids, proteins and nucleic acids within the cell (Halliwell and Gutteridge, 1986).

(1) $Fe^{3+} + O_2^{\bullet -} \longrightarrow Fe^{2+} + O_2$ (Haber-Weiss reaction)

(2) $Fe^{2+} + H_2O_2 \longrightarrow Fe^{3+} + OH^{\bullet} + OH^{-}$ (Fenton reaction)

Biological systems have evolved intricate transport, storage and regulatory proteins to achieve the correct balance of iron throughout the system.

1.1.2 Iron distribution

The total body iron content in the normal healthy adult man is approximately 3-4 grams, which remains fairly constant as the amount of iron absorbed is balanced by the amount lost through blood loss and sloughing of skin and mucosal cells (Anderson et al., 2007). Approximately 65% of total body iron is incorporated into erythroid cells, with 30% stored in the liver, spleen and bone marrow as ferritin or haemosiderin,

while the remaining 5% is distributed to myoglobin, haem enzymes and transferrin (Smith, 1969). Approximately 3 mg of iron is found in plasma. Despite its small proportion, the circulating iron found in the plasma represents one of the most dynamic compartments of the body with the highest turnover rate. Since there is no excretory mechanism for iron, the rate at which iron absorption occurs is tightly regulated.

1.1.3 Iron absorption

The absorption of iron takes place in the proximal small intestine, primarily in the duodenum. Iron obtained from the diet can be in two forms: haem iron or non haem iron. The absorption of haem iron is highly efficient as the proteolytic digestion of haemoglobin results in the release of haem which remains available for absorption (Uzel and Conrad, 1998). In contrast, the efficiency of non haem iron absorption is poor, as iron is found in the ferric form and needs to be reduced to the ferrous form before being absorbed.

Several studies have demonstrated that the brush-border surface of the enterocyte has ferric-reductase activities (Raja et al., 1992, Riedel et al., 1995, Ekmekcioglu et al., 1996). The first intestinal ferricreductase to be isolated was duodenal cytochrome b (DCYTB) (McKie et al., 2001). The expression of DCYTB was localised to the apical membrane and was upregulated during chronic anaemia, iron deficiency and hypoxia, all processes which stimulate iron absorption (McKie et al., 2001). However mice lacking functional DCYTB expression did not appear to become iron deficient, implying that there may be other mechanisms in place which are able to compensate for the DCYTB activity (Gunshin et al., 2005b). A limitation to the use of mouse models in these studies is that humans, unlike mice, are completely reliant on the diet to provide ascorbic acid which has been shown to increase the uptake of iron *in vitro* (Han et al., 1995). Mice however are able to produce endogenous ascorbate which may act as a reducing agent in the intestinal lumen (Gunshin et al., 2005b).

Ferrous iron is transported across the apical membrane by divalent metal transporter 1 (DMT1 – also known as SLC11A2/NRAMP2/DCT1). DMT1 was shown to accept a broad range of divalent cations including Ca^{2+}, Co^{2+}, Cu^{2+}, Ni^{2+}, Mn^{2+}, Pb^{2+}, Zn^{2+} (Gunshin et al., 1997). The cDNA encodes a 561 amino acid protein with 12- putative membrane spanning domains with a 3'-UTR iron response element (IRE) which may be subject to iron sensitive post-transcriptional regulation via the IRE-IRP system (discussed in 1.2.3) (Gunshin et al., 1997, Lee et al., 1998). Mice deficient in intestinal DMT1 are normal at birth, but their pre-natal iron stores are rapidly depleted after which they develop iron deficiency anaemia (Gunshin et al., 2005a). Additionally, the *Slc11a2*$^{-/-}$ animals where the gene was globally ablated, were unable to use iron efficiently for erythropoiesis demonstrating impairment in iron transport in the erythroid precursor cells (Gunshin et al., 2005a).

Intracellular iron is either stored in ferritin or exported out of the enterocyte through the basolateral iron transporter ferroportin (FPN1, MTP1) (Donovan et al., 2000, McKie et al., 2000, Abboud and Haile, 2000). Functional studies with *Xenopus Laevis* oocytes demonstrated that overexpression of ferroportin in the presence of DMT1 increased the efflux of iron (McKie et al., 2000). However, in order for the exported iron to be loaded on to apotransferrin (iron free transferrin), ferrous iron needs to be re-oxidised to ferric iron. This was shown to occur through the association of hephaestin and/or ceruloplasmin (Cp). The importance of these ferroxidases was demonstrated through the analysis of the defective mechanism that exists in the sex-linked anaemia (SLA) mouse model. In the SLA model, iron is taken up normally by the enterocyte, however iron is not released from the enterocyte into the bloodstream. The gene hephaestin was identified as a protein mutated in this strain and was shown to be required for the release of iron by a putative basolateral transporter, which we now know as ferroportin (Vulpe et al., 1999). Targeted gene deletion of ceruloplasmin (Cp) in mice caused iron over load in particularly in the liver and spleen. The uptake of iron was unaffected by Cp deletion, however *Cp*$^{-/-}$ mice displayed a marked impairment in the ability to efflux iron from hepatocytes as judged by a lack of radiolabelled iron in the serum of these animals. Interestingly administration of Cp protein in these mice resulted in a rapid

rise in radiolabelled serum iron, demonstrating the importance of this protein in iron efflux (Harris et al., 1999).

Ferroportin expression increased with iron loading in the liver (Abboud and Haile, 2000), lung (Yang et al., 2002) and macrophage (Delaby et al., 2008). This was supported by the identification of an iron responsive element (IRE) located at the 5′ untranslated region (UTR) of ferroportin mRNA. Under iron replete conditions, the expression of ferroportin protein is increased through the lack of iron regulatory protein (IRP) binding, thus promoting iron efflux from these cells (see section 1.2.3). However Ferroportin mRNA expression in the duodenum was shown to increase in iron deficiency (McKie et al., 2000). The later discovery of another transcript ferroportin1B (FPN1B) which lacked the IRE and was expressed in the duodenum now explains this anomaly (Zhang et al., 2009b).

It is now well known that the actions of ferroportin is also regulated by the hormone hepcidin which is released into the circulation when systemic iron levels are increased. The interaction of ferroportin with hepcidin was demonstrated through cell culture studies where the addition of hepcidin to cells expressing ferroportin tagged to green fluorescent protein (GFP) caused ferroportin to be internalised and degraded. Therefore hepcidin controls the amount of ferroportin on the cell surface and thus the amount of iron entering the circulation from the diet and from macrophages (Nemeth et al., 2004b).

Absorbed ferric iron is rapidly bound to Apotransferrin (the iron free form of transferrin). Transferrin (Tf) is an abundantly expressed protein with a molecular weight of approximately 80kDa. Transferrin can bind to two atoms of ferric iron per molecule (Fletcher, 1970). Therefore transferrin can exists in three forms: iron free apoTF; monoferric form or diferric/ holoTf. Plasma transferrin facilitates the transport of iron to cells that express transferrin receptors and also limits the ability of iron to generate reactive oxygen species.

Haem iron is an additional source of dietary iron and is absorbed via a different mechanism in comparison to non haem iron. Haem carrier protein 1 (HCP1) was described in 2005 and demonstrated an increased uptake of haem when expressed in *Xenopus* oocytes and Hela cells. (Shayeghi et al., 2005). Subsequently HCP1 was independently characterised as a folate/proton symporter and was shown to be necessary for folate homeostasis in man (Qiu et al., 2006). Thus the precise role of this haem/folate transporter requires further investigation. Upon entry into the enterocyte, the haem is degraded by haem oxygenases which release ferrous iron, which follows the same pathway as non-haem iron thereafter.

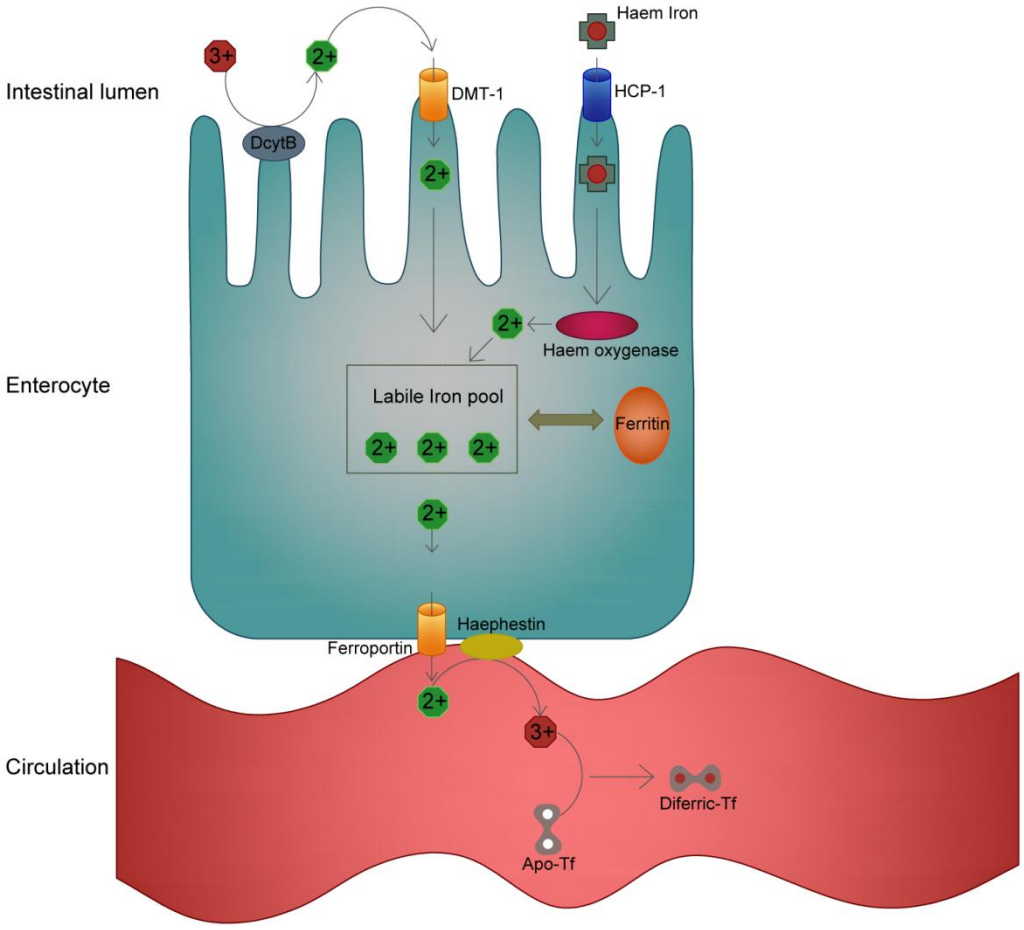

Figure 1.1 Mechanism of intestinal iron absorption

1.2 Regulation of iron homeostasis

Due to the limited ability to excrete iron, tight regulation between the sites where iron is absorbed, utilised and stored is essential.

1.2.1 Cellular iron uptake

The uptake of iron into cells is dependent on the expression of transferrin receptors (TfR). There are two transferrin receptors, TfR1, which is ubiquitously expressed and TfR2 whose expression is restricted to the liver (Kawabata et al., 1999). The binding of mono-Tf or holoTf at the cell surface to TfR1 causes the complex to be endocytosed into a clathrin-coated pit. The endosome is then acidified possibly by recruitment of a proton pump which causes a conformational change in Tf, releasing iron from transferrin (Aisen, 2004). The iron is reduced by the ferric reductase STEAP3 (Ohgami et al., 2006) to ferrous iron which exits the endosome through DMT1 (Fleming et al., 1998). The apoTf is recycled back to the cell surface where the protein is released for another cycle of iron transport (Aisen, 2004). The uptake of iron by TfR1 appears to be most important in the developing erythroid cell. Murine TfR1 deletion is embryonically lethal and haploinsuffiency results in impaired erythroid development and abnormal iron homeostasis (Levy et al., 1999). Thus red cell development is dependent on TfR1 function.

TfR2 is structurally similar to TfR1 and both receptors bind holoTf better than apoTf, however the affinity for TfR2 to bind diferric-Tf was shown to be 25-fold lower than TfR1 (Kawabata et al., 1999). Mutations in human and mouse TfR2 gene have been shown to cause severe hepatic iron overload termed type III haemochromatosis (section 1.6.1) (Camaschella et al., 2000, Fleming et al., 2002, Wallace et al., 2007). Although the effects of TfR2 mutations cause iron overload, studies involving TfR1 mutations demonstrated high mortality rates, suggesting that TfR2 was unable to compensate for TfR1 expression possibly due to its restricted tissue location.

Additionally, erythroid cells had reduced TfR2 protein expression and displayed limited mRNA expression (Calzolari et al., 2004), suggesting that the role of TfR2 may be more related to the iron sensing where TfR2 abundantly expressed by the hepatocyte.

1.2.2 Iron storage and recycling

Not all of the iron that is taken up by the cell is used for metabolism. Some of it can be stored to protect the cell from the toxic effects of free iron. Hepatocytes of the liver serve as major depots for iron storage where excess iron can be stored in ferritin. Ferritin is a water soluble molecule of 24 subunits which can bind up to 4500 atoms of iron (Harrison and Arosio, 1996). The protein is composed of heavy (21kDa) and light (19kDa) chains and the ratio of these are varied depending on the cell type. The heavy chain functions as a ferroxidase, which oxidises ferrous iron to ferric iron which is bound inside ferritin (Koorts and Viljoen, 2007). In addition to the iron that is absorbed from the diet, the recovery of iron from senescent erythrocytes also plays an important role in iron metabolism. The average life span of an erythrocyte is approximately 120 days. At the end of their life, the erythrocytes undergo surface alterations which targets them to be phagocytosed and digested by macrophages in the spleen, liver and bone marrow (Ganz, 2007). Haem from haemoglobin is degraded by the actions of haem oxygenases (Poss and Tonegawa, 1997). Iron is exported out of the phagosomal membrane into the cytoplasm by DMT1 where it can be stored in ferritin.

The stored iron can be used when iron is required by the cell through the help of ferroportin. Cells treated with exogenous iron increase cellular iron levels which in turn increase ferritin expression. This effect is lost through co-expression of ferroportin in the cells suggesting that ferroportin causes degradation of ferritin (Nemeth et al., 2004b). The mechanism by which this occurs has been proposed to require the activity of a proteosome (De Domenico et al., 2006). The expression of ferroportin is dependent on the expression of hepcidin (discussed in section 1.4.3). The importance of

ferroportin in erythrocyte recycling is demonstrated in mice that lack ferroportin which become anaemic and iron loaded due to the lack of iron export from macrophages and enterocytes (Ganz, 2007).

1.2.3 Regulation of cellular iron balance

The liver stores are mobilised if body iron levels are decreased; thus regulation between the sites where iron is absorbed, utilised and stored is essential to maintain iron homeostasis. Molecules involved in these processes can be regulated post-transcriptionally by intracellular iron levels through the interactions of iron regulatory proteins (IRPs) which bind to iron regulatory elements (IREs) found on the untranslated regions (UTR) of mRNA sequences (Casey et al., 1988).

There are two types of IRPs identified in the mammalian system, IRP1 and IRP2. IRP1 is an iron-sulphur cluster-protein containing a cubane [4Fe-4S]. IRP2 shares over 60% identity to IRP1 however lacks an iron-sulphur cluster (Ponka et al., 1998). The presence of IRE's located in the 3′ UTR of TfR1 and 5′ UTR of ferritin enables regulation of expression of these proteins by IRPs. Under iron depleting conditions, the IRE's in the 3′ UTR are occupied by IRP binding and this stabilises the TfR1 mRNA which increases iron uptake. In contrast, the translation of ferritin mRNA is inhibited through the binding of IRP on the 5′ IRE thus preventing iron from being stored. During iron repletion/excess, IRP1 binds iron-sulphur clusters converting it into a cytosolic aconitase and IRP2 undergoes iron dependent degradation (Guo et al., 1995, Iwai et al., 1995). Thus the IRPs fail to bind to IREs. In this situation, ferritin translation is stimulated while TFR1 mRNA containing 3′ IRE is degraded. The expression of ferroportin is also under the control of the IRE/IRP system (see section 1.1.3).

The roles of each of the IRPs in mammalian iron physiology have been investigated through genetic ablation studies. A lack of IRP1 did not appear to regulate iron

metabolism as indicated by the viability and health of *IRP1*$^{-/-}$ mice (Meyron-Holtz et al., 2004). Additionally, the authors proposed that IRP1 functions mainly as a cytosolic aconitase and is not critical for the regulation of iron (Meyron-Holtz et al., 2004). In contrast, iron deficiency increased the expression of IRP2 implying an iron sensing role of IRP2. The importance of IRP2 in maintaining iron homeostasis was demonstrated by two independent studies. *IRP2*$^{-/-}$ mice were shown to develop normally up to 6 months however mice older than 6 months of age developed progressive neurodegenerative disease along with increased liver and duodenal iron levels (LaVaute et al., 2001). However in a later study which generated another *IRP2*$^{-/-}$ model, the symptoms of overt neuropathy were not displayed and more systemic abnormalities with reduced TfR1 expression in the bone marrow were noted (Galy et al., 2005). The *in vivo* investigations demonstrate the importance of IRE/IRP regulation in maintaining cellular iron homeostasis.

1.3 Systemic iron regulation

The existence of the stores and erythroid regulators of systemic iron homeostasis was first coined by Clement Finch in 1994 many years before the discovery of hepcidin. In his review, Finch hypothesised that the stores regulator would regulate the amount of iron absorbed from the duodenum and a feedback mechanism would be involved to prevent iron overload. The erythroid regulator on the other hand would be involved when the demand for iron for erythropoiesis surpasses the capacity of storage cells to mobilise iron for erythropoiesis and thus intestinal iron absorption is increased (Finch, 1994). It is now well known that hepcidin is a key regulator of systemic iron homeostasis and that the stores and erythroid regulators are likely to modulate the expression of hepcidin through molecular components that are able to communicate signals between the sites of iron absorption/ storage utilisation.

1.4 Hepcidin: the iron regulatory peptide

1.4.1 Discovery

Before the iron connection emerged, hepcidin was regarded as an antimicrobial peptide expressed predominantly in the liver and was termed Liver Expressed Antimicrobial Peptide-1 (LEAP1) (Krause et al., 2000). LEAP1 could be isolated from human urine and was shown to be weakly active against bacteria and fungi (Park et al., 2001).

The relevance of hepcidin in iron metabolism was suggested later by Pigeon et al in 2001 who identified it from a search of new genes that were upregulated in the liver by iron excess. (Pigeon et al., 2001). The confirmation of the role of hepcidin in iron metabolism was initially completely serendipitous. A group in Paris had developed a knockout mouse for a gene involved in glucose metabolism named upstream stimulatory factor 2 (*USF2*$^{-/-}$). The *USF2*$^{-/-}$ mice developed liver iron overload which could not be explained. As it turned out the USF2 gene was located very close to the hepcidin gene and the later had been silenced by the insertion of the USF2 targeting construct. Nonetheless this strongly suggested a functional role of hepcidin in iron metabolism since mice had a similar phenotype to haemochromatosis patients (Nicolas et al., 2001b). The role of hepcidin was confirmed in a follow up paper from the same group showing that transgenic mice over expressing hepcidin developed severe iron deficiency (Nicolas et al., 2002a).

1.4.2 Structure

The human hepcidin gene (*HAMP*) is located on chromosome 19q13.1 and is synthesised by hepatocytes as a preprohepcidin of 84 amino acids. The full length preprohepcidin undergoes a series of enzymatic cleavages first to produce a

prohepcidin of approximately 64 amino acids. The proregion is post-translationally removed by a furin-like proprotein convertase resulting in a bio active 25 amino acid peptide (Valore and Ganz, 2008). The structure of hepcidin resembles that of other antimicrobial peptides such as defensins and proteogrin and is predicted to be an amphiphatic cationic disorted beta-sheet protein with four disulphide bridges (Hunter et al., 2002).

1.4.3 Mechanism of action

The molecular mechanisms governing the hepcidin response to iron came from cell culture studies, where hepcidin was found to interact with GFP- (green fluorescent protein) tagged ferroportin which caused ferroportin internalisation and degradation. The binding of hepcidin to ferroportin reduced the release of iron from hepatocytes, enterocytes and macrophages (Nemeth et al., 2004b). Hepcidin is therefore a negative regulator of iron efflux in these tissues. Loss of function studies suggested the N-terminal amino acid region of hepcidin was critical for its activity whereas the loss of the C-terminal did not affect its function (Nemeth et al., 2006).

The structural determinants governing hepcidin-mediated ferroportin degradation is currently under debate. Initial investigations demonstrated the importance of tyrosine residues 302 and 303 located on ferroportin which are phosphorylated by JAK2 following hepcidin binding (De Domenico et al., 2007, De Domenico et al., 2009). The phosphorylation of these residues was accompanied by the activation of the STAT3 pathway, thus providing evidence for downstream effectors (De Domenico et al., 2010). The studies conducted by De Domenico and colleagues have been recently challenged by findings that the neither JAK2 or phosphorylation of the tyrosine residues are required for hepcidin mediated internalisation (Ross et al., 2012). Ferroportin was found to be expressed in JAK2 null human fibrosarcoma cells and was shown to decrease upon hepcidin treatment with no reported phosphorylation of STAT3 or STAT5 (Ross et al., 2012). The authors highlight the significance of lysine residues 240

and 258 on ferroportin, which demonstrated a reduced rate of ferroportin internalisation when mutated to arginine upon hepcidin treatment *in vitro*. (Ross et al., 2012). In a separate study, the substitution of lysines in the third intracellular loop of ferroportin reduced ubiquitination upon hepcidin treatment and instead increased cellular iron export. This was determined by intracellular ferritin expression. HEK-293 cells expressing WT Ferroportin-GFP increased ferritin expression upon hepcidin treatment demonstrating iron retention in these cells. In contrast the expression of ferritin remained unchanged in mutant ferroportin-GFP expressing cells, demonstrating the continued export of iron in these cells (Qiao et al., 2012).

1.5 Regulation of hepcidin expression

Knowledge of the signals that repress and activate hepcidin expression has come from studies involving iron loading and iron deficient phenotypes in humans and mice, where hepcidin expression is increased during inflammation and iron loading and decreased by anaemia and hypoxia. Delineation of the regulatory circuits that govern hepcidin expression have identified the involvement of the Bone Morphogenetic Protein (BMP), JAK/STAT and the ERK/p38 MAP kinase pathways to be contributors to the transcriptional regulation of hepcidin expression. The BMP pathway is of interest in the present study and will be described in detail below.

1.5.1 The Bone morphogenetic proteins (BMPs)

Bone is the material that makes vertebrates unique from other animals. Providing support and protection for the visceral organs as well as allowing movement of limbs are but a few key features of bone. When a bone breaks, various signals are released to eventually produce a completely healed skeleton. Understanding how the bone regenerates has been central to the entire discipline of bone morphogenesis. In 1965, Dr Marshall Raymond Urist, implanted demineralised bone into a rabbit's muscle which then formed a bone at the site (Urist, 1965). He hypothesised that proteins released

from the bone are the cause of the regeneration at the site of implantation; he named the protein bone morphogenetic protein (BMP). Since their initial discovery in the formation of bone and cartilage, the BMPs have been shown to be a dynamic family of cytokines belonging to the TGF-β superfamily of ligands. They are involved in the regulation of a vast number of cellular processes ranging from tooth development to the maintenance of iron metabolism and vascular homeostasis *in vivo* (Miyazono et al., 2010).

Of the 20 members of the BMP family, BMP2 and BMP4 were amongst the first BMPs to be purified (Wozney et al., 1988). Purification of BMPs from bone has provided insight into the structure and sequence similarities between different BMPs and has enabled them to be sub-divided into groups (see Table 1.1). BMP2 and BMP4 have 83% amino acid sequence identity and are the best studied members of the BMP family (Kawabata et al., 1998). BMP5, BMP6, BMP7 (also known as osteogenic protein-1, OP-1) and BMP8 (OP-2) form another sub family which are slightly larger proteins in comparison to BMP2 and BMP4, with approximately 70% amino acid similarity between the sub-groups (Wozney, 2002).

The BMPs are processed as larger precursor proteins which are proteolytically processed to form dimeric proteins (Figure 1.2). A hydrophobic signal peptide is processed to produce a pro-BMP. This is further cleaved by a furin-like protease at the RXXR cleavage site to yield the mature C-terminal fragment. The mature BMP protein is a dimer which is formed by two BMPs molecules forming disulphide links at the highly conserved carboxy terminal region. In particular, seven cysteine residues are conserved in this domain and are present at analogous position in nearly all family members (Wozney et al., 1988). BMPs can form homo dimers between BMPs of the same subfamily or heterodimers between BMPs of different subfamilies. There is some evidence that heterodimeric BMPs are more potent in BMP signalling than homodimers (Ying et al., 2001).

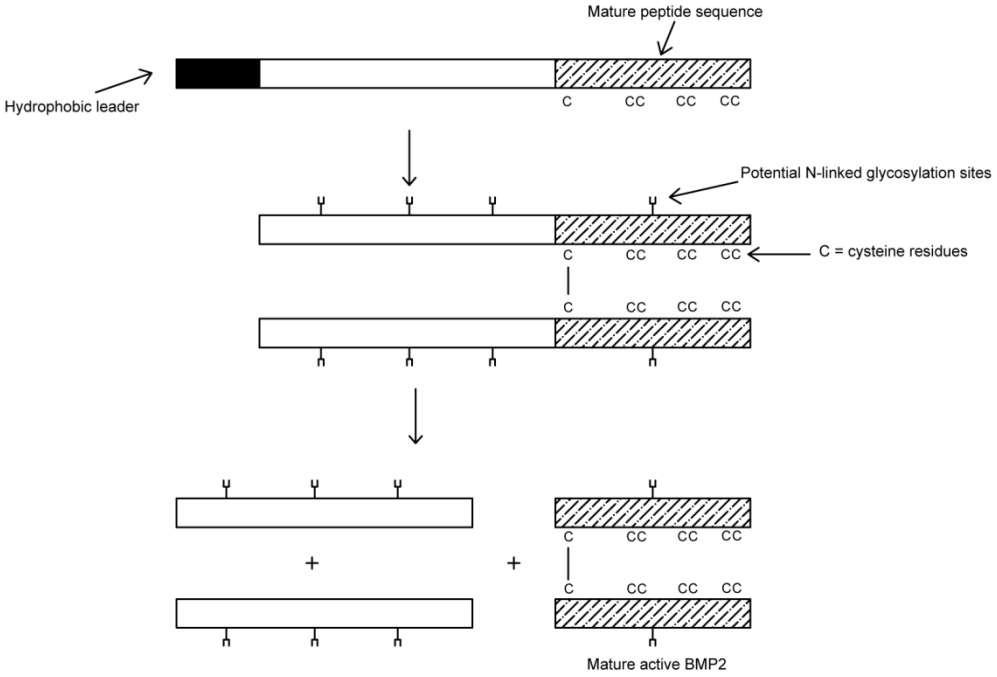

Figure 1.2 The proteolytic processing of BMP proteins (adapted from (Wozney et al., 1988))

The homo- or –heteromeric BMPs can bind to two types of serine-threonine kinase receptors, i.e. type I and type II receptors (de Gorter et al., 2009).

BMP type I receptors: there are 7 type I activin receptor-like kinases which are classified into three groups based on their structure and function (Table 1.1).

Table 1.1 BMP type I receptors

Group	Receptors	BMP binding preference	Downstream target
BMPR-I	**BMPR-IA / ALK3**	**BMP2/BMP4**	**Activates**
	BMPR-IB / ALK6	**GDF5**	**SMAD 1,5,8**
ALK-I	**ALK1**	**BMP9/ BMP10**	**Activates**
	ALK2	**BMP6/BMP7**	**SMAD 1,5,8**
TβR-I	**ALK4 / ACTR-IB**		**Activates**
	ALK5 / TβR-I		**SMAD2/3**
	ALK7		

BMP type II receptor: there are three BMP type II receptors which are widely expressed in mammals (Table 1.2).

Table 1.2 BMP type 11 receptors

Group	BMP binding preference
BMPR-II	**BMP specific**
ACTR-II	**Activins**
	Myostatin
	BMPs
ACTR-IIB	

Type I and type II receptors differ in certain structural features. Type I receptors have a glycine/serine residue rich stretch in the intracellular juxtamembrane region which becomes phosphorylated by type II receptors which are constitutively active and have extensions rich in serine and threonine residues (de Gorter et al., 2009). As well as BMP receptors type I and II, the regulation of certain ligands can be assisted by co-receptors (section 1.5.2).

The phosphorylation of type I receptors leads to the activation and phosphorylation of downstream signal transducers called SMADs. It was found that the *Drosophila* homologue of the *C.elegans* gene SMA, when mutated in the mother, repressed the gene decapentaplegic in the embryo. Hence the gene was called, "mothers against decapentaplegic". The human protein is called SMA and MAD related protein (SMAD) (Massague et al., 2005). The eight SMADs which have been identified in mammals can be sub-classed into three groups based on their functions:

- R-SMAD - receptor regulated
- Co-SMAD - common SMAD
- I-SMAD – inhibitory SMAD

Five R-SMADs have been identified in mammals whose actions are dependent on the BMP binding and receptor activation (outlined in Table 1.1 downstream target). Activated R-SMADs form a heteromeric complex with common SMAD4. This complex then translocates into the nucleus where it can bind to promoter regions located on target genes. Inhibitory SMADs also exist, which are also induced by BMPs and provide a feedback mechanism to prevent excessive BMP signalling (de Gorter et al., 2009).

In addition to the well defined BMP/SMAD pathway, BMPs are also able to activate alternative pathways including ERK/p38 MAP kinase pathways through TGF-β activated kinase I which associates with BMPR-II (Miyazono et al., 2010). BMPs are also able to activate PI3-kinase (PKB/AKT) and caspases which mediate BMP-induced osteoblast differentiation (de Gorter et al., 2009).

1.5.2 The BMP proteins and hepcidin transcription

Early investigations identified a connection between the BMP/SMAD pathway and iron metabolism through studies assessing the role of SMAD4 in liver development. *SMAD4*$^{-/-}$ resulted in embryonic lethality, however when a liver specific knockout was generated, investigators noted that the absence of SMAD4 resulted in iron overload and reduced hepcidin expression (Wang et al., 2005).

Since then a number of studies have been conducted in order to elucidate the role of factors that are upstream and downstream of the SMAD4 signalling cascade. Of the 20 different BMP ligands identified, BMP2, BMP4, BMP5, BMP6, BMP7 and BMP9 have been shown to be potent stimulators of hepcidin transcription *in vitro* (Truksa et al., 2006, Babitt et al., 2007). BMP2 positively regulates hepcidin transcription and reduces serum iron levels *in vivo* (Babitt et al., 2007). Shortly after the discovery of *SMAD4*$^{-/-}$ phenotype, Babitt and colleagues identified Hemojuvelin (HJV) as a co-receptor for the

BMP signalling pathway. The significance of HJV in modulating BMP signalling was demonstrated through cell cultures studies from primary hepatocytes isolated from *HFE2*$^{-/-}$ mice. These cells were unable to respond to BMP2/4 stimulation and failed to upregulate hepcidin expression. Transfection with HJV cDNA into hepatoma-derived cells increased hepcidin mRNA expression by quantitative real-time RT-PCR and increased hepcidin promoter reporter activity (Babitt et al., 2006).

Babitt et al were the first to show that a soluble form of HJV inhibits hepcidin expression *in vivo* (Babitt et al., 2006). HJV belongs to the RGM family of proteins of which RGMA and DRAGON were amongst the first described co-receptors for the BMP subfamily (Samad et al., 2005, Babitt et al., 2006). *HFE2*$^{-/-}$ mice displayed a similar phenotype to patients with HFE2 mutations where hepcidin levels are depressed, with marked tissue iron overload (Babitt et al., 2006). In addition, the expression of pSMAD 1,5,8, a downstream effector for BMP signalling, was significantly decreased in the *HFE2*$^{-/-}$ animals providing evidence that a loss of HJV reduced hepcidin by reducing BMP signalling.

HJV exists as two forms; a membrane bound (m-HJV) which acts as a BMP co-receptor and a soluble form (s-HJV). The soluble form has been shown to suppress hepcidin mRNA expression in primary human hepatocytes (Lin et al., 2007). Additionally, injections of s-HJV decreased hepatic hepcidin mRNA expression in mice (Babitt et al., 2007). s-HJV was shown to selectively bind and inhibit BMP2,4,5 and 6's ability to induce the hepcidin promoter without affecting BMP9 or BMP7 (Babitt et al., 2007). Having tested a wide array of ligands from both BMP and TGF-β sub-families, the authors concluded that the TGF-β sub-family may be less critical in modulating hepcidin transcription as these members showed no effect on hepcidin transcription *in vitro*. Additionally, when comparing the effects of BMP2/4 to other BMP's, BMP9 at first glance appeared to be the most potent inducer of hepcidin expression (Truksa et al., 2006). However further investigations revealed that BMP9 was only able to modulate basal hepcidin responses and did not appear to interact with HJV (Lin et al., 2007, Babitt et al., 2007).

The mechanism by which HJV is processed has been shown to occur in two ways which may account for its ability to switch from a co-receptor to a possible BMP-antagonist.

- Furin mediated cleavage

Silvestri and colleagues proposed that s-HJV is produced as a result of a furin cleavage that occurs in the endoplasmic reticulum (Silvestri et al., 2008a). Upon iron treatment the expression of s-HJV was reduced along with amount of furin protein which is consistent with increased hepcidin transcription. However under conditions of iron deficiency, where hepcidin expression is suppressed, s-HJV and furin expressions were increased suggesting that these proteins could be modulated by intrinsic iron levels. The absence of IRE's on the furin promoter ruled out the possibility of this regulation, however the identification of hypoxia responsive elements (HRE) on the furin promoter suggested that furin induced by hypoxia could release s-HJV under conditions of iron deficiency (Silvestri et al., 2008a). A more recent study however failed to show the effect of hypoxia on furin expression. Hypoxia induced by repeated phlebotomies had no effect on the expression of furin *in vivo* (Krijt et al., 2010). HJV has also been shown to interact with neogenin, an interaction which is considered to increase the susceptibility of cleavage by furin (Zhang et al., 2009a, Maxson et al., 2009).

- Cleavage by TMPRSS6 (Matriptase-2)

Matriptase-2 (MT-2) is a serine protease encoded by the gene TMPRSS6 (Velasco et al., 2002). The significance of MT-2 in iron metabolism came from studies investigating mutant MASK mice, which exhibited microcytic anaemia, low plasma iron levels and high hepcidin levels amongst other characteristics (Du et al., 2008). The results from this study suggested that a lack of a functional catalytic domain in MT-2 increased hepatic hepcidin expression and thus MT-2 was required for the suppression of hepcidin. This was supported by observations that human mutations of TMPRSS6 cause increased hepcidin expression leading to iron-refractory-iron-deficiency-anaemia (IRIDA) (Finberg et al., 2008). It was subsequently shown that MT-2 was able to bind

and cleave m-HJV and significantly reduce the hepcidin transcriptional response to BMP2 stimulation (Silvestri et al., 2008b).

The cleavage of m-HJV by furin results in a single product; conversely the cleavage of m-HJV by MT-2 results in a number of fragments. It remains to be determined if the cleavage products that result from m-HJV cleavage by MT-2 have any ability to antagonise BMP ligands. The absence of the catalytic domain within MT2 found in the MASK phenotype suggests this domain is required for cleavage of m-HJV. The regulation of MT-2 expression by iron still requires further investigation and is currently thought to occur through an autocatalytic mechanism.

Characterisation of *BMP6*$^{-/-}$ mice identified BMP6 as a potent regulator of iron metabolism (Meynard et al., 2009, Andriopoulos et al., 2009). Knockout mice of other BMP members appear to have skeletal and developmental defects; however *BMP6*$^{-/-}$ mice were viable and fertile with no apparent phenotype. However closer inspection revealed defects in iron metabolism; increased serum iron, increased tissue iron loading along with undetectable hepcidin mRNA expression (Meynard et al., 2009). Mice treated with a neutralising antibody against BMP6, had reduced liver hepcidin levels whereas mice injected with BMP6 peptide had increased hepcidin transcription (Andriopoulos et al., 2009). BMP6 expression was shown to be elevated by iron loading and reduced by iron deficiency (Kautz et al., 2008) a process which did not require HFE as demonstrated by increased BMP6 expression in *HFE*$^{-/-}$ mice by dietary iron loading (Corradini et al., 2009). Liver iron content was shown to correlate with hepatic BMP6 expression: liver iron loading induced by *HJV*$^{-/-}$ increased BMP6 mRNA expression. This effect was reduced having depleted *HJV*$^{-/-}$ mice of iron through dietary iron deficiency (Zhang et al., 2010a).

The mechanism by which iron (either liver iron stores or circulating iron) is able to regulate BMP6 expression is largely unknown. Studies which looked at the effect of increased circulating iron (by acute iron loading to increase transferrin saturation)

compared to increased tissue iron (chronic iron loading to increase liver iron content) on hepcidin regulation have highlighted the potential of hepcidin to be regulated by the BMP signalling pathway through differential mechanisms. Acute iron loading increased transferrin saturation which correlated with increased hepatic hepcidin expression without any changes in BMP6 expression. However chronic iron loading increased liver iron content (LIC) which correlated with increased hepatic BMP6 expression. Interestingly hepatic pSMAD 1,5,8 protein expression was increased in the acute iron administration setting where transferrin saturation was increased but LIC and hepatic BMP6 mRNA were not, demonstrating the activation of pSMAD 1,5,8 downstream of BMP6. In the chronic iron treatment setting, increases in LIC stimulate hepcidin expression by stimulating BMP6 mRNA expression, thereby activating the SMAD signalling pathway (Corradini et al., 2011).

In general, the regulation of signalling pathways can occur at multiple levels; intracellularly, extracellularly and at the membrane. Liver specific deletion of ALK2 and ALK3 (receptors for BMP2/4 and BMP6) caused iron loading in mice with significant reductions in hepcidin expression due to the lack of BMP signalling. Both receptors were required for the effect of BMP2 stimulation; however ALK3 appeared to be more abundantly expressed in the hepatocyte where mutations in ALK3 demonstrated a more marked iron overload. Thus ALK3 may be required for basal hepcidin expression (Steinbicker et al., 2011).

Just as important as activation of the BMP signalling pathway is, inhibition of the BMP pathway enables fine tuning of the responses elicited by the BMP ligands. The co-regulation of SMAD7, an inhibitory SMAD, through interaction with co-SMAD4 demonstrated the importance of a negative feedback loop in regulating hepcidin, expression where overexpression of SMAD7 strongly reduced hepcidin mRNA expression and prevented activation from both TGF-β and BMP ligands (Mleczko-Sanecka et al., 2010).

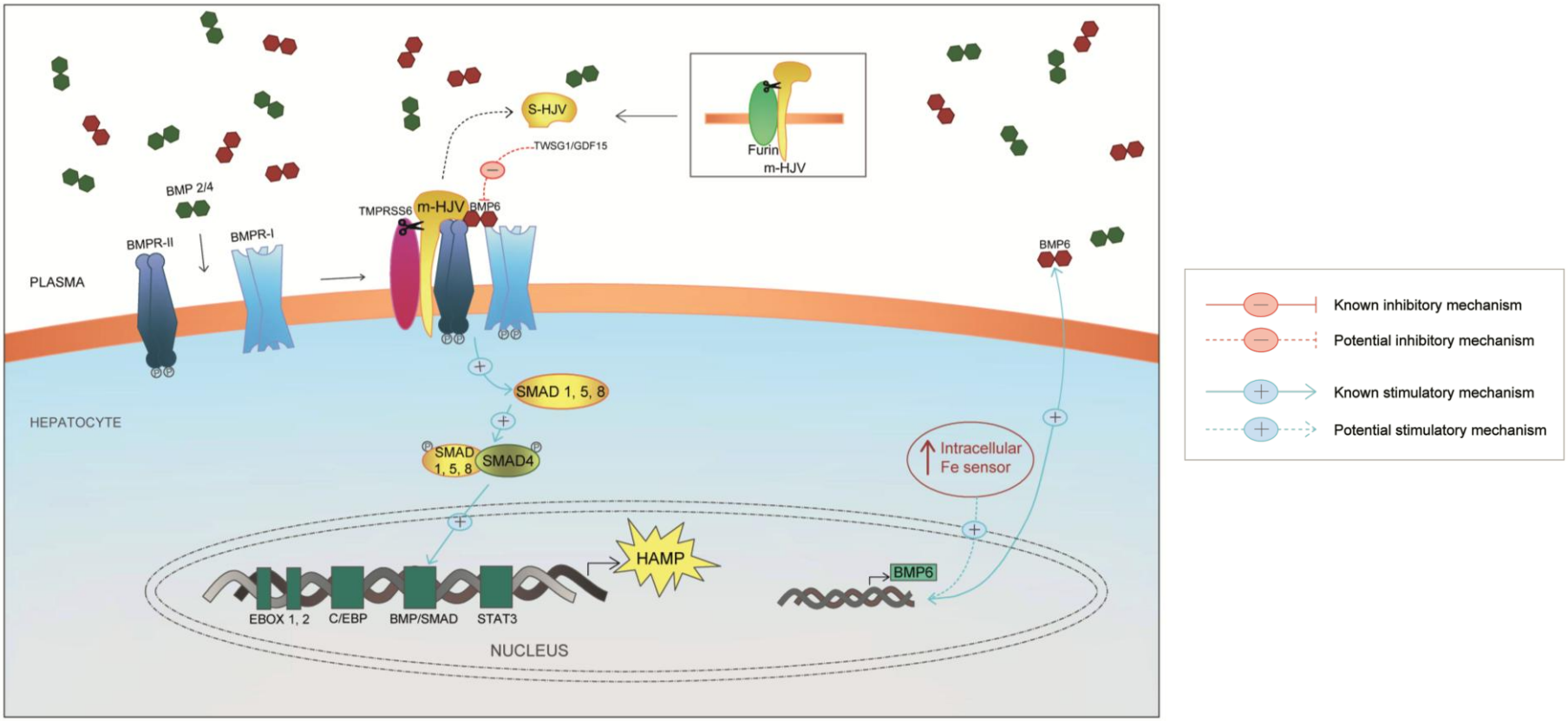

Figure 1.3 The regulation of hepcidin by the BMP pathway

1.5.3 The regulation of hepcidin by other stimuli

1.5.3.1 Iron

The regulation of hepcidin by iron has been demonstrated *in vivo* where human subjects ingesting 65mg of iron for three days increased urinary hepcidin excretion after the first day (Nemeth et al., 2004a). The mechanism by which this occurs is still under investigation. Insights into diseases where hepcidin fails to respond in the appropriate manner according to the iron burden have provided useful information into the molecular mechanisms behind the regulation of hepcidin by iron. Hereditary haemochromatosis (HH) are a group of disorders hallmarked by excessive iron loading. Various subtypes of HH have been characterised based upon the gene mutations (see Table 1.3). A common denominator between all of these disorders is the lack of an appropriate response of hepcidin to iron loading suggesting that the proteins encoding these genes are important for iron sensing and hepcidin regulation.

The HFE gene was identified by Feder and colleagues to be a MHC (major histocompatibility complex) class-I like protein in which a cysteine 282 tyrosine (C282Y) mutation prevented the binding of HFE to β_2-microglobulin (β_2-M) which in turn prevented HFE presentation on the cell surface (Feder et al., 1996). The C282Y missense mutation was present in 83% of HH patients and murine mutations of the HFE gene increased transferrin saturation and liver iron loading where hepcidin expression was decreased (Feder et al., 1996, Ahmad et al., 2002). HFE was shown to interact with TfR1 to form a stable complex thus regulating the amount of transferrin bound iron entering the cell (Feder et al., 1996). A study conducted by Schmidt et al demonstrated the nature of this interaction by carrying out mutational analysis in mouse strains which either favoured or interfered with the HFE/TfR1 complex. Interference with the HFE-TfR1 interaction increased hepcidin expression and caused iron deficiency suggesting that HFE induces hepcidin synthesis. However when HFE is complexed to TfR1, mice exhibited iron overload due to a lack of hepcidin expression (Schmidt et al., 2008). Additionally the HFE/TfR1 interaction greatly reduced the

affinity of TfR1 binding to diferric-Tf, suggesting HFE acts to repress the iron uptake by TfR1 (Lebron et al., 1999).

Mutations in TfR2 also cause HH, however unlike TfR1, the expression of TfR2 has been shown to be restricted to hepatocytes, erythroid cells lines and crypt cells (Subramaniam et al., 2002). Mutations in TfR1 cause mice to die *in utero* despite retaining a functional TfR2 gene. In contrast, *TfR2*$^{-/-}$ mice demonstrate hepatic iron loading (Levy et al., 1999). The modulation of TfR1 occurs through transcriptional and post-translational regulation by iron (see section 1.2.3). In contrast, TfR2 mRNA has no IRE's and hence the regulation of TfR2 by iron is largely unknown. Regulation has been proposed to occur through increases in protein stability where diferric-Tf increases TfR2 expression (Robb and Wessling-Resnick, 2004).

The importance of TfR2 in the regulation of hepcidin by iron was demonstrated through investigations into TfR2 knockout mice (*TfR2*$^{-/-}$). *TfR2*$^{-/-}$ mice failed to increase hepcidin expression after acute iron loading; however mice were able to respond to chronic iron loading in the correct manner (Ramos et al., 2011). The same study demonstrated a partial increase in hepcidin expression in *HFE*$^{-/-}$ mice in response to acute iron challenges suggesting a redundant role of HFE in acute iron changes. Similar to *TfR2*$^{-/-}$ mice, *HFE*$^{-/-}$ mice responded by increasing hepcidin mRNA expression in response to chronic iron loading. This was in contrast to *HJV*$^{-/-}$ and *BMP6*$^{-/-}$ mice which had impaired responses to both chronic and acute iron loading. The authors hypothesis that the pathways involved in regulating intracellular iron stores are mainly dependent on BMP6 and HJV with little contribution from HFE/TfR2 which may participate in the regulation of hepcidin by extracellular iron levels (Ramos et al., 2011) .

Recent investigations have shown attenuated BMP/SMAD signalling in *HFE*$^{-/-}$ (Corradini et al., 2009). In this mouse model, the expression of hepcidin was inappropriately low relative to the expression of BMP6. Additionally, these animals were unable to increase pSMAD 1,5,8 protein expression in response to dietary iron

loading thus implying HFE may regulate hepcidin expression through the BMP/SMAD pathway (Corradini et al., 2009). Transgenic overexpression of HFE was able to increase hepcidin expression in *HFE*$^{-/-}$ mice; an effect which was greatly attenuated in mice having lost HJV expression demonstrating the importance of both of these proteins in the regulation of hepcidin (Schmidt et al., 2010). Studies have demonstrated the ability of HJV to interact with HFE and TfR2. Co-localization of the three HH-associated proteins on the cell surface has been shown by glycerol gradient sedimentation where all three proteins co-sedimented in over-lapping fractions which were verified by immunofluorescence. The authors hypothesised the ability of both increased diferric iron levels in plasma as well as increased expression of TfR2 and/or HJV (which trigger the release of HFE from TfR1) may increase hepcidin expression (D'Alessio et al., 2012).

1.5.3.2 Hypoxia

The ability of cells to adapt to changes in oxygen tension is fundamental for their effective functioning. In order to correct for oxygen imbalances, oxygen sensitive transcription factors called hypoxia inducible factors (HIFs) have been identified which are able to regulate individual cellular responses to hypoxia (Semenza and Wang, 1992).

The HIFs are a family of transcription factors that mediate the response to hypoxia by increasing the expression of oxygen regulated genes. They are heterodimeric transcription factors consisting of a constitutively expressed HIF-β subunit which does not vary with oxygen availability and HIF-α subunits. To date, three HIF-α subunits have been identified; HIF-1α which is ubiquitously expressed, HIF-2α which is limited to certain cells such as endothelial cells, hepatocytes and enterocytes and HIF-3α where little is known about the expression and functional properties (Wenger, 2002). During hypoxia, the HIF-α subunits accumulate and translocate to the nucleus and interact with the constitutively expressed HIF-β subunit and other transcription factors, where

they are able to bind to recognition promoter sequences called hypoxia responsive elements (HRE). When oxygen is abundant, the HIF-α subunits are tightly regulated by oxygen dependent hydroxylation by specific prolyl hydroxylases (PHD) and the asparaginal hydroxylase factor inhibiting HIF (FIH). Prolyl hydroxylation enables ubiquitinylation and degradation of HIF-α by von Hippel-Lindau ligase (vHL) whereas asparaginal hydroxylation interferes with the association of transcriptional co-activators CBP and p300 and therefore with HIFα/β complex (Nakayama, 2009) (Figure 1.4).

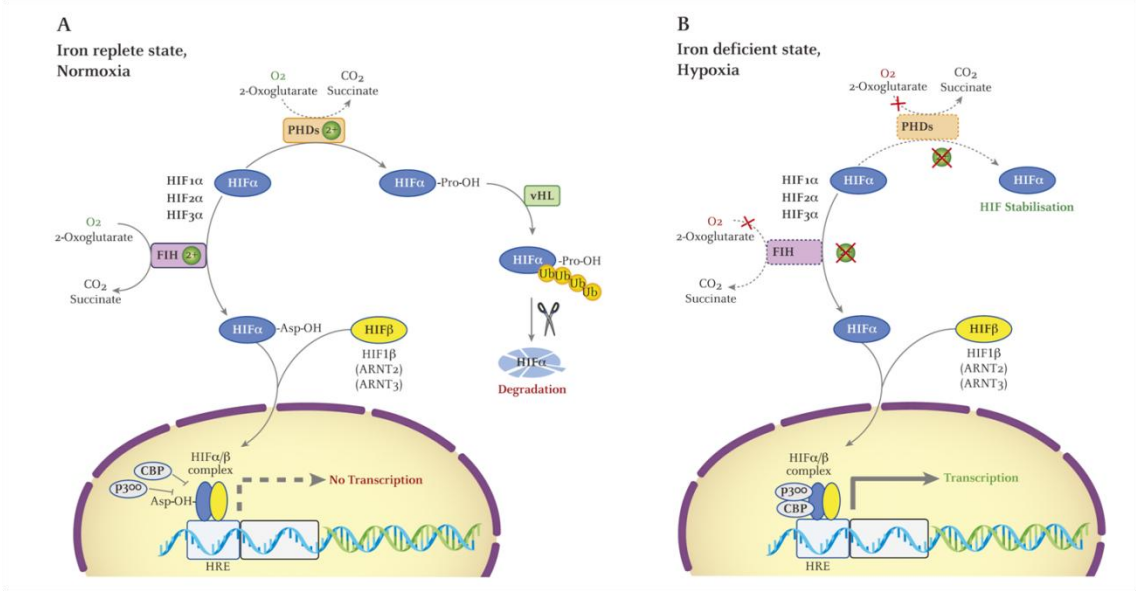

Figure 1.4 Regulation of the hypoxia inducible factors by iron and oxygen concentrations (adapted from (Evstatiev and Gasche, 2012))

Early investigations demonstrated the effect of hypoxia on iron absorption either through anaemia or changes in localised tissue hypoxia. Hypoxia increased intestinal iron absorption independently of erythropoiesis (Raja et al., 1988, Frazer et al., 2002) suggesting that the gut is able to sense hypoxia. The molecular mechanisms are still under investigation and have identified hepcidin and HIFs to play important roles in the local iron absorption which occurs during hypoxia.

The direct effect of hypoxia on hepcidin expression was shown by Nicolas and colleagues who demonstrated the negative regulation of hepcidin by hypoxia *in vivo* and *in vitro* (Nicolas et al., 2002b). This was supported by the discovery of putative HRE's located on hepcidin promoter which was shown to be occupied by HIF-1α. Treatment of the hepcidin promoter with the HIF agonist desferrioxamine (DFO), strongly reduced hepcidin promoter activity which correlated with increased HIF-1α binding, demonstrated by chromatin immunoprecipitation studies (Peyssonnaux et al., 2007). Additionally, the response of hepcidin to iron deficiency was partially blunted in liver specific HIF-1α knockout mice demonstrating the involvement of HIF-1α in the negative regulation of hepcidin (Peyssonnaux et al., 2007). Despite the strong evidence provided for the role of HIF-1α by Peyssonnaux and colleagues, other studies have proven that the effect of hypoxia is independent of HIF-1α where the binding of C/EBP and pSTAT3 to the hepcidin promoter were reduced by hypoxia (Choi et al., 2007). Co-culture of Huh7 cells with activated macrophages significantly reduced hepcidin expression upon exposure to hypoxia, an effect which was not significant on Huh7 cells alone (Chaston et al., 2011). Additionally the effects of hypoxia on co-culture studies significantly reduced SMAD4 protein expression suggesting the involvement of the BMP/SMAD pathway in the hypoxic repression of hepcidin *in vitro* (Chaston et al., 2011).

More recently the intestinal involvement of HIF-2α as a gene responsible for the increase in expression of genes involved in iron absorption (DMT1, DCYTB, FPN1) has been shown. Firstly Shah and colleagues and later Mastrogiannaki et al showed HIF-2α to be a critical regulator of intestinal iron absorption and iron metabolism generally (Shah et al., 2009, Mastrogiannaki et al., 2009). Using vHL/HIF-1α double knockout mice, Shah et al demonstrated an increased duodenal expression of DCYTB, DMT1 and FPN1 mRNAs resulting in systemic iron loading which was dependent on HIF-2 α expression. In the later paper by Mastrogiannaki the authors generated a specific intestinal *HIF-2$\alpha^{-/-}$* mouse and found decreases in duodenal DCYTB, DMT1 and FPN1 mRNA levels.

Recent studies have implicated the involvement of the BMP/HJV pathway in the regulation of hepcidin by hypoxia. The Pro- and anti- effects of HJV are thought to be dependent on the presence of membrane bound or soluble HJV where cleavage of HJV is thought to be carried out by furin whose promoter activity was increased by HIF stabilisation. Additionally, the serine protease matriptase-2 has been shown to degrade HJV, where recent studies have demonstrated the upregulation of matriptase-2 by hypoxia which was reduced upon silencing of HIF-1α or HIF-2α (Lakhal et al., 2011).

1.5.3.3 Inflammation

Hypoferraemia (low serum iron) is characteristic of anaemia of inflammation (AI) which results from reticuloendothelial sequestration of iron and interruption of intestinal iron absorption (Cartwright and Lee, 1971). The observation that inflammatory cytokines associated with AI increase hepcidin expression has established a role for hepcidin in inflammation. Evidence suggesting that hepcidin was playing a role in the dysregulation of iron homeostasis during inflammation came from investigations in mouse models of turpentine-induced inflammation, where mice demonstrated a six fold increase in hepatic hepcidin gene expression which correlated with a two-fold decrease in serum iron (Nicolas et al., 2001b). Additionally patients with AI had as much as a 100-fold increase in urinary hepcidin expression (Nemeth et al., 2003). Monocytes/ macrophages treated with LPS are able to produce cytokines which mediate either a type 1 (Il-1) or a type II (Il-6) acute phase response. Hepatocytes exposed to monocyte-induced LPS or IL-6 increased hepcidin expression, an effect which was not observed by Il-1 indicating that the induction of hepcidin was a type II acute phase response.

Mechanisms by which the inflammatory process stimulates hepcidin are still under investigation. The involvement of HFE in the hepcidin response to Il-6/inflammation has been controversial; studies which have stimulated inflammation in *HFE*$^{-/-}$ mice have either shown a HFE dependent or HFE independent mechanism (Roy et al., 2004, Lee

et al., 2004). The identification of STAT3 binding elements located on the hepcidin promoter have provided insights into the potential mechanisms that regulate the hepcidin response to inflammatory cytokines, in particular Il-6. The interaction of a complex of Il-6 receptor-α and gp130 results in the activation of Janus Kinase (JAK) which phosphorylates the Signal transducer and activators of transcription (STATs) which in turn translocate into the nucleus and bind to transcriptional target genes i.e. hepcidin (Verga Falzacappa et al., 2007, Wrighting and Andrews, 2006). STATs are a family of transcription factors involved in cytokine signal transduction during inflammation. STAT1 was unresponsive to Il-6 stimulation however STAT3 phosphorylation was increased by Il-6 (Pietrangelo et al., 2007). Additionally, the STAT3 binding motif at position -72/-64 on the hepcidin promoter was shown to be critical for basal hepcidin mRNA expression as well as hepcidin's response to the inflammatory cytokine IL-6 (Verga Falzacappa et al., 2007, Wrighting and Andrews, 2006). The observation that SMAD4$^{-/-}$mice failed to respond to Il-6 stimulation indicated that SMAD signalling may also play a role in staging the appropriate response to inflammation.

Mice deficient in Il-6 are still able to increase hepcidin expression in response to LPS suggesting that other cytokines may also be governing the response. This has been demonstrated by the effect of TNF-α on HJV expression; injection of LPS to normal mice increased hepcidin expression and decreased HJV expression (Krijt et al., 2004). These effects were independent of HFE as HJV expression remained reduced in *HFE*$^{-/-}$ mice exposed to LPS (Constante et al., 2007). The suppressive effect of LPS on HJV was shown to be independent of Il-6 and the cytokine responsible for the suppression was TNF-α. The treatment of hepatocytes with exogenous TNF-α suppressed HJV mRNA expression, an effect that was not observed on treatment with Il-6. Thus it could be hypothesised that the suppression of HJV by TNF-α would uncouple the iron-regulatory pathway and promote the Il-6 inflammatory pathway (Constante et al., 2007).

1.5.3.4 Erythropoiesis

The majority of body iron is found in the circulating erythrocytes bound to haem; therefore the production of erythrocytes and iron homeostasis are closely linked. When the erythropoietic demands of the body are increased for example under anaemic conditions, iron absorption is increased by reducing the hepcidin expression. This process occurs regardless of the iron storage abilities of the organism and is observed in iron loading anaemia's. The inhibition of hepcidin despite iron overload can be considered as an inappropriate physiological response and demonstrates the ability of the suppressive erythroid signal to over-ride the effects of a stores regulator. The effect appears to be dependent on erythropoiesis rather than anaemia or hypoxia since inhibition of erythropoiesis using carboplatin or irradiation attenuated the response (Pak et al., 2006, Vokurka et al., 2006).

The mechanism by which hepcidin suppression occurs as a result of erythropoiesis is currently an area of active research. It was hypothesised that one or more humoral factors are secreted from erythroblasts during erythropoiesis could contribute to the suppression of hepcidin. Patients suffering from β-Thalassaemia develop chronic anaemia due to defective haemoglobin production. The chronic anaemia causes tissue hypoxia which in turn stimulates erythropoiesis (Tanno et al., 2007). Frequent blood transfusions are able to correct the anaemia however this results in sever tissue iron over load which is not compensated for by increased hepcidin and in turn increases iron absorption causing secondary iron overload (Tanno et al., 2007). The expression of growth differentiating factor 15 (GDF15) and twisted gastrulation (TWSG1) were found to be significantly increased in patients and mice with β-Thalassaemia (Tanno et al., 2007, Tanno et al., 2009). Additionally both proteins were able to inhibit hepcidin production *in vitro*. One could argue that the increase in GDF15 in β-Thalassaemia patients could be due to iron loading however this was not the case as GDF15 levels were not increased in the blood of patients with primary haemochromatosis (Tanno et al., 2007). The study conducted by Tanno and colleagues utilised the serum from β-Thalassaemia patients to treat hepatocytes which reduced hepcidin expression.

Interestingly, the same effect was also observed having depleted the serum of GDF15 suggesting other molecules could be assisting with GDF15 to suppress hepcidin. Investigators hypothesised TWSG1 to be the second erythroid regulator of hepcidin which was able to inhibit hepcidin production through inhibiting the action of BMP2 and BMP4 (Tanno et al., 2009). In this context, the function of TWSG1 is of an anti-BMP factor, however earlier investigations have demonstrated TWSG1 to be a secreted protein that has a permissive role in BMP signalling. Chordin is a well defined BMP antagonist and has been shown to bind to BMP molecules through interactions of its four cysteine rich domains (Zhang et al., 2007b). Additionally, the binding of chordin to BMP's has been shown to be facilitated by TWSG1, where the formation of a ternary complex improves the antagonising ability of chordin. Thus in this context TWSG1 functions as an anti-BMP factor (Chang et al., 2001). The cleavage of chordin by the zinc metalloproteinase Xolloid generates fragments of chordin which are bound by BMP molecules. The expression of TWSG1 in this context however promotes the degradation of chordin fragments thus acting as a pro-BMP molecule (Larrain et al., 2001).

Recombinant erythropoietin (EPO) injections in mice significantly stimulated erythropoiesis and decreased serum iron status, non haem iron concentrations and hepcidin expression (Kong et al., 2008). The mechanism by which EPO suppressed hepcidin was shown to occur by preventing the binding of CCAAT/enhancer-binding protein alpha (C/EBPα) to C/EBP domains located on the hepcidin promoter. EPO significantly decreased the ability of C/EBPα to bind to the hepcidin promoter through the action of erythropoietin receptor (EPOR) (Pinto et al., 2008). Additionally an effect of EPO on hepcidin levels *in vivo* was shown through inhibition of STAT3 and SMAD phosphorylation (Huang et al., 2009). These results suggest that EPO may affect hepcidin by modulating the STAT/BMP signalling pathway, however the proteins involved need to be further investigated. Additionally, EPO alone does not appear to directly modulate hepcidin transcription. Inhibition of erythropoiesis through the cytotoxic inhibitor carboplatin, increased hepcidin expression without affecting serum

EPO levels (Pak et al., 2006). In a more recent study, the importance of the BMP signalling cascade in regulating hepcidin expression during increased erythropoiesis was demonstrated through the use of a mouse model of chronic stimulated erythropoiesis with secondary iron loading by treatment of mice with the haemolytic agent phenylhydrazine (PHZ). BMP6 levels were increased (a sign of increased stores), however hepcidin remained suppressed with reduced pSMAD 1,5,8 expression, suggesting the erythroid regulator may attenuate hepcidin expression through effects on BMP signalling (Frazer et al., 2012).

1.5.3.5 Oxidative stress

The labile iron pool (LIP) represents non ferritin bound iron that is able to react with oxygen to form reactive oxygen species (ROS). β-Thalassaemia patients have increased LIP which may contribute to increased oxidative stress in these patients (Staubli and Boelsterli, 1998, Rachmilewitz et al., 2005). Additionally, oxidative stress has been shown to suppress hepcidin expression in patients with alcoholic liver disease. Treatment of mice with 10 or 20% alcohol for seven days significantly reduced liver hepcidin expression which correlated with increased expression of duodenal iron transporters DMT1 and ferroportin. A similar trend was observed *in vitro* in HepG2 cells transfected with alcohol metabolising enzymes, providing a direct link between alcohol and hepcidin expression (Harrison-Findik et al., 2006).

The mechanism by which ethanol induces oxidative stress has been shown to involve the C/EBP proteins. Evidence of this comes from the findings that exposure of the hepcidin promoter encompassing the C/EBP responsive element to ethanol, reduced promoter activity by reducing the binding ability of C/EBPα protein (Harrison-Findik et al., 2006). A similar finding was observed in rats where the effect of chronic alcohol consumption reduced the expression of C/EBPα in the liver. More recent findings have identified the importance of the TGF-β signalling pathway in the involvement of alcohol mediate hepcidin suppression. Chronic alcohol consumption increased the

expression of the cytokine TGF-β which correlated with increased pSMAD2 protein expression. The expression of pSMAD 1,5,8 however was unchanged suggesting no involvement of the BMP pathway in this effect. Additionally, the authors report the lack of BMP receptor-1 phosphorylation despite increased BMP2 expression after alcohol consumption suggesting that the simultaneous activation of the TGF-β with the inhibition of the BMP pathway may contribute to the suppressive effects of hepcidin by alcohol *in vivo* (Gerjevic et al., 2012).

So far the effects of ethanol mediated c/EBPα suppression have been reversed by treatment with Vitamin E or antioxidant N-acetyl cysteine. Since the effects of C/EBPα can be reversed, C/EBPα activators may be therapeutically useful for iron overload prevention in HH of thalassemia syndromes (Harrison-Findik et al., 2006).

1.6 Disorders of hepcidin regulation

1.6.1 Primary disorders of hepcidin dysregulation

Primary disorders of hepcidin regulation are those which result from mutations in genes that are directly involved in the regulation of hepcidin. These can result in excess or absence of hepcidin production.

1.6.1.1 Hepcidin deficiency

Hereditary haemochromatosis (HH) are a group of inherited disorders characterised by hyper-absorption of iron from the diet leading to increased transferrin saturation which result in increased uptake non transferrin bound iron (NTBI) by the liver and other organs (Pietrangelo, 2006). The listed characteristics are associated with an inappropriately low of production of hepcidin. HH can be classified into four groups

based on the gene mutated. These are listed in Table 1.3 (adapted from (Deugnier et al., 2008)). Heritable iron overload has also been shown to occur through ablation of the genes encoding BMP6 and SMAD4 in mice, however no known human clinical equivalents have been reported (Ganz, 2011).

1.6.1.2 Hepcidin excess

Iron refectory iron deficiency anaemia (IRIDA) is a rare heritable form of iron deficiency anaemia characterised by hypochromic, microcytic anaemia, low serum iron and low transferrin saturation despite apparent marrow, spleen or hepatic iron stores (Ramsay et al., 2009). Patients with IRIDA show inappropriately high hepcidin expression which may explain why these patients are unresponsive to oral iron therapy but partially responsive to parenteral iron administration (Finberg et al., 2008). Studies have linked the IRIDA phenotype to mutations of the TMPRSS6 gene encoding the serine protease matriptase-2 (MT-2) (Finberg et al., 2008). Mutations lead to reduced MT-2 activity in hepatocytes which results in increased hepcidin synthesis, and as a result decreased plasma iron concentration leading to anaemia, suggesting that the normal function of MT-2 is to repress hepcidin expression in response to iron deficiency. At the molecular level, mutations of MT-2 lead to increased HJV expression and therefore increased BMP signalling (Ramsay et al., 2009).

1.6.2 Secondary disorders of hepcidin dysregulation

Secondary disorders of hepcidin dysregulation are those which result in iron overload or iron deficiency as a phenomenon secondary to a number of different causes.

1.6.2.1 Hepcidin deficiency in acquired disorders

Ineffective erythropoiesis is a condition which results in the premature death of red blood cells which in turn results in anaemia. Diseases associated with ineffective erythropoiesis with anaemia include the thalassaemia syndromes and dyserythropoietic anaemia's. In these diseases, severe iron overload develops as a result of blood transfusion and of greatly expanded erythropoiesis which suppresses hepatic hepcidin production and increases dietary iron absorption. Despite the iron overload, hepcidin expression remains low, highlighting the importance of the dominant effect of the erythroid regulator in the suppression of hepcidin irrespective of the iron stores (Origa et al., 2007).

It has been shown at the molecular level that the suppression of hepcidin in these conditions could be carried out by one or more mediators produced during ineffective erythropoiesis. The candidate mediators are members of the BMP family, GDF15 and TWSG1 (discussed in section 1.5.3.4). However the role of these mediators in hepcidin suppression was not demonstrated in other studies in which inhibition of erythropoiesis decreased both GDF15 and TWSG1 without affecting hepcidin expression (Bartnikas et al., 2011).

1.6.2.2 Hepcidin excess in acquired disorders

In contrast to hepcidin deficiency, hepcidin excess has been associated with the development of anaemia (anaemia of inflammation/anaemia of chronic disease) as a result of chronic infections and inflammation. Disorders resulting from these conditions are characterised by an over production of inflammatory cytokines in particular Il-6 and TNF-α (Weiss and Goodnough, 2005). Increased inflammatory cytokines, increase hepcidin expression via the STAT3 pathway which causes iron retention in macrophages and hepatocytes due to a lack of ferroportin expression and decreased erythropoiesis due to the limited availability of iron (Nicolas et al., 2001b, Nemeth et al., 2004a).

Table 1.3 the main characteristics of hereditary haemochromatosis (adapted from (Deugnier et al., 2008))

Genetic iron overload disease	Gene mutated	Chromosome	Transmission	Onset	Phenotype/ clinical features
Type 1 HH	*HFE*	6p21.3	Recessive	Late	Most common form of HH, predominantly a Cys282Tyr mutation; Increased serum ferritin, transferrin saturation, iron absorption, plasma iron
Type 2A HH Type 2B HH	*Hjv* *Hamp*	1p21 19q13.1	Recessive Recessive	Early Early	Much more severe phenotype 2A is more prevalent that 2B Increased transferrin saturation, severe parenchymal iron loading, cardiomyopathy, diabetes and hypogonadism
Type 3 HH	*TfR2*	7q22	Recessive	Late	Relatively rare with a moderate phenotype similar to *HFE* with a slowly progressive nature
Type 4 HH	*SLC40A1*	2q32	Dominant	Late	Two categories: type 4A includes the loss of function mutant which reduces cell surface localisation of ferroportin, reducing its ability to export iron leading to macrophage iron accumulation. Type 4B is less common which includes gain of function mutation, which does not alter the cell surface expression but rather abolishes the ability of hepcidin induced ferroportin internalisation causing increased iron efflux and parenchymal iron loading.

1.7 Aims and hypothesis

Hypotransferrinaemia is a rare genetic disorder characterised by severe deficiency in serum transferrin (Trenor et al., 2000). The affected patients and mouse models demonstrate chronic anaemia with parenchymal iron overload and severe hepcidin deficiency. The precise mechanism of hepcidin suppression in this mouse model remains unclear and may involve a number of signalling pathways.

The aims of the present study were to investigate four potential regulators of hepcidin (BMPER, BMP8b, VWF and ATOH8) identified in hypotransferrinaemic mice liver, with a focus on the regulation of hepcidin by the BMP/SMAD signalling pathway.

Chapter 2 .

Material and methods

2.1 Cell culture

2.1.1 Cell lines

Human hepatocellular carcinoma cells (HepG2 and Huh7 cells) and Human Embryonic Kidney cells (HEK-293 cells) were purchased from the American Type Culture Collection (ATCC) and were cultured in Dulbecco Modified Eagles Medium (DMEM) supplemented with 10% heat inactivated FBS/FCS, Penicillin G (3 mg/L), Streptomycin (5 mg/L) and L-glutamine (200 mM) (Sigma Aldrich, UK). Cells were maintained at 37ºC under 95% air and 5% CO_2. Adherent cells were harvested and/or re-seeded using trypsin/EDTA(Sigma Aldrich, UK). Briefly, cells were washed with PBS, before being treated with trypsin/EDTA for 5 minutes at 37ºC, after which the cells were resuspended in cell culture media for immediate use or freezing media. Cells were initially placed at -80ºC prior to storage in liquid nitrogen.

Cell number and viability were determined using a haemocytometer and trypan blue staining. Depending on the format of the experiment, the concentration of the cells was counted and plated at approximately 2.5 X 10^5 cells/mL. The concentration was calculated as follows:

Cells per mL = average number of cells in primary square x 10^4 x dilution factor.

2.1.2 Primary cell cultures

Primary human hepatocytes were obtained and cultured in collaboration with Dr. Ragai Mitry (King's College Hospital, UK). Human hepatocytes were isolated from donor liver segments/lobes. All tissues were consented for research in accordance with the Research Ethics Committee of King's College Hospital. Cell isolation was carried out using a modified two-step collagenase perfusion technique, and hepatocytes were

purified by low speed centrifugation at 50*g* for 5 minutes at 4ºC (Mitry et al., 2003). Cells were cryopreserved in University of Wisconsin solution containing 10% DMSO using a controlled-rate freezer and stored at -140ºC.

Before plating the primary cells, the collagen coated cell culture plates were prepared. This was carried out by washing the collagen coated wells in MEM-Eagle media and incubation at 37ºC for 20 minutes. This is carried out to neutralise the acetic acid used to make the collagen coated plates. Having washed the wells, the previously isolated hepatocytes were thawed out quickly ensuring that the cells do not reach room temperature. They were then diluted in ice cold MEM-eagle media (Sigma Aldrich, UK) in a drop-wise manner to prevent cell shock. Percoll (Sigma Aldrich, UK) density gradient centrifugation of cell suspensions was carried out to improve the viability of cells. Approximately 25% percoll was added to a final volume of 50 mL of cells. The cells were then centrifuged at 250*g* for 20 minutes at 4ºC. The pellet contained viable cells whilst any cells found floating were decanted and were considered to be dead cells. The cells were resuspended in Williams' E medium supplemented with 10mM HEPES (Cambrex, UK), 10% heat inactivated FCS, 2mM L-Glutamine (Invitrogen, UK), 0.1 μM dexamethasone, 0.1 μM insulin, penicillin (50 IU/mL) and streptomycin (50 μg/mL Sigma Aldrich, UK) on ice to maintain cell viability before being subjected to low speed centrifugation at 50*g* for 5 minutes at 4ºC. Cells were then counted using a haemocytometer as described previously and plated out. Cells were incubated at 37ºC over night before being used for experiments.

2.1.3 Recombinant peptide treatments

Recombinant peptides were purchased from R&D Systems (USA) or PeproTech (USA) and were reconstituted according to manufacturer's instructions. The concentrations of individual peptides are listed in Table 2.1.

Table 2.1 list of recombinant peptides used *in vitro* studies

Peptide name	Concentration of stock solution
Recombinant Human BMP 2 (R&D Systems, USA)	100 μg/ mL
Recombinant Human BMP 4 (R&D Systems, USA)	100 μg/ mL
Recombinant Human BMP 6 (R&D Systems, USA)	380 μg/ mL
Recombinant Human BMP 8b (R&D Systems, USA)	100 μg/ mL
Recombinant Human Crossveinless-2 (BMPER) (R&D Systems, USA)	50 μg/ mL
Recombinant Human Twisted Gastrulation Protein (TWSG1) (PeproTech, UK)	1000 μg/ mL
Recombinant Human BMP8B (Adipo Bioscience, Inc, USA)	200 μg/ mL

2.1.4 Apo- and holotransferrin treatment

Human apo- and holotransferrin were purchased from Sigma Aldrich (UK) and were reconstituted with sterile water as per manufacturer's instructions. HepG2 cells were grown in 6-well plates until 60-80% confluence was reached. The medium was replaced with serum-free DMEM and the cells were incubated for several hours prior to treatment. A working solution of 100 μM was prepared and added to the cells to give the desired final concentrations. Holotransferrin and apotransferrin were added to cells at various ratios to reach a constant total transferrin concentration of 30 μM. Cells were treated over night at 37ºC before harvesting.

2.2 Animals

2.2.1 Mouse models

All mice were maintained on standard commercial diet (Rodent Maintenance diet; RM1, Special Diet Services; UK) and were fed *ad libitum* unless indicated. Mice were sacrificed by isofluorane anaesthesia followed by neck dislocation. The central lobe of the liver was collected for further analysis. Blood samples were withdrawn by cardiac puncture and were allowed to clot before being centrifuged at 16,000*g* for 5 minutes to collect serum. All animal experiments were performed under the authority of a UK Home Office licence.

Hypotransferrinaemic (HPX, $Trf^{hpx/hpx}$) were bred on the Balb/c background strain and were maintained on Biosure diet CRM (Special Diet Services, Cambs). Homozygous HPX mice were obtained through HPX/+ * HPX/+ crosses (Simpson et al., 1991). HPX mice were maintained by weekly intraperitoneal injections of 50-250 μL mouse serum obtained from wild type/heterozygous littermates. The mice were sacrificed and tissue samples were collected at the age of 7-8 weeks or 10-11 weeks. In the case of HPX mice aged 10-11 weeks, mice were able to survive in the absence serum injections. Wild type or heterozygous littermates which were healthy and have normal iron metabolism were used as controls.

CD1 mice were purchased from Charles River (Margate, UK). All mice were maintained on the RM1 diet as described above. Animal treatments were commenced between 6-8weeks of age.

Bmper knockout heterozygous ($Bmper^{+/-}$) mouse samples were obtained through collaboration by Dr. Cam Patterson (Carolina Cardiovascular Biology Centre, University of North Carolina (Kelley et al., 2009)). Liver and serum samples from 12-

week old wild type and Bmper$^{+/-}$ mice were transported to King's College on dry ice and further analysed

Mouse models in which the *HFE* gene has been disrupted display a similar phenotype to patients who have haemochromatosis (Zhou et al., 1998). Male homozygote *HFE* knockout mice (*HFE*$^{-/-}$) of 8 weeks of age on a 129/Ola*C57BL/6 mixed background were used (Simpson et al., 2003).

The *Hepcidin1* knockout mouse model (*Hamp1*$^{-/-}$) (mixed C57BL/6*129 background strain backcrossed for at least 5 generations on C57BL/6) was obtained through collaboration with Dr. Sophie Vaulont (Institute of Cochin; Paris, France). Female *Hamp1*$^{-/-}$ mice and wild type littermates aged 5-7 weeks old were utilized.

2.2.1.1 Hypoxia

Male CD1 mice aged 8 weeks were exposed to 24 hours or 72 hours of hypoxia (0.5atm in a hypobaric chamber) after which the treated mice were immediately anaesthetised with isofluorane and samples were collected. Control mice were maintained at normoxia.

2.2.1.2 Bmper treatment

Male CD1 mice aged 6 weeks were given an intraperitoneal injection of 2 μg, 20 μg, or 50 μg of recombinant mouse BMPER peptide (R&D systems, USA) dissolved in 0.5 mL of sterile PBS. Control mice were injected with 0.5 mL sterile PBS. The mice were sacrificed after 18 hours and serum and tissues were collected for further analysis. In a similar experiment, mice of the same age and sex were in injected with 10 μg of recombinant mouse BMPER peptide. The mice were sacrificed at 2 hours or 6 hours

post-injection where serum and tissues were collected for further analysis. Control mice were injected with PBS as described above.

2.2.1.3 Phenylhydrazine treatment

Phenylhydrazine (PHZ) is a commonly used experimental procedure to induce haemolysis in animals to create a mouse model of acute haemolytic anaemia. The reaction of PHZ with ferrihaemoglobin forms ferrihaemochrome along with reactive oxidants which denature oxyhaemoglobin. As a result, PHZ treated mice have enhanced erythropoietic activity, increased iron absorption and tissue iron loading, all characteristics that mirror haemolytic anaemia (Latunde-Dada et al., 2006). Female *Hamp*$^{-/-}$ mice along with wild type littermates aged 5-7 weeks were intraperitoneally injected with 60 mg/kg body weight of neutralized phenylhydrazine or saline solution twice on consecutive days. In a separate study, male CD1 mice aged 8 weeks were treated in the same way. The mice were sacrificed and samples were collected three days after the last injection.

2.3 General molecular biology techniques

2.3.1 RNA extraction from cells and tissues

RNA was extracted using the TRIzol reagent protocol (Invitrogen, UK). Briefly, cells were washed with ice cold phosphate buffered saline (PBS) before being resuspended in 0.5 mL TRIzol reagent. Tissue samples were snap frozen by immersion into liquid nitrogen upon collection and were stored at -80ºC. Approximately 40-100 mg of mouse tissues (liver and muscle) was homogenised in 1 mL of TRIzol using a glass homogeniser. The cell and tissue lysates were incubated at room temperature for 5 minutes and phase separation was achieved by adding 200 μL of chloroform per 1 mL of TRIzol reagent and shaken vigorously for approximately 15 seconds. The samples

were centrifuged at 12,000*g* for 15 minutes at 4ºC. The top aqueous phase containing RNA was removed and further precipitated by the addition of half a volume of isopropanol. The samples were left at room temperature for 10 minutes before being centrifuged at 12,000*g* for 10 minutes at 4ºC. The isopropanol was decanted and the RNA pellet was washed in 1 mL of 75% ethanol and further centrifuged at 7,500*g* for 5 minutes. The ethanol was then removed and the pellet was air dried and resuspended in nuclease-free water. The quality of RNA was determined by running 1 µL of RNA on an agarose-formaldehyde gel and quantified using a Nanodrop spectrophotometer (ND-1000, Nanodrop Technologies, USA). The level of protein and phenol contamination was determined by the Data provided by the nanodrop where $A^{260/280}$ and $A^{260/A270}$ ratios indicated protein and phenol contamination, respectively.

2.3.2 Complementary DNA (cDNA) synthesis

Complementary DNA (cDNA) was synthesised from total RNA extracted from either cells or tissues using a Transcriptor High Fidelity cDNA Synthesis Kit (Roche Diagnostics, Germany). The RNA amount was quantified using a NanoDrop spectrophotometer and the ratio of $A^{260/280}$ was used to assess the purity of the RNA. One microgram of RNA was primed with 1 µL of anchored oligo-dT, in a final reaction volume of 12 µL which was made up with nuclease-free water. The mixture was denatured by heating at 65ºC for 10 minutes before being transferred on to ice to cool down. The mixtures were briefly spun after which the following reaction mixture was added to each sample: 4 µL of reaction buffer, 2 µL of dNTP mix (10mM each), 1 µL of 0.1M DTT, 0.5 µL of protector RNase inhibitor, 0.25 µL of transcriptor high fidelity reverse transcriptase and 0.25 µL of nuclease-free water. The reaction mix was incubated at 50ºC for 30 minutes followed by 85ºC for 5 minutes. The cDNA was stored at -20ºC for future use.

2.3.3 Semi-quantitative reverse transcription polymerase chain reaction (RT-PCR)

Semi-quantitative RT-PCR was carried out using Go-Taq polymerase (Promega, USA) using the cDNA templates obtained from section 2.3.2. Cycle numbers and template concentrations were optimized to avoid over saturation of the final PCR product. The products were resolved on either a 1% or 2% agarose/ethidium bromide gel depending on the size of the product. Messenger RNA from the gene encoding mouse beta actin (*Actb*) and human beta actin (*ACTB*) were expression controls. The band intensities were quantified using ImageJ software (NIH; USA) and normalized to beta actin expression where possible. The sequences of the utilised primers are listed in Appendix 2: Primers.

2.3.4 Real-time polymerase chain reaction (Q-PCR)

Real-time PCR was conducted using the cDNA obtained from section 2.3.2. Real-Time PCR primers were designed using the Universal Probe Library system software (Roche Diagnostics, Germany). Probes for the corresponding primers were provided by the Genomics centre, King's College London. Briefly per reaction, 0.05 μL of forward and reverse primers were mixed with 0.25 μL of the universal probe. This reaction was mixed with 12.5 μL of FastStart Universal Probe Master mix (Rox) (Roche Diagnostics, Germany). The reaction was made up to a final volume of 20 μL with nuclease free water with an additional 5 μL of diluted cDNA. Quantitative real-time PCR was carried out using ABI Prism 3700 PCR machine (Applied Biosystems, USA) and analysed using SDS software at King's College Genomics centre. Messenger RNA from the gene encoding mouse beta actin (*Actb*), human beta actin (*ACTB*), mouse Rpl19 (*Rpl19*) and human Rpl19 (*RPL19*) were used as house-keeping genes. The expression of the gene of interest was normalised to those of a house-keeping gene to obtain relative gene expression. The relative expression of the gene of interest in each group was compared to the relative expression in the control group. The relative gene expression in the treatment group was expressed as a fold change compared to the relative gene expression in control group. The method was based on that of Livak and Schmittgen (Livak and Schmittgen, 2001). The sequences of the utilised primers are listed in Appendix 2: Primers.

2.3.5 Gel electrophoresis

Depending on the estimated size of the fragment, DNA was resolved on 1% to 2% agarose gels made by using 1X TBE buffer (1M Tris, 0.9 M Boric Acid, and 0.5 M EDTA). The integrity of RNA was verified before any gene expression analysis was carried out. RNA was resolved on a 1% MOPS gel (10% 10X MOPS buffer, 8% formaldehyde in water). The RNA samples were denatured at 99ºC for 3 minutes in 6X loading dye spiked with ethidium bromide before being loaded on the gel. Samples were resolved at 100-120V (Bio-Rad power pack, USA).

2.3.6 Transformation and plasmid DNA preparation

The pGL3 vector expressing 0.9kb and 2.7kb of the human hepcidin promoter along with a mutant BMP-responsive element (BMP-RE) were a gift from Dr. Pavle Matak (Duke University Medical Center, North Carolina, USA) (Matak et al., 2009). The pcDNA 3.1-Matriptase-2 FLAG expressing vector were kindly provided by Professor Carlos Lopez-Otin (University of Oviedo, Spain) and the MASK and R774C vectors were kindly provided by Professor Clara Camaschella (University Vita-Salute San Raffaele, Italy) (Silvestri et al., 2008b). The vectors were transformed into chemically competent *E.coli* cells by heat shocking at 42ºC for 30 seconds and immediately transferred on to ice before being recovered in LB broth at 37 ºC for an hour on a shaker. The transformed bacterial cells were plated on agar-ampicillin plates and left overnight. Colonies were picked and grown up in LB broth containing ampicillin (50 µg/mL) overnight at 37ºC shaking. Plasmid DNA was purified using QIAGEN Plasmid Mini/Midi/Maxi kits as per the manufacturer's instructions (QIAGEN, Germany).

Plasmids expressing Myc-DDK-tagged ORF clones of *Homo sapiens*, Atonal homologue 8 (*Drosophila*) (ATOH8 – RC203005), Bone morphogenetic protein 8b (BMP8B –

RC215336) and von Willebrand factor C domain containing protein 2-like (VWC2L – RC212458) were purchased from OriGene Technologies (Rockville, MD) as transfection-ready DNA. The plasmids were transformed into *E.coli* cells and grown up to yield larger amounts of plasmid DNA, as described above, using Kanamycin as the antibiotic for selecting positive clones for use as transfection ready DNA. Plasmid vector maps can be found in Appendix 3: Plasmid maps.

2.3.7 Diagnostic restriction enzyme digest

A diagnostic restriction enzyme digest was carried out in order to screen for the plasmid DNA obtained in section 2.3.6. The plasmid DNA was digested with the same enzymes that were used to insert DNA fragments into the vector backbone. Briefly, 1-2 μg of plasmid DNA was incubated with 1 μL of restriction enzyme (0.5 μL each for a double digest), 1 μL of BSA and 5 μL of compatible buffer in a final reaction volume made up to 20 μL at 37ºC for 1-4 hours. The products were resolved on a 1% agarose gel. The expected size of fragments for each plasmid are listed in Table 2.2.

Table 2.2 Restriction enzymes utilised in diagnostic restriction digest of all constructs used

Plasmid	Restriction enzymes	Expected size of product(s)
Tk-Renilla	MluI , BamHI	Single digest: 4045bp Double digest: 2535bp; 1510bp
WT 0.9b/ BMP-RE1/ E-box 1,2	MluI, Xhol	Single digest: 5718bp Double digest: 4818bp; 900bp
WT 2.7/ BMP-RE2	MluI, Xhol	Single digest: 7518bp Double digest: 4818bp; 2700bp
Myc-DDK-tagged ORF clones	BamHI, NotI,	Single digest: 4900bp Double digest: 4800bp; 1,00bp
Matriptase -2/ MASK/ R774C	KpnI, Xhol	Single digest: 7924bp Double digest: 5374bp; 2550bp

pSecTag2BMPER	AscI, XhoI	Single digest: 7026bp Double digest: 5080bp, 1946bp

2.4 Protein analysis

2.4.1 Protein extraction

2.4.1.1 Total cell lysate extraction

Total cell lysates were extracted from mouse tissues by homogenisation in 500 µL of RIPA buffer (10mM TRIS, 150mM NaCl, 1mM EDTA, 1% NP-40, 0.1% SDS) and protease inhibitor cocktail (1:100 dilution, Sigma Aldrich, UK). The same extraction buffer was used to extract whole cell lysates from cells. In general, cells were washed in ice cold PBS and harvested in RIPA buffer containing protease inhibitor by scraping and incubating on ice for 5 minutes. Tissue and cell extracts were prepared using NET-TRITON (150mM NaCl, 5mM EDTA, 10mM TRIS pH 7.4 and 1% Triton X-100) as described by Zhang et al (Zhang et al., 2007a) for the immunodetection of pSMAD 1,5,8 and total SMAD 1,5,8. The homogenates were centrifuged at 1,000*g* at 4ºC for 5 minutes.

2.4.1.2 Nuclear protein extraction

Nuclear protein from cells and tissues was extracted using the NE-PER nuclear and cytoplasmic extraction kit (Thermo scientific, UK) according to the manufacturer's instructions. Briefly, cells or tissues were homogenised in buffer CERI and subjected to vortex for 15 seconds and then incubated on ice for 10 minutes after which 11 µL of buffer CERII was added. The cells were then vortex for 5 seconds and centrifuged at 16,000*g* at 4ºC for 5 minutes. The remaining supernatant (cytoplasmic extract) was transferred to a clean pre-chilled tube. The insoluble pellet (nuclei) was suspended in buffer NER, after which the samples were vortex for 15 seconds every 10 minutes for a total of 40 minutes. Nuclear extracts were obtained by centrifugation at 16,000*g* at 4ºC for 10 minutes.

2.4.1.3 Protein quantification

The resulting supernatants from total cell lysates and nuclear protein lysates were quantified using a BSA assay (Bio-Rad, USA) according to the manufacturer's protocol. Briefly, buffer A was added to reagent S in a 1:50 ratio. 5 µL of sample was added to 15 µL of nuclease free water to which 100 µL of reagent A + S mixture and 800 µL of reagent B were added and incubated for 15 minutes at room temperature. The optical densities of the samples were measured by spectrophotometry at 750nm. A protein standard curve was generated using bovine serum albumin (BSA) as a reference protein from which protein concentrations of the samples were determined.

2.4.2 Western blot analysis

50-100 µg of proteins from section 2.4.1 or 5 µl of mouse sera was separated by SDS-PAGE on either 4-15% Mini-Protean precast gel or 4-15% Criterion TGX precast gradient gel depending on the number of samples loaded and protein to be detected (Bio-Rad, USA). Beta-mercaptoethanol was added to Laemmli loading dye according to the manufacturer's instructions (Bio-Rad, USA). The loading dye was added to protein samples in a 1:1 ratio, before being separated and transferred to a PVDF membrane or nitrocellulose membrane using a trans-blot turbo transfer system (Bio-Rad, USA). The membrane was blocked with 5% milk in PBST for 1-2 hours at room temperature followed by an overnight incubation with primary antibody in blocking solution at 4ºC. This was followed by three 5 minute wash steps with PBST at room temperature after which the membranes were incubated with secondary antibody coupled with horse radish peroxidase. The membrane was washed for a second time (three 5 minutes wash steps) and immunoreactive bands were visualised with Pierce ECL western blot substrate (Thermo Scientific, USA) on Hyperfilm ECL (GE Healthcare, UK). The band intensities were quantified using ImageJ software (NIH, USA) and normalized to beta actin expression where possible. For the detection of pSMAD, 5% BSA was used as the blocking solution as opposed to 5% milk to prevent

the high background caused by phosphoproteins present in milk. The antibodies and their dilutions are listed in Table 2.3.

Table 2.3 List of antibodies used for western blot analysis

Primary antibodies	Dilution
Goat anti-mouse Crossveinless-2 (BMPER) (R&D Systems, USA)	1:1,000
Rabbit anti-Phospho-Smad1/Smad5/Smad8 (Cell Signaling technology, USA)	1:1,000
Rabbit polyclonal Smad1/5/8 (Santa Cruz Biotechnology, USA)	1:1,000
Rabbit anti- Smad1 (Cell Signaling technology, USA)	1:1,000
Rabbit anti-FLAG(TM) (Sigma Aldrich, UK)	1:1,000
Mouse anti-c-Myc (9E10) (Santa Cruz Biotechnology, USA)	1:1,000
Mouse anti-DDK (IgG2a) (OriGene Technologies, USA)	1:2,000
Rabbit anti VWF (H-300) (Santa Cruz Biotechnology, USA)	1:1,000
Rabbit anti-ATOH8 (OriGene Technologies, USA)	1:1,000
Sheep anti-BMP8b (R&D Systems, USA)	1:1,000
Rabbit anti-actin (Sigma Aldrich, UK)	1:1,000
Secondary Antibodies	
Polyclonal Rabbit anti-Goat Immunoglobulin/HRP (Dako Cytomation, Denmark)	1:5,000

Polyclonal Goat anti-Rabbit Immunoglobulin/HRP (Dako Cytomation, Denmark)	1:2,000
Polyclonal Goat anti-Mouse Immunoglobulin/HRP (Dako Cytomation, Denmark)	1:2,000
Goat anti-Mouse Immunoglobulin/HRP (OriGene Technologies, USA)	1:5,000
Polyclonal Donkey anti-sheep Immunoglobulin/HRP (R&D Systems, USA)	1:2,000

2.4.3 Immunostaining

Tissue sections were collected and immediately submerged in OCT embedding matrix (Thermo Scientific, USA) and stored at -80ºC. Cryostat sections were cut to approximately 5 μM thickness and mounted on poly-lysine coated slides (Sigma Aldrich, UK). All samples were stored -80ºC. Prior to staining, slides were air dried for 30 minutes to 1 hour after which the slides were fixed in pre chilled acetone for 10 minutes at 4ºC. The acetone was allowed to evaporate after which the sections were blocked with 1% BSA in PBS for 1 hour at room temperature in a humid chamber. Blocking buffer was removed and the sections were covered with primary antibody diluted 1:100 in blocking buffer for 1 hour at room temperature in a humid chamber. The slides were washed three times in a stream of PBS and then incubated with FITC-conjugated secondary antibody (Dako Cytomation, Denmark) diluted 1:100 in PBS for 45 minutes. After incubation, the slides were washed with PBS as before, and counter-stained with VECTASHIELD Mounting Medium with Propidium Iodide (Oxford instruments, UK). Images were captured on DM IRE2 Confocal microscope (Leica; Wetzlar, Germany). The antibodies and their dilutions are listed in Table 2.4

Table 2.4 List of antibodies used for immunostaining

Primary antibodies	Dilution
Goat anti-mouse Crossveinless-2 (BMPER)	1:100

(R&D Systems, USA)	
Rabbit anti-ATOH8	1:100
(OriGene Technologies, USA)	
Secondary Antibodies	
Polyclonal Rabbit anti-Goat Immunoglobulin/FITC	1:200
(Dako Cytomation, Denmark)	
Polyclonal Goat anti-Rabbit Immunoglobulin/FITC	1:200
(Dako Cytomation, Denmark)	

2.5 Reporter gene assay

A 'dual' luciferase reporter assay system was utilised for measuring luminescence in a Glo-max luminometer (Promega, USA). This approach utilises the expression and detection of two reporter enzymes, firefly (*Photinus pyralis*) and renilla (*Renilla reniformis*) simultaneously. Both enzymes have distinct evolutionary origins and therefore share no similarities in terms of structure and substrate requirements. They can therefore be used in the same system, where the luminescence from the experimental vector which expresses firefly can be quenched whilst activating the luminescence of the internal control which expresses renilla. In addition, neither enzyme requires any post translational processing and can therefore be detected as soon as they are translated.

2.5.1 Cell transfection

Plasmid DNA was transiently transfected into either HepG2 cells, Huh7 cells or HEK-293 cells using FuGENE 6 or x-tremeGENE 9 DNA transfection reagent (Roche, Germany) according to manufacturer's protocol. In brief, cells were seeded and grown to 50-70% confluence overnight in complete DMEM. The final amount of DNA, transfection reagent and media was dependent on the experiment. In general, the

transfection reagent was added to serum-free DMEM and the mixture was incubated for 5 minutes after which plasmid DNA was added. The hepcidin promoter and renilla were added in a 1:50 ratio. After a minimum of 15 minute incubation of the transfection reagent and plasmid DNA, the mixture was aliquoted out into each individual well in a drop-wise manner. The cells were left in the cell culture incubator for 6-8 hours after which over-night treatments of recombinant peptides, where appropriate, were commenced.

2.5.2 Luminescence measurement

Luciferase activity was assayed according to manufacturer's protocol (GloMax Luminometer, Promega, USA). All reactions were carried out at room temperature in order to maintain efficient enzyme activity. Briefly, cells were washed in PBS before being lysed with 1X passive lysis buffer (PLB) for 15 minutes on a shaker. The volume of PLB used was dependent on the plate format. 20 μL of cell lysate was mixed with 100 μL of luciferase buffer after which the firefly signal from the experimental vector was read. This was followed by the addition of Stop and Glo buffer, which consists of a firefly signal quencher and renilla substrate. A second reading was taken from the internal control renilla. The ratio of firefly/renilla was calculated allowing normalisation of the signal from the experimental vector (firefly) to the internal control (renilla) and thus minimising experimental variability caused by transfection efficiencies or cell viability.

2.6 Measurement of iron parameters

2.6.1 Haemoglobin measurement

Haemoglobin was determined using the methods described by Beutler (Beutler, 1971). Briefly, 5 μL of blood was added to 1 mL of Drabkin's solution (2 mM sodium cyanide

and 1 mM potassium ferricyanide, Sigma Aldrich, UK). This converted the haemoglobin into cyanmethaemoglobin, a stable complex which can be read spectrophotometrically at 540nm, where 1 mL of Drabkin's solution was used as a blank measurement. The concentrations of haemoglobin were quantified using the following equation:

Haemoglobin = (A540 x reaction volume)/(sample volume x extinction coefficient)

= (A540 x 1.005)/(5 x 5.6) g/dL

Where A540 represents the absorbance of the samples at 540nm.

2.6.2 Serum iron measurement

Serum iron was measured using the Bio-Assay Systems kit (Hayward, USA) according to manufacturer's instructions. In brief, 100 µl of working reagent containing reagent A, B and C in a 20:1:1 ratio was added to 25 µl samples and iron standards. The intensity of the colour was measured at 590nm. Serum iron was calculated from the following formula:

Serum iron (µg/dL) = (Absorbance unknown – Absorbance blank) / slope

Where 1mg/dL iron equals 179µM.

2.6.3 Tissue non haem iron measurement

The weight of each individual tissue sample was recorded before being homogenised in 500µl of HEPES saline (pH 7.4) with a glass homogeniser. 100 µl of tissue homogenate was added to 200 µl of 25% trichloroacetic acid and 2M sodium pyrophosphate. The mixtures were then boiled for 10 minutes and centrifuged at 10,000*g* for 5 minutes after which the supernatant was collected and the sediment was resuspended in 100 µl of TCA/sodium pyrophosphate. The samples were again boiled for 10 minutes and centrifuged at 10,000*g* for 5 minutes. The sediment was

resuspended in TCA/sodium pyrophosphate for the final time and the process of boiling and centrifugation was repeated. Non haem iron measurements were carried out by mixing 200 µl from the total supernatant with 100 µl of 0.23 M ascorbate, 80 µl of 10 mM ferrozine and 420 µl of 2 M sodium acetate pH 4.78. Samples were measured spectrophotometrically at 562nm. 1 µl of 10 mM $FeCl_3$ in 10 mM HCL was added to 199 µl of TCA/sodium pyrophosphate to obtain a standard and was mixed with ascorbic acid, ferrozine and sodium acetate as for the samples. The following calculation was used to calculate tissue nonhaem iron concentration:

$$\text{Non haem iron concentration} = (A_{562}\ \text{unknown} \times 125)/(A_{562}\ \text{standard} \times \text{wet weight})$$

Where Non haem iron concentration = nmol/mg wet weight; A_{562} unknown and A_{562} standard represent the absorbance of unknown samples and the standard at 562 nm, respectively (Simpson and Peters, 1990).

2.7 Statistical analysis

Data are presented as mean ± standard deviation (SD). The comparisons of multiple groups for significant effects were conducted by 1-way analysis of variance (1-way ANOVA) with Tukey post-hoc test. 2-way analysis of variance (2-way ANOVA) was used to test significant differences between two or more groups and their interactions with Bonferroni post-hoc test. Unpaired Student *t*-test was used for simple comparison between control and treatment groups. A p value less than 0.05 was considered significant. Data analysis was performed using SPSS (IBM, USA).

Chapter 3 .

BMPER is a negative regulator of hepcidin

3.1 Introduction

A growing body of evidence has outlined the importance of the BMP signalling pathway during vascular development. Gain- and loss- of functions studies have identified BMP2 and BMP4 to be important pro-angiogenic factors. Treatment of bone explants with BMP2 and BMP4 increased the production of vascular endothelial growth factor A (VEGFA), a protein that induces angiogenesis (Deckers et al., 2002). Treatment of human umbilical vein endothelial cells (HUVEC) with increasing concentrations of BMP4 and BMP2 increased capillary sprouting (Zhou et al., 2007, Finkenzeller et al., 2012). Failure to co-ordinate the expression of these proteins *in vivo* can lead to increased angiogenesis which can promote tumour growth and development. Investigations into antagonising the effects of BMPs during increased vascular development identified Bone morphogenetic protein (BMP) binding endothelial precursor derived regulator (BMPER) to play a pivotal role in fine-tuning BMP activity during angiogenesis.

The formation and patterning of veins is a well defined process in *Drosophila* wing development. The BMP signalling pathway plays a pivotal role in the maintenance of cross veins during the later stages of wing development (Conley et al., 2000). By investigating a Drosophila mutant ''crossveinless'' where the mutant fly lacked small cross vein between the wing capillaries, a group identified the causative gene naming it Crossveinless-2 (Cv-2) (Conley et al., 2000). The orthologous mouse protein named Bone morphogenetic protein (BMP) binding endothelial precursor derived regulator (BMPER) was identified from a screen of differentially expressed transcripts during early endothelial cell development (Moser et al., 2003). Altered BMPER expression in zebrafish as in fly adversely affected the development of blood vessels, (Moser et al., 2007).

BMPER is a secreted protein that contains five cysteine-rich von Willebrand type-C like domains (CR-domains) at the N-terminus followed by a von Willebrand factor type D located at the C-terminus. The presence of CR domains are characteristic of many BMP binding proteins such as chordin (Zhang et al., 2007b). Although both drosophila and mouse proteins are structurally similar, the presence of a trypsin domain in mouse BMPER may confer differences in the function compared to its drosophila homologue.

The mRNA expression of BMPER was highest in the heart, lung, skin and brain; tissues which are of endothelial lineage as judged by FLK-1 (fetal liver kinase-1) positive expression, thus further emphasising the importance of the role of this protein in endothelial cell development (Moser et al., 2003). Additionally, the expression of BMPER was also found in regions which were important for angiogenesis in the developing embryo; the yolk sac where BMP2, BMP4 and BMP6 are expressed, and the AGM (aorto-gonadal-mesonepheric) region where increased expression of BMP4 was observed (Moser et al., 2003, Farrington et al., 1997, Marshall et al., 2000).

The ability of BMPER to influence BMP signalling is closely linked to its ability to bind BMP2, BMP4 and BMP6 (Moser et al., 2003). Studies conducted in *Drosophila* wing suggest a pro-BMP effect where mutations in the CV-2 gene reduced BMP signalling and cross-vein formation (Conley et al., 2000, Coffinier et al., 2002, Rentzsch et al., 2006). However, studies conducted in mouse suggest an anti-BMP effect (Binnerts et al., 2004, Moser et al., 2003). The biphasic nature of BMPER function has been suggested to occur via two potential mechanisms:

(a) Firstly, several studies have demonstrated a concentration dependent effect of BMPER on BMP signalling, where the ratio of BMPs to BMPER determine the function of BMPER. This was demonstrated in functional assays using endothelial cell sprouting and migration of HUVEC cells; low concentrations of BMPER demonstrated faster migration which was prevented at higher concentrations. In addition to the concentrations of

BMP present, the type of BMP present may also determine the nature of BMPER's actions. For example, BMPER inhibits DPP signalling (BMP2 and BMP4) without promoting the effects of BMP signalling at any given concentrations. In contrast the effects of BMPER on Gbb signalling demonstrated biphasic properties (Serpe et al., 2008).

(b) Secondly, the protein exists in two forms, a full-length membrane bound associated form and a soluble form consisting of a heterodimer of C- and N-terminal cleavage fragments connected by disulphide bonds (Rentzsch et al., 2006). The cleavage of the protein at a conserved acid sensitive autocatalytic cleavage site (FGDPH) through an undefined protease has been suggested to account for the ability of the protein to act as a pro- or anti- BMP modulator *in vivo* (Rentzsch et al., 2006); and hence may function in a manner similar to m-HJV and s-HJV where one is pro-BMP and the other an anti-BMP.

In agreement with the former mechanism, the ratio of BMPER to BMP4 was shown to modify the cellular responses to BMP signalling where BMPER was shown to bind to BMP4 with a 2:1 molar stoichiometry; a low ratio of BMPER:BMP4 increased signalling and excess BMPER:BMP4 inhibited signalling through a trap and sink mechanism (Kelley et al., 2009). Based on this, the N-terminus of BMPER which is rich in CR domains, was shown to bind to BMP4 which prevented SMAD interaction and the C-terminus of BMPER was required to sink the BMP4 further into the cell to ensure efficient lysosomal degradation (Kelley et al., 2009).

The pro-angiogenic ability of BMP4 was shown to be dependent on the expression of BMPER where both proteins were required to stimulate endothelial cell production *in vitro* (Heinke et al., 2008). However later studies demonstrated that the expression of BMPER was negatively regulated in response to hypoxia, a pro-angiogenic stimulus, both *in vivo* and *in vitro* and these effects were independent of BMP4 expression. Since BMPER null mice do not survive beyond birth (Ikeya et al., 2006, Kelley et al., 2009) the

authors utilised heterozygote mice which displayed increased revascularisation in the retina along with increased BMP signalling compared to wild type controls upon exposure to hypoxia, demonstrating that the ratio of BMPER to BMP is critical in determining the *in vivo* angiogenic response to a physiological stimulus (Moreno-Miralles et al., 2011).

A plethora of factors have been shown to participate in the regulation of hepcidin. The studies in this chapter were conducted in order to elucidate the function of BMPER, a known BMP antagonist, in the regulation of hepcidin. The expression of BMPER and other iron related genes were investigated in various mouse models of altered iron metabolism along with the effects of BMPER on the hepcidin transcriptional response to BMP signalling.

3.2 BMPER expression in Hypotransferrinaemic mice (HPX)

To identify factors which could potentially regulate or suppress liver hepcidin expression, microarray analysis was conducted on HPX livers and WT/Het liver. *Bmper* mRNA was found to be significantly upregulated in HPX mouse liver (McKie unpublished data). These results were confirmed by real-time PCR (Figure 3.1) and western blot/ immunostaining analysis on the liver and serum of HPX mice (Figure 3.2 and Figure 3.3). Hepcidin mRNA transcripts were also measured to confirm hepcidin mRNA suppression compared to WT/Het.

In order to explore the mechanisms of hepcidin suppression in the HPX mouse model, the mRNA expression of other known BMP antagonists (*Noggin*, *Chordin*, *Twsg1*, *Hjv*) as well as other hepcidin inhibitors such as *Gdf15* were also measured by real-time PCR in HPX mouse liver (Figure 3.4A). There were no significant changes in any of the BMP antagonists listed with the exception of *Gdf15* where hepatic levels were significantly increased.

Hepcidin antagonists such as soluble HJV (s-HJV) have been reported to be highly expressed in other tissues as well as the liver (Papanikolaou et al., 2004, Rodriguez Martinez et al., 2004); therefore the suppression of hepcidin could be generated from more than one tissue. The levels of *Hjv*, *Noggin* and *Chordin* were also measured in the skeletal muscle of HPX mice and controls. No significant changes were observed (Figure 3.4B and Figure 3.4C).

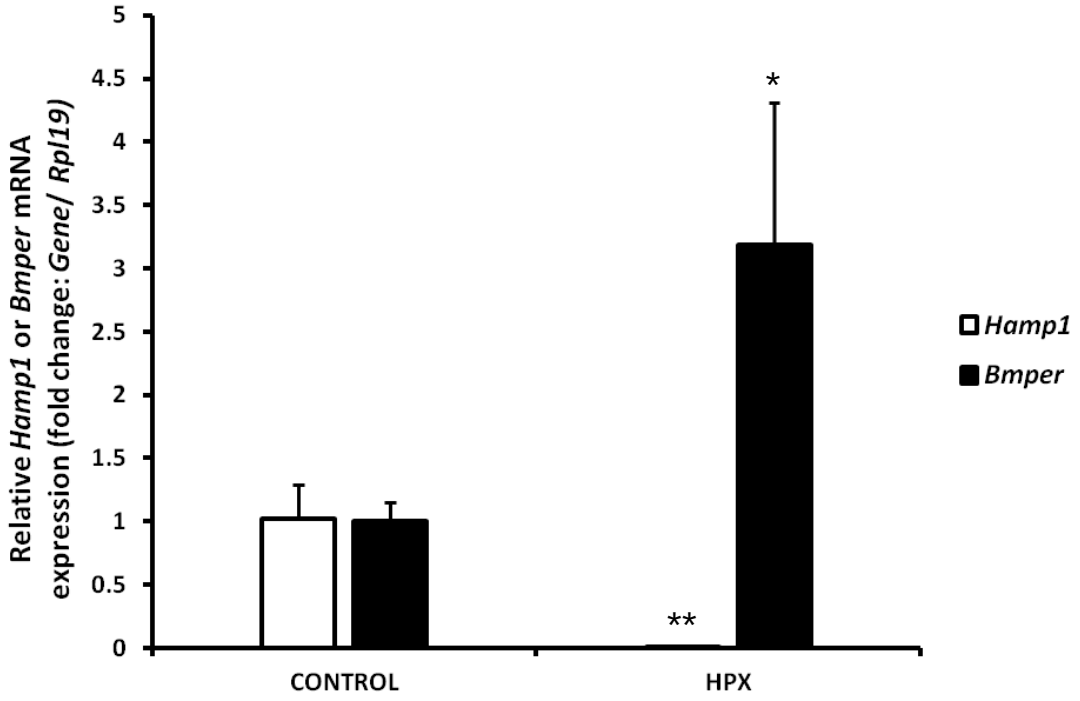

Figure 3.1 Real-time PCR measurement of hepatic *Bmper* and *Hamp1* mRNA levels in HPX mouse liver

Liver *Hamp1* and *Bmper* mRNA expression were measured in 10-11 week old male HPX mice (n=3). Wild type and heterozygous mice were used as controls. Relative mRNA expression was normalised against the house keeping gene *Rpl19*. Data are presented as mean ± SD for fold change as compared with wt/het mice (n=3 per group). The samples were measured in triplicate. Statistical analysis was performed by Student *t*-test. *p<0.05; **p<0.01 for CONTROL vs. HPX comparisons.

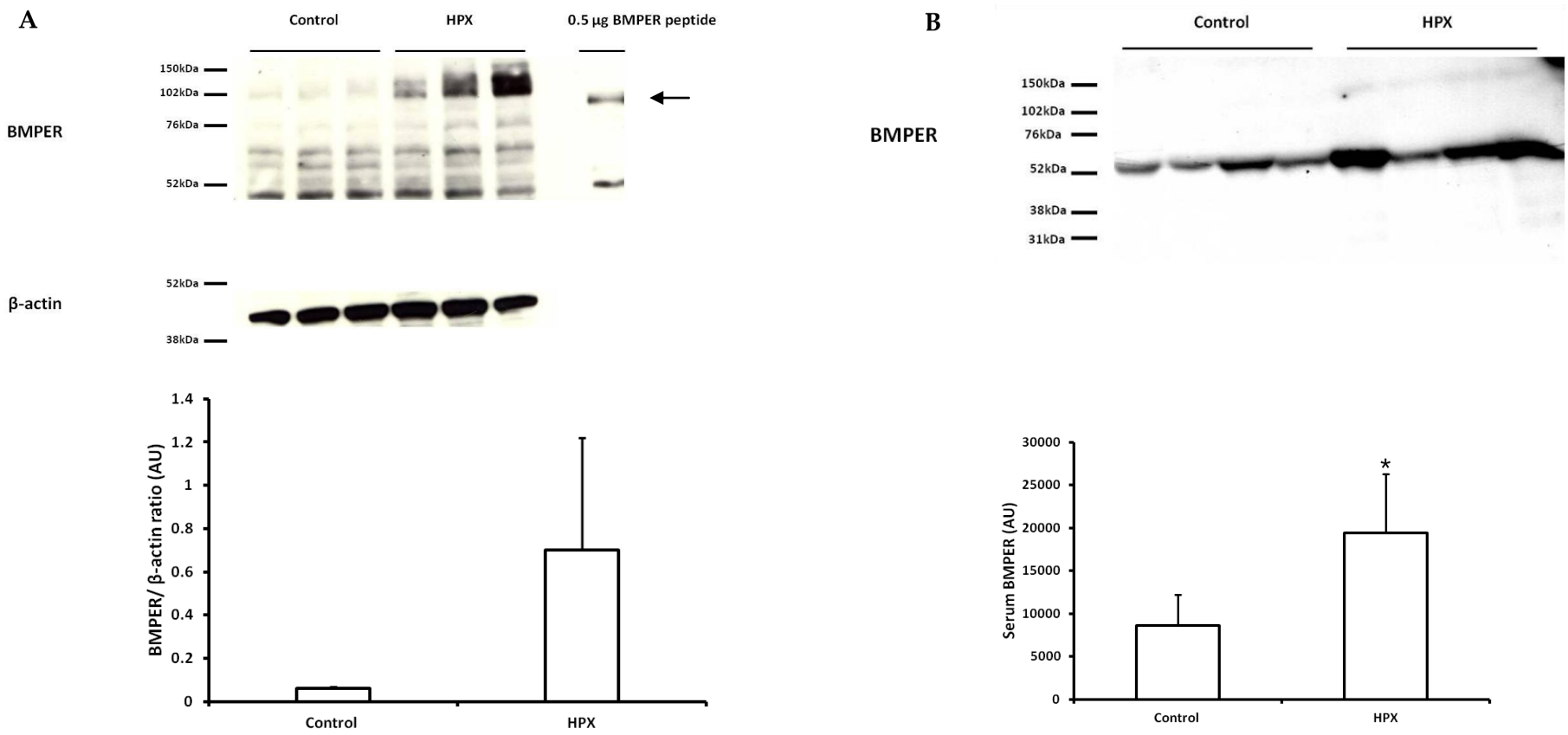

Figure 3.2 Western blot analysis of liver and serum BMPER protein expression in HPX mouse liver

Western blot analysis of (A) liver and (B) serum of 10-11 week old male HPX mice (n=3). Wild type/heterozygous mice were used as controls. (A) BMPER expression was normalised to the expression of β-actin and presented in arbitrary units (AU). The expression of BMPER was verified by loading 0.5 µg of recombinant BMPER peptide which may have separated faster due the absence of other endogenous proteins which may have affected the separation of liver BMPER. Densitometry is displayed below the blot. Data are presented as mean ± SD for three biological replicates. Statistical analysis was performed by Student *t*-test. *$p<0.05$ for CONTROL vs. HPX comparisons.

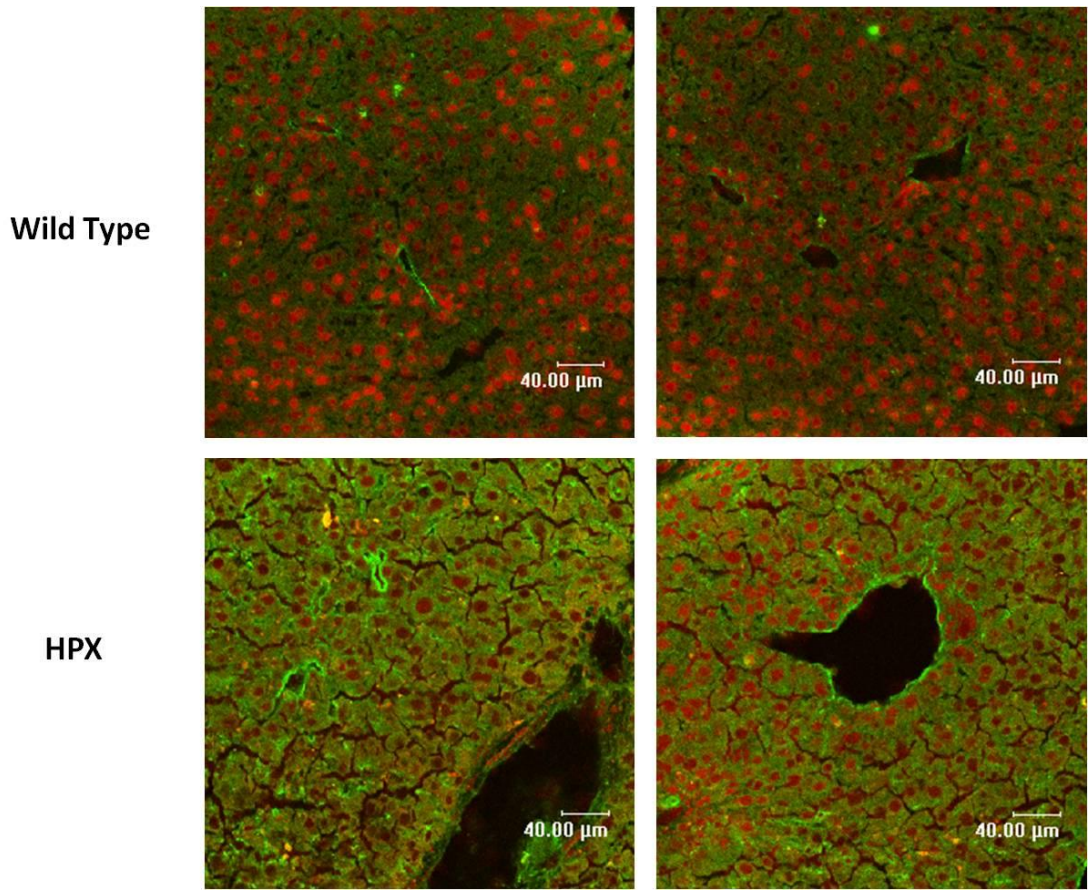

Figure 3.3 Immunofluorescence of liver BMPER expression in HPX mice

The expression of BMPER from frozen liver sections of 10-11 week old male HPX mice was demonstrated though immunofluorescence technique. BMPER protein was visualised as green fluorescence and nuclei were counterstained in red (Leica DM-IRE2 confocal microscope, magnification x630).

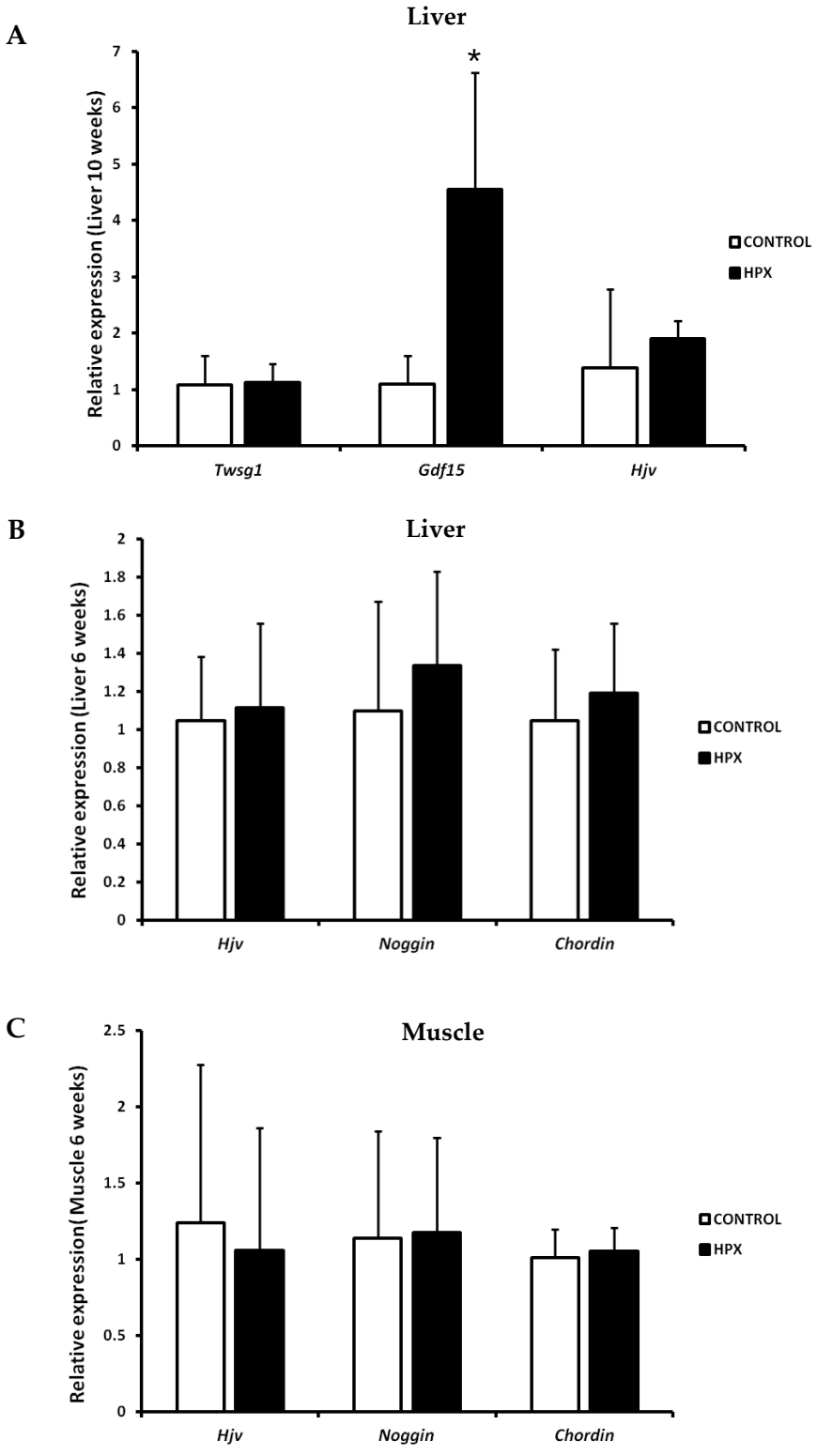

Figure 3.4 Expression levels of other potential hepcidin modifiers in HPX mouse liver and muscle

The mRNA expression of potential hepcidin modifiers were measured in the liver (A) (B) and muscle (C) of HPX mice. WT/Het mice were used as control. Relative mRNA expression was normalised against the house keeping gene *Rpl19*. Data are presented as mean ± SD for fold change as compared with Wt/Het mice (n=3 per group). The samples were measured in triplicate. Statistical analysis was performed by Student *t*-test. *p<0.05 for CONTROL vs. HPX comparisons.

3.3 Effects of recombinant BMPER peptide on hepcidin transcription

Identification of the BMP-responsive elements (BMP-RE 1/2/3) present within the hepcidin promoter has provided a direct link between the BMP signalling pathway and hepcidin expression. BMP-RE1 at position -84/-79 and BMP-RE2 at position -2,255/-2,250 of the human hepcidin promoter function together to regulate basal hepcidin mRNA expression under control conditions (Casanovas et al., 2009). There is also the third BMP-RE however, unlike BMP-RE1/2, it is not full conserved between species and is not required for BMP signalling.

pGL3 vectors expressing 0.9kb and 2.7kb of the human hepcidin promoter encompassing the BMP-REs were utilised together with controls in which the BMP-REs were mutated. The expression vectors were transiently transfected into to the HepG2 and Huh7 cell lines which were treated with recombinant BMP peptides (BMP2/4/6) in the absence and presence of various concentrations of BMPER peptide. Western blot analysis of phosphorylated SMAD 1,5,8 (pSMAD 1,5,8) was carried out in order to investigate the effects on the SMAD signalling.

As shown in Figure 3.5 and Figure 3.6, BMPER peptide strongly inhibited BMP2-dependent hepcidin promoter activity in both HepG2 cells and Huh7 cells. pSMAD 1,5,8 protein expression was increased by BMP2 treatment and this induction was suppressed in the presence of BMPER in both cell lines (Figure 3.7 and Figure 3.8). The effects of BMPER on BMP6-dependent hepcidin promoter were also investigated. Similar to BMP2, addition of increasing amounts of BMPER resulted in a significant inhibition of BMP6 induced hepcidin promoter activity (Figure 3.9 and Figure 3.10).

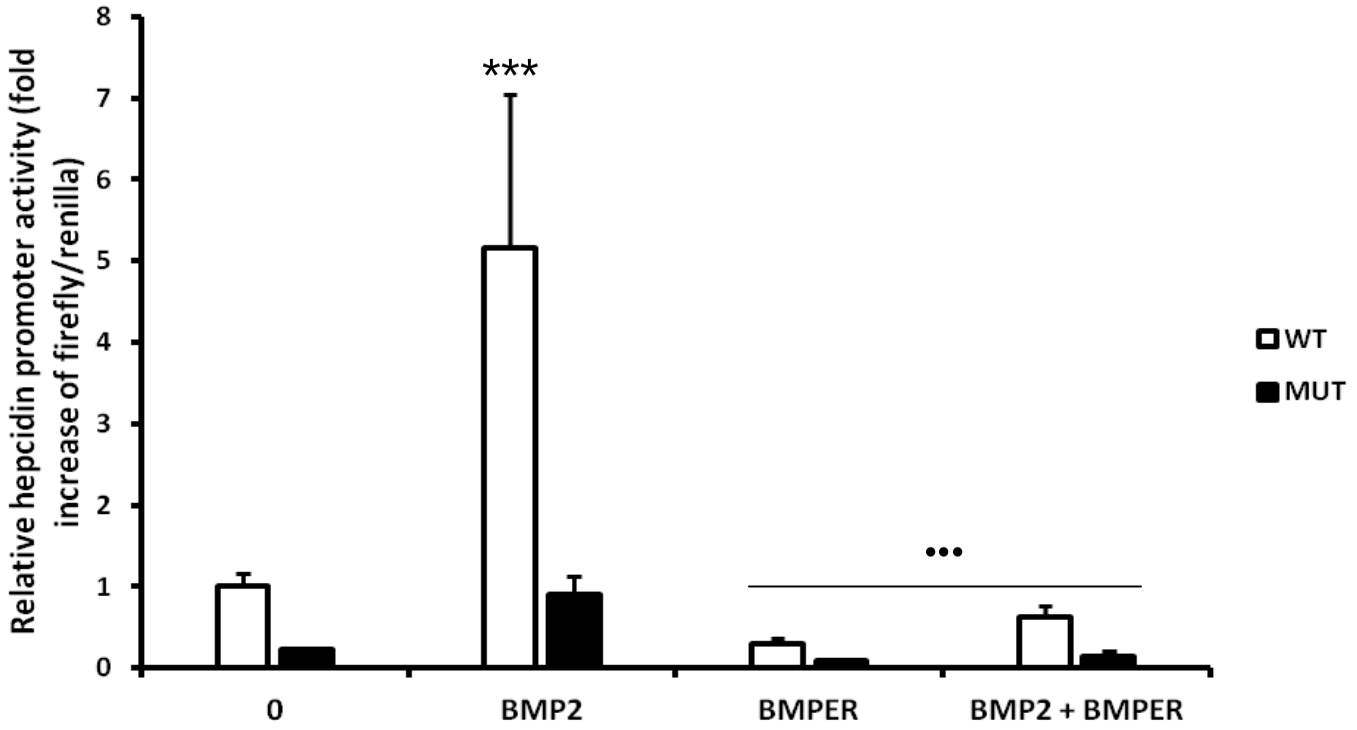

Figure 3.5 Effects of recombinant BMPER peptide on BMP2 dependent hepcidin promoter activity in HepG2 cells

HepG2 cells transiently transfected with wild-type 2.7 kb (WT) or BMP-RE2 mutant (MUT) hepcidin constructs for 6-8 hours were treated with 25ng/mL BMP2 and 2500ng/mL BMPER or a combination of both. Data are presented as mean ± SD derived from a single experiment with three biological replicates. The experiment shown is representative of 3 similar experiments. Statistical analysis was performed by 1-way ANOVA with Tukey's post hoc test. ***$p<0.001$ for –BMP2 vs. treatment comparisons; •••$p<0.001$ for +BMP2 vs. treatment comparisons.

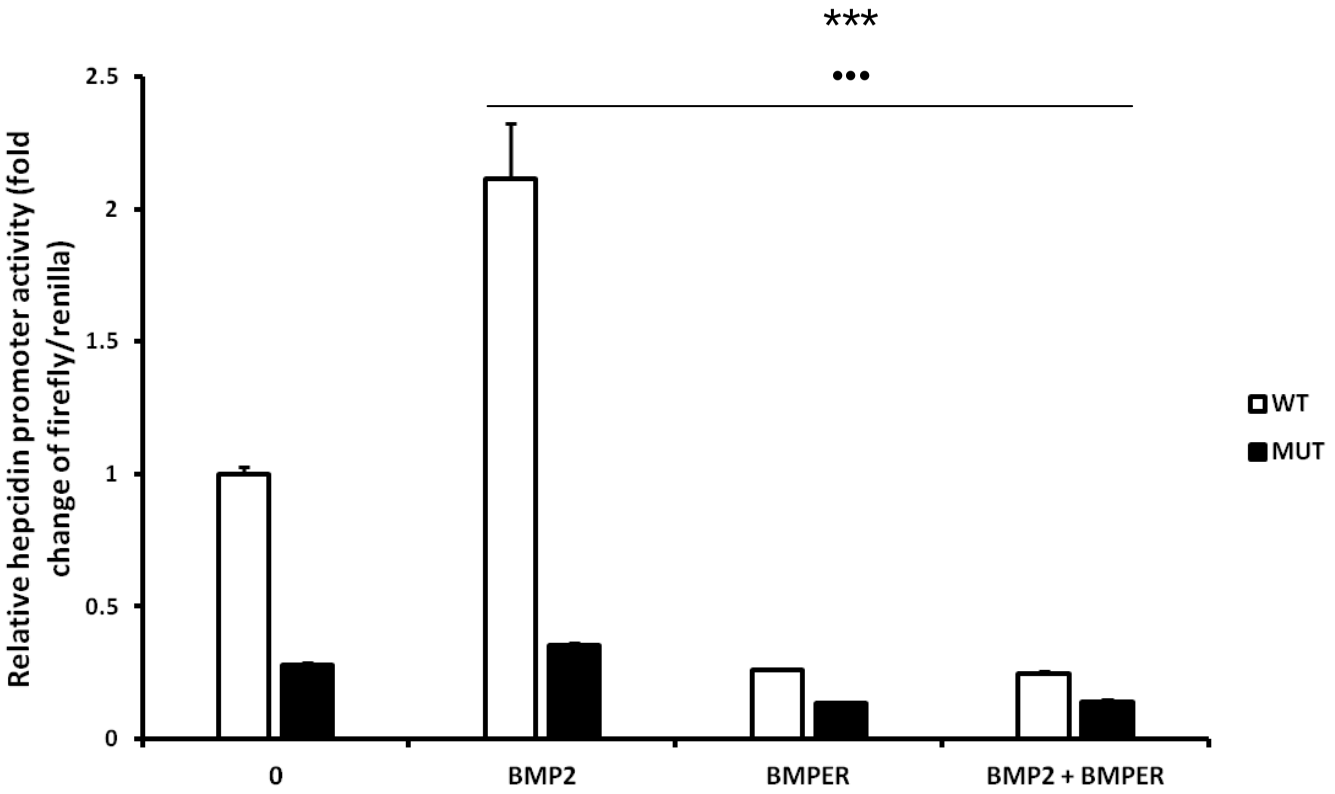

Figure 3.6 Effects of recombinant BMPER peptide on hepcidin promoter activity in Huh7 cells

Huh7 cells transiently transfected with 2.7 kb wild type (WT) or BMP-RE2 mutant (MUT) hepcidin construct for 6-8 hours were treated with 25ng/mL BMP2 and 2500ng/mL BMPER or a combination of both. Data are presented as mean ± SD derived from a single experiment with three biological replicates. The experiment shown is representative of 3 similar experiments. Statistical analysis was performed by 1-way ANOVA with Tukey's post hoc test. ***$p<0.001$ for –BMP2 vs. treatment comparisons; •••$p<0.001$ for +BMP2 vs. treatment comparisons.

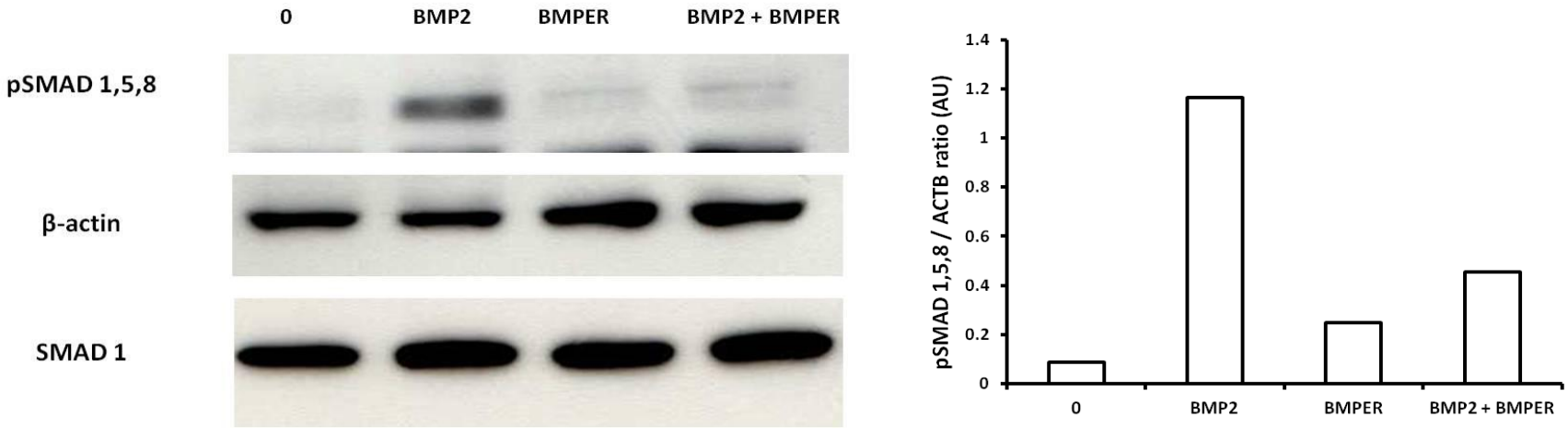

Figure 3.7 Effects of recombinant BMPER peptide on pSMAD 1,5,8 protein expression in HepG2 cells

Western blot analysis showing pSMAD 1,5,8 expression in HepG2 cells treated with 25ng/mL BMP2 and 2500ng/mL BMPER or a combination of both. pSMAD expression was normalised to the expression of SMAD1 and presented in arbitrary unit (AU). Densitometry is displayed next to the blot. Data are presented as mean ± SD derived from a single experiment with three biological replicates. The experiment shown is representative of 3 similar experiments. Statistical analysis was performed by 1-way ANOVA with Tukey's post hoc test. *$p<0.05$ for -BMP vs. BMP2+BMPER comparison; •••$p<0.001$ for +BMP2 vs. BMP2+BMPER comparison.

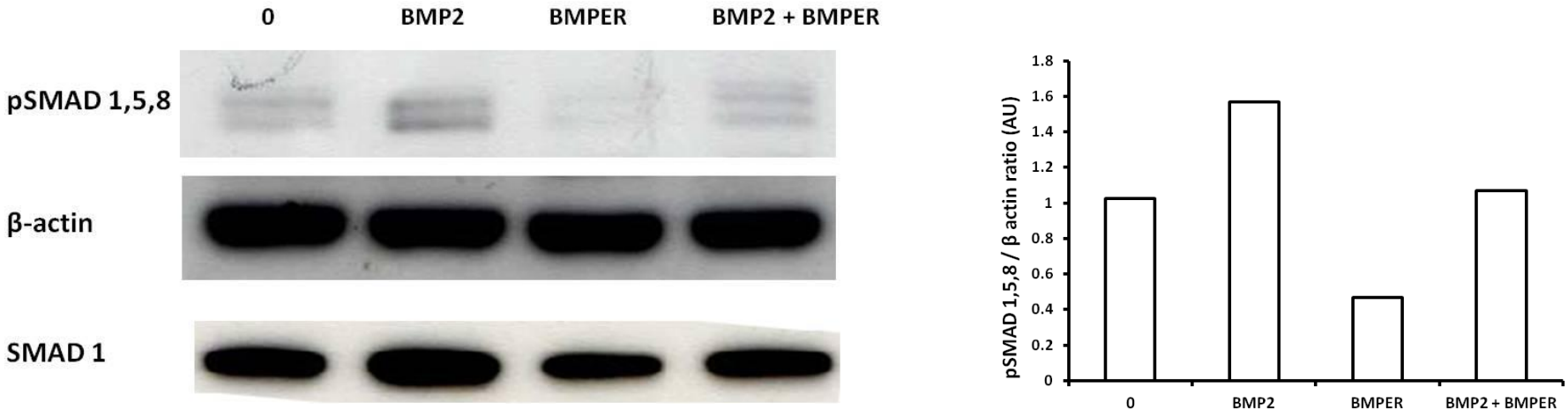

Figure 3.8 Effects of recombinant BMPER peptide on pSMAD 1,5,8 protein expression in Huh7 cells

Western blot analysis showing pSMAD 1,5,8 levels in Huh7 cells treated with 25ng/mL BMP2 and 2500ng/mL BMPER or a combination of both. pSMAD expression was normalised to the expression of β-actin. Data are presented in arbitrary units (AU) for a single experiment with one biological replicate. Densitometry is displayed next to the blot.

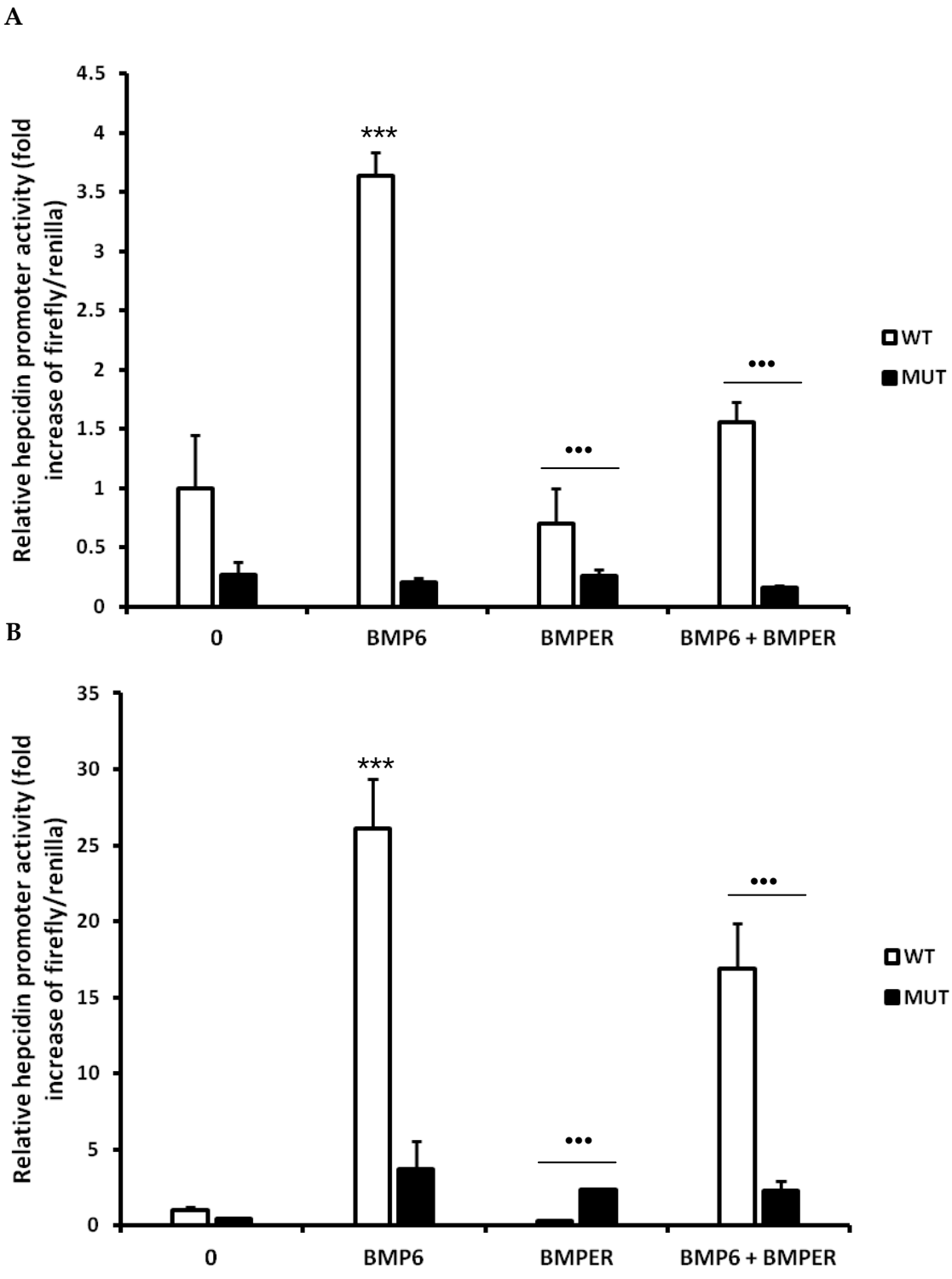

Figure 3.9 Effect of BMPER on BMP6 induced hepcidin promoter activity in HepG2 cells

HepG2 cells transiently transfected with (A) 0.9kb wild type (WT) or BMP-RE1 mutant (MUT) hepcidin construct; (B) 2.7kb wild type (WT) or BMP-RE2 mutant (MUT) construct for 6-8 hours were treated with 25ng/mL BMP6 and 2500ng/mL BMPER or a combination both. Data are presented as mean ± SD derived from a single experiment with three biological replicates. The experiment shown is representative of 3 similar experiments. Statistical analysis was performed by 1-way ANOVA with Tukey's post hoc test. ***$p<0.001$ –BMP6 vs. treatment comparison; •••$p<0.001$ for +BMP6 vs. treatment comparisons.

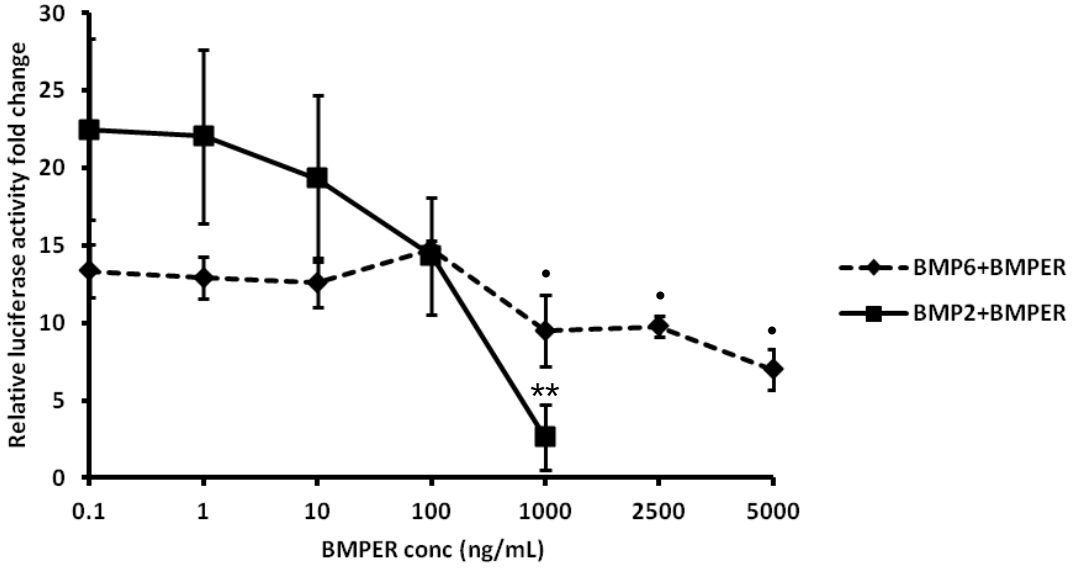

Figure 3.10 Effect of BMPER on BMP2- and BMP6 dependent hepcidin promoter activity in HepG2 cells

HepG2 cells transiently transfected for 6 hours with wild type 2.7kb (WT) hepcidin promoter were treated with BMPER (1-1000 ng/mL), in the presence of BMP2 (25 ng/mL) or BMP6 (25ng/mL). Data are presented as mean ± SD derived from a single experiment with three biological replicates. The experiment shown is representative of 3 similar experiments. Statistical analysis was performed by 1-way ANOVA with Tukey's post hoc test. **$p<0.01$ for +BMP2 vs. BMP2+BMPER; •$p<0.05$ for +BMP6 vs. BMP6+BMPER.

3.4 BMPER inhibits hepcidin transcription in primary human hepatocytes

The effects observed on the hepcidin promoter were confirmed on isolated primary hepatocytes (in collaboration with The Liver Unit, King's College hospital). Endogenous hepcidin mRNA expression, measured by real-time PCR, increased upon exposure of the primary cells to BMP2. This effect was abolished in the presence of BMPER (Figure 3.11).

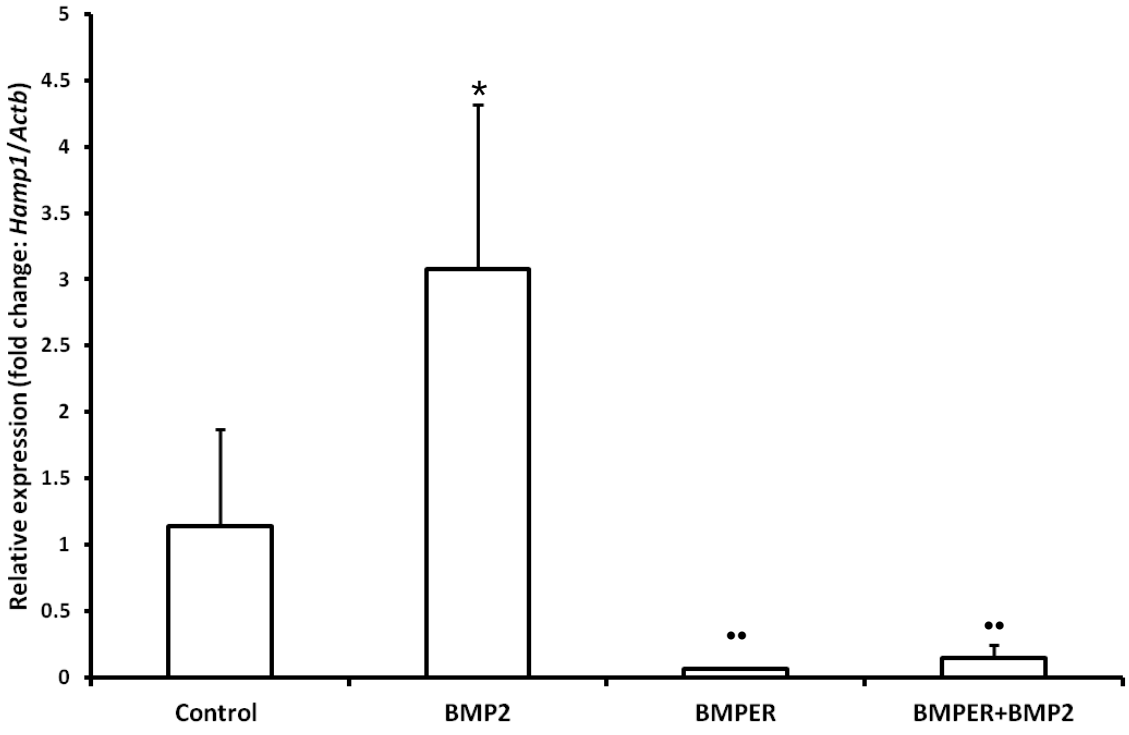

Figure 3.11 Effect of recombinant BMPER on *Hamp1* mRNA in primary human hepatocytes

Primary human hepatocytes were treated with 2500ng/mL BMPER in the presence or absence of 25ng/mL BMP2 for 16 hours. *Hamp1* mRNA expression was measured by real-time PCR. Relative mRNA expression was normalised against the house keeping gene *Actb*. Data are presented as mean ± SD for fold change compared to control (n=3 per group). The samples were measured in triplicate. Statistical analysis was performed by 1-way ANOVA with Tukey's post hoc test. *$p<0.05$ for –BMP2 vs. treatment comparison; ••$p<0.01$ for +BMP2 vs. treatment comparisons.

3.5 Effects of recombinant BMPER and Twisted gastrulation (TWSG1) on hepcidin transcription

It has been proposed that, in iron-loading anaemia's such as hypotransferrinaemia, one or more humoral factors are released from the marrow under increased erythropoietic drive that can influence hepatic hepcidin levels (Tanno et al., 2007, Tanno et al., 2009).

The expression of growth differentiating factor 15 (GDF15) and twisted gastrulation (TWSG1) was found to be significantly increased in patients (GDF15) and mice (TWSG1) with β-Thalassaemia and both have been shown to inhibit hepcidin expression *in vitro* (Tanno et al., 2009, Tanno et al., 2007). Additionally, TWSG1 has also been proposed to form a ternary complex with BMPER and BMPs. The binding of BMP4 to BMPER was enhanced in the presence of TWSG1 (Ambrosio et al., 2008). It was therefore hypothesised that the inhibitory effects observed on the hepcidin promoter by BMPER may be further enhanced in the presence of TWSG1. The effects of TWSG1 and BMPER on hepcidin transcription were tested.

BMPER exhibited a clear dose response inhibition of BMP2-dependent hepcidin promoter activity. In this study TWSG1 did not appear to inhibit BMP-2 dependent hepcidin promoter activity. When given together, BMP2-dependent hepcidin promoter activity was decreased to a similar level to that observed with BMPER alone demonstrating no additive or interactive effects of BMPER with TWSG1 on BMP2-dependent hepcidin promoter activity (Figure 3.12).

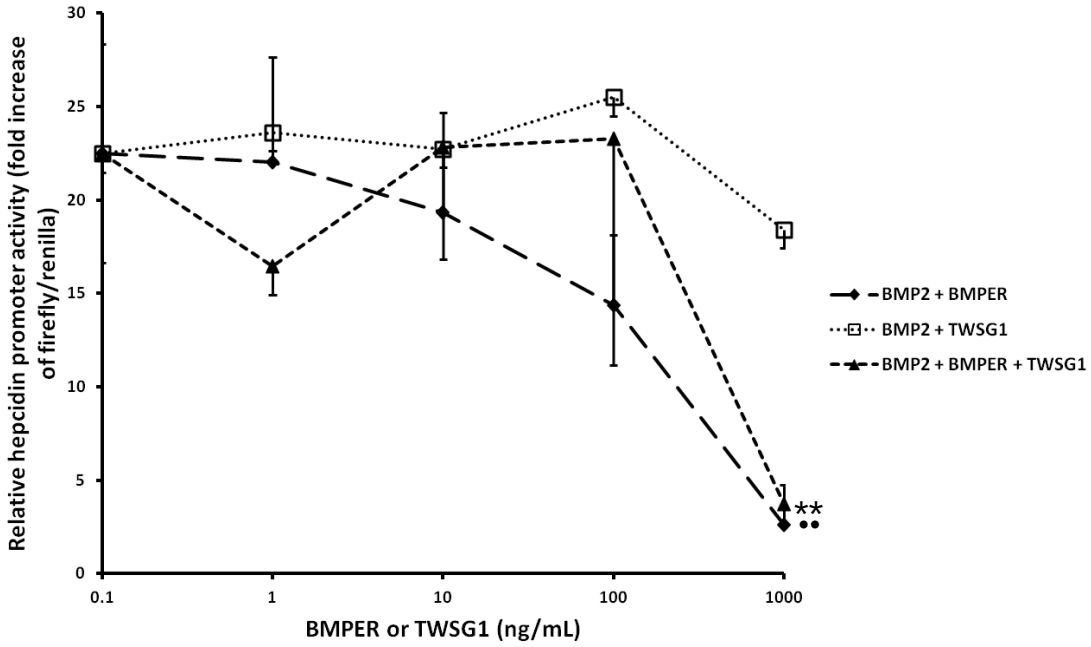

Figure 3.12 Effect of BMPER and TWSG1 on BMP2-dependent hepcidin promoter activity in HepG2 cells

HepG2 cells transiently transfected with wild type 2.7kb (WT) hepcidin promoter were treated with BMPER (◆1-1000 ng/mL) or TWSG1 (□ 1-1000 ng/mL) alone or in combination (▲), in the presence of BMP2 (25ng/mL). Data are presented as mean ± SD derived from a single experiment with three biological replicates. The experiment shown is representative of 3 similar experiments. Statistical analysis was performed by 1-way ANOVA with Tukey's post hoc test. **p<0.01 for +BMP2 vs. BMP2+BMPER; ••p<0.01 +BMP2 vs. BMP2+BMPER+TWSG1.

3.6 Effects of recombinant BMPER peptide on hepcidin transcription and serum iron in CD1 mice

Recombinant BMPER peptide was administered to CD1 mice in order to investigate the effects of BMPER *in vivo*. Various studies were carried out in order to optimise the dose and duration of treatment.

3.6.1 Effect of BMPER injections: optimising the dose of BMPER injections

A range of doses of BMPER peptide were administered in order to identify an optimal concentration of BMPER which causes significant changes in the measured iron parameters. The mice were sacrificed after 18 hours.

The highest dose (50 μg) was associated with a tendency for hepcidin mRNA expression to decrease (Figure 3.13) which correlated with increased serum iron levels (Table 3.1). Tissues nonhaem iron was unchanged with a trend towards decreased liver nonhaem iron at the highest dose (Table 3.1). No changes in hepatic pSMAD 1,5,8 protein expression was observed (Figure 3.14).

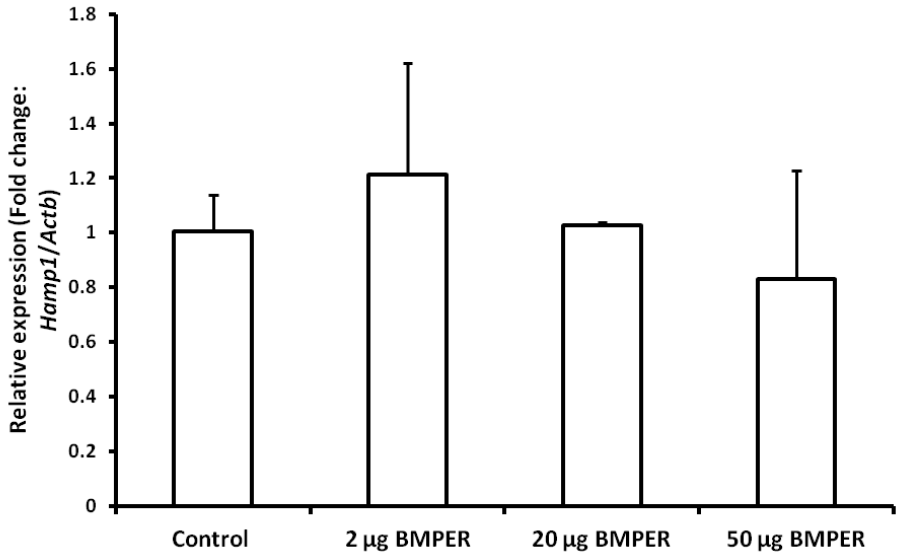

Figure 3.13 Effect of different doses of recombinant BMPER peptide on liver *Hamp1* mRNA

Seven week old male CD1 mice received an intraperitoneal injection of either 2 µg, 20 µg or 50 µg of BMPER peptide dissolved in PBS or PBS alone. Mice were sacrificed 18 hours after injection. *Hamp1* mRNA expression was measured by real-time PCR and results were normalised to the expression of *Actb*. Data are presented as mean ± SD for fold change compared with control (n=2 per group). The samples were measured in triplicate.

Table 3.1 Blood and tissue indicators of iron status in 7 week old male CD1 mice treated with PBS or varying doses of recombinant BMPER peptide

Sample ID (n=2)	Haemoglobin (g/dL)	Serum iron (µM)	Liver non haem iron (nmol/mg wet weight)
Control PBS injections	13.53 ± 0.65	28.34 ± 13.07	3.75 ± 0.18
2 µg BMPER	12.99 ± 0.20	60.56 ± 25.73	2.63 ± 0.86
20 µg BMPER	12.61 ± 0.02	53.99 ± 1.26	3.03 ± 1.24
50 µg BMPER	13.80 ± 0.83	64.44 ± 12.65	2.51 ± 0.61

Data are presented as mean ± SD for (n) determinations.

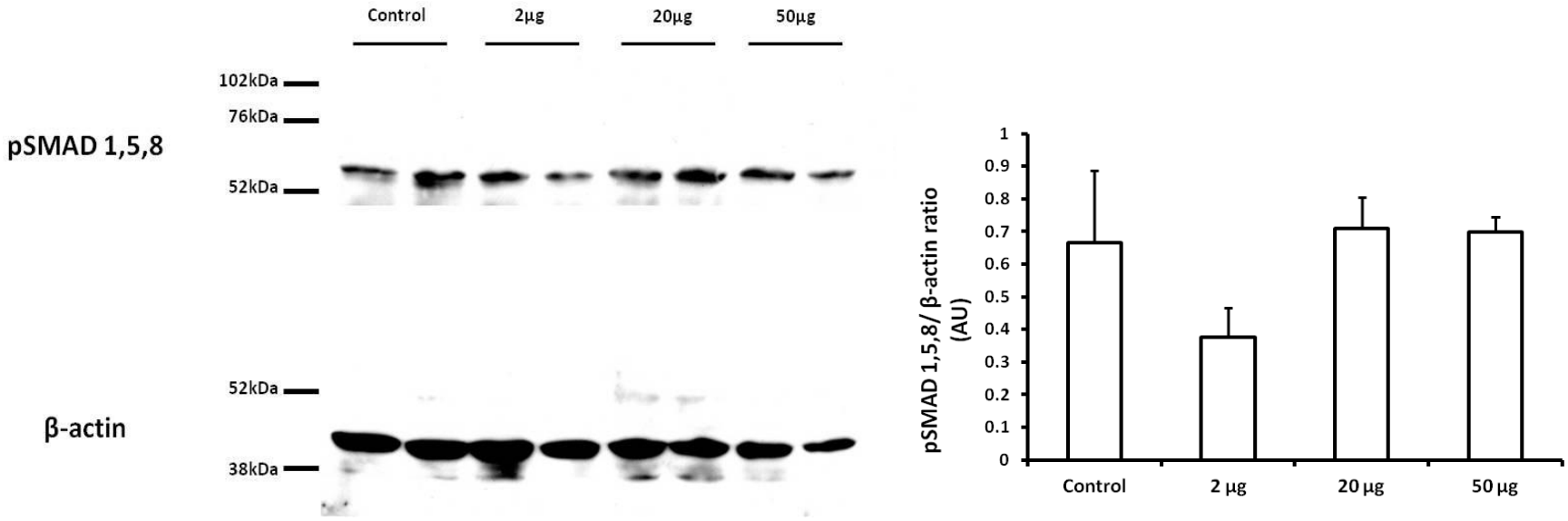

Figure 3.14 Effect of different doses of recombinant BMPER peptide on liver pSMAD 1,5,8 protein expression

Seven week old male CD1 mice received an intraperitoneal injection of either 2 µg, 20 µg or 50 µg of BMPER peptide dissolved in PBS or PBS alone (n=2 per group). Mice were sacrificed 18 hours after injection. Liver pSMAD 1,5,8 protein expression was normalised to the expression of β-actin and presented in arbitrary unit (AU). Densitometry is displayed next to the blot.

3.6.2 Effect of BMPER injections: optimising the duration of BMPER injections

Small doses of BMPER at shorter time points were also investigated to see if BMPER has a rapid response compared to 18hrs. 10μg of peptide was injected intraperitoneally and mice were sacrificed after 2 hours or 6 hours respectively. Trends towards decreased hepcidin mRNA expression were observed after 2 hours of treatment (Figure 3.15). There were no changes in hepcidin mRNA expression, pSMAD 1,5,8 protein expression, serum iron and liver non haem iron after 6 hours (Figure 3.15, Figure 3.16 and Table 3.2).

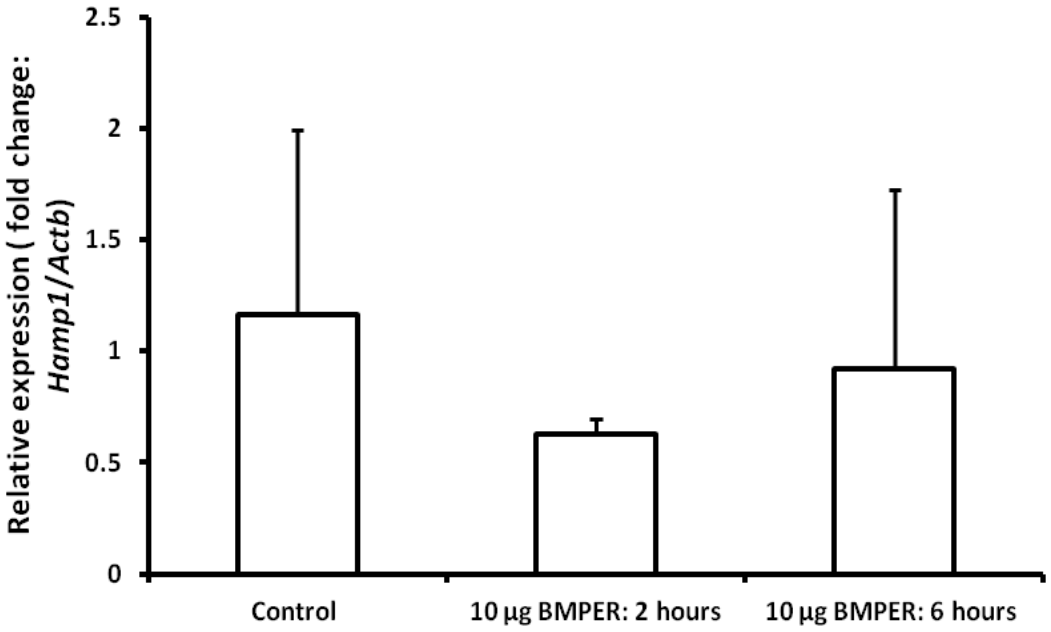

Figure 3.15 Effect of various treatment times after recombinant BMPER peptide on liver *Hamp1* mRNA expression

Seven week old male CD1 mice received an intraperitoneal injection of 10 µg BMPER peptide dissolved in PBS or PBS alone. Mice were sacrificed 2 hours or 6 hours after injection. *Hamp1* mRNA expression was measured by real-time PCR and results was normalised to the expression of *Actb*. Data are presented as mean ± SD for fold change compared with control (n=2 per group). The samples were measured in triplicate.

Table 3.2 Blood and tissue indicators of iron status in 7 week old male CD1 mice treated with PBS or 10 µg of recombinant BMPER peptide for different lengths of time

Sample ID (n=2)	Haemoglobin (g/dL)	Serum iron (µM)	Liver non haem iron (nmol/mg wet weight)
Control PBS injections	15.03 ± 0.862	40.57 ± 5.90	3.78 ± 0.09
10 µg BMPER injection: 2hrs	13.81 ± 0.20	41.17 ± 1.68	2.81 ± 1.69
10 µg BMPER injection: 6hrs	14.14 ± 0.30	46.62 ± 2.95	3.26 ± 0.83

Data are presented as mean ± SD for (n) determinations

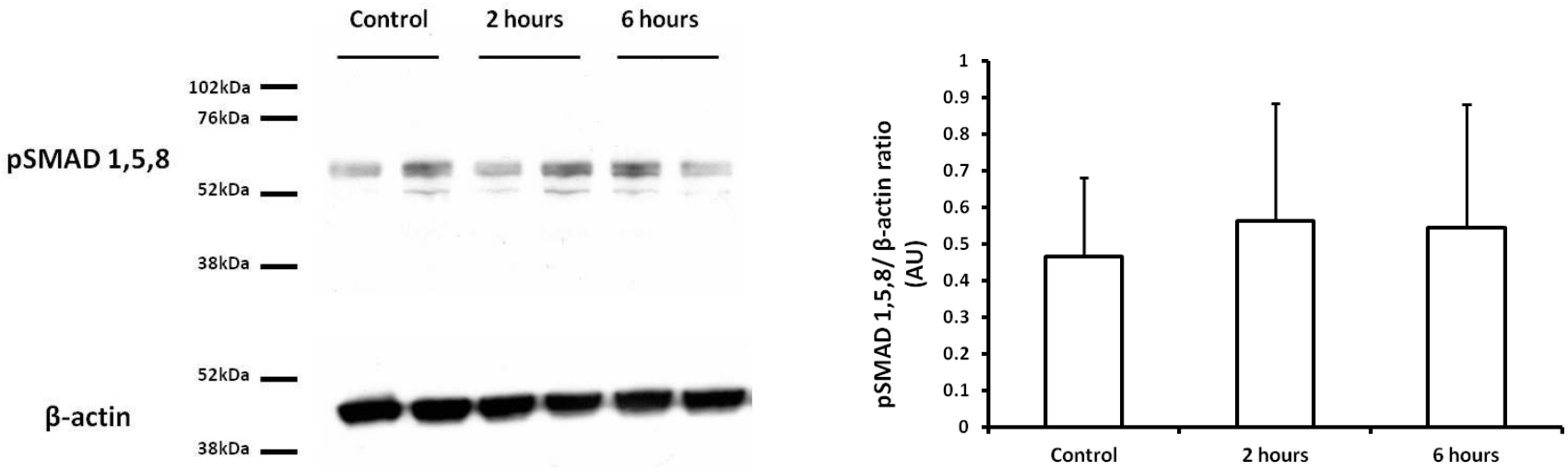

Figure 3.16 Effect of various time point of recombinant BMPER peptide on liver pSMAD 1,5,8 protein expression

7 week old male CD1 mice received an intraperitoneal injection of 10 μg BMPER peptide dissolved in PBS or PBS alone (n=2). Mice were sacrificed 2 hours or 6 hours after injection. Liver pSMAD 1,5,8 protein expression was normalised to the expression of β-actin and presented in arbitrary unit (AU). Densitometry is displayed next to the blot.

In another set of experiments male CD1 mice of 7 weeks of age received an intraperitoneal injection of 50 μg BMPER peptide dissolved in PBS or PBS alone. Mice were sacrificed 18 hours later. Compared to control mice, mice injected with 50 μg BMPER peptide showed significant increases in serum iron levels (Table 3.3) together with a significant decrease in liver hepcidin mRNA levels (Figure 3.17). Hepatic pSMAD 1,5,8 protein expression remained unaltered (data not shown).

Table 3.3 Blood and tissue indicators of iron status in 7 week old male CD1 mice treated with PBS or 50 μg of recombinant BMPER peptide

Sample ID (n=4)	Haemoglobin (g/dL)	Serum iron (μM)	Liver non haem iron (nmol/mg wet weight)
Control PBS injection	13.62 ± 1.24	19.39 ± 6.56	3.02 ± 0.78
50 μg BMPER injection	12.39 ± 0.56	26.94 ± 4.08*	2.07 ± 0.51

Data are presented as mean ± SD for (n) determinations. *$p<0.05$ for control PBS injections vs. 50μg BMPER injections.

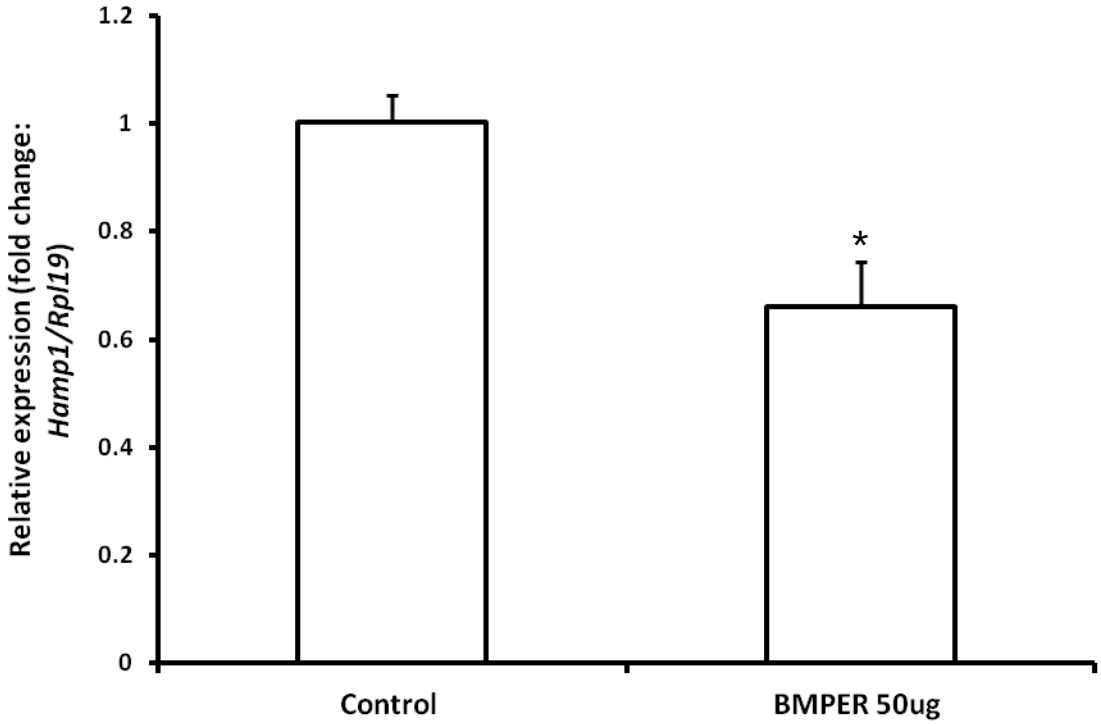

Figure 3.17 Effect of 50 μg recombinant BMPER peptide on liver *Hamp1* mRNA expression

7 week old male CD1 mice received an intraperitoneal injection of 50 μg BMPER peptide dissolved in PBS or PBS alone. Mice were sacrificed 18 hours after later. *Hamp1* mRNA expression was measured by real-time PCR and results was normalised to the expression of *Rpl19.* Data are presented as mean ± SD for fold change compared with control (n=4 per group). The samples were measured in triplicate. Statistical analysis was performed by Student *t*-test *p<0.05 for Control vs. BMPER 50 μg comparison.

3.7 Effects of hypoxia on BMPER expression

Amongst other factors, hypoxia has been shown to reduce hepcidin levels. BMPER was originally identified in developing endothelial cells where it was postulated to play a role in blood vessel sprouting (Moser et al., 2003). It was therefore hypothesised that under hypoxic conditions the levels of BMPER may alter in attempts to increase the production of blood vessels. This in turn may cause hepcidin levels to be suppressed to increase iron absorption.

To test this, CD1 mice were exposed to 24 hours or 72 hours of hypoxia (0.5atm in a hypobaric chamber). Haemoglobin measurements were significantly increased upon exposure to hypoxia (Table 3.4). This correlated with significant reductions in hepcidin mRNA expression after 24 hours of hypoxia and trends towards decreased hepcidin mRNA expression after 72 hours of hypoxia (Figure 3.18). BMPER expression was measured by real-time PCR and western blot analysis (Figure 3.18 and Figure 3.19). Interestingly, trends towards increased BMPER mRNA and protein expression were also observed after 24 hours and reduced almost back to basal levels after 72 hours of hypoxia. The expression of adrenomedullin (*Adm*) was measured as a marker for hypoxia which was significantly increased with hypoxic treatment (Ribatti et al., 2005) (Figure 3.20).

Table 3.4 Haemoglobin measurements in 7 week old CD1 mice exposure to 24hr or 72hr of hypoxia

Sample ID (n=6)	Normoxia	24hr hypoxia	72hr hypoxia
Haemoglobin (g/dL)	14.17 ± 0.90	16.92 ± 0.81*	17.32 ± 0.56*

Data are presented as mean ± SD for (n) determinations. *p<0.05 for normoxia vs. 24hr and 72hr hypoxia by 1-way ANOVA.

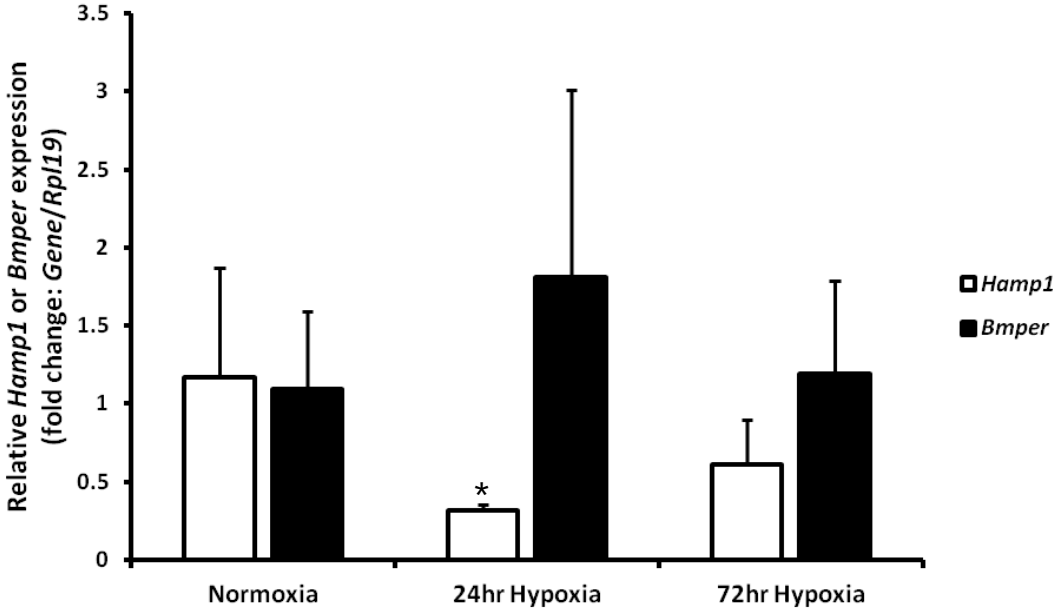

Figure 3.18 Real-time PCR measurement of *Hamp1* and *Bmper* mRNA levels in CD1 mice exposed to 24 hours or 72 hours of hypoxia

Hepatic *Hamp1* and *Bmper* mRNA levels were measured in 7 week old male CD1 mice (n=6) treated with normoxia, 24 hours or 72 hours of hypoxia. mRNA expression was normalised to the housekeeping gene *Rpl19*. The samples were measured in triplicates. Data are presented as mean ± SD for fold change compared with normoxic mice (n=6 per group). Statistical analysis was performed by 1-way ANOVA with Tukey's post hoc test. *$p<0.05$ for normoxia vs. 24hr hypoxia.

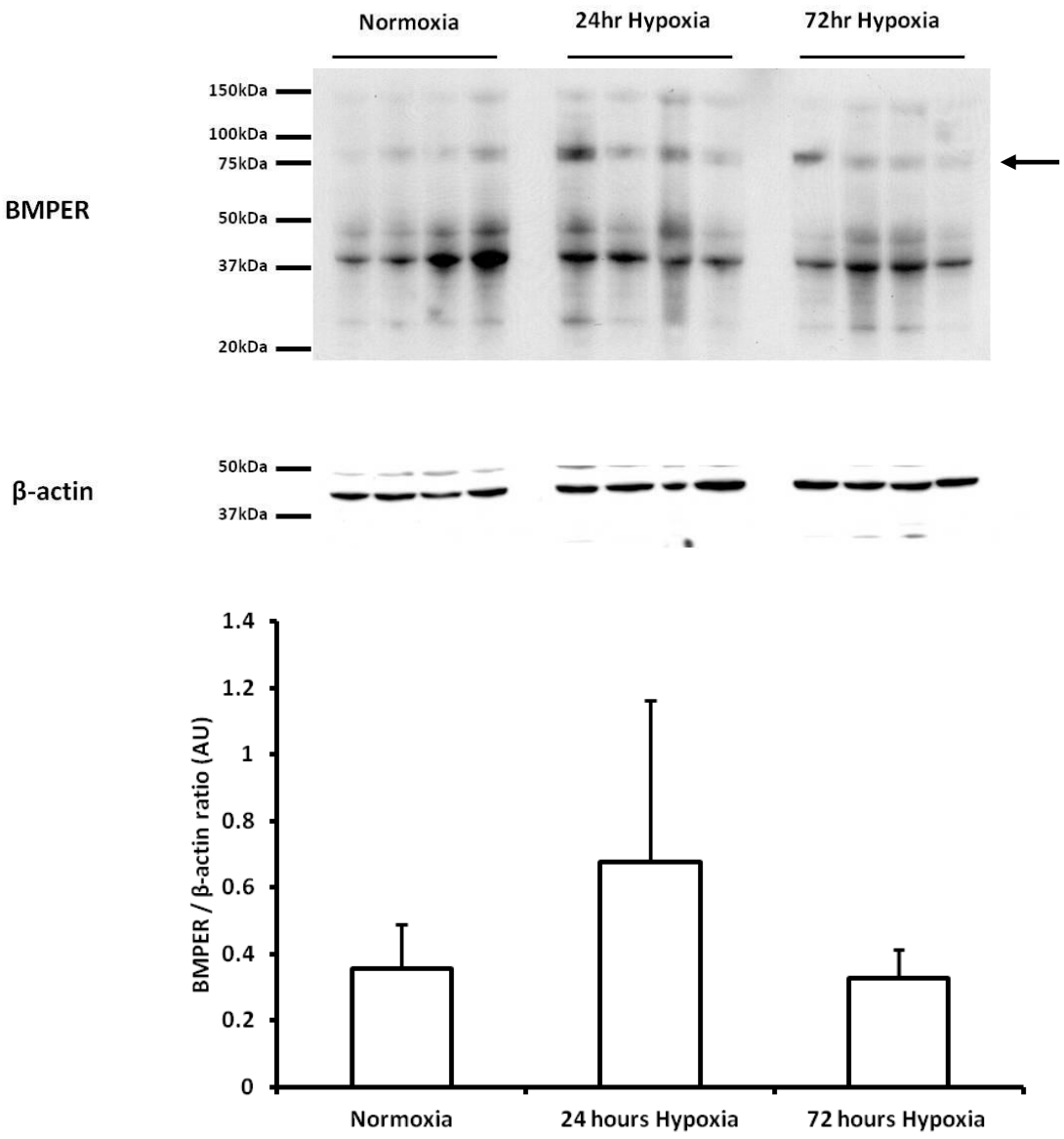

Figure 3.19 Western blot analysis of liver BMPER expression after 24 hours and 72 hours of hypoxia

Western blot analysis of liver total cell lysates of 7 week old male CD1 mice treated with normoxia, 24 hours or 72 hours of hypoxia (n=4 per group). BMPER expression (full length band indicated by arrow) was normalised to the expression of β-actin and are presented in arbitrary units (AU). Densitometry is displayed below the blot. Data are presented as mean ± SD. Statistical analysis was performed by 1-way ANOVA with Tukey's post hoc test.

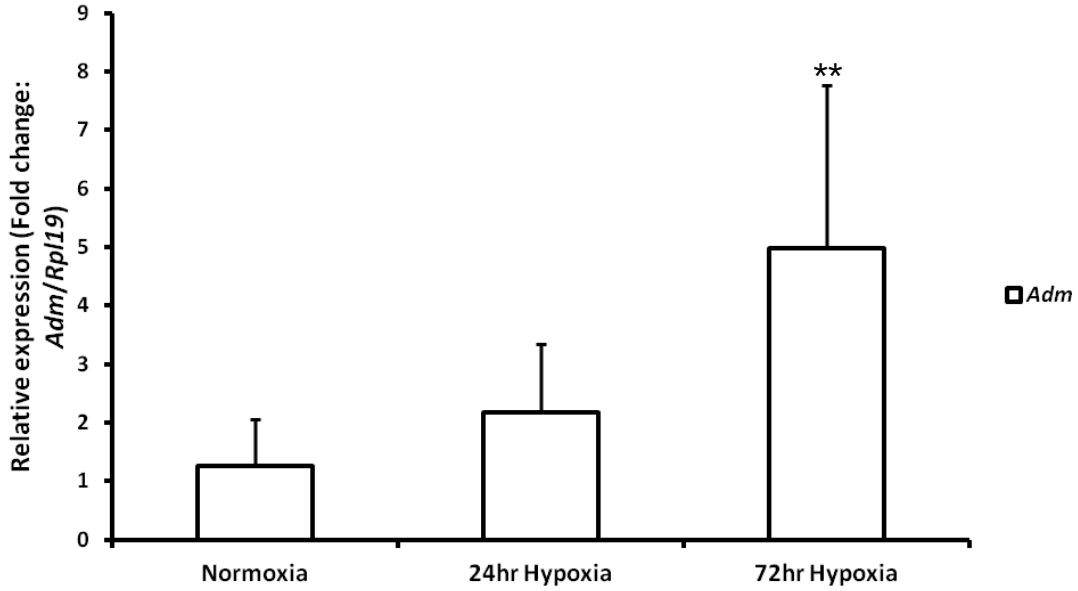

Figure 3.20 Real-time PCR measurement of *Adm* mRNA expression after 24 hours and 72 hours of hypoxia

Liver *Adm* mRNA levels were measured as a marker for hypoxia (Ribatti et al., 2005) in 7 week old male CD1 mice treated with normoxia, 24 hours or 72 hours of hypoxia. Relative mRNA expression was normalised to the housekeeping gene *Rpl19*. Data are presented as mean ± SD for fold change compared with normoxia (n=6 per group). The samples were measured in triplicates. Statistical analysis was performed by 1-way ANOVA with Tukey's post hoc test. **p<0.01 for normoxia vs. 24hr hypoxia.

The trends observed at mRNA and protein level were further investigated through immunostaining of liver sections (Figure 3.21). Due to the poor quality of sample at 24 hours, only control sections and 72 hours hypoxic treatment were stained for BMPER expression. A noticeable increase in BMPER expression as judged by staining of the smaller surrounding blood vessels (indicated by arrows) in the liver was observed after 72 hours of treatment.

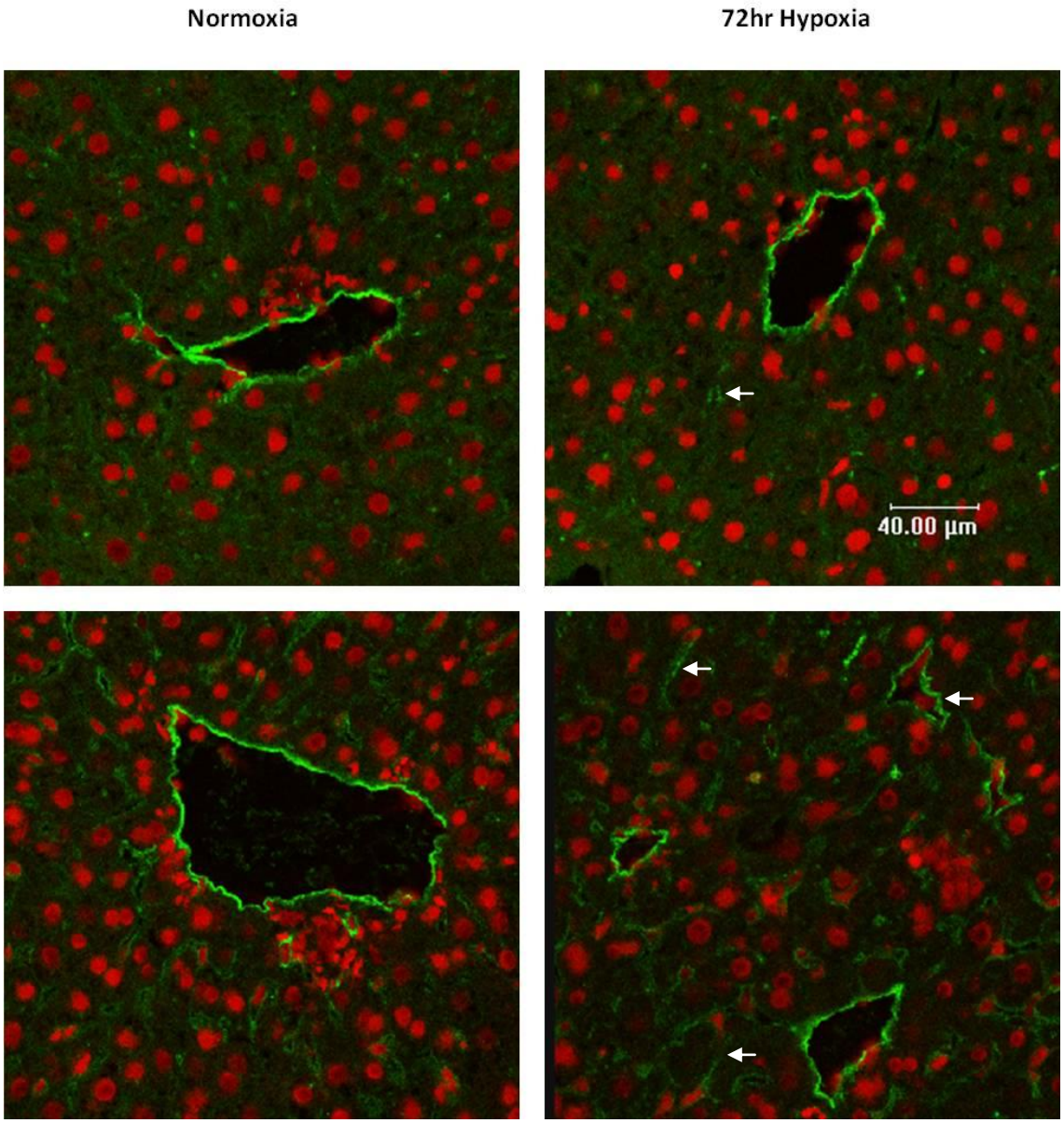

Figure 3.21 Immunofluorescence of liver tissue from normoxic and 72 hours hypoxic treatment stained with BMPER

The expression of BMPER in frozen liver tissues of 7 week old male CD1 mice from normoxia and 72 hours of hypoxia were investigated by immunofluorescence technique. BMPER protein was visualised as green fluorescence and nuclei were counterstained in red (Leica DM-IRE2 confocal microscope, magnification x630).

3.8 Measurement of iron parameters in BMPER heterozygous mice

BMPER knockout mice do not survive beyond birth however heterozygous mice are viable. Liver samples from BMPER heterozygous mice (aged 12 weeks) were kindly provided by the Patterson laboratory (University of North Carolina, USA). Hepcidin mRNA expression (Figure 3.22), serum iron and liver nonhaem iron were measured (Table 3.5). Although not statistically significant, trends towards increased liver hepcidin levels and decreased serum iron in the BMPER knockout heterozygous samples were observed.

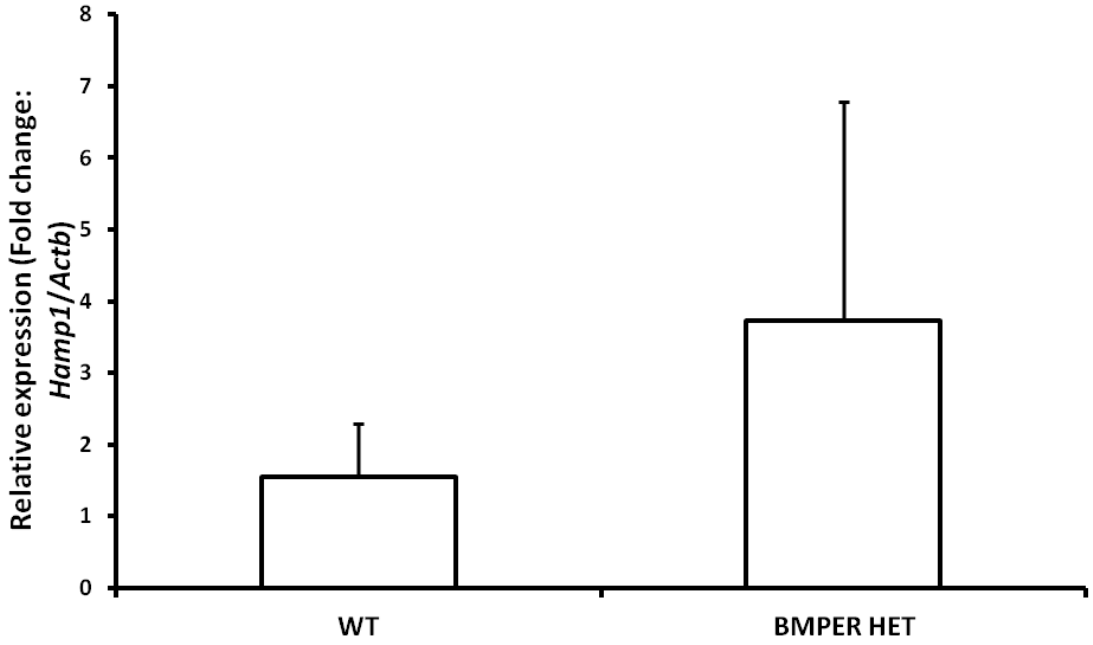

Figure 3.22 Real-time PCR measurement of *Hamp1* mRNA expression in BMPER knockout heterozygous mice

Liver *Hamp1* mRNA expression was measured in 12 week old BMPER knockout heterozygous mice (n=13) and compared against wild type mice (n=4) Relative mRNA expression was normalised to the housekeeping gene *Actb*. Data are presented as mean ± SD for fold change compared with WT. The samples were measured in triplicates. Statistical analysis was performed by Student *t*-test.

Table 3.5 Blood and tissue indicators of iron status in wild type and BMPER heterozygous mice

Sample ID	Haemoglobin (g/dL)	Serum iron (μM)	Liver non haem iron (nmol/mg wet weight)
Wt (n=4)	16 ± 2.66	22.47 ± 1.24	0.86 ± 0.22
Het (n=13)	18.38 ± 2.95	17.42 ± 4.57	1.02 ± 0.31

Data are presented as mean ± SD for (n) determinations.

3.9 Proteolytic processing of BMPER

BMPER is a secreted protein which can undergo proteolytic cleavage to generate two fragments bound together by disulphide bonds (Rentzsch et al., 2006). Multiple sequence alignments of BMPER and HJV revealed certain structural similarities between the two proteins (Figure 3.23). The cleavage mechanism of HJV has been proposed to involve furin as well as the serine protease TMPRSS6 otherwise known as matriptase-2 (MT-2) (Babitt et al., 2006, Silvestri et al., 2008a). Co-transfection of HEK-293 cells with MT-2 and BMPER was performed to determine if BMPER was also a substrate for MT-2 cleavage.

HEK-293 cells were co-transfected with 10 μg of MT-2, MASK, R774C which are mutants of MT-2 in the presence and absence of 10 μg BMPER. Western blot analysis was carried out to assess the expression of MT-2 and BMPER. Co-expression of BMPER and MT-2 increased the expression of MT-2, without significantly altering the expression of BMPER (Figure 3.24).

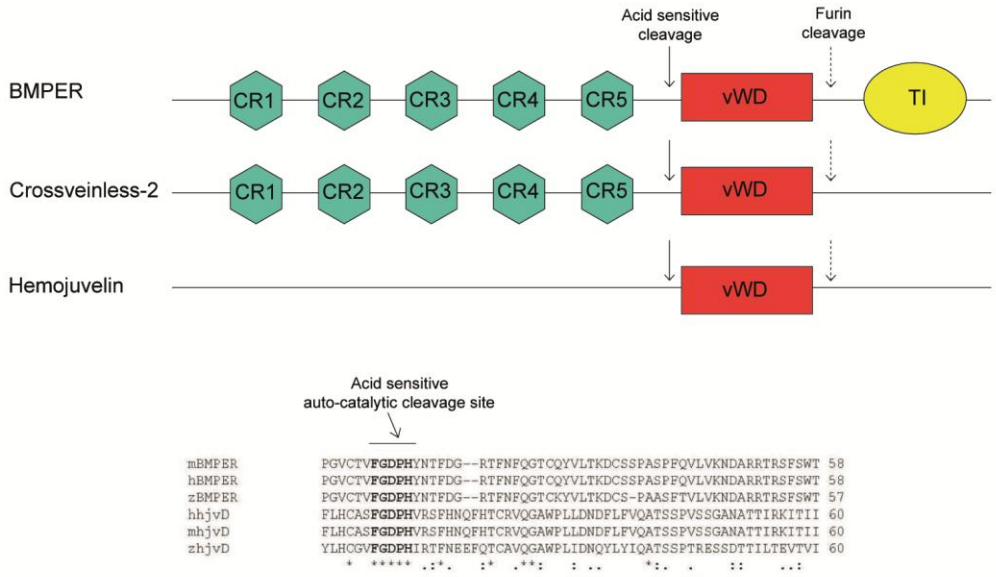

Figure 3.23 Sequence comparison of BMPER, CV-2 and HJV

Upper panel BMPER, HJV and CV-2 share a common von Willebrand type D domain (vWD) a fully conserved acid-sensitive autocatalytic cleavage site and C terminal furin cleavage site. BMPER and CV-2 contain 5 N-terminal cysteine rich regions (CR1-5) which are involved in binding BMPs; these domains are absent in HJV. Lower panel multiple alignment (Clustal) of mouse, human and zebra fish BMPER and HJV sequences showing fully conserved acid-sensitive auto catalytic cleavage site.

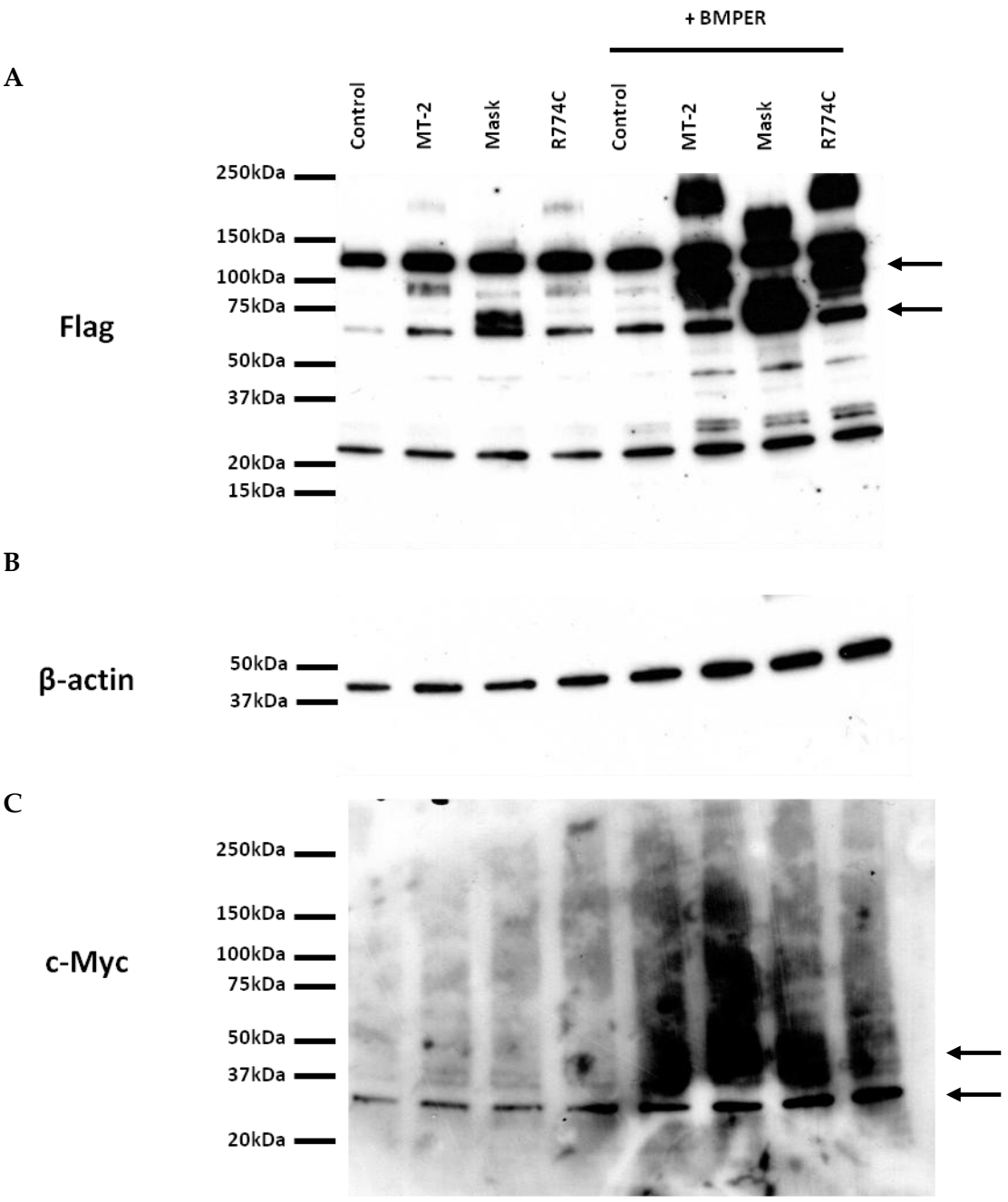

Figure 3.24 Proteolytic cleavage of BMPER by MT-2 in HEK-293 cells

HEK-293 cells were transfected with 10 μg of MT-2, MASK, R774C which are mutants of MT-2 in the presence and absence of 10 μg BMPER. Western blot analysis was carried out to assess the expression of MT-2 (A) which was tagged with Flag and BMPER (C) which was tagged with c-Myc. The MT-2 plasmid and mutants were detected with a Flag antibody. The BMPER protein was detected with a c-Myc antibody. β-actin was used as a loading control (middle panel, B).

3.10 Discussion

BMPER is a known regulator of the BMP pathway and was found to be significantly upregulated in the HPX mouse model both at the mRNA and protein level. The expressions of other known antagonists were also measured and only GDF-15 was found to be significantly increased. Hepcidin downregulation in the HPX mouse model can occur through various mechanisms, each targeting and affecting various signalling pathways. The study described in this chapter has been able to highlight the importance of the BMP pathway and its involvement in hepcidin transcription.

The effects observed *in vivo* were investigated *in vitro* through the use of hepcidin promoter constructs. Recombinant BMPER peptide was able to inhibit basal hepcidin promoter activity as well as the hepcidin promoter response to BMP2 and BMP6. Initial studies have highlighted the importance of BMP2, -4 and -6 in the hepcidin response to BMP signalling. The discovery that BMP6 deficient mice induce iron overload together with the finding that other BMPs are unable to compensate for the lack of BMP6 now corroborates BMP6 to be the key regulator of hepcidin transcription (Meynard et al., 2009, Andriopoulos et al., 2009). BMPER has been shown to bind BMP2,-4, and -6 (Moser et al., 2003). This was evident from the current study where BMPER was able to inhibit BMP2 and BMP6 dependent hepcidin promoter activity. The ability of BMPER to inhibit BMP6 dependent hepcidin promoter activity was somewhat dampened in comparison to BMP2. The reasons for this are not clear as yet, however this is likely to be due to different binding affinities of BMPER to individual BMPs.

The effects of BMPER were also correlated with reduced pSMAD 1,5,8 protein expression in two independent cell lines as well as direct effects on hepcidin mRNA expression in primary human hepatocytes. This result verifies the effects elicited by BMPER are via the SMAD signalling pathway. However further investigations could be carried out to see if upstream or downstream effectors are also being affected. For example, one could disrupt the expression of endogenous BMPER levels through RNA

interference and examine the hepcidin response to BMP stimulation. If the expression of hepcidin is increased above basal levels, one could hypothesise that BMPER directly affects hepcidin transcription. The importance of the BMP pathway could be reinforced if the effects of BMPER-RNAi affect pSMAD 1,5,8 protein expression. It can be noted that the pSMAD1,5,8 antibody appeared to recognise a doublet of bands which may represent different R-SMAD members. Knockdown of individual R-SMADs maybe be required in order to confirm the identities of the bands. Primary human hepatocytes can be considered as the gold standard for hepcidin expression studies, however due to the scarce availability of freshly isolated human liver samples, primary human hepatocytes were only used once in this study. The effects of BMPER on hepcidin mRNA expression should be repeated in immortalised cell lines for further confirmation.

The mechanism of BMPER is likely based on the ability of BMPER to bind BMP molecules with high affinity and therefore prevent the binding of the BMPs to their receptors. It is noteworthy that this effect may only be observed when BMPER levels are in excess. Previous studies have suggested that BMPER can have both pro- and anti -BMP effects; at low levels BMPER acts to promote BMP signalling, and high levels acts to sequester the BMPs in the extracellular space (Serpe et al., 2008, Kelley et al., 2009). This effect was not reproducible in the current study and hence this could be a species/organ specific effect.

TWSG1 was previously suggested to form a ternary complex with BMPER and BMP4, thus increasing the binding of BMP4 to BMPER and reducing BMP signalling (Ambrosio et al., 2008). In the current study, no significant additive anti-BMP effects were observed when BMPER and TWSG1 were used in combination on hepcidin promoter activity. When comparing the molar ratio's used, 1:23 molar of BMP2:TWSG1 compared to 1:6 molar of BMP2:BMPER, it was evident that using approximately four times less BMPER resulted in a more significant decrease in hepcidin promoter activity, highlighting the potency of BMPER compared to TWSG1.

Mutations of the *Bmper* gene adversely affect the formation of small blood vessels in the *Drosophila* wing. It has been suggested that BMPER may play a role in blood vessel sprouting (Conley et al., 2000). Hypoxia as a result of chronic anaemia may stimulate angiogenesis. This has been hypothesised in breast cancer patients where iron deficiency due to menstruation in premenopausal women increased HIF-1α stability which in turn increased the angiogenic factor, VEGF. Additionally, bovine capillary endothelial cells demonstrated increased elongation and extension when cultured under premenopausal conditions (Jian et al., 2011). Since BMPER was identified as an early marker of vasculogenesis (Moser et al., 2003) it was hypothesized that under hypoxic/anaemic conditions, increased BMPER levels may be required for blood vessel remodelling, leading to increased sequestration of BMPs and the downregulation of hepcidin in the liver. The effect of hypoxia on hepcidin expression *in vivo* has been shown to be variable with some studies demonstrating reduced hepatic hepcidin levels after 4 days, however in other studies only mild effects have been reported (Nicolas et al., 2002b, Latunde-Dada et al., 2011, Benedict et al., 2007). In the current study, trends towards increased *Bmper* mRNA expression were observed after 24 hours of hypoxia which correlated with significant decreases in *Hamp1* mRNA levels. 72 hours of hypoxia normalised the expression of hepcidin to that of normoxic mice suggesting an adaptive or short-lived response to hypoxia by hepcidin. In a similar way, *Bmper* levels reduced back to almost the same levels as normoxic mice. The small effects of hypoxia could be explained by an increase in BMPER expression which was localised to smaller blood vessels when liver sections were stained for BMPER protein. The effect of hypoxia on BMPER expression was small compared to those brought about in the HPX mice suggesting that BMPER maybe more relevant under pathophysiological conditions as opposed to a physiological adaptive situations such as hypoxia.

In a recent study, BMPER heterozygous mice demonstrated increased BMP signalling as judged by increased pSMAD expression in retinal sections from oxygen-induced retinopathy (OIR)–subjected mice (Moreno-Miralles et al., 2011), corroborating the notion that a loss of one functional BMPER allele removes the anti-BMP effect. These

results provide an explanation to the trends towards increased hepcidin expression observed in BMPER heterozygous mouse liver samples. Although BMPER knockout mice do not survive beyond birth (Ikeya et al., 2006), it would be interesting to see if a liver specific knockout or inducible knockout of BMPER would alter hepcidin expression and ultimately iron metabolism in adult mice.

The way in which BMPER modulates BMP signalling is not very well understood. Several mechanisms have been proposed:

- A concentration dependent mechanism where low concentrations promote BMP signalling and high concentrations inhibit BMP signalling (Serpe et al., 2008). This effect was not observed in the current study.
- A membrane bound versus cleaved mechanism (Zhang et al., 2007b).

Following the latter theory, hemojuvelin has been shown to be processed in a similar way where the membrane-bound form acts as a co-receptor for BMP signalling, however the cleaved soluble form of HJV has been shown to reduce the BMP signalling cascade (Babitt et al., 2006, Babitt et al., 2007). Cleavage of m-HJV has been shown to occur in two ways, where the cleavage of HJV by furin results in a single product where as the cleavage of m-HJV by MT-2 results in a ladder of products. The precise nature of the binding of BMPs to HJV is not very well understood, however the binding of BMPs to BMPER has been shown to occur through the cysteine-rich (CR) domains (Zhang et al., 2007b). Multiple sequence alignments between several species of BMPER to HJV have revealed sequence similarities in particular the acid sensitive auto-catalytic domain FGDPH. Co-expression of MT-2 with BMPER increased the expression of MT-2 as measured by increased FLAG expression; levels of soluble BMPER appeared to increase somewhat with treatment with MT-2 compared to mutants, as determined by c-MYC western blot analysis, suggesting BMPER could also be a substrate for MT2. However the experiments conducted in this study were preliminary investigations and were only conduced once, therefore future work would be required to confirm these observations.

To conclude, the evidence presented in this chapter emphasises the importance of the BMP signalling pathway in the regulation of hepcidin. The mechanism by which hepcidin is downregulated in the HPX mouse model appears to involve a number of factors, with BMPER adding to the list of potential modulators that can suppress hepcidin levels *in vitro* and *in vivo.* BMPER was able to effectively suppress the effects of BMP2 and BMP6-mediated hepcidin promoter induction. Increased BMPER levels in HPX mice would also explain why increased BMP6 expression fails to induce an increase in hepcidin levels. One cannot exclude the potential of other BMP modulators such as TWSG1 and GDF15 to interact with BMPER. Although the effect of recombinant TWSG1 demonstrated no additive effect on BMPER, the levels of GDF15 were significantly increased in the HPX mouse model. Further investigations need to be conducted to see if GDF15 could be co-operating with BMPER to reduced hepcidin expression. BMPER may play a role in the suppression of hepcidin in other forms severe chronic anaemia with iron loading or in diseases where there is a significant amount of angiogenesis.

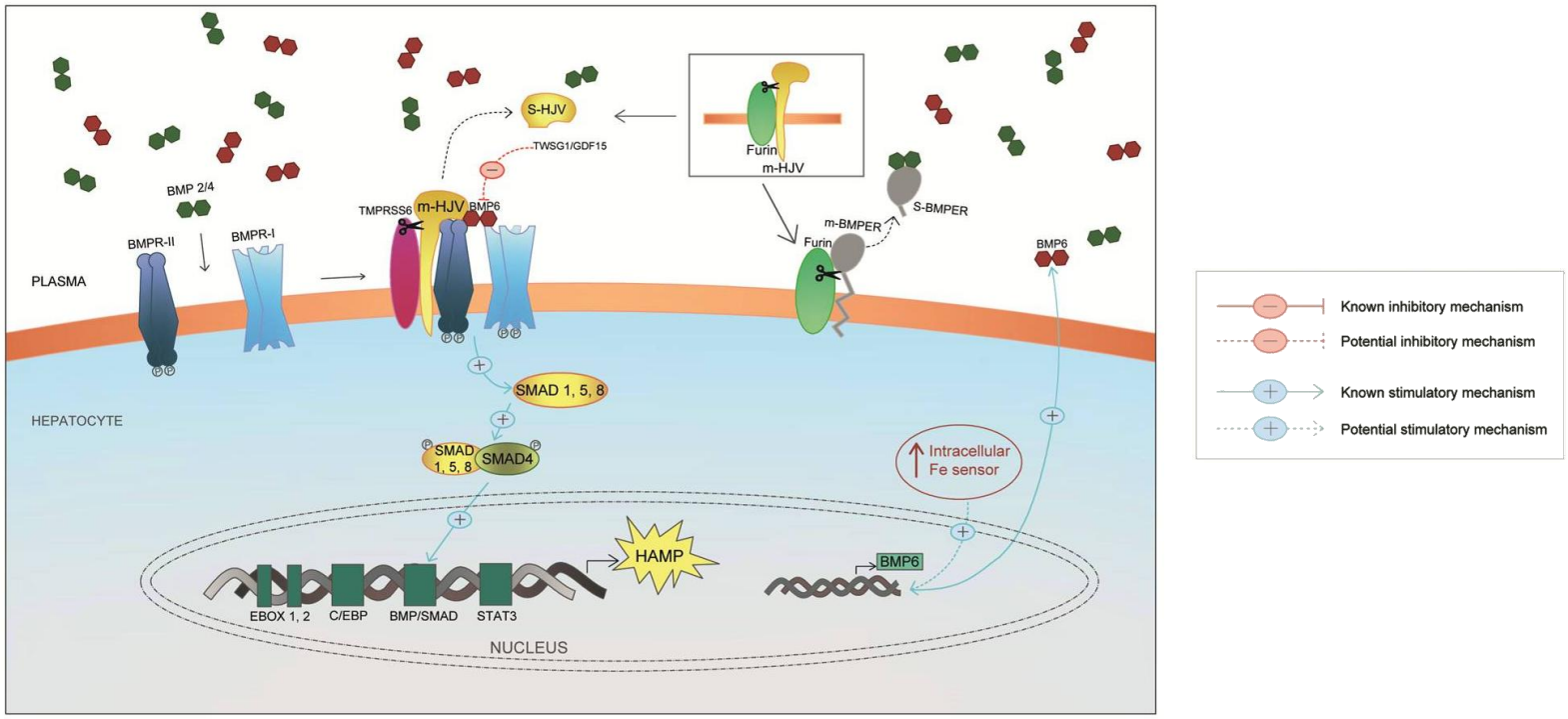

Figure 3.25 Regulation of hepcidin by BMPER

Increased hepatic intracellular iron stores increases BMP6 mRNA and protein expression. The binding of BMP6 to BMPR-I/II stimulates hepcidin transcription via the BMP/SMAD signalling cascade which is facilitated by the BMP co-receptor HJV. The release of erythropoietic signals, GDF15/TWSG1, by erythroid precursor cells inhibits BMP/SMAD activation which is characteristic of iron loading anaemia's. The studies conducted in this chapter identified BMPER to be significantly upregulated in the HPX mouse liver. Chronic anaemia may stimulate blood vessel remodelling which in turn may increase the expression of BMPER. The binding of BMPER to BMP2/4/6 prevents BMP/SMAD activation and thus contributes to the suppression of hepcidin. BMPER may also be susceptible to cleavage by matriptase-2 (TMPRSS6) and furin.

Chapter 4 .

Atonal homologue 8 (ATOH8) regulates hepcidin transcription

4.1 Introduction

The differentiation and development of an organism is a tightly regulated process where the patterning of undifferentiated cells into specialised cells requires rapid changes in gene expression to occur. The involvement of the basic helix-loop-helix family of transcription factors (b-HLH) in the regulation of various biological processes in the eukaryotic organism has been well documented (Massari and Murre, 2000). As their name implies, the structure comprises of two regions: the basic (b) region which is a highly conserved region responsible for interaction with recognitions sequences on DNA; and the HLH region, which are two alpha helices separated by a loop which can be of variable length. The HLH are able to form homo- and heterodimers with other b-HLH proteins, increasing their biological activities depending on the availability of other transcription factors (Massari and Murre, 2000). The b-HLH proteins have been categorised into six groups based on their phylogenetic relationships and different biochemical properties (Ledent et al., 2002). Group A is of relevance to the current study which belongs to the neuronal bHLH proteins.

Insights into the importance of neuronal bHLH proteins came from studies conducted in *Drosophila* which have two classes of proneural genes namely aschaete-scute complex (as-c) and atonal (ato) (Hassan and Bellen, 2000). The cloning of Atonal in 1993 by Jarman and colleagues identified it to be a bHLH transcription factor involved in the development of the peripheral nervous system (PNS) of *Drosophila* (Jarman et al., 1993). The mouse homologue, ATOH8/MATH6 (Atonal Homologue 8/Mouse Atonal Homologue 6), was also shown to be expressed by neural precursor cells (Inoue et al., 2001). Despite a reported function in neural development, the expression of ATOH8 extended over a range of tissues; brain, heart, kidney, lung and pancreas (Ross et al., 2006, Lynn et al., 2008). The expression of ATOH8 was required for the differentiation and maturation of podocytes in mouse kidney development (Ross et al., 2006) and also for the development of the endocrine cell lineage during mouse pancreatic development (Lynn et al., 2008). Additionally, mice deficient in ATOH8 demonstrated

malformation of the retina and muscle which affected the expression of another bHLH protein, MyoD (Yao et al., 2010). Inactivation of ATOH8 gene expression resulted in embryonic lethality in mice demonstrating a pivotal role of this protein during the embryogenesis (Lynn et al., 2008).

Sequence alignment of ATOH8 orthologs revealed all vertebrate ATOH8 proteins to have 100% sequence conservation through the bHLH region, which persisted through the rest of the sequence (Ross et al., 2006). Additionally, the mammalian ATOH8 promoter was found to be enriched with CpG islands which characteristically have multiple transcriptional start sites (TSS). Which TSS is adopted is dependent on the cellular context. The observation of CpG islands in the ATOH8 promoter supports the functionally dynamic expression observed in multiple tissues (Chen et al., 2011a).

The transcriptional regulation of hepcidin has been extensively studied. In addition to the previously discussed BMP-response elements (chapter 3), the CCAAT/enhancer binding protein alpha (CEBPα) is required for the hepcidin response to oxidative stress as well as basal promoter activity (Harrison-Findik et al., 2006). Additionally, the inflammatory response induces hepcidin via activation of the Janus kinases (JAK/STAT3) pathway, where Il-6 is the principle cytokine activator (Pietrangelo et al., 2007, Verga Falzacappa et al., 2007). The actions of Il-6 are dependent on a STAT3 consensus site present on the proximal hepcidin promoter. bHLH proteins, such as ATOH8, bind to the core consensus DNA sequence CANNTG within promoter regions known as E-boxes. There are 4 such E-boxes within the hepcidin promoter. The current study focused on two canonical E-boxes with the core sequence CACGTG within the core hepcidin promoter previously reported to bind other bHLH factors (Bayele et al., 2006).

In the current study, the effect of Atonal homologue 8 (ATOH8), was investigated to determine its role in the regulation of hepcidin and iron metabolism. Prior research has examined the ability of other members of the b-HLH family, USF1 and USF2 and c-

Myc and Max to occupy E-Boxes located on the hepcidin promoter (Bayele et al., 2006). *Atoh8* mRNA expression has been show to be regulated by iron *in vivo* in parallel with other genes known to be regulated by the BMP pathway (Kautz et al., 2008). The studies conducted in this chapter aimed to characterise the role ATOH8 in the regulation of hepcidin transcription *in vitro*. Additionally, the expression of ATOH8 was examined *in vivo* using various mouse models of altered iron metabolism.

4.2 ATOH8 expression in Hypotransferrinaemic mice (HPX)

The hepatic expression of ATOH8 was measured by real-time PCR and western blot analysis (Figure 4.1 and Figure 4.2). Hepatic ATOH8 localization was examined by immunohistochemistry in HPX liver sections (Figure 4.3). Contrary to the concept of ATOH8 upregulation by iron loading, HPX mice, despite being severely iron loaded, demonstrated decreased expression of ATOH8 at both mRNA and protein levels as demonstrated by real time PCR, western blot analysis and immunohistochemistry.

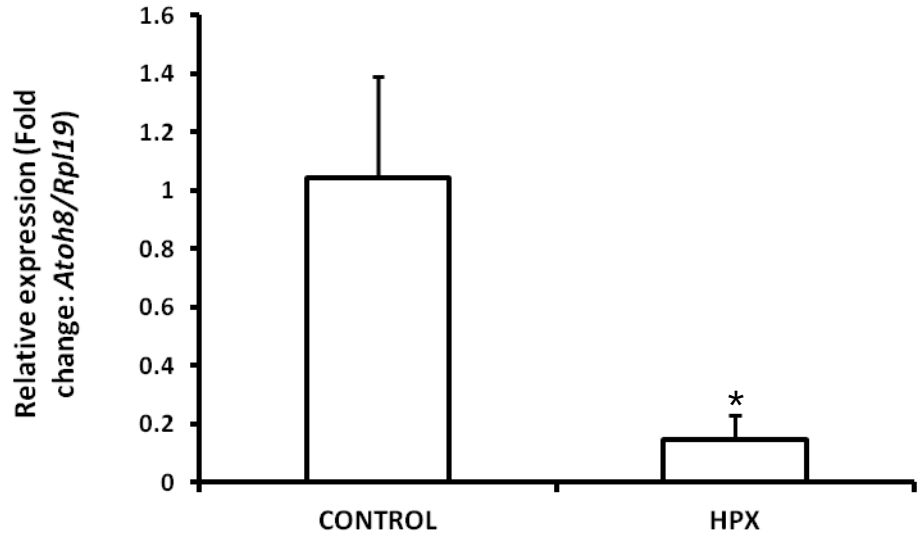

Figure 4.1Real-time PCR measurement of hepatic *Atoh8* mRNA expression in HPX mouse liver

Liver *Atoh8* mRNA expression was measured in 10-11 week old male HPX mice. Wild type and heterozygous mice were used as controls. Relative mRNA expression was normalised against the house keeping gene *Rpl19*. Data are presented as mean ± SD for fold change compared with wild type and heterozygous mice (n=3 per group). The samples were measured in triplicate. Statistical analysis was performed by Student *t*-test. *$p<0.05$ for CONTROL vs. HPX comparisons.

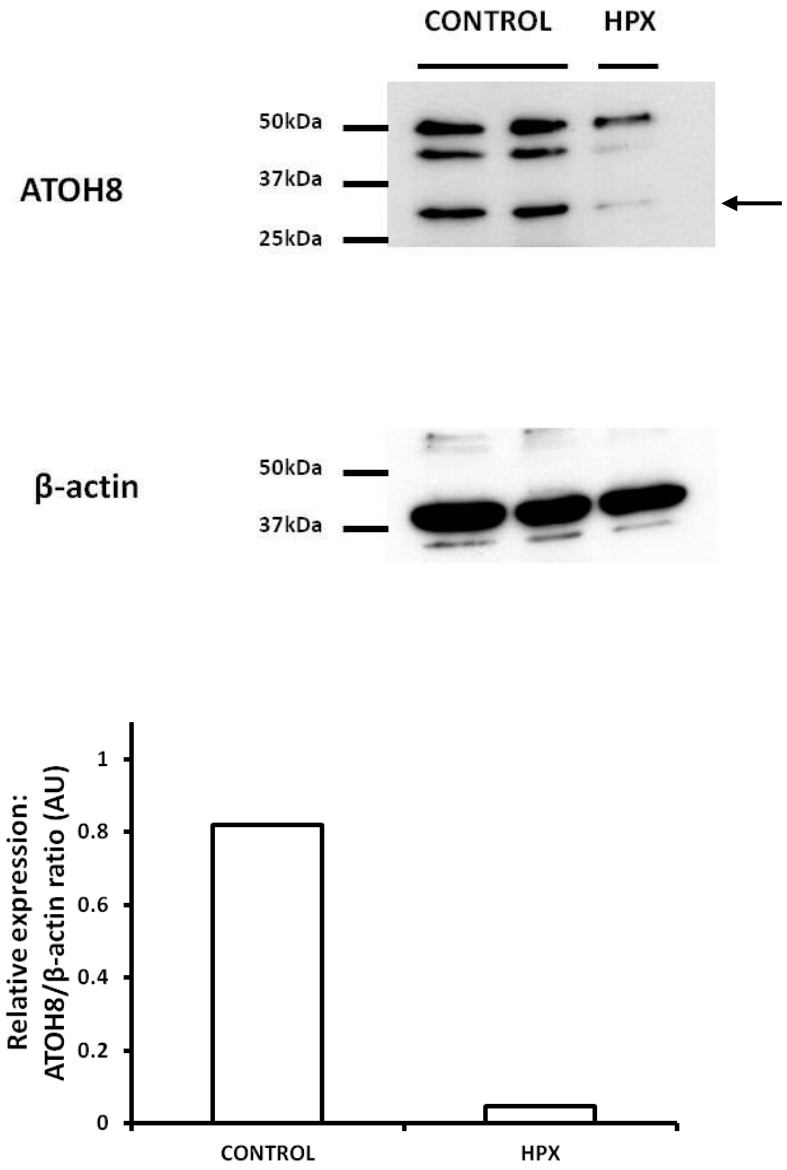

Figure 4.2 Western blot analysis of ATOH8 expression in HPX mouse liver

Western blot analysis of nuclear liver extract of 10-11 week old male HPX mice (n=1). Wild type/heterozygous mice were used as controls (n=2). ATOH8 expression was normalized to the expression of β-actin and presented in arbitrary unit (AU). Densitometry is displayed below the blot.

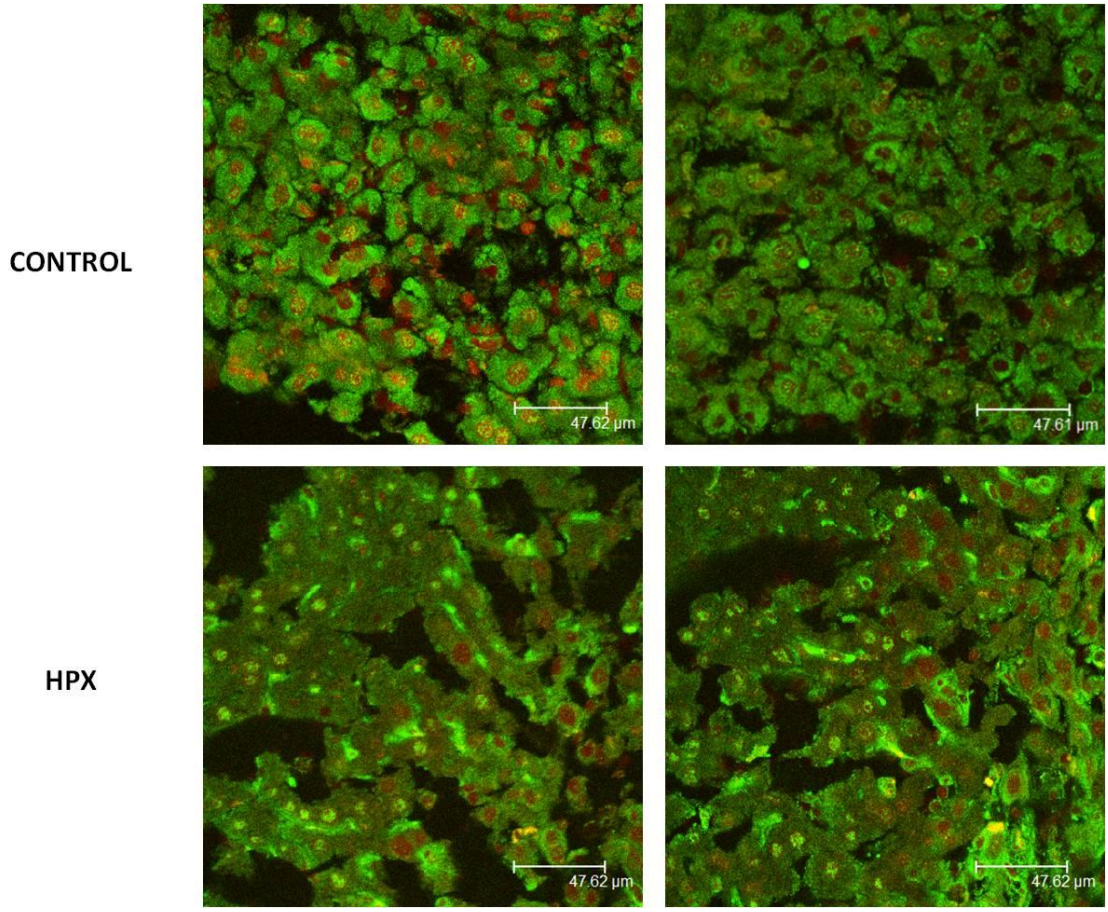

Figure 4.3 Immunofluorescence of liver ATOH8 expression in HPX mice

The expression of ATOH8 from frozen liver sections of 10-11 week old male HPX mice was demonstrated though immunofluorescence technique. ATOH8 protein was visualised as green fluorescence and nuclei were counterstained in red (Leica DM-IRE2 confocal microscope, magnification x630).

4.3 Effect of ATOH8 on hepcidin transcription *in vitro*

In preliminary experiments, HepG2 cells were co-transfected with 0.5 μg of the 2.7kb hepcidin promoter cloned into the pGL3 luciferase vector together with 2 μg, 4 μg, or 6 μg of the ATOH8 expression plasmid in the absence or presence of 25ng/mL recombinant BMP2. Luciferase activities were determined and results were compared to wild-type hepcidin promoter activity without BMP2 treatment (Figure 4.4A). The transfection efficiency of the ATOH8 plasmid was determined through western blotting analysis (Figure 4.4B). ATOH8 expression significantly increased hepcidin promoter activity in the presence of BMP2 stimulation but had no effect in the absence of BMP2 stimulation. There was no significant effects on endogenous pSMAD 1,5,8 protein expression.

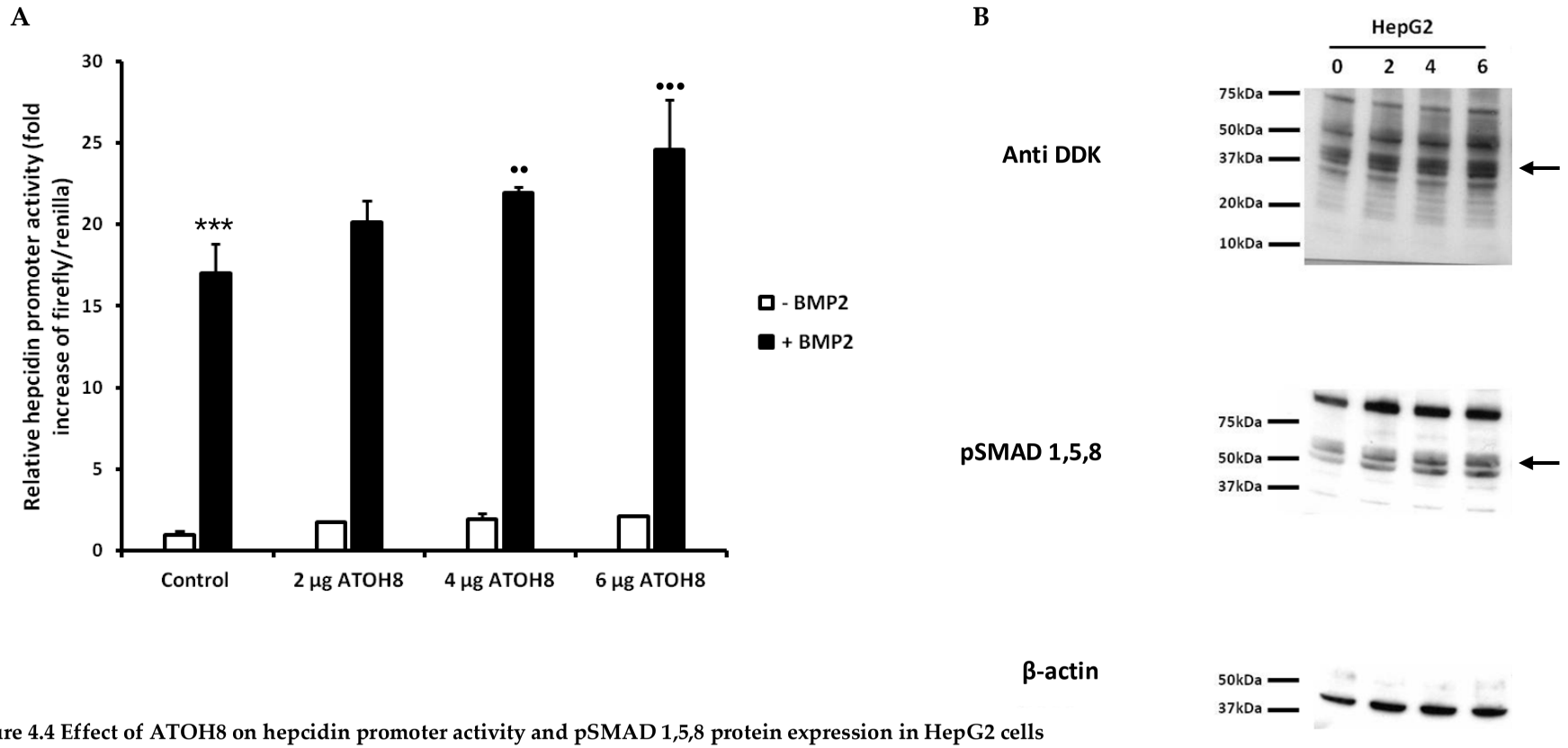

Figure 4.4 Effect of ATOH8 on hepcidin promoter activity and pSMAD 1,5,8 protein expression in HepG2 cells

(A) HepG2 cells were co-transfected with the wild-type 2.7 kb hepcidin promoter (WT) construct along with increasing concentrations of ATOH8 plasmid construct in the presence or absence of 25ng/mL BMP2. Data are presented as mean ± SD derived from a single experiment with three biological replicates. The experiment shown is representative of 3 similar experiments. Statistical analysis was performed by 1-way ANOVA with Tukey's post hoc test. ***$p<0.001$ for –BMP2 vs ATOH8 treatment comparisons; ••$p<0.01$; •••$p<0.001$ for +BMP2 vs ATOH8 treatment comparisons. (B) HepG2 cells were transfected with increasing concentration of the ATOH8 plasmid for 24 hours. Western blot analysis was performed on whole cell lysates. The expression of the plasmid was determined through detection of anti-DDK (indicated by arrow). The expression of pSMAD 1,5,8 (indicated by arrow) and β-actin was also determined.

4.3.1 ATOH8 titration significantly increased basal and BMP2-mediated hepcidin promoter activity in HEK-293 cells

The transfection efficiency and/or protein expression from the ATOH8 plasmid in HEK-293 cells appeared to be much higher than HepG2 cells (Figure 4.5D). HEK-293 cells treated with the same concentrations of ATOH8 plasmid as HepG2 cells, demonstrated a significant increase hepcidin promoter activity in the presence or absence of BMP stimulation. Concentrations above 4 μg produced no further increase in promoter activity, suggestive of saturation of the hepcidin promoter activity at high concentrations of ATOH8 (Figure 4.5A-C). Interestingly pSMAD 1,5,8 protein expression increased in a dose dependent manner with ATOH8 transfection suggesting ATOH8 affects the BMP signalling pathway (Figure 4.6). The increase in hepcidin promoter activity correlated with increased expression of endogenous hepcidin in HEK-293 cells (Figure 4.7).

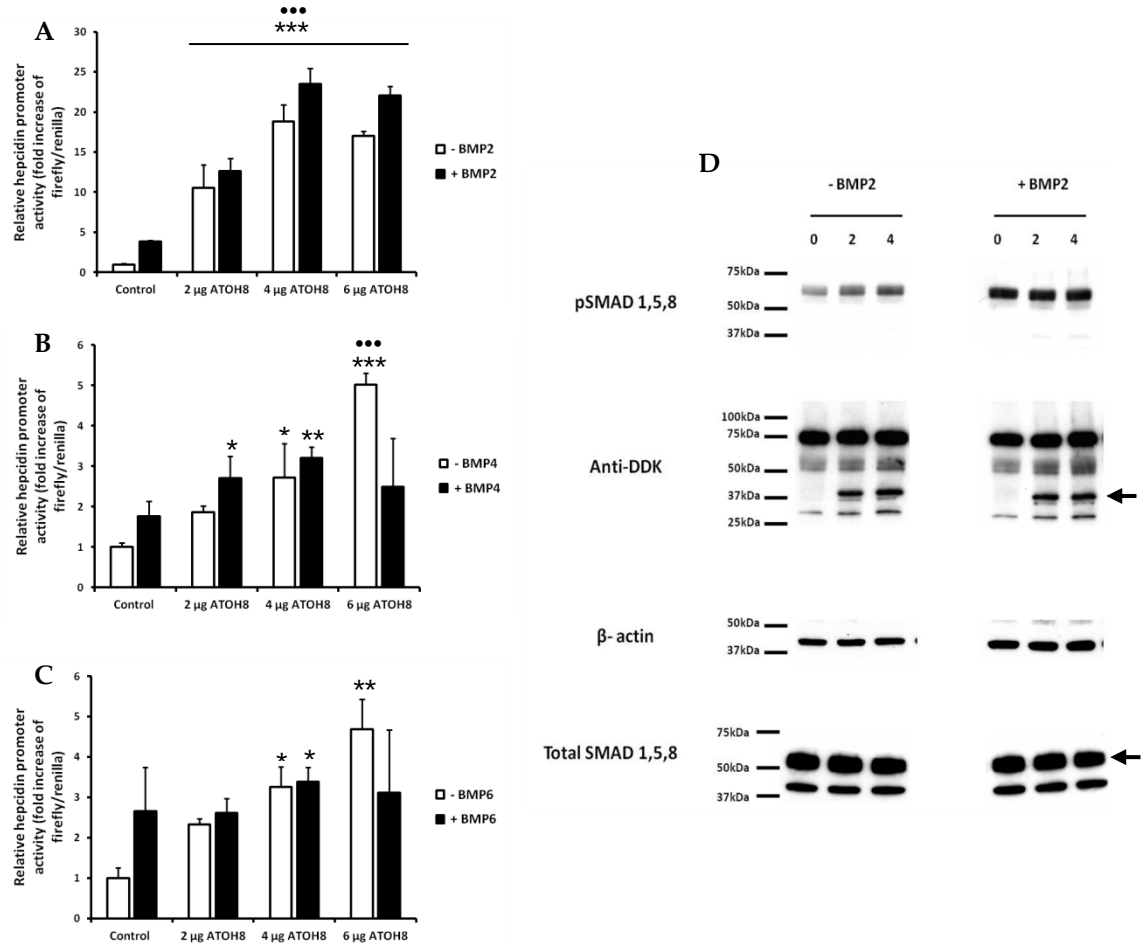

Figure 4.5 Effect of ATOH8 on hepcidin promoter activity and pSMAD 1,5,8 protein expression in HEK-293 cells

HEK-293 cells were co-transfected with the wild-type 2.7 kb hepcidin promoter construct along with increasing concentrations of ATOH8 plasmid in the presence or absence of 25ng/mL BMP2 (A), BMP4 (B) or BMP6 (C). Data are presented as mean ± SD derived from a single experiment with three biological replicates. The experiment shown is representative of 3 similar experiments. Statistical analysis was performed by 1-way ANOVA with Tukey's post hoc test. *p<0.05; **p<0.01; ***p<0.001 for –BMP vs. ATOH8 treatment comparisons; •••p<0.001 for +BMP vs. ATOH8 treatment comparisons. (D) HEK-293 cells were transfected with increasing concentration of the ATOH8 plasmid in the presence or absence or 25ng/mL BMP2. Western blot analysis was performed on whole cell lysates. The expression of the plasmid was determined through detection of anti-DDK (indicated by arrow). The expression of pSMAD 1,5,8, Total SMAD 1,5,8 (indicated by arrow) and β-actin were also determined.

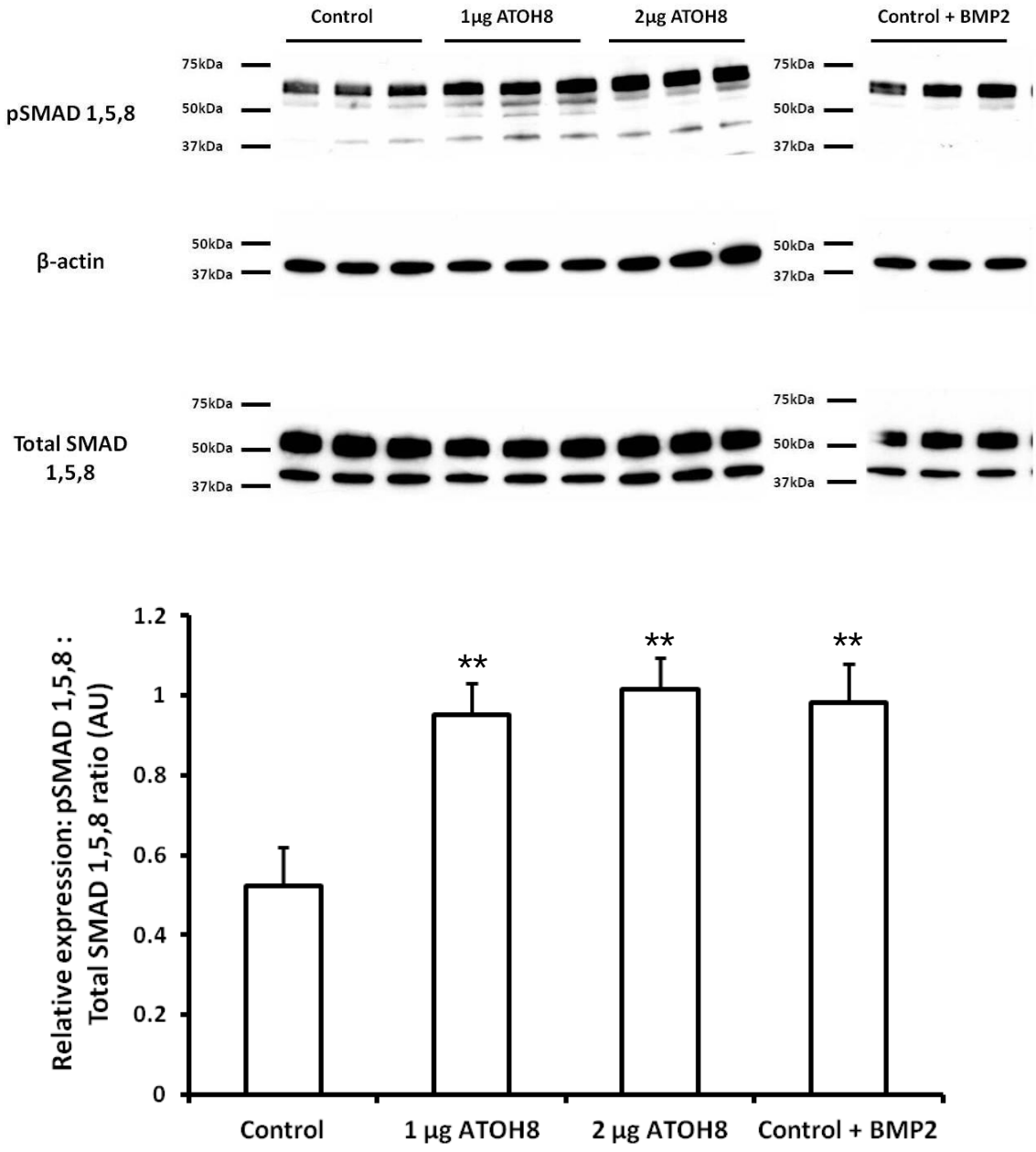

Figure 4.6 Western blot analysis of HEK-293 cells transfected with ATOH8

HEK-293 cells were transfected with different concentrations of ATOH8 plasmid. Western blot analysis was performed on whole cell lysates where pSMAD 1,5,8 expression was normalized to the expression of total SMAD 1,5,8 and presented in arbitrary unit (AU). Densitometry is displayed below the blot. Data are presented as mean ± SD (n=3 per groups). Statistical analysis was performed by 1-way ANOVA with a Tukey's post hoc test. **p<0.01 control vs. ATOH8 treatment comparisons.

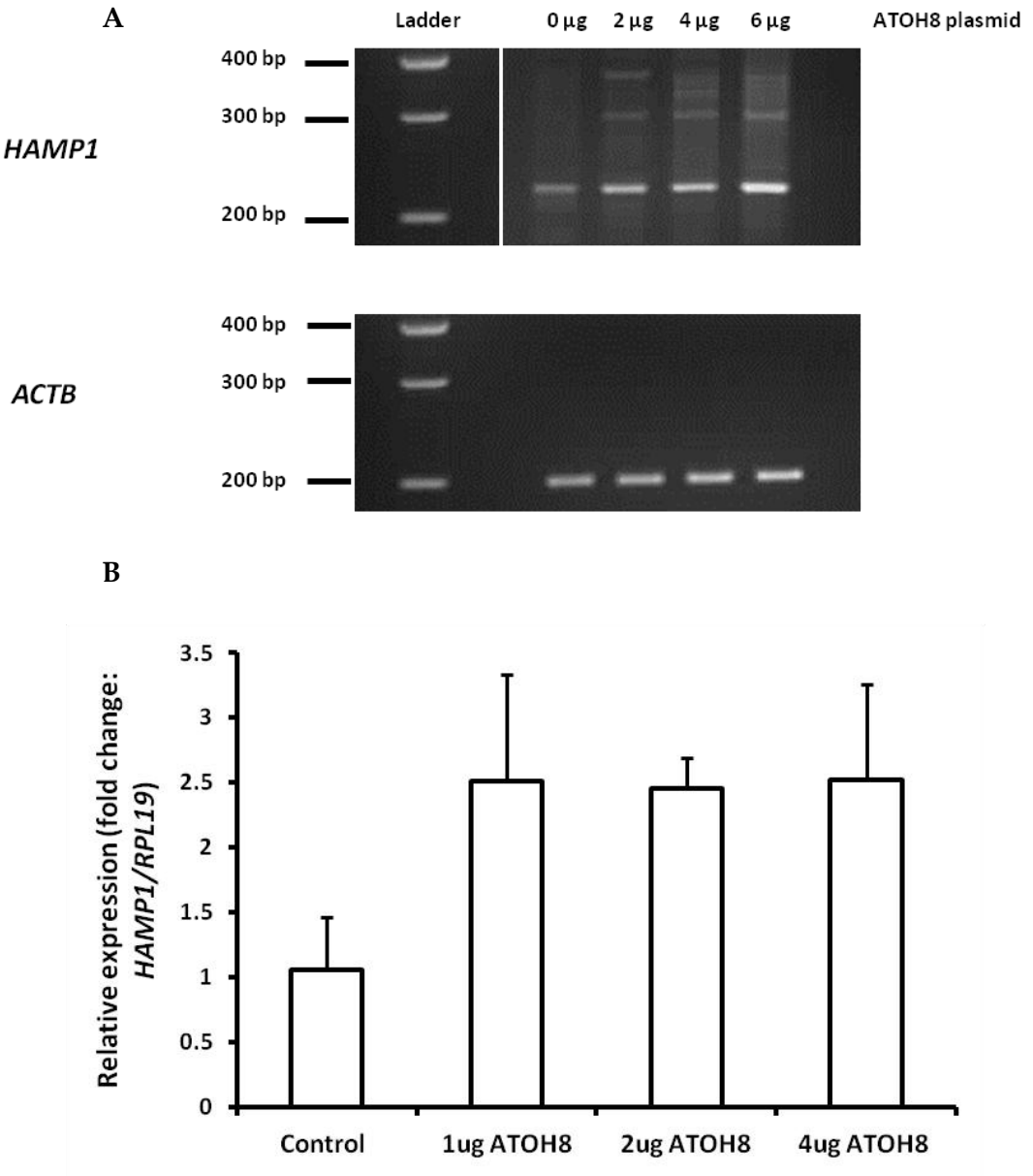

Figure 4.7 Endogenous *HAMP1* mRNA expression in HEK-293 cells transfected with increasing concentrations of ATOH8 plasmid

HEK-293 cells were transfected with increasing amounts of ATOH8 plasmid. *HAMP1* mRNA expression was determined through semi-quantitative PCR (A) where *ACTB* was used as the housekeeping gene, and by real-time PCR (B) where relative mRNA expression was normalized to the housekeeping gene *RPL19*. Data are presented as mean ± SD for fold change as compared with control (n=3 per group). The samples were measured in triplicates. Statistical analysis was performed by 1-way ANOVA with Tukey's post-hoc test.

4.3.2 Mutations in the enhancer elements (E-boxes) and BMP response elements (BMP-RE) reduces hepcidin promoter activation by ATOH8

Two E-Boxes located on the proximal hepcidin promoter were previously shown to bind the basic helix-loop-helix leucine zipper family of transcription factors (b-HLH-ZIP) USF1 and USF2 (Bayele et al., 2006). Given that ATOH8 also belongs to the b-HLH family of transcription factors, the ability of ATOH8 to activate the hepcidin promoter in constructs bearing mutations in the two E-boxes (E-box MUT 1, 2) was explored (Figure 4.8A). This was compared to a WT hepcidin promoter of the same length (0.9kb). As described for the WT 2.7kb promoter, increasing concentrations of ATOH8 plasmid significantly increased the wild type hepcidin promoter. However this effect was ablated in the E-Box mutants (Figure 4.8B). Interestingly, the hepcidin promoter response to ATOH8 was also reduced in constructs which had the BMP-RE1 mutated supporting the notion that ATOH8 also affects BMP signalling.

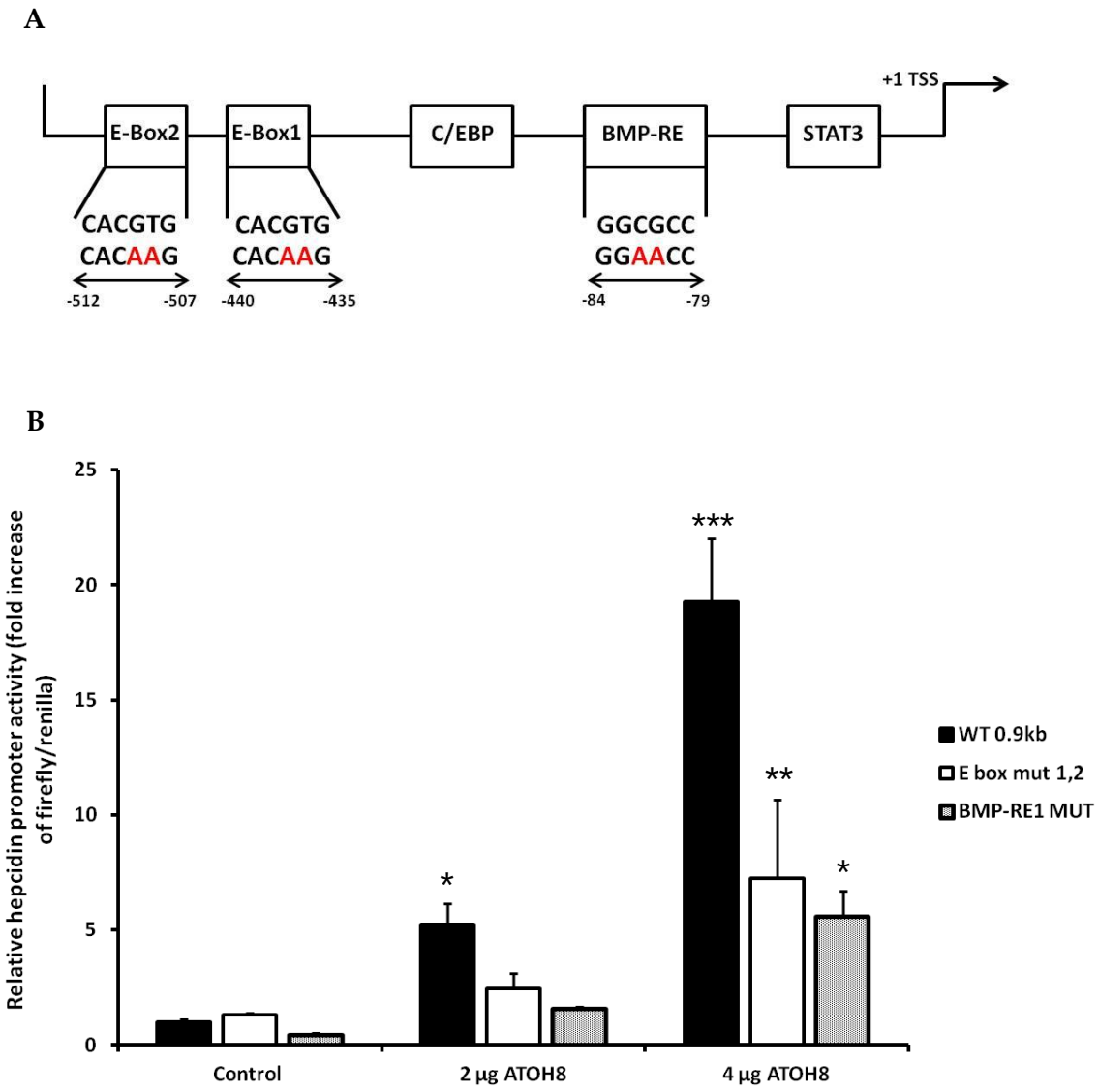

Figure 4.8 Effect of mutations on hepcidin promoter induction by ATOH8 in HEK-293 cells

(A) Schematic representation of the 0.9kb hepcidin promoter. Positions of particular consensus elements and their mutations are highlighted (Matak et al., 2009). (B) The ability of ATOH8 to induce the hepcidin promoter in the absence of known consensus elements, E-box 1,2 and BMP-RE1 were investigated through promoter mutational analysis. HEK-293 cells were transfected with WT 0.9kb, E Box 1,2 mutant or BMP-RE1 mutant hepcidin promoter constructs in the absence or presence of 2- or 4 µg of ATOH8 plasmid. Data are presented as mean ± SD derived from a single experiment with three biological replicates. The experiment shown is representative of 3 similar experiments. Statistical analysis was performed by 1-way ANOVA with Tukey's post hoc test. *$p<0.05$; **$p<0.01$; ***$p<0.001$ for control vs. treatment comparisons.

4.4 Effect of hypoxia and increased erythropoiesis on ATOH8 expression

The hepatic expression of ATOH8 in the HPX mouse model demonstrates that iron loading alone is not the sole regulator of ATOH8 expression. Amongst other factors, the HPX mouse serves as a model for iron-restricted erythropoiesis due to the lack of transferrin (Bartnikas et al., 2011). Therefore, to examine the effects of erythropoiesis on ATOH8 expression in another setting, mice were exposed to hypoxia. *Atoh8* mRNA expression was significantly reduced after 24 hours and 72 hours of hypoxia; ATOH8 protein expression was reduced after 24 hours of hypoxia, with no significant change observed after 72 hours of hypoxia (Figure 4.9 and Figure 4.10). Immunostaining of liver sections demonstrated small reductions in ATOH8 expression after 72 hours of hypoxia. Immunostaining was not conducted in liver section of 24 hours hypoxia treatment due to the poor quality of liver samples (Figure 4.11).

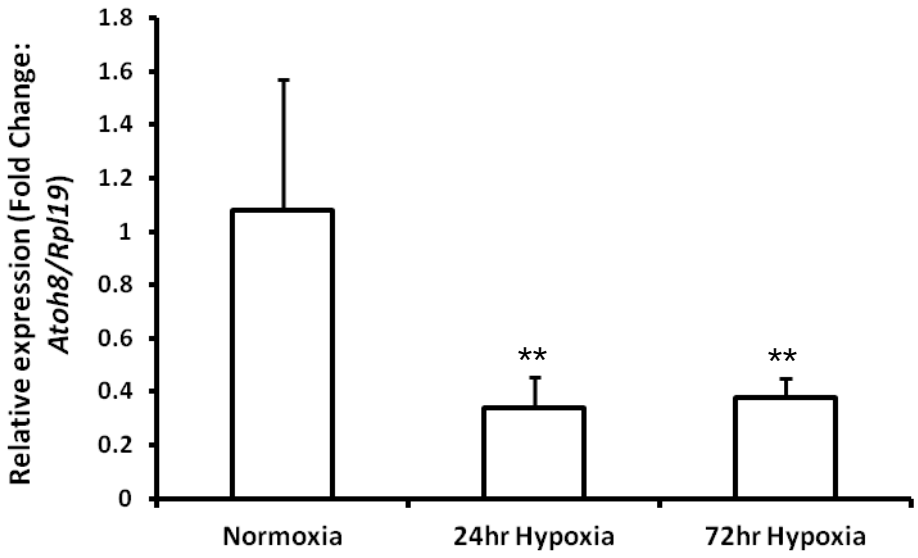

Figure 4.9 Real-time PCR measurement of *Atoh8* mRNA levels in CD1 mice exposed to 24 hours or 72 hours of hypoxia

Liver *Atoh8* mRNA expression was measured in 7 week old male CD1 mice treated with normoxia, 24 hours or 72 hours of hypoxia. Relative mRNA expression was normalized to the housekeeping gene *Rpl19*. Data are presented as mean ± SD for fold change compared with normoxic mice (n=6 per group). The samples were measured in triplicates. Statistical analysis was performed by 1-way ANOVA with Tukey's post hoc test. **p<0.01 for normoxia vs. Hypoxia treatment.

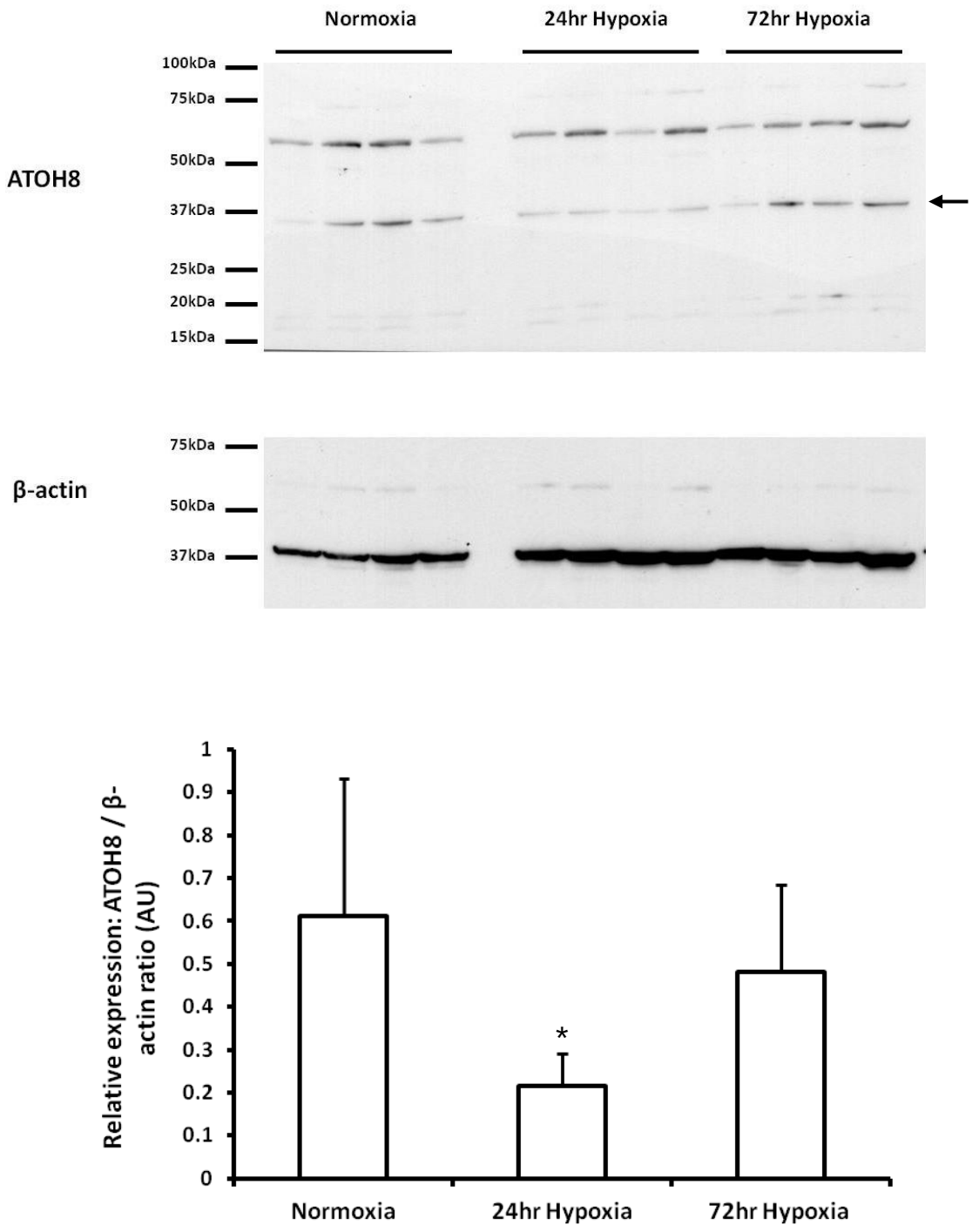

Figure 4.10 Western blot analysis of liver ATOH8 expression after 24 hours and 72 hours of hypoxia

Western blot analysis of liver nuclear protein extracts of 7 week old male CD1 mice treated with normoxia, 24 hours or 72 hours of hypoxia. ATOH8 expression was normalized to the expression of β-actin and presented in arbitrary unit (AU). Densitometry is displayed below the blot. Data are mean ± SD (n=4 for per group). Statistical analysis was performed by 1-way ANOVA with Tukey's post hoc test. *$p<0.01$ for normoxia vs. 24hr hypoxia.

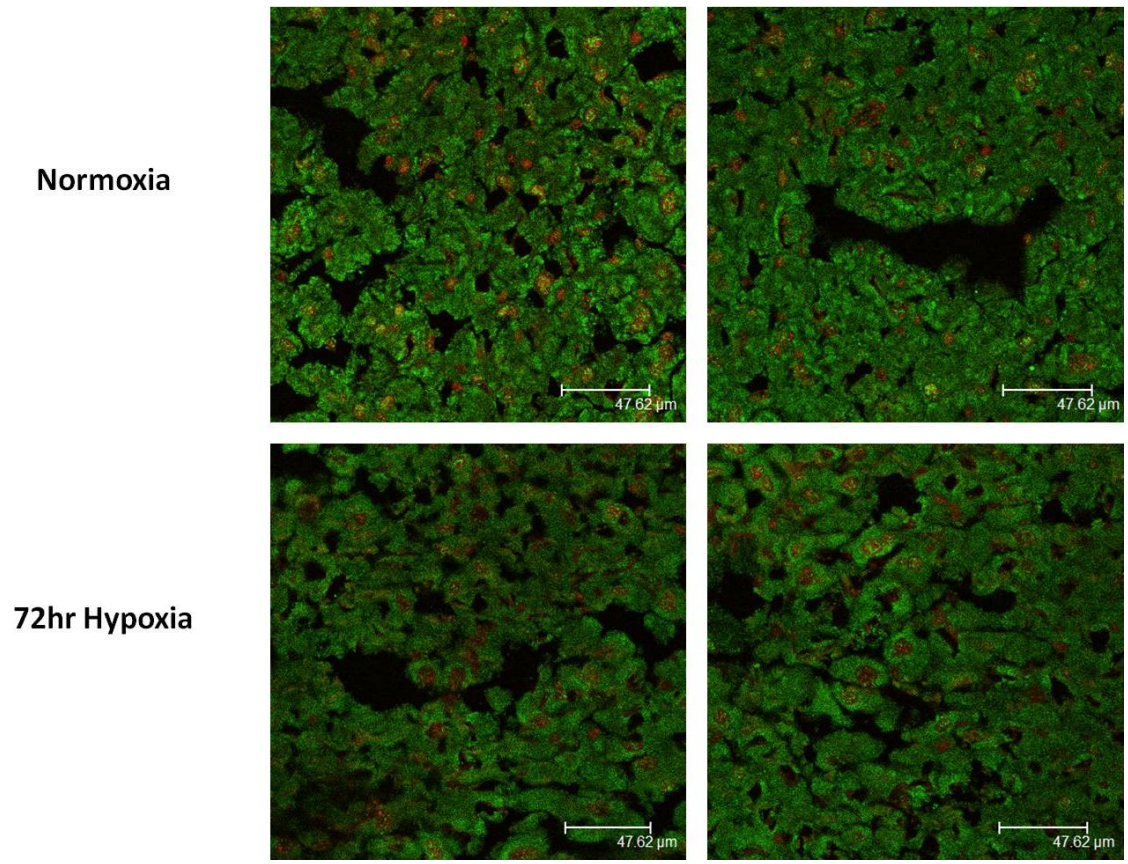

Figure 4.11 Immunofluorescence of liver tissue from normoxic and 72 hours hypoxic treatment stained with ATHO8

The expression of ATOH8 in frozen liver tissues of 7 week old male CD1 mice treated with normoxia and 72 hours of hypoxia were investigated by immunofluorescence technique. ATOH8 protein was visualised as green fluorescence and nuclei were counterstained in red (Leica DM-IRE2 confocal microscope, magnification x630).

4.5 Effects of iron loading and erythropoiesis on ATOH8 expression

The expression of ATOH8 was examined in wild type mice and *Hamp1*$^{-/-}$ mice treated with PHZ in order to investigate the effect of iron loading and haemolytic anaemia (in which there is increased erythropoietic demand) on hepatic ATOH8 expression. The effect of PHZ treatment in wild type mice showed trends towards decreased *Atoh8* liver mRNA expression as measured by real-time PCR (Figure 4.12). The effect of the global hepcidin1 gene disruption caused iron loading and significantly increased both *Atoh8* and *Bmp6* mRNA expression which is in line with previous reports by Kautz et al (Kautz et al., 2008). This effect was significantly decreased upon PHZ challenge in *Hamp1*$^{-/-}$. The effect of PHZ on ATOH8 protein expression was significant in both genotypes as measured by western blotting (Figure 4.13).

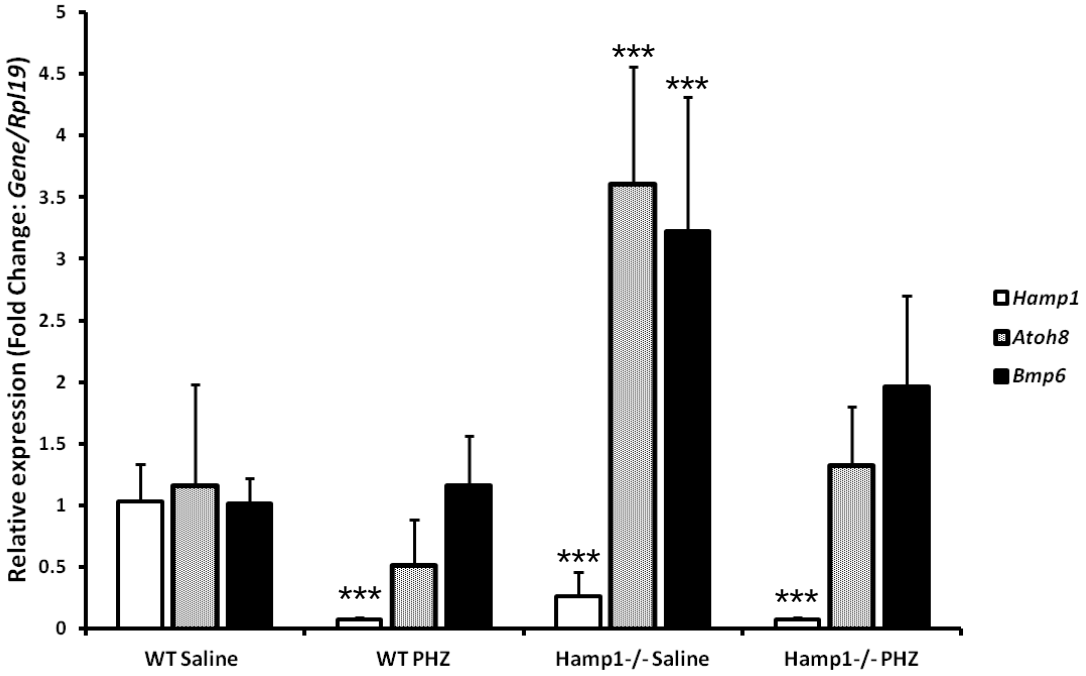

Figure 4.12 Real- time PCR measurement of *Hamp1*, *Atoh8* and *Bmp6* mRNA expression in livers of WT and *Hamp1*$^{-/-}$ mice treated with saline or PHZ

Hepatic *Hamp1*, *Atoh8* and *Bmp6* mRNA expression was measured in Female *Hamp1*$^{-/-}$ mice and wild type littermates (5-7weeks old) treated with saline or PHZ injections. Relative mRNA expression was normalized to the housekeeping gene *Rpl19*. Data are presented as mean ± SD as compared with saline-treated wild type mice (n=5 and 6 for saline-, PHZ treated wild type mice and n=6, 7 for saline-, PHZ-treated *Hamp1*$^{-/-}$ mice respectively). The samples were measured in triplicates. Statistical analysis was performed by 2-way ANOVA with Bonferroni post-hoc test. ***p<0.001 as compared to saline treated WT mice.

Significant effects of genotype: *Hamp1* (p<0.0001), *Atoh8* (p<0.0001), *Bmp6* (p<0.0001)

Significant effects of treatment: *Hamp1* (p<0.0001), *Atoh8* (p<0.0001), *Bmp6* (p<0.05)

Significant interaction: *Hamp1* (p<0.0001), *Atoh8* (p<0.001), *Bmp6* (p<0.05)

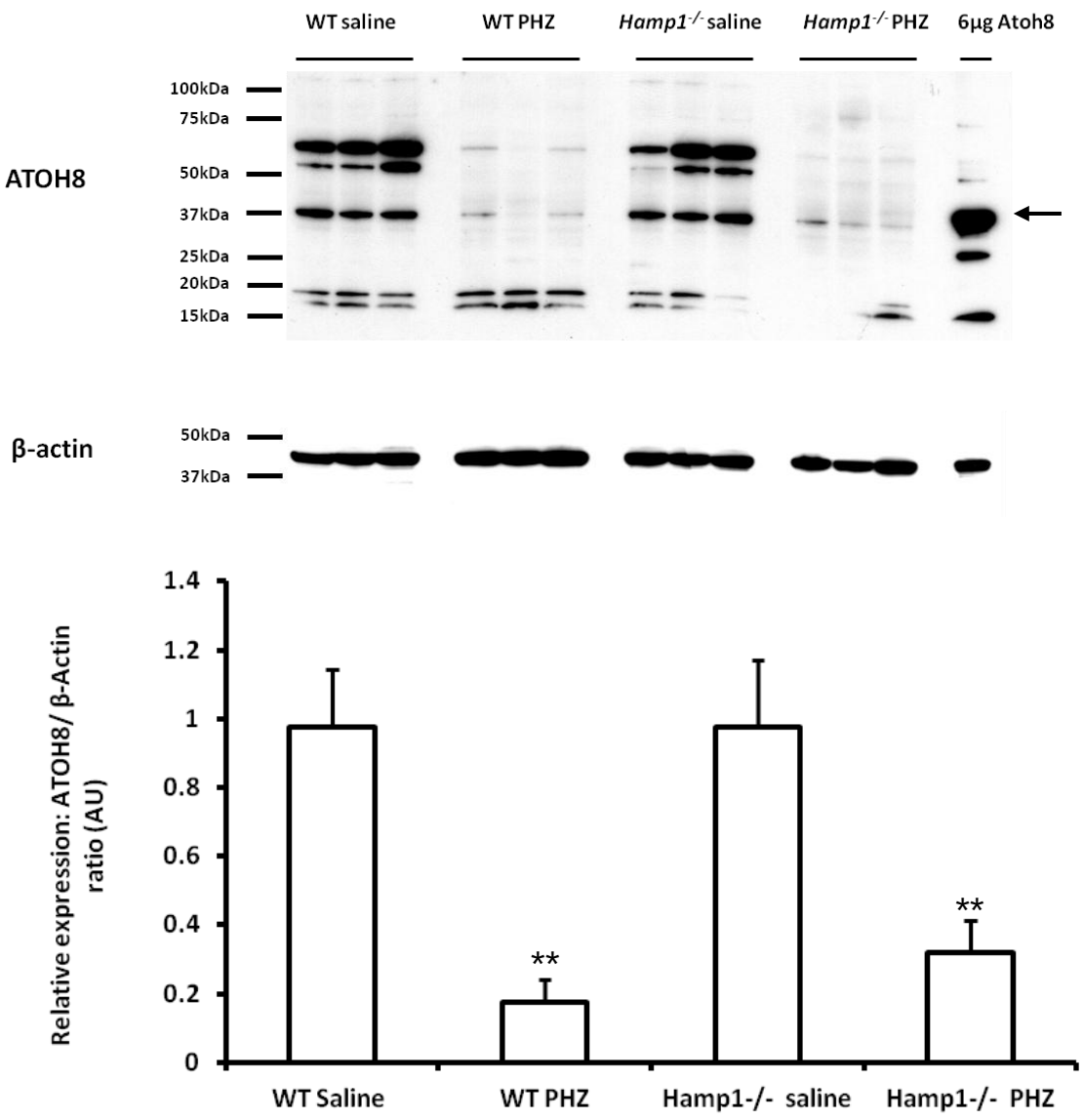

Figure 4.13 Western blot analysis of ATOH8 expression in the liver of WT and *Hamp1*$^{-/-}$ mice treated with saline or PHZ

Western blot analysis of ATOH8 expression in liver nuclear protein extracts of WT mice and *Hamp1*$^{-/-}$ mice treated with saline or PHZ. The expression of ATOH8 (indicated by arrow) was verified by running lysates obtained from HEK-293 cells over-expressing ATOH8. ATOH8 expression was normalized to the expression of β-actin and presented in arbitrary unit (AU). Densitometry is displayed below the blot. Data are presented as mean ± SD (n=3 for per group). Statistical analysis was performed by 2-way ANOVA with a Bonferroni post hoc test. **p<0.01 as compared to saline treated WT mice.

No significant effect of genotype

Significant effect of treatment p<0.0001

No significant interaction

4.6 ATOH8 expression in *HFE*$^{-/-}$ mice

The downstream signalling cascade as a result of HFE gene disruption which reduces hepcidin transcription remains elusive. By utilising the HFE knockout mouse model (*HFE*$^{-/-}$), several studies have accentuated the involvement of the BMP signalling cascade where *HFE*$^{-/-}$ mice, despite having elevated hepatic BMP6 expression due to iron loading, show decreased pSMAD 1,5,8 expression, suggesting an impairment of the BMP signalling cascade (Corradini et al., 2009). Consequently the expression of ATOH8 was assessed in the *HFE*$^{-/-}$ mouse model in order to determine its role in the BMP signalling cascade. Surprisingly, despite the iron loading in *HFE*$^{-/-}$ mouse liver and in contrast to *Hamp1*$^{-/-}$ mice, ATOH8 mRNA and protein expression was not altered (Figure 4.14 and Figure 4.15).

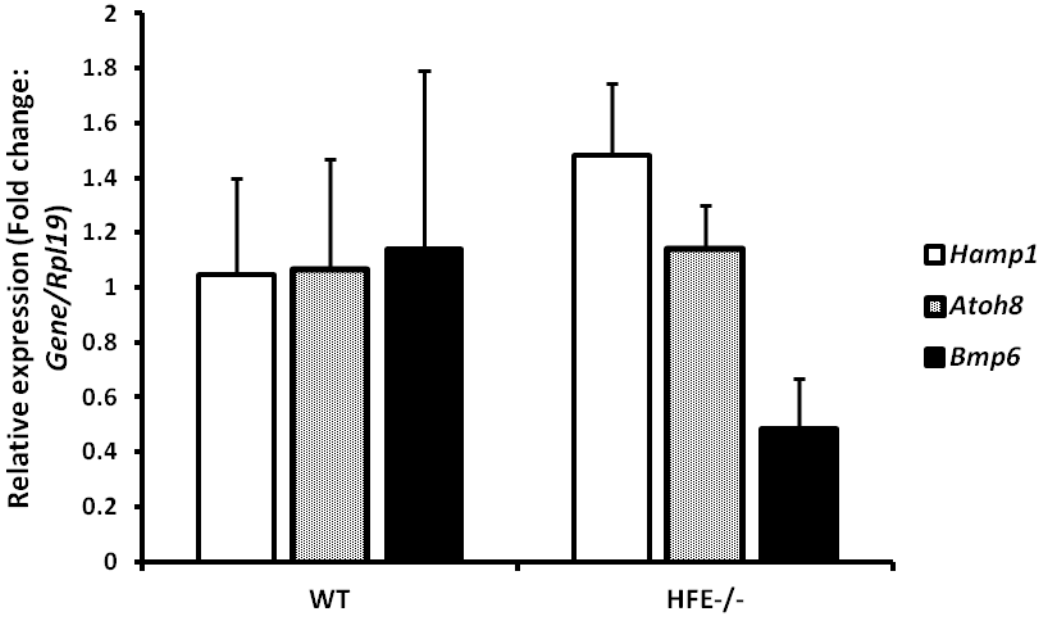

Figure 4.14 Real-time PCR measurement of *Hamp1*, *Atoh8* and *Bmp6* in *HFE*$^{-/-}$ mice

Hepatic *Hamp1*, *Atoh8* and *Bmp6* mRNA expression was measured in 8 week old male WT and *HFE*$^{-/-}$ mice. Relative mRNA expression was normalized to the housekeeping gene *Rpl19*. Data are presented as mean ± SD for fold change compared with WT mice (n=4 per group). The samples were measured in triplicates. Statistical analysis was performed by Student *t*-test.

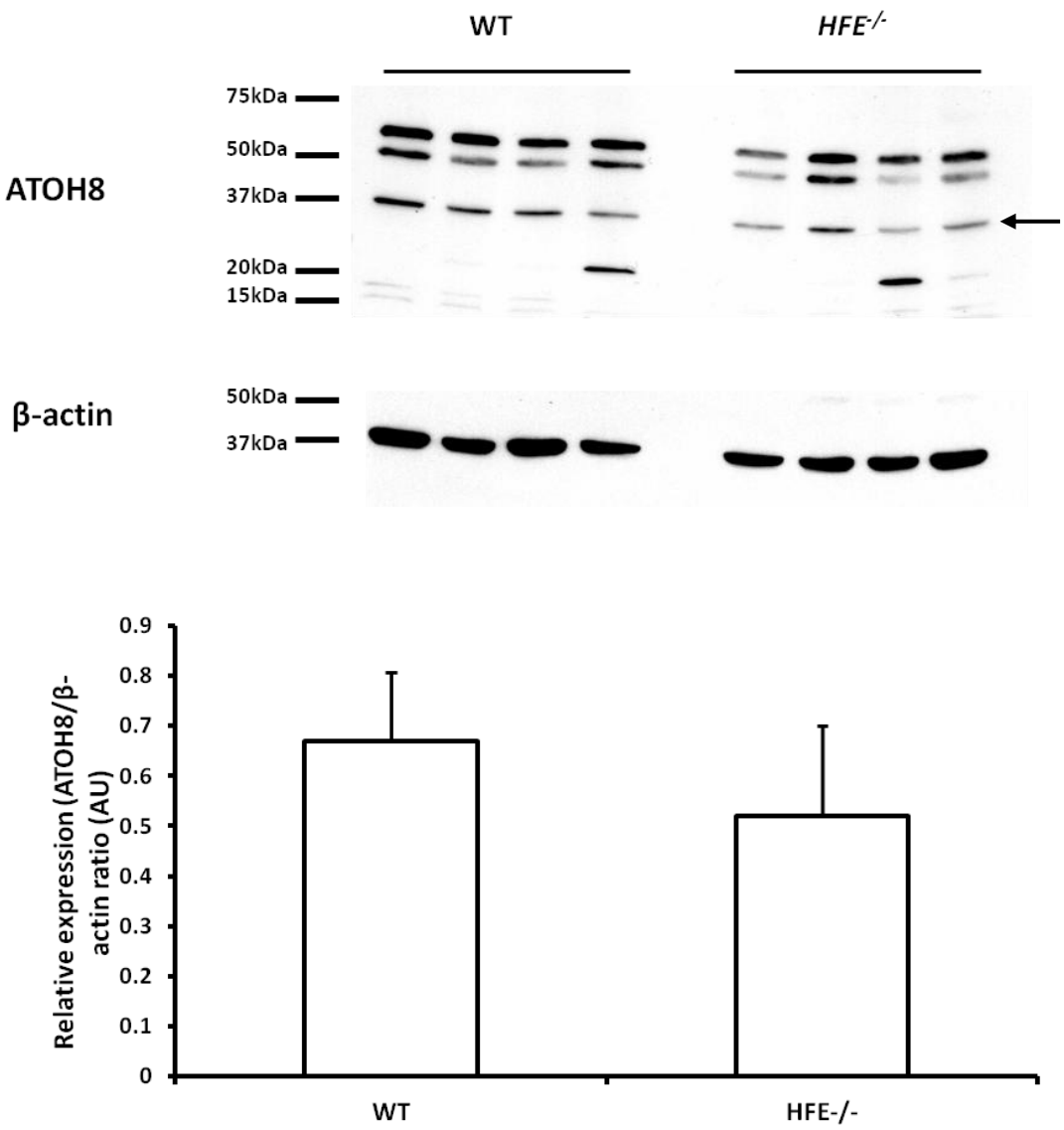

Figure 4.15 Western blot analysis of liver ATOH8 expression in *HFE*$^{-/-}$ mice

Western blot analysis of ATOH8 expression in liver nuclear protein extracts of 8 week old male WT and *HFE*$^{-/-}$ mice. ATOH8 expression (indicated by arrow) was normalized to the expression of β-actin and presented in arbitrary unit (AU). Densitometry is displayed below the blot. Data are presented as mean ± SD (n = 4 for all groups). Statistical analysis was performed with Student's *t*-test.

4.7 Effect of transferrin saturation on *HAMP1* and *ATOH8* mRNA expression *in vitro*

Initial investigations identified ATOH8 to be increased by dietary iron loading and decreased by dietary iron deficiency (Kautz et al., 2008). Both liver iron stores and transferrin saturation change in these experimental settings. In order to investigate the effect of transferrin saturation on *ATOH8* mRNA expression, HepG2 cells were exposed to different ratios of apo- and holotransferrin where *ATOH8* mRNA expression was measured by real-time PCR. *HAMP1* and *ATOH8* mRNA expression showed a steady decrease in expression when treated with increasingly iron-saturated transferrin, where treatment of 100% iron-saturated holotransferrin significantly reduced the expression of *ATOH8* by approximately 5-fold in comparison to iron free apotransferrin treatment (Figure 4.16).

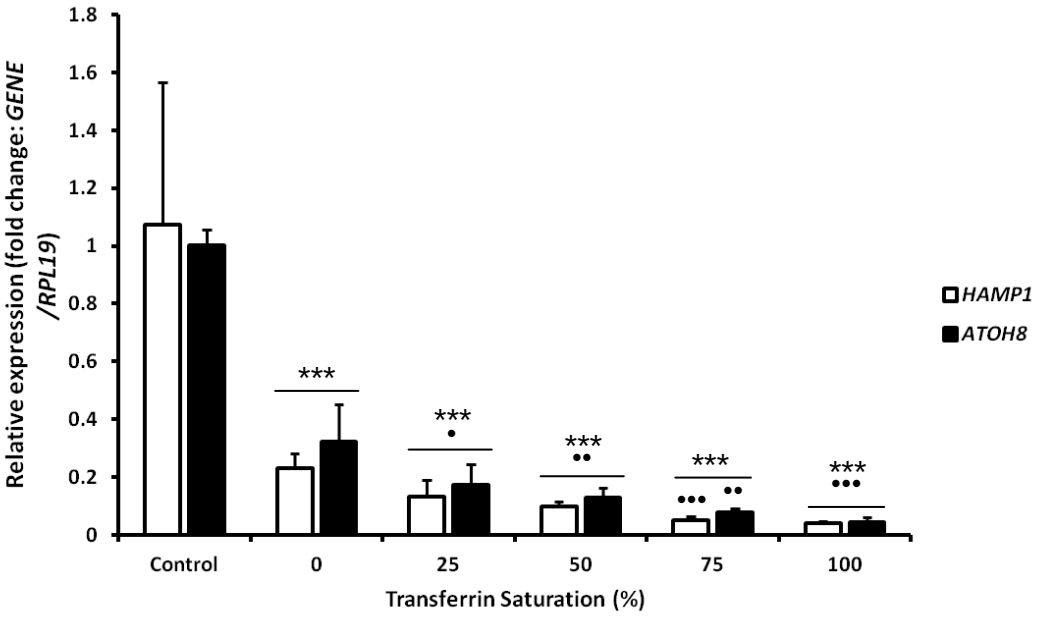

Figure 4.16 Real-time PCR measurement of *HAMP1* and *ATOH8* mRNA expression in response to different transferrin saturation in HepG2 cells

Mixtures of apotransferrin and holotransferrin were added to HepG2 cells at a total transferrin concentration of 30 μM. *HAMP1* and *ATOH8* mRNA expression was measured at each transferrin saturation level and was plotted as fold increase in comparison to untreated cells. Relative mRNA expression(s) was normalised to the housekeeping gene *RPL19*. Data are presented as mean ± SD for fold change compared with control (n=3 per group). The samples were measured in triplicates. Statistical analysis was performed by 1-way ANOVA with Tukey's post-hoc test. ***p<0.001 as compared to control; •p<0.05; ••p<0.01; •••p<0.001 as compared to 0% transferrin saturation.

4.8 Discussion

The present study was designed to determine the role of ATOH8 in the regulation of hepcidin. The findings from the study are consistent with those of Kautz et al who demonstrated the ability of iron to influence *Atoh8* gene expression (Kautz et al., 2008). Through the use of mouse models in which iron metabolism is altered, a striking correlation between the effect of iron and erythropoiesis on ATOH8 expression was observed.

The first line of evidence came from the analysis of hepatic ATOH8 expression in the HPX mouse model. In this model, despite extensive tissue iron loading, the expression of ATOH8 was found to be significantly reduced. The HPX mice used in the current study only received haematologic support for the first few weeks, where mice were able to survive without therapy. In agreement with previous reports by Trenor and colleagues, the liver of these mice was particularly noteworthy for its dark brown colour where iron deposition was seen in both Kupffer cells and hepatocytes (Trenor et al., 2000). Immunostaining studies demonstrated ATOH8 staining to be localised to the hepatocytes in WT mice with reduced staining in the HPX liver.

It was hypothesised that in addition to iron loading, the effect of increased erythropoietic activity or reduced transferrin saturation may also regulate hepatic ATOH8 levels. The effect of increased erythropoiesis on ATOH8 expression was pursued through the induction of acute hypoxia. The hypoxic induction of erythropoietin (EPO) has been extensively studied; EPO serves to prevent apoptosis of developing erythrocytes and therefore increases their viability under hypoxic conditions through the actions of hypoxia inducible factors (see section 1.5.3.2) (Haase, 2010). Although the expression of EPO was not measured in the current study, increased erythropoiesis was assumed from the significant increases in haemoglobin (Hb) levels after 24 and 72 hours of hypoxia (see Table 3.4 chapter 3). The increased exposure to hypoxia was correlated with a significant reduction in hepatic *Hamp1* and

Atoh8 mRNA expression, providing further evidence to support the suggestion that increased erythropoiesis affects hepcidin expression possibly through ATOH8.

Prior studies have associated increased *Atoh8* mRNA expression in the *Hamp1*$^{-/-}$ mouse model which have increased iron stores (Kautz et al., 2008). In this report the authors hypothesised that *Atoh8* may be regulated by iron stores provided that SMAD4 was functional and is a downstream target for BMP signalling induced by dietary iron loading. The present study showed that ATOH8 levels were robustly decreased by treatment with PHZ which causes haemolysis of the erythrocytes and thus increases erythropoietic activity. Upon PHZ injection, haemoglobin levels demonstrated a tendency towards reduced levels in WT mice which correlated with reduced ATOH8 protein expression (17.98±1.63 g/dL in WT PHZ treated, n=6, vs. 19.10±1.28 g/dL in WT saline treated, n=5). Although not significant, haemoglobin levels were increased by PHZ treatment in *Hamp1*-/- however ATOH8 protein and mRNA expression was significantly reduced (24.74±1.64 g/dL in *Hamp1*-/- PHZ treated, n=7, vs. 21.95±0.87 g/dL in *Hamp1*-/-saline treated, n=6) (Masaratana et al., 2012).This evidence provides further support for the notion that *Atoh8* mRNA expression is reduced by increased erythropoietic demand even in the face of iron overload and perhaps anaemia and reinforces the idea that ATOH8 could be involved in the erythropoietic regulation of hepcidin. Although the mice in this study were not significantly anaemic after PHZ treatment, prolonged treatment with PHZ with smaller doses may be more effective and inducing anaemia as was observed by Frazer and colleagues (Frazer et al., 2012).

The regulation of hepcidin is dependent on erythropoietic activity. This was demonstrated through studies in which erythropoiesis was inhibited using carboplatin, doxorubicin, EPO-blocking antibody (Pak et al., 2006) and irradiation or posttransfusion polycythemia (Vokurka et al., 2006). Hepcidin expression was increased upon inhibition of erythropoiesis even when challenged with anaemia or EPO. Additionally the inhibition of erythropoiesis did not affect the ability of the tissue to sense hypoxia as demonstrated by an increase in vascular endothelial growth factor (VEGF) in all mice with or without the treatment with erythropoiesis inhibitors (Pak et

al., 2006). These studies demonstrate that hepcidin was not suppressed by anaemia and hypoxia in absence of erythropoietic activity. Evidence presented throughout this chapter suggests an important role of ATOH8 in the regulation of hepcidin by erythropoiesis. Future studies will focus on hepatic ATOH8 expression under conditions of enhanced erythropoiesis and anaemia to investigate whether ATOH8 is responding to the former, as demonstrated for hepcidin by Pak et al and Vokurka et al (Pak et al., 2006, Vokurka et al., 2006).

It is clear from the *in vivo* investigations conducted in this chapter that multiple stimuli such iron and erythropoietic demands are able to influence both ATOH8 mRNA and protein expression. In each case, the expression of ATOH8 paralleled that of hepcidin. Further investigations were conducted in order to establish whether ATOH8 had a direct effect of on hepcidin transcription. ATOH8 increased hepcidin promoter activity in a dose dependent manner in the absence or presence of BMP stimulation which correlated with increased pSMAD 1,5,8 protein expression. In support of this, mutation of the BMP-RE element reduced ATOH8-dependent hepcidin promoter activity by around 50% demonstrating the potential of ATOH8 to regulate hepcidin transcription thorough pSMAD/SMAD4.

In addition to the BMP-RE's, the enhancer elements (E-Boxes) which have been shown to be occupied by other members of the b-HLH family of transcription factors i.e. USF1 and USF2 and also c-Myc and c-Max were also of particular interest to this study (Bayele et al., 2006). Despite increasing hepcidin transcription *in vitro*, mutations of USF1 and USF2 do not appear to affect hepcidin expression or iron metabolism *in vivo* (Nicolas et al., 2001a). Interestingly, mutation of the E-boxes also reduced the ability of ATOH8 to activate the hepcidin promoter indicating the potential of ATOH8 to bind to the E-box regions. Further studies involving chromatin immunoprecipitation (ChIP) studies would ascertain that the promoter regions highlighted are bound by ATOH8.

The results presented in this chapter could offer an explanation for the recent findings by Frazer and colleagues who report decreased hepatic hepcidin levels, increased BMP6 levels with no change in liver pSMAD 1,5,8 levels in mice treated with PHZ. The authors noted two important findings; firstly that in PHZ treated mice, increased hepatic BMP6 levels failed to elicit an increase in pSMAD 1,5,8 levels and secondly that hepcidin levels decreased without any change in pSMAD1/5/8 levels suggesting SMAD independent suppression of hepcidin (Frazer et al., 2012). In the current study the expression of BMP6 was not changed with PHZ treatment, however hepcidin expression was significantly reduced along with ATOH8 protein expression. This data suggests that a reduction in ATOH8 expression could attenuate BMP signalling via reduction of pSMAD 1,5,8 independently of BMP6 levels by reducing E-box dependent hepcidin transcription.

In addition to the b-HLH transcription factors, HIF-1 was also shown to inhibit hepcidin promoter activity through the binding of putative HRE located at -582bp in the proximal hepcidin promoter (Peyssonnaux et al., 2007). It is noteworthy that these regions lie very close to the E-boxes and therefore it is possible that there may be interaction or interferences between the various transcription factors which are activated by different pathways. The crosstalk between pathways will require further clarification.

HFE knockout mice are phenotypically iron loaded due to impaired hepcidin production. A trend towards decreased ATOH8 expression was observed in the *HFE*$^{-/-}$ mouse model. However the expression of hepcidin appeared to be unaffected. This could be interpreted in a few ways; firstly, age-related changes between WT and *HFE*$^{-/-}$ mice have previously been reported where younger mice of 4-week of age have significantly reduced hepatic hepcidin expression compared to mice which are of 8-weeks of age (which was the age used in the present study), where hepcidin expression was not statistically different between WT and *HFE*$^{-/-}$ (Ahmad et al., 2002). Furthermore, the background strains of mice have been shown to respond differently to HFE mutations where mice of the AKR strain are more susceptible to iron loading

compared to the C57BL/6 which is what was used for analysis in the present study (Fleming et al., 2001, Simpson et al., 2003). The fact that ATOH8 levels did not increase in *HFE*$^{-/-}$ mice despite the liver iron loading is intriguing and may indicate that HFE is required for ATOH8 regulation. Further studies in *HFE*$^{-/-}$ mice will be required to confirm this.

Hepcidin can be regulated by both serum and liver iron levels perhaps independently as demonstrated in studies where mice challenged with acute or chronic iron administration through dietary intervention (Corradini et al., 2011). Mice treated with PHZ displayed increased liver iron stores (demonstrated by increased BMP6 expression) with reduced serum diferric-transferrin and increased apotransferrin levels (Frazer et al., 2012). It seems unlikely that ATOH8 is predominantly regulated by iron stores as PHZ treatment significantly reduced its expression. Therefore changes in the ratios of apo-to holotransferrin levels could be a factor regulating ATOH8 levels. In support of this, treatment of HepG2 cells with either apo- or holotransferrin significantly reduced *ATOH8* mRNA expression. Previous reports have outlined the inconsistencies that exist with an *in vitro* system that mimics *in vivo* conditions of iron loading. The current study outlines the lack of *HAMP1* mRNA expression from treatment of HepG2 cells with holotransferrin. The reasons for this are not fully understood and are thought to be due to the loss of liver-specific gene expression over prolonged time periods in the absence of differentiation-promoting factors (Lin et al., 2007). As a result of immortalisation, some effects one observes *in vivo* cannot be mimicked with an *in vitro* system in an immortalised cell line such as HepG2 cells. It is possible that *ATOH8* expression may change in response to changes in either holo- or apotransferrin which could be sensed by the hepatocyte via the HFE/TfR1 and TfR2 complex, leading to signals which increase ATOH8 expression. However further work in primary hepatocytes will be required to confirm this. Additionally, the transferrin used in the current study was sourced from a commercial company and may have contained contaminants which could have contributed to the reduction in hepcidin and Atoh8 expression. Future studies will involve precise analysis of the transferrin by HPLC prior to experimental use to establish the baseline transferrin saturation. Furthermore, the current study was carried out in the absence of serum

supplementation to the cell culture media. Previous studies have shown that serum affects hepcidin (Ramey et al., 2009). This may have also contributed to the reduction in hepcidin and/or Atoh8 expression. Further studies would test the effect of serum supplementation in the culture media.

Recent studies have demonstrated the ability of HJV to interact with HFE and/or TfR2 (D'Alessio et al., 2012). The authors hypothesised that increased diferric iron levels in plasma as well as increased expression of TfR2 and/or HJV may trigger the release of HFE from TfR1 causing increased hepcidin expression through modulation of the BMP/SMAD signalling cascade (D'Alessio et al., 2012). Whether ATOH8 is a downstream target of HFE or TfR2 requires further investigation perhaps through the use of HFE and TfR2 KO mice.

In summary, the studies carried out in this chapter have shown that a previously little studied iron regulated gene, *Atoh8*, is significantly influenced erythropoietic demand and moreover can regulate hepcidin levels. ATOH8 was able to influence hepcidin transcription through the actions of the BMP/SMAD signalling cascade and E-box' regions. Further clarification of this binding needs to be carried out, taking into consideration the potential of other transcription factors that could be co-operating to induce hepcidin transcription. The expression of other signalling pathways such a MAPK/ERK1,2 was not analysed in the current study and the crosstalk between pathways (if any) will require further clarification. Prior studies have shown the effect of transferrin saturation on hepcidin expression; however the intracellular signalling pathway involved in this regulation has not been clarified. Preliminary investigations have identified ATOH8 to be a potential candidate that could be influenced by changes in either holo- or apotransferrin which in turn could be signalling via HFE/ TfR2 complex possibly through interactions with the BMP/SMAD4 pathway. Taken together, these findings add another dimension to the complex regulatory mechanisms that are already known to influence hepcidin transcription. The ability of ATOH8 to be regulated both by iron and erythropoiesis makes it an attractive candidate for future

studies which will involve analysis of any regulatory elements contained with its promoter sequences.

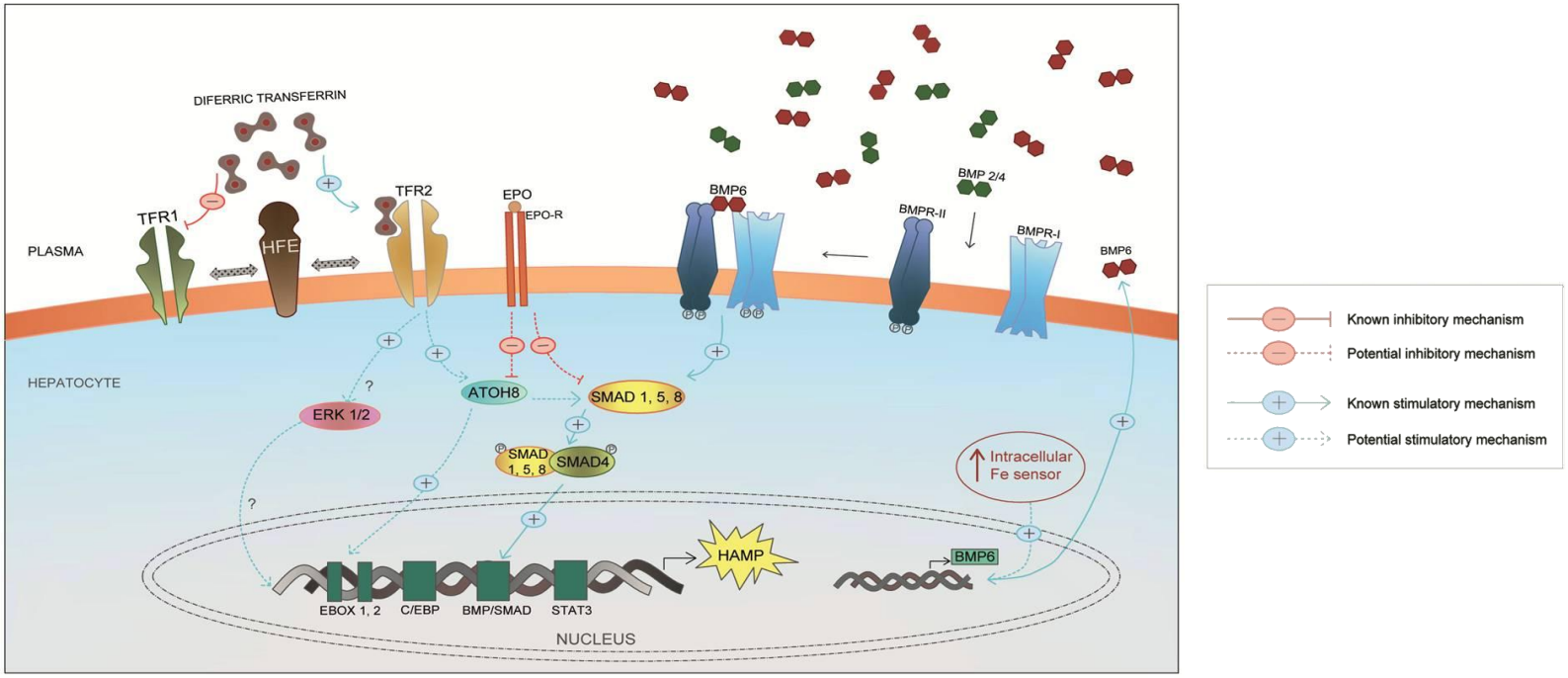

Figure 4.17 Regulation of hepcidin transcription by ATOH8

Increased hepatic intracellular iron stores increases the expression of BMP6 mRNA and protein expression. The binding of BMP6 to BMPR-I/II stimulates hepcidin transcription via the BMP/SMAD signalling cascade which is facilitated by the BMP co-receptor HJV. The studies conducted in this chapter identified ATOH8 as a potential downstream transcription factor which could potentiate hepcidin transcription through the BMP/SMAD signalling cascade as well as binding to E-Box regions located on the hepcidin promoter. Liver ATOH8 mRNA and protein levels were markedly downregulated *in vivo* under several conditions with increased erythropoietic activity including: haemolytic anaemia; hypotransferrinaemia and hypoxia. The erythroid signal modulating ATOH8 remains to be identified. Levels of ATOH8 may also be modulated by changes is diferric transferrin levels, which acts via the iron-sensing molecules. Increased diferric transferrin levels, promotes the binding of HFE to TfR2 and stabilises it. The HFE-TfR2 then potentiates BMP-receptor signalling possibly through modulation of ATOH8. Additional pathways such as the MAP kinase/ERK1/2 pathway, may also be participating in the regulation of hepcidin.

Chapter 5 .

The regulation of hepcidin by other potential modulators of BMP signalling: BMP8b and von Willebrand Factor C

5.1 Introduction

BMP8 belongs to the 60A subfamily of BMP proteins (Zhao et al., 1998) and exists as two highly related and closely linked genes namely, BMP8a and BMP8b found on chromosome 4 in mice and humans (Zhao and Hogan, 1996). Despite their similarities, the expression profile of each gene has been shown to be variable. The expression of BMP8a was reported to be high in the maternal elements of the placenta however the expression of BMP8b was shown to be in the male germ cells (Zhao et al., 1996, Zhao and Hogan, 1996). Unlike many of the other BMP knockout mice, BMP8a and BMP8b deficient mice appear to be healthy and viable implying a redundant role in the developmental stages. Of the two genes, mice homozygous for the mutant allele in BMP8b demonstrated impaired development of the male germ cells however BMP8a mutant mice failed to show any obvious germ cell defects. Investigators ascribe the role of BMP8a to be important in the maintenance rather than the induction of spermatogenesis (Zhao et al., 1996, Zhao et al., 1998).

Studies have demonstrated that the members of the 60A class are often co-expressed with members of the DPP class (BMP2 and BMP4) in numerous tissues and cell types (Ying et al., 2001). BMPs are functionally active as dimers where heterodimeric complexes have been shown to be more potent at activating BMP signalling than homodimeric complexes (Valera et al., 2010), thus increasing the variability of the downstream effector molecules. This was evidenced for BMP8b and BMP4 in the induction of primordial germ cells (PGCs), where a combination of BMP8b and BMP4 was more effective for the induction of PGCs compared to homodimers (Ying et al., 2000).

Although the roles of each of these proteins have been established, the mechanism by which BMP8a and BMP8b proteins mediate their effects are still poorly understood. Recent investigations have demonstrated the importance of BMP8b in the regulation of thermogenesis. BMP8b was shown to stimulate the p38-MAP kinase pathway in brown

adipocytes where the transcription factor, cAMP-responsive element binding protein (CREB), was implicated to be a potential downstream target of BMP8b (Whittle et al., 2012). The involvement of this pathway in spermatogenesis however requires further investigations.

The biological activities of BMPs are largely influenced by extracellular modulators, allowing many of the BMPs to have a dual function. Chordin is one of the most extensively studied BMP modulators which has shown to bind to BMP proteins through four cysteine rich (CR) regions similar to those found in the extracellular protein von Willebrand factor C (VWC) (Larrain et al., 2000, Sasai et al., 1994). The VWC domain has a common conserved CXXCXC and CCXXC consensus where its expression has been noted in approximately 70 human extracellular proteins (Zhang et al., 2007b). The expression of VWC domains has also been noted in the chordin family member CV-2/BMPER (chapter 3). BMPER has 5 closely spaced VWC domains at its N-terminal region, where truncation studies have demonstrated the first VWC domain to be important for the binding of BMP2 (Zhang et al., 2007b).

In addition to genes discussed in previous chapters (BMPER and ATOH8) the expression of BMP8b and VWC, were also identified by microarray analysis, to be significantly increased in the HPX mouse liver (McKie unpublished data). The expression of BMP8b was not found to be reported in any of the iron related disorders and hence the potential of BMP8b to modulate hepcidin was further explored. Following on from the negative regulation of hepcidin by BMPER (chapter 3), since VWC domains bind to BMPs with high affinities, the potential of the VWC domains alone to inhibit BMP signalling were thus investigated. The expression of BMP8b and VWC were also investigated in various mouse models of altered iron metabolism along with the effects of BMP8b and VWC on the hepcidin promoter.

5.2 BMP8b Expression in Hypotransferrinaemic mouse liver (HPX)

The overexpression of BMP8b in the HPX mouse liver was confirmed by real-time PCR and western blot analysis (Figure 5.1A and Figure 5.2). The levels of *Hamp1* mRNA transcripts were measured previously (Figure 3.1, chapter 3). The mRNA expression of other BMP proteins (*Bmp2*, *Bmp4* and *Bmp6*) was also measured by real-time PCR (Figure 5.1B). The mRNA expression of *Bmp6* and *Bmp8b* were significantly upregulated amongst the BMP molecules analysed.

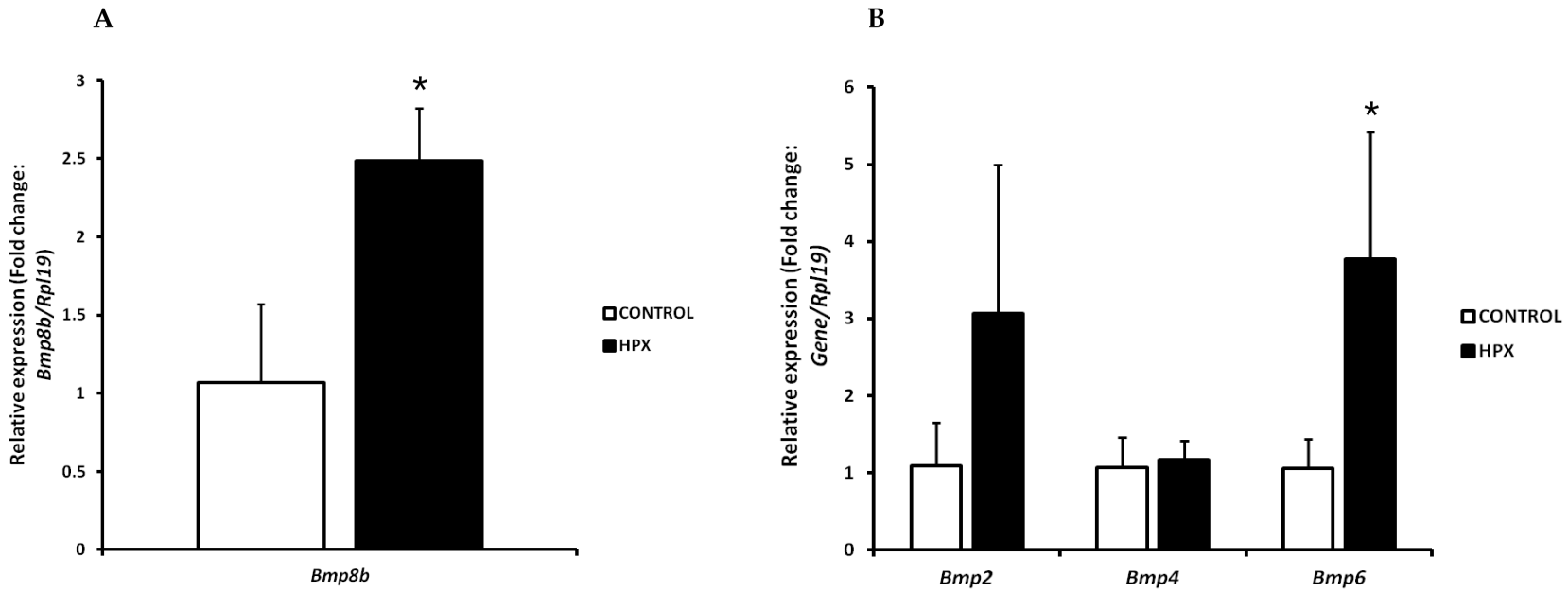

Figure 5.1 Real-time PCR measurement of *Bmp8b*, *Bmp2*, *Bmp4* and *Bmp6* mRNA expression in HPX mouse liver

Liver mRNA expression levels of *Bmp8b*(A), *Bmp2*, *Bmp4* and *Bmp6* (B) were measured in 10-11 week old male HPX mice. Wild type and heterozygous mice were used as controls. Relative mRNA expression was normalised against the house keeping gene *Rpl19*. Data are presented as mean ± SD for fold change compared with wild type and heterozygous mice (n=3 per group). The samples were measured in triplicate. Statistical analysis was performed by Student *t*-test. *p<0.05 for CONTROL vs. HPX comparisons.

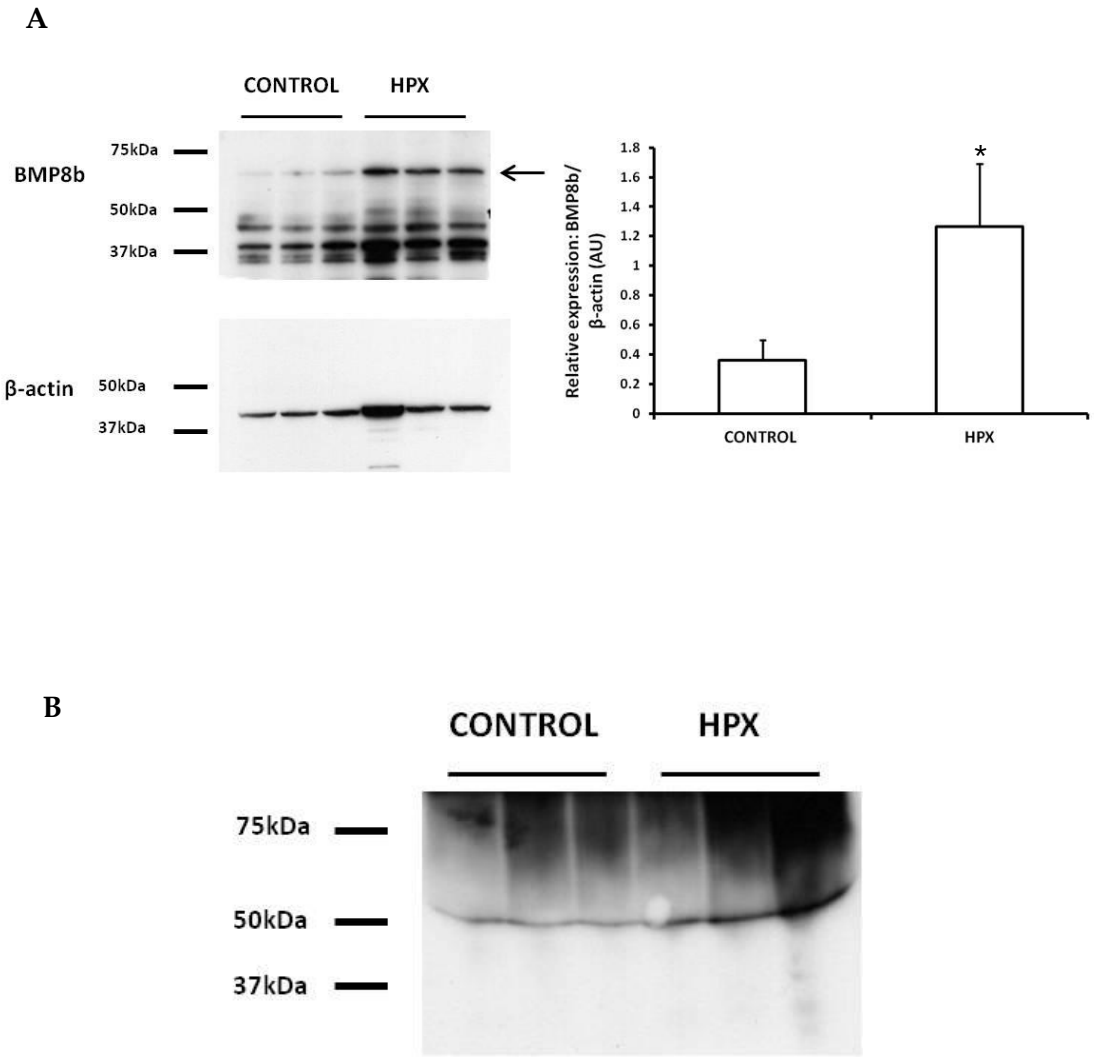

Figure 5.2 Western blot analysis of liver and serum BMP8b expression in HPX

Western blot analysis of (A) liver and (B) serum of 10-11 week old male HPX mice (n=3). Wild type and heterozygous mice were used as controls. BMP8b expression (indicated by arrow) was normalised to the expression of β-actin and presented in arbitrary units (AU). Densitometry is displayed next to the blot. Data are presented as mean ± SD. Statistical analysis was performed by Student *t*-test. *$p<0.05$ for CONTROL vs. HPX comparisons.

5.3 Effect of BMP8b on hepcidin promoter activity

5.3.1 Recombinant BMP8b peptide

The pGL3 vector expressing 2.7kb of the human hepcidin promoter encompassing the BMP-REs was utilised together with controls in which the BMP-RE2 was mutated. The expression vectors were transiently transfected into the HepG2 cells which were then treated with recombinant BMP peptides (BMP4/6) in the absence and presence of 40 to 100 times excess BMP8b peptide.

The results showed that BMP8b peptide significantly enhanced BMP6 dependent hepcidin promoter activity (Figure 5.3A). However no such response was noted in BMP4 dependent hepcidin promoter activity (Figure 5.3B).

5.3.2 BMP8b plasmid constructs

HEK-293 cells were transfected with the human hepcidin promoter along with increasing concentrations of BMP8b plasmid ranging from 2 to 6 micrograms in the presence or absence of BMP2 stimulation (Figure 5.4A). Phosphorylated SMAD 1,5,8 (pSMAD 1,5,8) protein expression was measured by western blot analysis (Figure 5.4B). BMP8b plasmid was able to significantly reduce the BMP2 dependent hepcidin promoter induction without significantly altering pSMAD 1,5,8 protein expression.

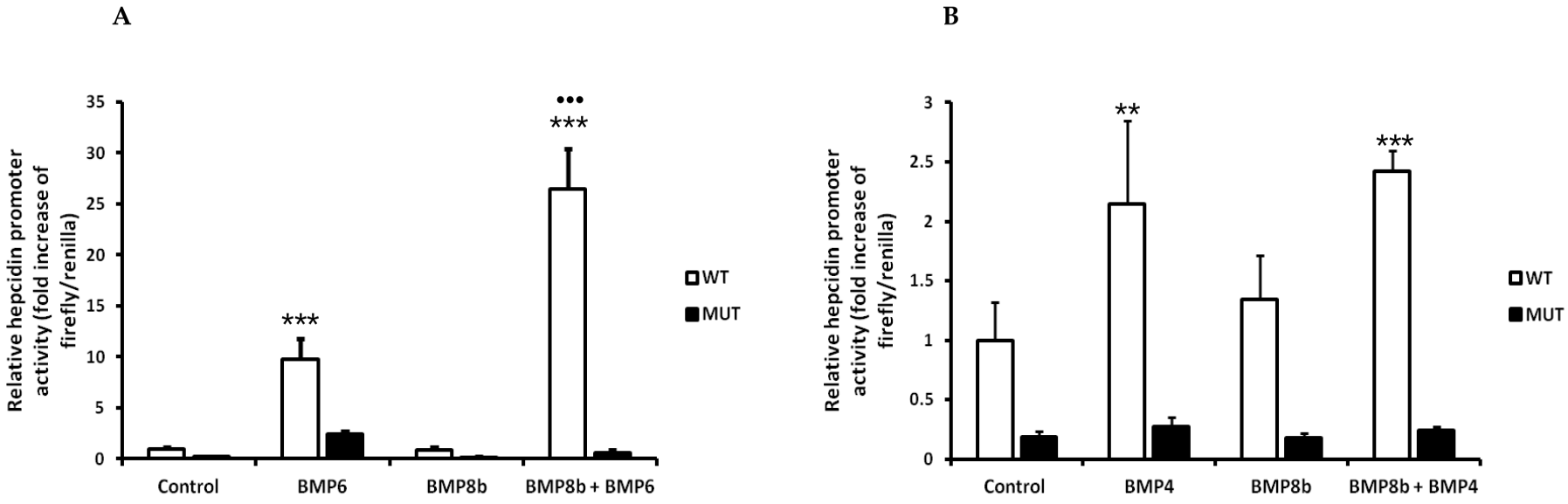

Figure 5.3 Effects of BMP8b on BMP6- and BMP4-dependent hepcidin promoter activity in HepG2 cells

HepG2 cells transiently transfected with the wild type 2.7kb (WT) hepcidin promoter, along with the BMP-RE2 mutant (MUT) were treated with (A) 25ng/mL BMP6 or 2500ng/mL BMP8b or a combination of both; or (B) 25ng/mL BMP4 and 1000ng/mL BMP8b or a combination of both. Data are presented as mean ± SD derived from a single experiment with three biological replicates. The experiment shown is representative of 3 similar experiments. Statistical analysis was performed by 1-way ANOVA with Tukey's post hoc test. **p<0.01;***p<0.001 for –BMP6/4 vs. treatment; •••p<0.001 for +BMP6 vs. BMP6+BMP8b.

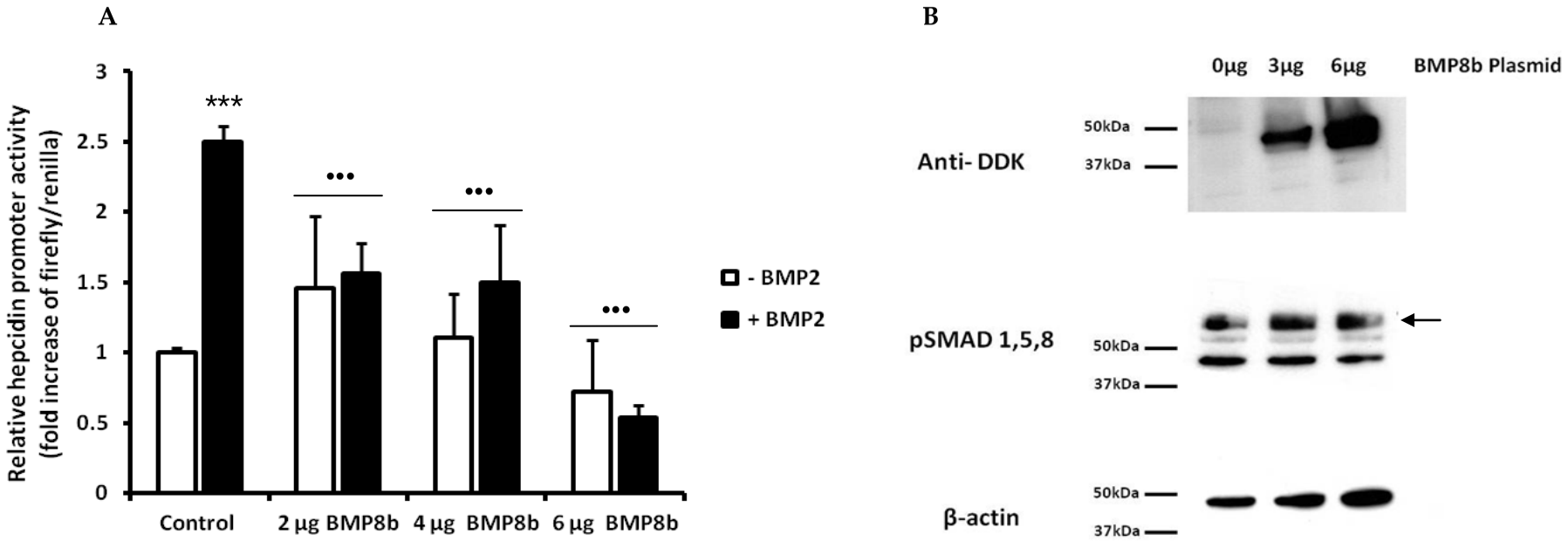

Figure 5.4 Effect of BMP8b plasmid on hepcidin promoter activity and pSMAD 1,5,8 expression in HEK-293 cells

(A) HEK-293 cells were transiently co-transfected with the wild-type 2.7kb hepcidin promoter construct and 2, 4 or 6 µg of BMP8b plasmid before being treated with 25ng/ml BMP2. Samples were compared against the wild type hepcidin promoter without BMP2 treatment. Data are presented as mean ± SD derived from a single experiment with three biological replicates. The experiment shown is representative of 3 similar experiments. Statistical analysis was performed by 1-way ANOVA with Tukey's post hoc test. ***$p<0.001$ for -BMP2 vs. treatment; •••$p<0.001$ for +BMP2 vs. treatment comparison. (B) HEK-293 cells were transfected with 3 or 6 µg of BMP8b plasmid for 16-18 hours. The expression of the BMP8b plasmid was detected by an anti-DDK antibody. pSMAD 1,5,8 levels were determined in the same samples and were normalised to the expression of β-actin.

5.4 Effect of iron loading and haemolytic anaemia on BMP8b expression

HPX mouse is a complex model which has secondary iron overload with chronic anaemia, low levels of transferrin, and increased erythropoietic drive (Trenor et al., 2000). The effects of these factors were investigated individually. A model of iron loading was induced by intramuscular injection of iron dextran (Fe dextran); haemolytic anaemia was induced by intraperitoneal injection of phenylhydrazine (PHZ 60mg/kg body weight). *Hamp1* and *Bmp8b* expression was measured by real-time PCR (Figure 5.5). In agreement with previous reports, the mRNA expression of *Hamp1* increased and decreased upon iron dextran and PHZ treatment respectively (Nicolas et al., 2002b). Interestingly, *Bmp8b* mRNA expression altered in the same direction as hepcidin after both Fe dextran and PHZ treatment indicative of a correlation between the two genes (Figure 5.5).

This was investigated further through the use of a model in which iron loading and haemolytic anaemia co-exist. *Hamp1*$^{-/-}$ mice, which are characteristically iron loaded, were treated with PHZ to induce haemolysis as described previously (Masaratana et al., 2012). The mRNA expression of *Bmp8b* in this mouse model did not retain the same expression pattern observed when the factors (iron loading or PHZ) were manipulated individually (Figure 5.6). Two-way ANOVA indicated a significant effect of genotype with no significant effect of treatment on *Bmp8b* expression, implying the effect of haemolysis in this model had no effect on *Bmp8b* expression.

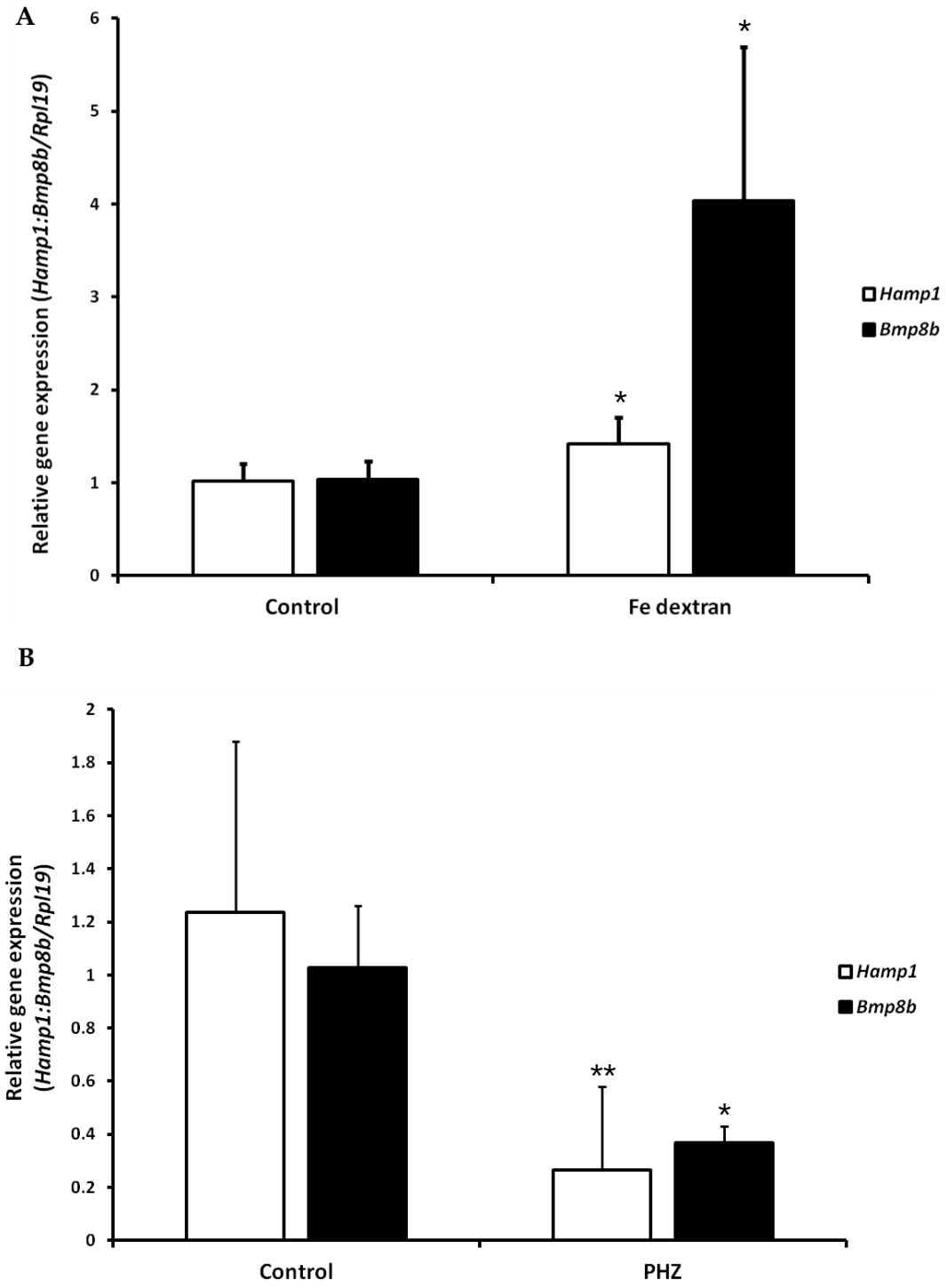

Figure 5.5 Real-time PCR measurement of *Hamp1* and *Bmp8b* mRNA levels in CD1 mice treated with iron dextran or phenylhydrazine

Liver *Hamp1* and *Bmp8b* levels were measured in 6 week old male CD1 mice (n=6) treated with iron dextran (A) or phenylhydrazine (B). Relative mRNA expression was normalised to the housekeeping gene *Rpl19*. Data are presented as mean ± SD for fold change compared to control (n=6 per group). The samples were measured in triplicates. Statistical analysis was performed by Student *t*-test. *p<0.05; **p<0.01 for Control vs. PHZ/Fe dextran.

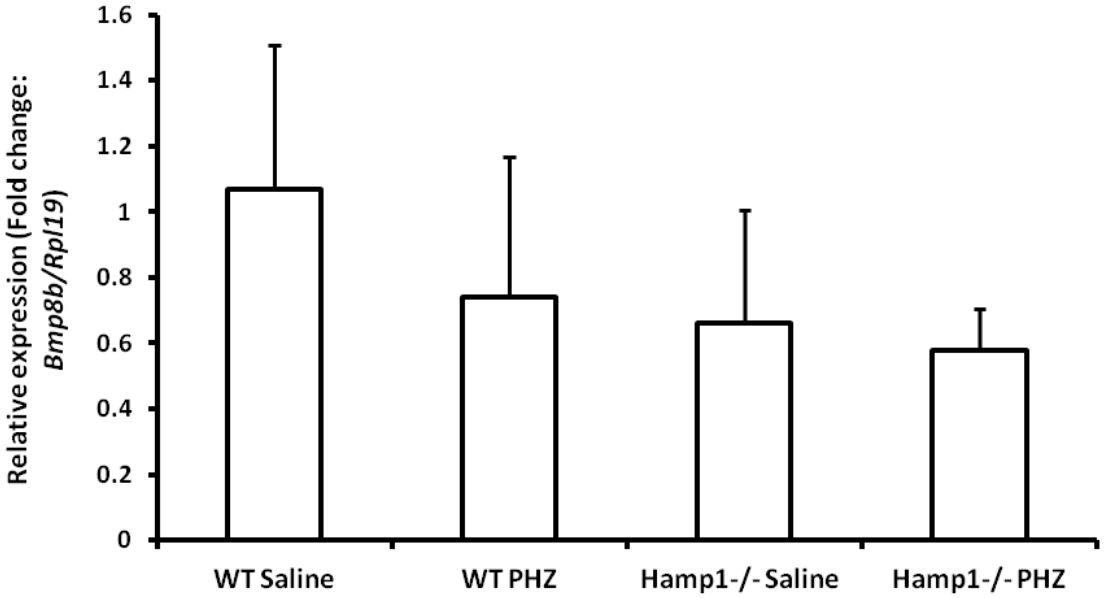

Figure 5.6 Real-time PCR measurement of *Bmp8b* mRNA expression in livers of WT and *Hamp1*$^{-/-}$ mice treated with saline or PHZ

Liver *Bmp8b* levels was measured in WT and *Hamp1*$^{-/-}$ treated with saline or phenylhydrazine. Relative mRNA expression was normalised to the housekeeping gene *Rpl19*. Data are presented as mean ± SD as compared with saline-treated wild type mice (n=5 and 6 for saline-, PHZ treated wild type mice and n=6, 7 for saline-, PHZ-treated *Hamp1*$^{-/-}$ mice respectively). The samples were measured in triplicates. Statistical analysis was performed by 2-way ANOVA with Bonferroni post-hoc test.

Significant effects of genotype: *Bmp8b* (p=0.049)

No Significant effect of PHZ treatment: *Bmp8b* (p=0.150)

No Significant interaction: *Bmp8b* (p=0.388)

5.5 VWC expression in Hypotransferrinaemic mouse liver (HPX)

The expression of BMPER was shown to be significantly increased in the HPX mouse liver (Figure 3.1, chapter 3). The VWC domains of BMPER have been shown to bind BMPs; thus the expression of VWF (a monomer encompassing VWC) was investigated in the same mouse model. The expression of BMPER was mirrored by a significant increase in the expression of VWF at both mRNA and protein level (Figure 5.7 and Figure 5.8).

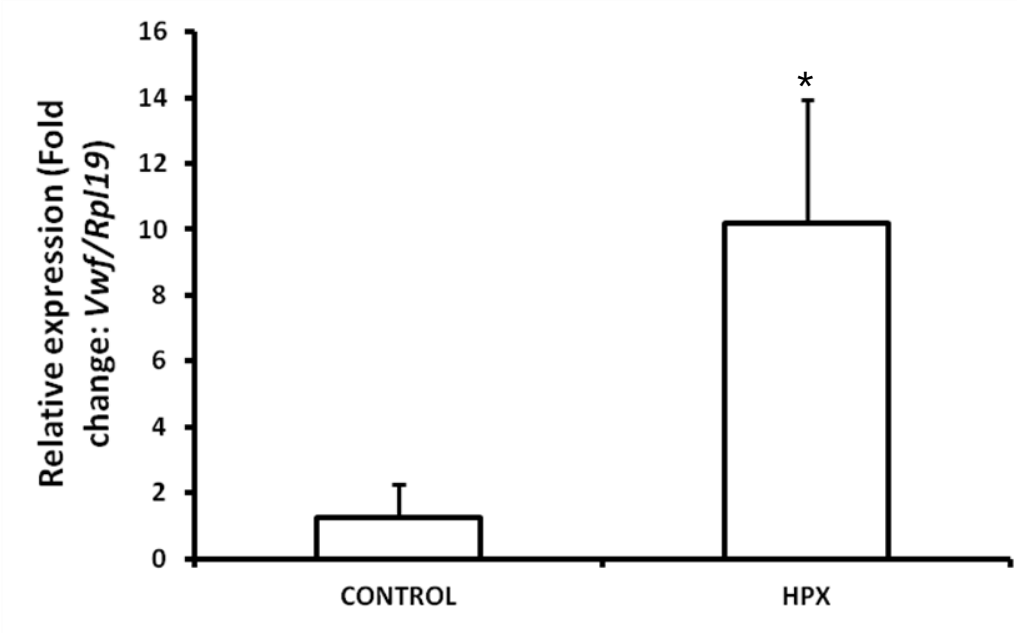

Figure 5.7 Real-time PCR measurement of *Vwf* in the HPX mouse liver

Liver *Vwf* mRNA expression levels were measured in 10-11 week old male HPX mice (n=3). Wild type and heterozygous mice were used as controls. Relative mRNA expression was normalised against the house keeping gene *Rpl19*. Data are presented as mean ± SD for fold change as compared with wild type and heterozygous mice. The samples were measured in triplicate. Statistical analysis was performed by Student *t*-test. *p<0.05 for CONTROL vs. HPX comparisons.

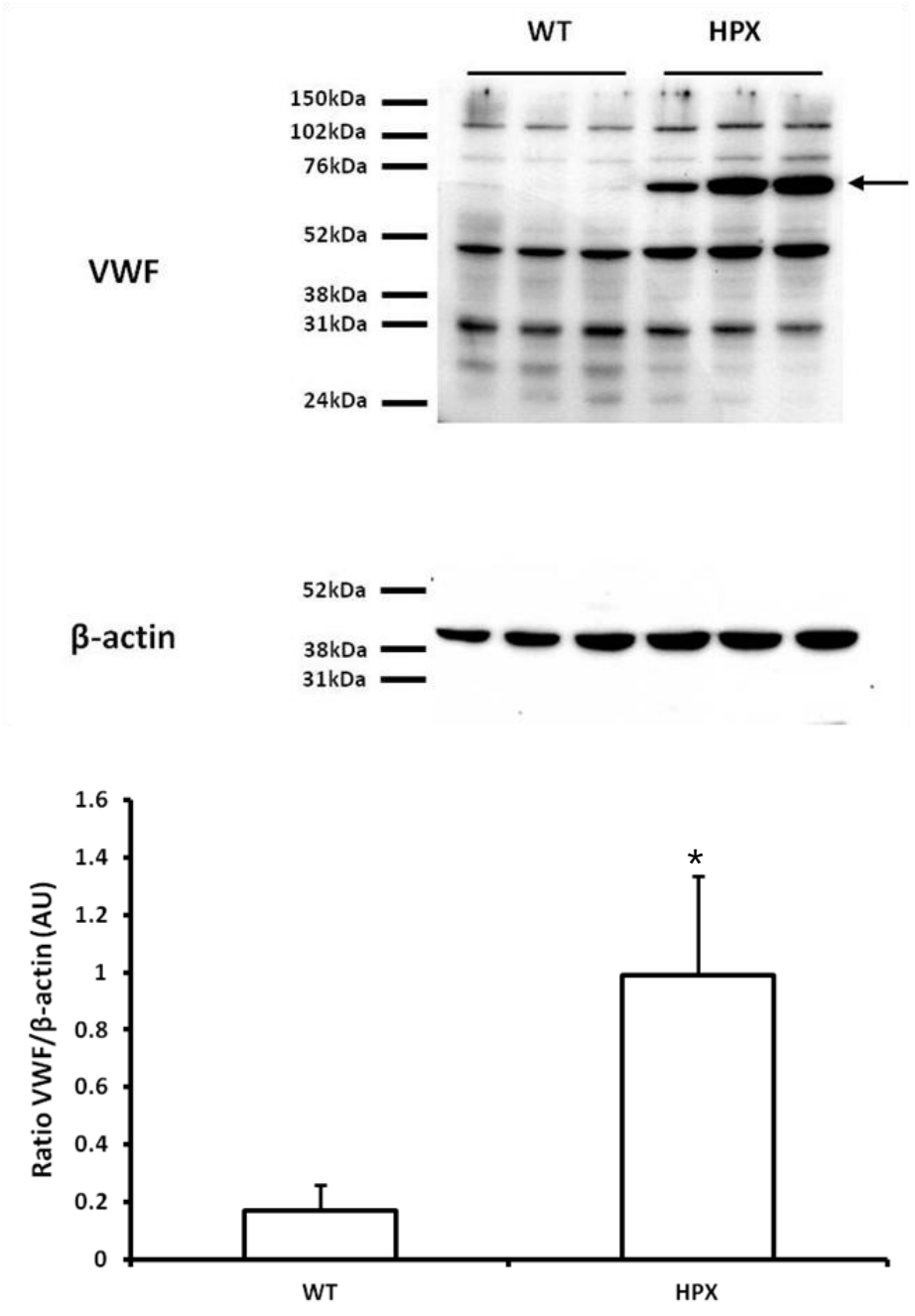

Figure 5.8 VWF protein expression in the HPX mouse model

VWF protein expression was measured in 10-11 week old male HPX mice (n=3). Wild type and heterozygous mice were used as controls. VWF expression (indicated by arrow) was normalised to the expression of β-actin. Densitometry is displayed below the blot and presented in arbitrary units (AU). Data are presented as mean ± SD. *$p<0.05$ for WT vs. HPX comparison.

5.6 Effect of VWC on hepcidin promoter activity

The human hepcidin promoter was co-transfected with increasing concentrations of VWC plasmid ranging from 2 to 6 micrograms into HepG2 or HEK-293 cells in the presence or absence of BMP2 or BMP4 stimulation. The transfection efficiency of the HepG2 cells was not as good as that of the HEK-293 cells and therefore measurement of pSMAD 1,5,8 protein expression was only carried out in HEK-293 cells by western blot analysis. VWC potentiated BMP2-dependent hepcidin promoter activity with no effect on BMP4 in HepG2 cells (Figure 5.9). VWC suppressed BMP4-dependent hepcidin promoter activity in HEK-293 cells at the highest concentration (Figure 5.10). This was not correlated with reduced pSMAD 1,5,8 expression as demonstrated by western blot analysis (Figure 5.11).

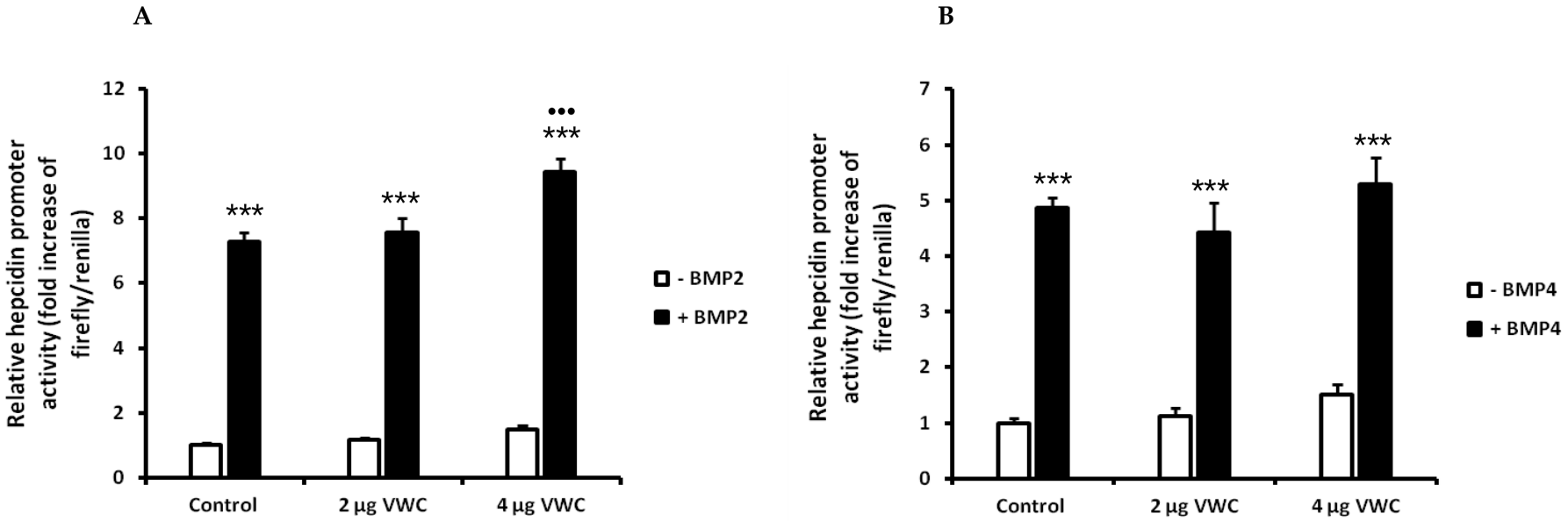

Figure 5.9 Effects of VWC plasmid on BMP2 (A) and BMP4 (B) dependent hepcidin promoter activity in HepG2 cells

HepG2 cells were transiently co-transfected with the wild-type 2.7kb hepcidin promoter construct and/or 2 or 4 µg of VWC plasmid before being treated with 25ng/ml BMP2 (A) or BMP4 (B) for 16 hours. Samples were compared against the wild type hepcidin promoter without any BMP2 treatment Data are presented as mean ± SD derived from a single experiment with three biological replicates. The experiment shown is representative of 3 similar experiments. Statistical analysis was performed by 1-way ANOVA with Tukey's post hoc test. ***$p<0.001$ for –BMP vs. +BMP comparison; •••$p<0.001$ for +BMP vs. VWC treatment comparisons.

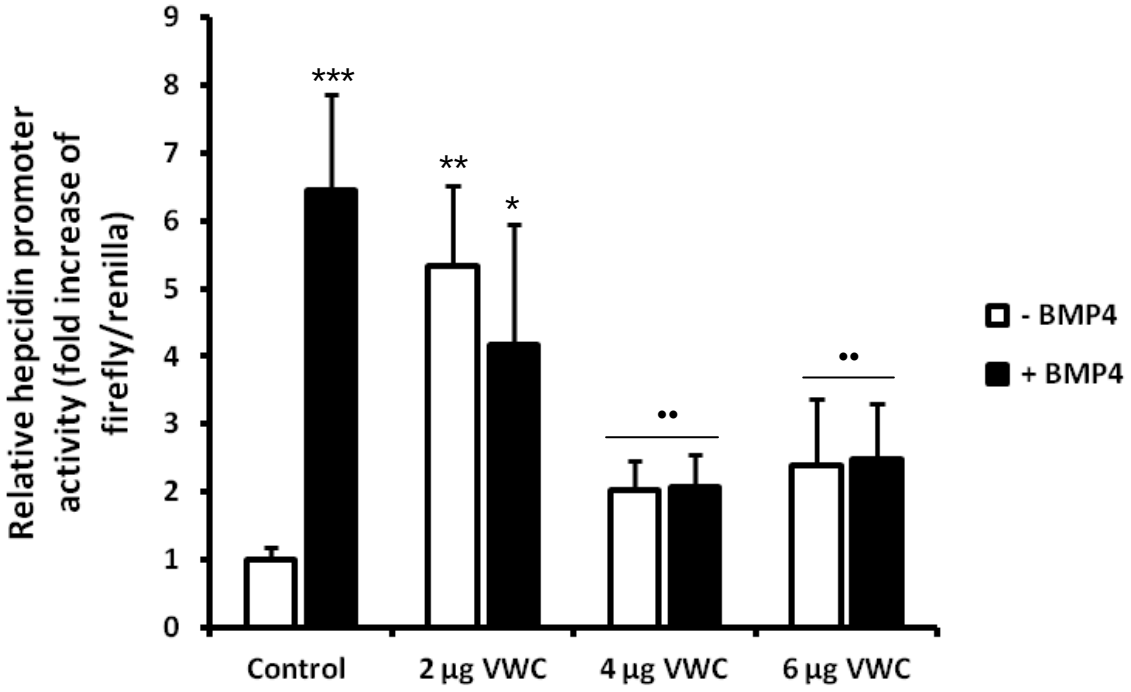

Figure 5.10 Effects of VWC plasmid on hepcidin promoter activity in HEK-293 cells

HEK-293 cells were transiently co-transfected with the wild-type 2.7kb hepcidin promoter construct and 2, 4 or 6 µg of VWC plasmid before being treated with 25ng/mL BMP4. Samples were compared against the wild type hepcidin promoter without any BMP4 treatment Data are presented as mean ± SD derived from a single experiment with three biological replicates. The experiment shown is representative of 3 similar experiments. Statistical analysis was performed by 1-way ANOVA with Tukey's post hoc test. *$p<0.05$; **$p<0.01$; ***$p<0.001$ for –BMP4 vs. treatment comparisons. ••$p<0.05$ for +BMP4 vs. treatment.

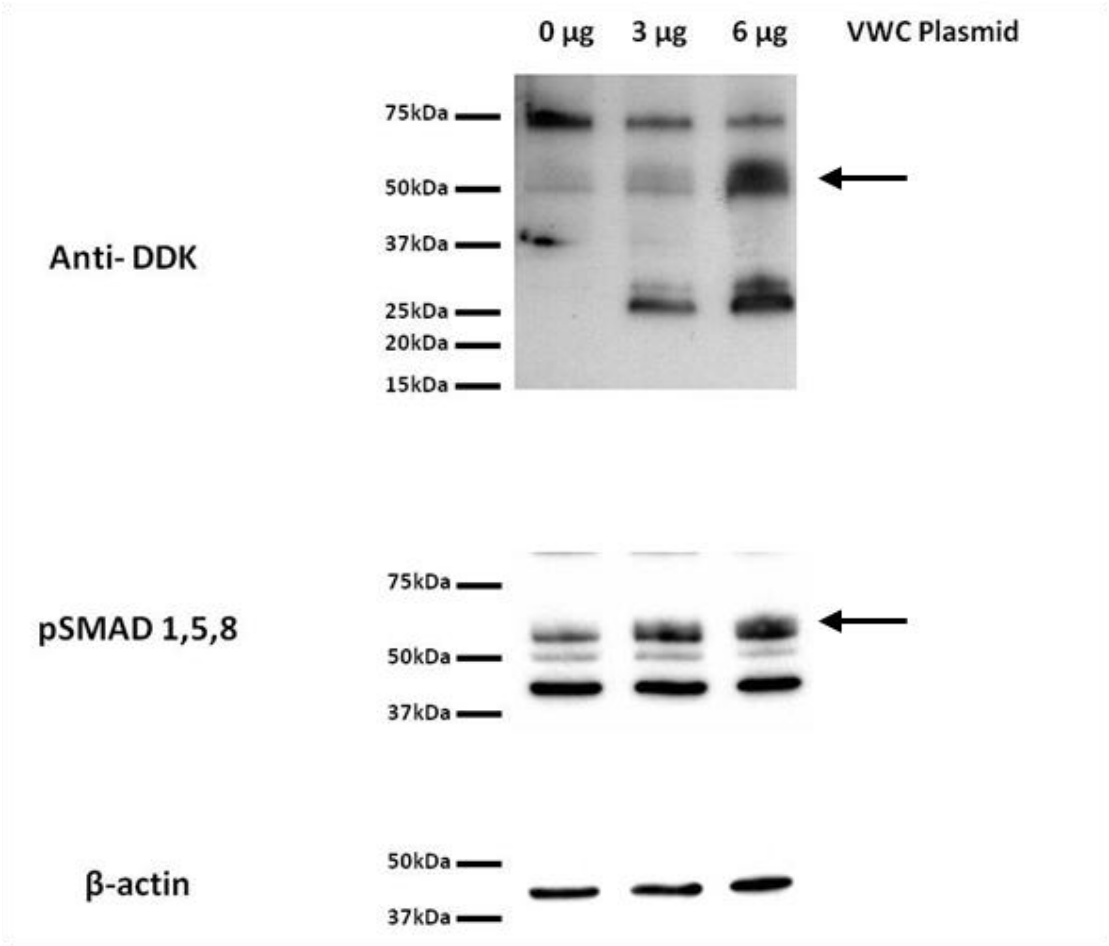

Figure 5.11 pSMAD 1,5,8 expression in HEK-293 cells transfected with VWC plasmid

HEK-293 cells were transfected with 3 or 6 µg of VWC plasmid for 16-18 hours. The expression of the VWC plasmid was detected by an anti-DDK antibody (indicated by arrow). pSMAD 1,5,8 levels were determined in the same samples. β-actin was used as a loading control.

5.7 Expression of VWC in phenylhydrazine treated mice

The von Willebrand factors are a family of glycoprotein's involved in the process of blood clotting. The effect of PHZ-induced anaemia on *Vwf* and *Bmper* mRNA expression was measured by real-time PCR in order to determine the potential of *Vwf* to reduce hepcidin expression in response to haemolysis. Hepatic *Hamp1* mRNA expression was significantly reduced after PHZ treatment with no significant changes in *Bmper* or *Vwf* (Figure 5.12).

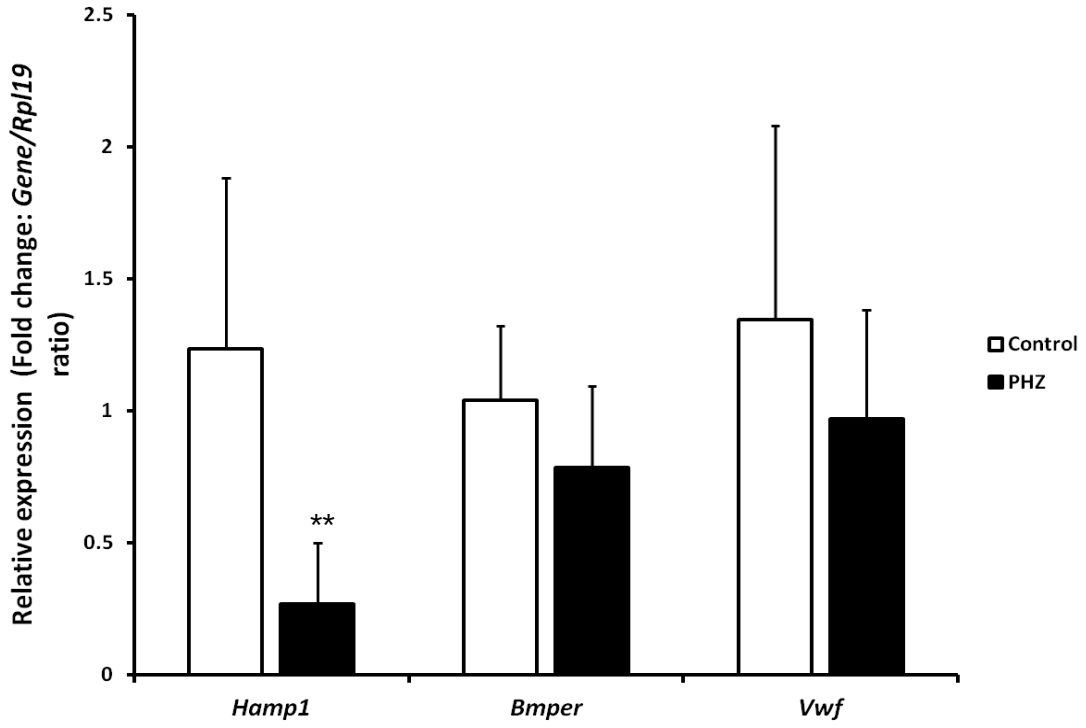

Figure 5.12 Real-time PCR measurement of *Hamp1*, *Bmper* and *Vwf* mRNA expression after phenylhydrazine injection

6 week old male CD1 mice were intraperitoneally injected with 60 mg/kg body weight of neutralized phenylhydrazine or saline solution twice on consecutive days. The expression on *Hamp1*, *Bmper* and *Vwf* were determined though real-time PCR. Relative mRNA expression were normalised against the house keeping gene *Rpl19*. Data are presented as mean ± SD for fold change as compared with saline injected mice (n=6 per group). The samples were measured in triplicate. Statistical analysis was performed by Student *t*-test. **p< 0.01 for Control vs. PHZ comparison.

5.8 Discussion

The BMP signalling pathway and its involvement in the regulation of hepcidin has been extensively researched. The present study was designed to investigate the effects BMP8b and VWC on hepcidin transcription.

BMP6 knockout mice are the only BMP knockout model so far to demonstrate altered iron metabolism. Iron overload appears to induce BMP6 mRNA expression in the liver but not other BMPs (Kautz et al., 2008, Andriopoulos et al., 2009, Meynard et al., 2009). The current study demonstrated the expression of BMP8b as well as BMP6 to be significantly increased in the HPX mouse model, which has not been identified in previous studies. Various mouse models of altered iron metabolism were utilised in order to identify a correlation between BMP8b expression and iron loading. The effects of iron dextran injections significantly increased *Bmp8b* mRNA expression. In contrast the effect of PHZ significantly reduced *Bmp8b* expression. Although it was not measured in the current study, PHZ treatment has been shown to increase liver iron stores while decreasing the expression of diferric transferrin (Frazer et al., 2012). Thus the expression of BMP8b could be dependent on the levels of circulating transferrin bound iron, where injections of iron dextran or PHZ may have increased or decreased transferrin saturation respectively. In the case of the HPX mouse model, in the absence of a functional transferrin gene, the expression of BMP8b may have been upregulated by increased circulating non-transferrin bound iron.

This study demonstrates that iron loading and anaemia (caused by haemolysis from PHZ treatment) are both able to influence the expression of BMP8b individually. However when both factors are present, for instance in hypotransferrinaemia, the effect of iron appears dominant. Studies conducted utilising the *Hamp1*$^{-/-}$ model treated with PHZ, do not agree with this paradigm, since BMP8b expression was not affected. Therefore other factors maybe influencing the expression of BMP8b in the HPX model

which may have not been present in the *Hamp1*$^{-/-}$ model treated with PHZ. Further investigations need to be carried out in order to identify the factor(s) responsible.

Prior studies have noted the importance of homo- and heterodimeric complexes that can form between different BMP proteins. In particular, the DPP family (BMP2 and BMP4) have been shown to be more potent activators when forming heterodimeric complexes with members from the 60A class (BMP5,6,7,8a,8b) (Ying et al., 2001). There was some evidence that BMP8b peptide appeared to potentiate BMP6-dependent hepcidin promoter activity in HepG2 cells however BMP8b had no effect on basal hepcidin promoter activity in HEK-293 cells. The lack of BMP8b effect on hepcidin and pSMAD 1,5,8 expression suggests it may require other BMPs to heterodimerise for full activity. The effect of BMP8b on hepcidin promoter activity was negative and in general appeared to inhibit effects of other BMPs. Therefore BMP8b could form heterodimeric complexes with BMP6 and other BMPs and thus modify their effects, however further investigations into these complexes need to be undertaken before the association between BMP8b, BMP6 and other BMPs are more clearly understood.

Future work could involve analysis of hepatic hepcidin and BMP6 expression in *BMP8b*$^{-/-}$ mice or conversely BMP8b expression could be assessed in *BMP6*$^{-/-}$ mice, where the expression of other BMPs (BMP2 and BMP4) were shown not to be significantly altered in this mouse model (Andriopoulos et al., 2009). Additionally, the effects of BMP8b could be explored *in vivo* through peptide injections in the presence and absence of BMP6 to see if hepcidin expression is affected by the combination of different BMPs.

Recent studies have highlighted the potential of BMP8b to be a regulator of thermogenesis. *BMP8b*$^{-/-}$ mice were shown to have lower metabolic rates and displayed increased propensity for weight gain which was significantly exacerbated when the mice were fed a high fat diet (Whittle et al., 2012). Interestingly, obesity has been associated with decreased serum iron concentrations with assumptions that the

adipose tissues are able to release cytokines which increase hepcidin production and as a result cause anaemia in obese individuals (Yanoff et al., 2007). Further studies which take these variables into account could be carried out to investigate the relationship between BMP8b and hepcidin levels in a mouse model of obesity.

Thrombospondin and types I and III procollagen alpha-1 have two internally homologous domains known as von Willebrand type C domains. These domains are now referred to as VWC due to their C-terminal location on VWF protein (Hunt and Barker, 1987). These regions are rich in cysteine residues which are thought to participate in the intramolar formation of disulphide bonds between proteins. This is supported by more recent findings which shows the first VWC repeat of BMPER to be involved in the molecular interaction between BMPER and BMPs and accounts for the pro and anti-BMP effects of BMPER (Zhang et al., 2007b). BMPER has more than one VWC domain and it is thought that the second VWC domain contributes to the pro-BMP effect of BMPER. This is mediated by the interaction of the second VWC domain on BMPER with the BMP antagonist, chordin. The interaction between BMPER and chordin relieves the inhibitory effect of chordin to BMPs and therefore promotes BMP signalling (Zhang et al., 2010b). The presence of endogenous chordin or other factors could thus modify the function of VWC domains as an anti- or pro- BMP molecules. In the studies carried out in HepG2 and HEK-293 cells, the expression of VWC in HepG2 cells produced a small increase in hepcidin promoter activity, however in HEK-293 cells the expression of VWC decreased hepcidin promoter activity. The presence of such extracellular modifiers such as chordin could provide an explanation for the variations observed in the *in vitro* studies carried out with the VWC plasmid. One could hypothesise that expression of chordin may vary in different cell lines used. Future studies could therefore measure the expression of chordin in the cell lines.

The expression of VWF (which is the monomer encompassing VWC) was significantly increased in HPX mouse liver. The hypothesis behind this increase could be that the HPX mice, as a result of anaemia may increase the remodelling of blood vessels where

VWF has been proposed to be synthesised by endothelial cells (Chen et al., 2011b). This increase in vessel development is only assumed and further investigations are required to confirm this. Evidence from immunostaining (Figure 3.3, chapter 3) has revealed small amounts of increased vasculature in the HPX mouse model. Additionally, the expression of chordin was unchanged in the HPX liver (see Figure 3.4, chapter 3), providing further evidence that the anti-BMP effect observed in the HPX mouse could be mediated by the binding of BMPs to the first VWC domain of BMPER. Increasing the expression of chordin in the HPX mouse could displace the binding of the BMPs to BMPER and ultimately increase BMP signalling.

Moreover it was hypothesized that conditions such as haemolysis may lead to increased VWF protein production in attempts to increase clotting factors. Surprisingly mice treated with phenylhydrazine however did not show any changes in VWF expression. In other studies VWF was increased with increased rate of haemolysis (Chen et al., 2011b). While in a separate study, it has been demonstrated that PHZ prolongs bleeding in rats (Naughton et al., 1989) and therefore maybe acting to decrease clotting factors.

In summary, the studies carried out in this chapter have shown increased expression of BMP8b in the HPX mouse model. The effects of iron loading are most likely to be influencing the expression of BMPs of different sub-classes, although the studies in this chapter did not demonstrate a direct effect of BMP8b on BMP signalling. The effect of BMP8b on hepcidin transcription appears to be less clear in comparison to other BMPs which have demonstrated a direct effect on hepcidin promoter activity. This study has been unable to demonstrate the strongly additive heterodimeric effect of BMP8b and BMP4 as shown in other studies during the development of primordial germ cells (Ying et al., 2000). Hence it appears the interaction may be a cell specific effect. The effect of VWF protein on hepcidin transcription appears cell-type dependent and may be modulated by other extracellular molecules such as chordin. However it would be interesting to look at the effect of VWF on hepcidin levels *in vivo* in future studies.

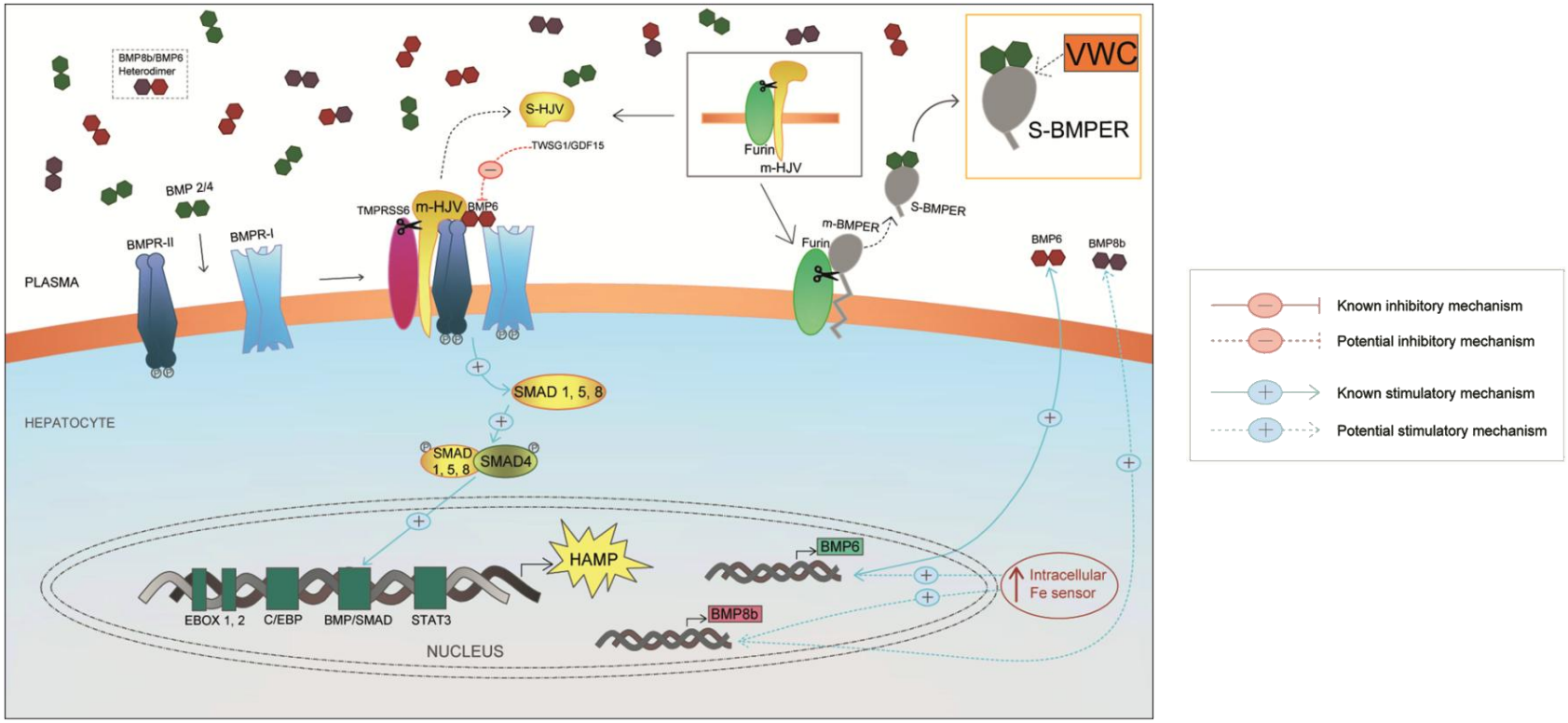

Figure 5.13 Regulation of hepcidin by BMP8b and VWC

Increased hepatic intracellular iron stores increases the expression of BMP6 mRNA and presumably protein. The binding of BMP6 to BMPR-I/II stimulates hepcidin transcription via the BMP/SMAD signalling cascade which is facilitated by the BMP co-receptor HJV. The studies conducted in this chapter identified BMP8b to be significantly increased by iron loading, which may co-operate with BMP6 to influence hepcidin transcription. Additionally, the binding of BMPER to BMP2/4/6 (chapter 3) was shown to be partially dependent on the VWC domains of BMPER.

Chapter 6 .

Conclusion

Hepcidin has emerged as the master regulator of iron homeostasis. Understanding the molecular basis by which hepcidin is regulated has enabled us to further our knowledge of the underlying mechanisms which contribute to the pathogenesis of primary haemochromatosis, secondary iron loading and iron-restricted anaemia. The regulation of hepcidin is principally transcriptional with the BMP/SMAD signalling pathway central to the regulatory network governing hepcidin expression. The studies presented in this thesis have provided new insights into the regulation of hepcidin by the BMP pathway, by the extracellular BMP antagonist BMPER and the transcriptional regulation by ATOH8. Both molecules contribute to regulation of hepcidin expression and will open up new avenues of research.

Experimental animal models of altered iron metabolism have provided a great deal of insight into the systemic regulation of iron metabolism and the relevance of hepcidin in genetic iron disorders such as hereditary haemochromatosis and the anaemia of chronic disease. The hypotransferrinaemic (HPX) mouse model, where the suppression of hepcidin is drastic despite secondary hepatic iron loading has proved particularly useful. Due to the transferrin deficiency, these animals suffer from severe iron restricted anaemia despite having undetectable levels of hepcidin. In these mice is it not clear whether the anaemia, increased erythropoietic drive and possibly tissue hypoxia or all contribute to the suppression of hepcidin. The first study conducted in this thesis demonstrated an increase in the hepatic expression of a known BMP antagonist, BMPER, in HPX mice. Exogenous BMPER was able to inhibit hepcidin expression *in vivo* causing alterations in serum iron levels and *in vitro* via suppression of BMP2/6 dependent hepcidin promoter activity. Since BMPER has a role in blood vessel generation and sprouting, levels may be increased in HPX mice in response to severe chronic anaemia and/or hypoxia that may occur in pathophysiological situations. However BMPER was not significantly affected by hypoxia or iron deficiency induced anaemia. BMPER or peptides based on the structure of the BMP binding sites (VWC domains, chapter 5) have therapeutic potential for the treatment of iron-restrictive disorders in which hepcidin excess contributes to the pathogenesis of anaemia with the proviso that inhibitors of the BMP pathway may disturb other important process dependent on BMP signalling. Additionally, identifying the

cleavage mechanism of BMPER may provide some additional regulatory mechanism of hepcidin expression.

Hepcidin remains suppressed even with the greatly increased iron stores in the HPX model. This has been attributed to an enhanced erythropoietic activity in the HPX mouse which serves as an attractive system for identifying the 'erythroid regulator' which is able to stimulate iron absorption even in the face of iron loading. The second major finding of this thesis identified ATOH8 as a transcription factor that is significantly suppressed in the liver of the HPX mouse. The expression of ATOH8 was influenced by iron and erythropoiesis in various mouse models simulating the iron-loading anaemia phenotype. ATOH8 was shown to positively regulate hepcidin transcription through the BMP signalling cascade as well as through E-box' regions located on the hepcidin promoter, demonstrating the importance of this molecule in the regulation of iron metabolism. Further work will be required to determine whether ATOH8 represents part of the true erythroid regulatory mechanism of hepcidin; however it is certainly a strong candidate. Identifying the molecules that regulate ATOH8 can become important drug targets for disorders of iron metabolism where hepcidin expression is greatly disturbed.

The major findings of this thesis can be summarised in brief as depicted in Figure 6.1. Collectively, the data presented in this thesis provides an in depth of knowledge on the regulation of hepcidin by the BMP signalling pathway. The *in vivo* models of altered iron metabolism have been compared to normal circumstances throughout the thesis, highlighting the importance of the genes identified under diseased conditions. Ultimately, disease results from the disruption of normal signalling pathways, and prevention depends upon our knowledge of these signalling pathways and how they were perturbed. The iron-loading diseases are strong examples of hepcidin dysregulation that rely on current research for treatment.

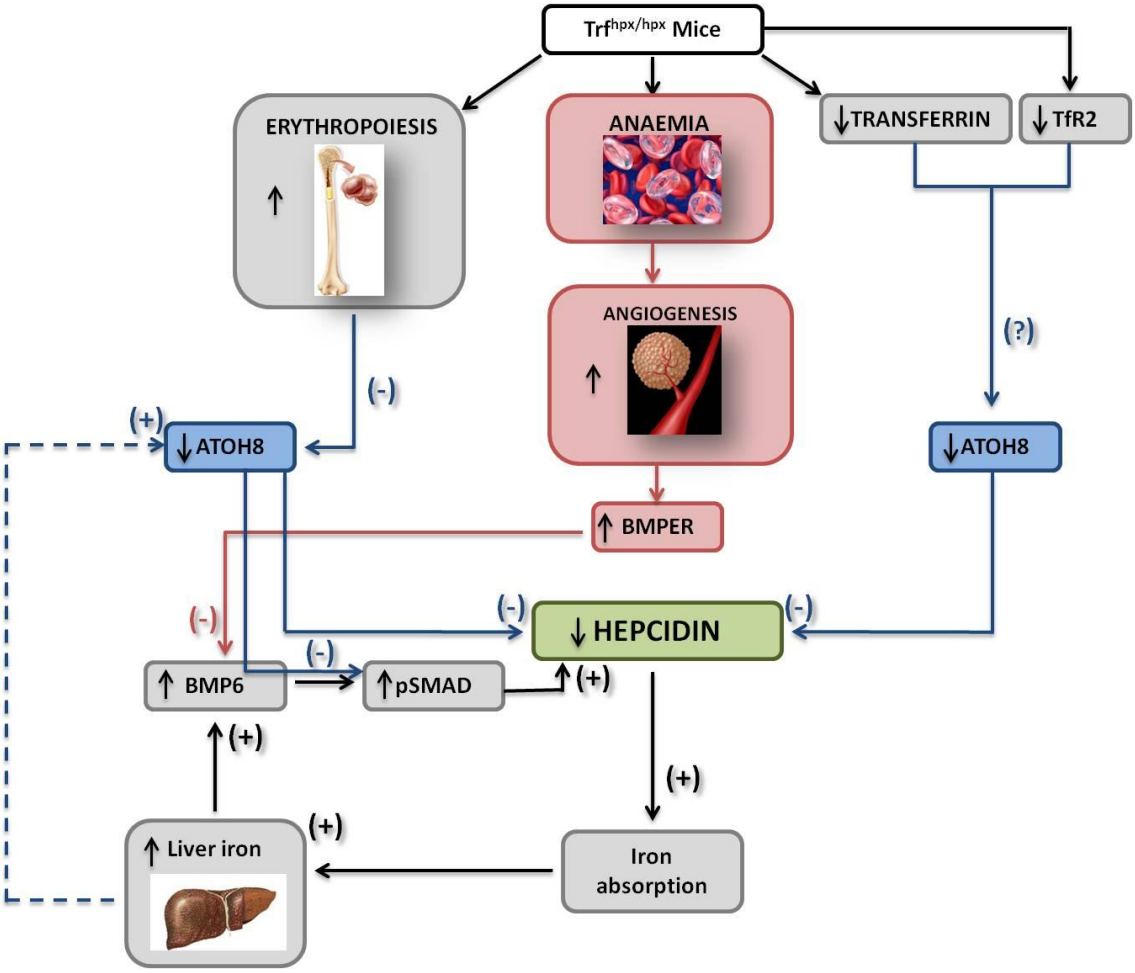

Figure 6.1 Schematic summary of the work presented

The suppression of hepcidin is thought to occur through multiple stimuli. Following the red arrows (→), as a result of anaemia and possibly hypoxia, chapter 3 hypothesised that an increase in blood vessel remodelling increases the expression of BMPER which is able to inhibit hepcidin transcription through modulation of the BMP/SMAD signalling cascade. The binding of BMPs to BMPER was partially shown to occur to through the VWC domain indentified in chapter 5. Following the blue arrows (→), chapter 4 demonstrated the upregulation of ATOH8 by increased liver iron stores, whose expression was suppressed during conditions of enhanced erythropoietic demands. This is turn reduced hepcidin expression through an undefined erythroid signal. Evidence from chapter 4 demonstrated the involvement of pSMAD 1,5,8 and E-box regions on the hepcidin promoter. Furthermore ATOH8 may also be regulated by the ratio of apo- to holotransferrin which may signal via TfR2/HFE receptor complex. As well as reduced hepcidin expression, non-transferrin bound iron uptake is another cause of liver iron overload in the HPX model. Chapter 5 introduced a novel member of the BMP family of cytokines namely BMP8b who's expression was the only BMP member besides BMP6 to be significantly increased in the liver of the HPX mouse. The nature of the signal that regulates BMP8b expression and how this affects hepcidin regulation requires further investigation. In addition, increased oxidative stress may also be contributing to the suppression of hepcidin in this model which was not examined in the current study (images adapted from science photo library).

Bibliography

ABBOUD, S. & HAILE, D. J. 2000. A novel mammalian iron-regulated protein involved in intracellular iron metabolism. *J Biol Chem,* 275**,** 19906-12.

AHMAD, K. A., AHMANN, J. R., MIGAS, M. C., WAHEED, A., BRITTON, R. S., BACON, B. R., SLY, W. S. & FLEMING, R. E. 2002. Decreased liver hepcidin expression in the Hfe knockout mouse. *Blood Cells Mol Dis,* 29**,** 361-6.

AISEN, P. 2004. Transferrin receptor 1. *Int J Biochem Cell Biol,* 36**,** 2137-43.

AMBROSIO, A. L., TAELMAN, V. F., LEE, H. X., METZINGER, C. A., COFFINIER, C. & DE ROBERTIS, E. M. 2008. Crossveinless-2 Is a BMP feedback inhibitor that binds Chordin/BMP to regulate Xenopus embryonic patterning. *Dev Cell,* 15**,** 248-60.

ANDERSON, G. J., DARSHAN, D., WILKINS, S. J. & FRAZER, D. M. 2007. Regulation of systemic iron homeostasis: how the body responds to changes in iron demand. *Biometals,* 20**,** 665-74.

ANDREWS, N. C. 2000. Iron metabolism: iron deficiency and iron overload. *Annu Rev Genomics Hum Genet,* 1**,** 75-98.

ANDRIOPOULOS, B., JR., CORRADINI, E., XIA, Y., FAASSE, S. A., CHEN, S., GRGUREVIC, L., KNUTSON, M. D., PIETRANGELO, A., VUKICEVIC, S., LIN, H. Y. & BABITT, J. L. 2009. BMP6 is a key endogenous regulator of hepcidin expression and iron metabolism. *Nat Genet,* 41**,** 482-7.

BABITT, J. L., HUANG, F. W., WRIGHTING, D. M., XIA, Y., SIDIS, Y., SAMAD, T. A., CAMPAGNA, J. A., CHUNG, R. T., SCHNEYER, A. L., WOOLF, C. J., ANDREWS, N. C. & LIN, H. Y. 2006. Bone morphogenetic protein signaling by hemojuvelin regulates hepcidin expression. *Nat Genet,* 38**,** 531-9.

BABITT, J. L., HUANG, F. W., XIA, Y., SIDIS, Y., ANDREWS, N. C. & LIN, H. Y. 2007. Modulation of bone morphogenetic protein signaling in vivo regulates systemic iron balance. *J Clin Invest,* 117**,** 1933-9.

BARTNIKAS, T. B., ANDREWS, N. C. & FLEMING, M. D. 2011. Transferrin is a major determinant of hepcidin expression in hypotransferrinemic mice. *Blood,* 117**,** 630-7.

BAYELE, H. K., MCARDLE, H. & SRAI, S. K. 2006. Cis and trans regulation of hepcidin expression by upstream stimulatory factor. *Blood,* 108**,** 4237-45.

BENEDICT, C., GHIO, A. J., GEHRING, H., SCHULTES, B., PETERS, A. & OLTMANNS, K. M. 2007. Transient hypoxia and downregulation of circulating prohepcidin concentrations in healthy young men. *Haematologica,* 92**,** 125-6.

BEUTLER, E. 1971. Red Cell Metabolism: a manual of biochemical methods. *Grune & Stratton.*

BINNERTS, M. E., WEN, X., CANTE-BARRETT, K., BRIGHT, J., CHEN, H. T., ASUNDI, V., SATTARI, P., TANG, T., BOYLE, B., FUNK, W. & RUPP, F. 2004. Human Crossveinless-2 is a novel inhibitor of bone morphogenetic proteins. *Biochem Biophys Res Commun,* 315**,** 272-80.

CALZOLARI, A., DEAGLIO, S., SPOSI, N. M., PETRUCCI, E., MORSILLI, O., GABBIANELLI, M., MALAVASI, F., PESCHLE, C. & TESTA, U. 2004.

Transferrin receptor 2 protein is not expressed in normal erythroid cells. *Biochem J,* 381**,** 629-34.

CAMASCHELLA, C., ROETTO, A., CALI, A., DE GOBBI, M., GAROZZO, G., CARELLA, M., MAJORANO, N., TOTARO, A. & GASPARINI, P. 2000. The gene TFR2 is mutated in a new type of haemochromatosis mapping to 7q22. *Nat Genet,* 25**,** 14-5.

CARTWRIGHT, G. E. & LEE, G. R. 1971. The anaemia of chronic disorders. *Br J Haematol,* 21**,** 147-52.

CASANOVAS, G., MLECZKO-SANECKA, K., ALTAMURA, S., HENTZE, M. W. & MUCKENTHALER, M. U. 2009. Bone morphogenetic protein (BMP)-responsive elements located in the proximal and distal hepcidin promoter are critical for its response to HJV/BMP/SMAD. *J Mol Med (Berl),* 87**,** 471-80.

CHANG, C., HOLTZMAN, D. A., CHAU, S., CHICKERING, T., WOOLF, E. A., HOLMGREN, L. M., BODOROVA, J., GEARING, D. P., HOLMES, W. E. & BRIVANLOU, A. H. 2001. Twisted gastrulation can function as a BMP antagonist. *Nature,* 410**,** 483-7.

CHASTON, T. B., MATAK, P., POURVALI, K., SRAI, S. K., MCKIE, A. T. & SHARP, P. A. 2011. Hypoxia inhibits hepcidin expression in HuH7 hepatoma cells via decreased SMAD4 signaling. *Am J Physiol Cell Physiol,* 300**,** C888-95.

CHEN, J., DAI, F., BALAKRISHNAN-RENUKA, A., LEESE, F., SCHEMPP, W., SCHALLER, F., HOFFMANN, M. M., MOROSAN-PUOPOLO, G., YUSUF, F., BISSCHOFF, I. J., CHANKIEWITZ, V., XUE, J., YING, K. & BRAND-SABERI, B. 2011a. Diversification and molecular evolution of ATOH8, a gene encoding a bHLH transcription factor. *PLoS One,* 6**,** e23005.

CHEN, J., HOBBS, W. E., LE, J., LENTING, P. J., DE GROOT, P. G. & LOPEZ, J. A. 2011b. The rate of hemolysis in sickle cell disease correlates with the quantity of active von Willebrand factor in the plasma. *Blood,* 117**,** 3680-3.

CHOI, S. O., CHO, Y. S., KIM, H. L. & PARK, J. W. 2007. ROS mediate the hypoxic repression of the hepcidin gene by inhibiting C/EBPalpha and STAT-3. *Biochem Biophys Res Commun,* 356**,** 312-7.

COFFINIER, C., KETPURA, N., TRAN, U., GEISSERT, D. & DE ROBERTIS, E. M. 2002. Mouse Crossveinless-2 is the vertebrate homolog of a Drosophila extracellular regulator of BMP signaling. *Mech Dev,* 119 Suppl 1**,** S179-84.

CONLEY, C. A., SILBURN, R., SINGER, M. A., RALSTON, A., ROHWER-NUTTER, D., OLSON, D. J., GELBART, W. & BLAIR, S. S. 2000. Crossveinless 2 contains cysteine-rich domains and is required for high levels of BMP-like activity during the formation of the cross veins in Drosophila. *Development,* 127**,** 3947-59.

CONSTANTE, M., WANG, D., RAYMOND, V. A., BILODEAU, M. & SANTOS, M. M. 2007. Repression of repulsive guidance molecule C during inflammation is independent of Hfe and involves tumor necrosis factor-alpha. *Am J Pathol,* 170**,** 497-504.

CORRADINI, E., GARUTI, C., MONTOSI, G., VENTURA, P., ANDRIOPOULOS, B., JR., LIN, H. Y., PIETRANGELO, A. & BABITT, J. L. 2009. Bone morphogenetic protein signaling is impaired in an HFE knockout mouse model of hemochromatosis. *Gastroenterology,* 137**,** 1489-97.

CORRADINI, E., MEYNARD, D., WU, Q., CHEN, S., VENTURA, P., PIETRANGELO, A. & BABITT, J. L. 2011. Serum and liver iron differently regulate the bone

morphogenetic protein 6 (BMP6)-SMAD signaling pathway in mice. *Hepatology,* 54**,** 273-84.

D'ALESSIO, F., HENTZE, M. W. & MUCKENTHALER, M. U. 2012. The hemochromatosis proteins hfe, tfr2 and hjv form a membrane-associated protein complex For hepcidin regulation. *J Hepatol*.

DE DOMENICO, I., LO, E., WARD, D. M. & KAPLAN, J. 2009. Hepcidin-induced internalization of ferroportin requires binding and cooperative interaction with Jak2. *Proc Natl Acad Sci U S A,* 106**,** 3800-5.

DE DOMENICO, I., VAUGHN, M. B., LI, L., BAGLEY, D., MUSCI, G., WARD, D. M. & KAPLAN, J. 2006. Ferroportin-mediated mobilization of ferritin iron precedes ferritin degradation by the proteasome. *EMBO J,* 25**,** 5396-404.

DE DOMENICO, I., WARD, D. M., LANGELIER, C., VAUGHN, M. B., NEMETH, E., SUNDQUIST, W. I., GANZ, T., MUSCI, G. & KAPLAN, J. 2007. The molecular mechanism of hepcidin-mediated ferroportin down-regulation. *Mol Biol Cell,* 18**,** 2569-78.

DE DOMENICO, I., ZHANG, T. Y., KOENING, C. L., BRANCH, R. W., LONDON, N., LO, E., DAYNES, R. A., KUSHNER, J. P., LI, D., WARD, D. M. & KAPLAN, J. 2010. Hepcidin mediates transcriptional changes that modulate acute cytokine-induced inflammatory responses in mice. *J Clin Invest,* 120**,** 2395-405.

DE GORTER, D. J. J., VAN BEZOOIJEN, R. L. & TEN DIJKE, P. 2009. Bone Morphogenetic Proteins and Their Receptors. *Encyclopedia of Life Sciences (ELS).* 15/09/2009 ed. Chichester: John Wiley&Sons, Ltd.

DECKERS, M. M., VAN BEZOOIJEN, R. L., VAN DER HORST, G., HOOGENDAM, J., VAN DER BENT, C., PAPAPOULOS, S. E. & LOWIK, C. W. 2002. Bone morphogenetic proteins stimulate angiogenesis through osteoblast-derived vascular endothelial growth factor A. *Endocrinology,* 143**,** 1545-53.

DELABY, C., PILARD, N., PUY, H. & CANONNE-HERGAUX, F. 2008. Sequential regulation of ferroportin expression after erythrophagocytosis in murine macrophages: early mRNA induction by haem, followed by iron-dependent protein expression. *Biochem J,* 411**,** 123-31.

DEUGNIER, Y., BRISSOT, P. & LOREAL, O. 2008. Iron and the liver: update 2008. *J Hepatol,* 48 Suppl 1**,** S113-23.

DONOVAN, A., BROWNLIE, A., ZHOU, Y., SHEPARD, J., PRATT, S. J., MOYNIHAN, J., PAW, B. H., DREJER, A., BARUT, B., ZAPATA, A., LAW, T. C., BRUGNARA, C., LUX, S. E., PINKUS, G. S., PINKUS, J. L., KINGSLEY, P. D., PALIS, J., FLEMING, M. D., ANDREWS, N. C. & ZON, L. I. 2000. Positional cloning of zebrafish ferroportin1 identifies a conserved vertebrate iron exporter. *Nature,* 403**,** 776-81.

DU, X., SHE, E., GELBART, T., TRUKSA, J., LEE, P., XIA, Y., KHOVANANTH, K., MUDD, S., MANN, N., MORESCO, E. M., BEUTLER, E. & BEUTLER, B. 2008. The serine protease TMPRSS6 is required to sense iron deficiency. *Science,* 320**,** 1088-92.

EKMEKCIOGLU, C., FEYERTAG, J. & MARKTL, W. 1996. A ferric reductase activity is found in brush border membrane vesicles isolated from Caco-2 cells. *J Nutr,* 126**,** 2209-17.

EVSTATIEV, R. & GASCHE, C. 2012. Iron sensing and signalling. *Gut,* 61**,** 933-52.

FARRINGTON, S. M., BELAOUSSOFF, M. & BARON, M. H. 1997. Winged-helix, Hedgehog and Bmp genes are differentially expressed in distinct cell layers of the murine yolk sac. *Mech Dev,* 62**,** 197-211.

FEDER, J. N., GNIRKE, A., THOMAS, W., TSUCHIHASHI, Z., RUDDY, D. A., BASAVA, A., DORMISHIAN, F., DOMINGO, R., JR., ELLIS, M. C., FULLAN, A., HINTON, L. M., JONES, N. L., KIMMEL, B. E., KRONMAL, G. S., LAUER, P., LEE, V. K., LOEB, D. B., MAPA, F. A., MCCLELLAND, E., MEYER, N. C., MINTIER, G. A., MOELLER, N., MOORE, T., MORIKANG, E., PRASS, C. E., QUINTANA, L., STARNES, S. M., SCHATZMAN, R. C., BRUNKE, K. J., DRAYNA, D. T., RISCH, N. J., BACON, B. R. & WOLFF, R. K. 1996. A novel MHC class I-like gene is mutated in patients with hereditary haemochromatosis. *Nat Genet,* 13**,** 399-408.

FINBERG, K. E., HEENEY, M. M., CAMPAGNA, D. R., AYDINOK, Y., PEARSON, H. A., HARTMAN, K. R., MAYO, M. M., SAMUEL, S. M., STROUSE, J. J., MARKIANOS, K., ANDREWS, N. C. & FLEMING, M. D. 2008. Mutations in TMPRSS6 cause iron-refractory iron deficiency anemia (IRIDA). *Nat Genet,* 40**,** 569-71.

FINCH, C. 1994. Regulators of iron balance in humans. *Blood,* 84**,** 1697-702.

FINKENZELLER, G., HAGER, S. & STARK, G. B. 2012. Effects of bone morphogenetic protein 2 on human umbilical vein endothelial cells. *Microvasc Res,* 84**,** 81-5.

FLEMING, M. D., ROMANO, M. A., SU, M. A., GARRICK, L. M., GARRICK, M. D. & ANDREWS, N. C. 1998. Nramp2 is mutated in the anemic Belgrade (b) rat: evidence of a role for Nramp2 in endosomal iron transport. *Proc Natl Acad Sci U S A,* 95**,** 1148-53.

FLEMING, R. E., AHMANN, J. R., MIGAS, M. C., WAHEED, A., KOEFFLER, H. P., KAWABATA, H., BRITTON, R. S., BACON, B. R. & SLY, W. S. 2002. Targeted mutagenesis of the murine transferrin receptor-2 gene produces hemochromatosis. *Proc Natl Acad Sci U S A,* 99**,** 10653-8.

FLEMING, R. E., HOLDEN, C. C., TOMATSU, S., WAHEED, A., BRUNT, E. M., BRITTON, R. S., BACON, B. R., ROOPENIAN, D. C. & SLY, W. S. 2001. Mouse strain differences determine severity of iron accumulation in Hfe knockout model of hereditary hemochromatosis. *Proc Natl Acad Sci U S A,* 98**,** 2707-11.

FLETCHER, J. 1970. Iron transport in the blood. *Proc R Soc Med,* 63**,** 1216-8.

FRAZER, D. M., WILKINS, S. J., BECKER, E. M., VULPE, C. D., MCKIE, A. T., TRINDER, D. & ANDERSON, G. J. 2002. Hepcidin expression inversely correlates with the expression of duodenal iron transporters and iron absorption in rats. *Gastroenterology,* 123**,** 835-44.

FRAZER, D. M., WILKINS, S. J., DARSHAN, D., BADRICK, A. C., MCLAREN, G. D. & ANDERSON, G. J. 2012. Stimulated erythropoiesis with secondary iron loading leads to a decrease in hepcidin despite an increase in bone morphogenetic protein 6 expression. *Br J Haematol,* 157**,** 615-26.

GALY, B., FERRING, D., MINANA, B., BELL, O., JANSER, H. G., MUCKENTHALER, M., SCHUMANN, K. & HENTZE, M. W. 2005. Altered body iron distribution and microcytosis in mice deficient in iron regulatory protein 2 (IRP2). *Blood,* 106**,** 2580-9.

GANZ, T. 2007. Molecular control of iron transport. *J Am Soc Nephrol,* 18**,** 394-400.

GANZ, T. 2011. Hepcidin and iron regulation, 10 years later. *Blood,* 117**,** 4425-33.

GERJEVIC, L. N., LIU, N., LU, S. & HARRISON-FINDIK, D. D. 2012. Alcohol Activates TGF-Beta but Inhibits BMP Receptor-Mediated Smad Signaling and Smad4 Binding to Hepcidin Promoter in the Liver. *Int J Hepatol,* 2012**,** 459278.

GUNSHIN, H., FUJIWARA, Y., CUSTODIO, A. O., DIRENZO, C., ROBINE, S. & ANDREWS, N. C. 2005a. Slc11a2 is required for intestinal iron absorption and erythropoiesis but dispensable in placenta and liver. *J Clin Invest,* 115**,** 1258-66.

GUNSHIN, H., MACKENZIE, B., BERGER, U. V., GUNSHIN, Y., ROMERO, M. F., BORON, W. F., NUSSBERGER, S., GOLLAN, J. L. & HEDIGER, M. A. 1997. Cloning and characterization of a mammalian proton-coupled metal-ion transporter. *Nature,* 388**,** 482-8.

GUNSHIN, H., STARR, C. N., DIRENZO, C., FLEMING, M. D., JIN, J., GREER, E. L., SELLERS, V. M., GALICA, S. M. & ANDREWS, N. C. 2005b. Cybrd1 (duodenal cytochrome b) is not necessary for dietary iron absorption in mice. *Blood,* 106**,** 2879-83.

GUO, B., PHILLIPS, J. D., YU, Y. & LEIBOLD, E. A. 1995. Iron regulates the intracellular degradation of iron regulatory protein 2 by the proteasome. *J Biol Chem,* 270**,** 21645-51.

HAASE, V. H. 2010. Hypoxic regulation of erythropoiesis and iron metabolism. *Am J Physiol Renal Physiol,* 299**,** F1-13.

HALLIWELL, B. & GUTTERIDGE, J. M. 1986. Oxygen free radicals and iron in relation to biology and medicine: some problems and concepts. *Arch Biochem Biophys,* 246**,** 501-14.

HAN, O., FAILLA, M. L., HILL, A. D., MORRIS, E. R. & SMITH, J. C., JR. 1995. Reduction of Fe(III) is required for uptake of nonheme iron by Caco-2 cells. *J Nutr,* 125**,** 1291-9.

HARRIS, Z. L., DURLEY, A. P., MAN, T. K. & GITLIN, J. D. 1999. Targeted gene disruption reveals an essential role for ceruloplasmin in cellular iron efflux. *Proc Natl Acad Sci U S A,* 96**,** 10812-7.

HARRISON-FINDIK, D. D., SCHAFER, D., KLEIN, E., TIMCHENKO, N. A., KULAKSIZ, H., CLEMENS, D., FEIN, E., ANDRIOPOULOS, B., PANTOPOULOS, K. & GOLLAN, J. 2006. Alcohol metabolism-mediated oxidative stress down-regulates hepcidin transcription and leads to increased duodenal iron transporter expression. *J Biol Chem,* 281**,** 22974-82.

HARRISON, P. M. & AROSIO, P. 1996. The ferritins: molecular properties, iron storage function and cellular regulation. *Biochim Biophys Acta,* 1275**,** 161-203.

HASSAN, B. A. & BELLEN, H. J. 2000. Doing the MATH: is the mouse a good model for fly development? *Genes Dev,* 14**,** 1852-65.

HEINKE, J., WEHOFSITS, L., ZHOU, Q., ZOELLER, C., BAAR, K. M., HELBING, T., LAIB, A., AUGUSTIN, H., BODE, C., PATTERSON, C. & MOSER, M. 2008. BMPER is an endothelial cell regulator and controls bone morphogenetic protein-4-dependent angiogenesis. *Circ Res,* 103**,** 804-12.

HUANG, H., CONSTANTE, M., LAYOUN, A. & SANTOS, M. M. 2009. Contribution of STAT3 and SMAD4 pathways to the regulation of hepcidin by opposing stimuli. *Blood,* 113**,** 3593-9.

HUNT, L. T. & BARKER, W. C. 1987. von Willebrand factor shares a distinctive cysteine-rich domain with thrombospondin and procollagen. *Biochem Biophys Res Commun,* 144**,** 876-82.

HUNTER, H. N., FULTON, D. B., GANZ, T. & VOGEL, H. J. 2002. The solution structure of human hepcidin, a peptide hormone with antimicrobial activity that is involved in iron uptake and hereditary hemochromatosis. *J Biol Chem,* 277**,** 37597-603.

IKEYA, M., KAWADA, M., KIYONARI, H., SASAI, N., NAKAO, K., FURUTA, Y. & SASAI, Y. 2006. Essential pro-Bmp roles of crossveinless 2 in mouse organogenesis. *Development,* 133**,** 4463-73.

INOUE, C., BAE, S. K., TAKATSUKA, K., INOUE, T., BESSHO, Y. & KAGEYAMA, R. 2001. Math6, a bHLH gene expressed in the developing nervous system, regulates neuronal versus glial differentiation. *Genes Cells,* 6**,** 977-86.

IWAI, K., KLAUSNER, R. D. & ROUAULT, T. A. 1995. Requirements for iron-regulated degradation of the RNA binding protein, iron regulatory protein 2. *EMBO J,* 14**,** 5350-7.

JARMAN, A. P., GRAU, Y., JAN, L. Y. & JAN, Y. N. 1993. atonal is a proneural gene that directs chordotonal organ formation in the Drosophila peripheral nervous system. *Cell,* 73**,** 1307-21.

JIAN, J., YANG, Q., DAI, J., ECKARD, J., AXELROD, D., SMITH, J. & HUANG, X. 2011. Effects of iron deficiency and iron overload on angiogenesis and oxidative stress-a potential dual role for iron in breast cancer. *Free Radic Biol Med,* 50**,** 841-7.

KAUTZ, L., MEYNARD, D., MONNIER, A., DARNAUD, V., BOUVET, R., WANG, R. H., DENG, C., VAULONT, S., MOSSER, J., COPPIN, H. & ROTH, M. P. 2008. Iron regulates phosphorylation of Smad1/5/8 and gene expression of Bmp6, Smad7, Id1, and Atoh8 in the mouse liver. *Blood,* 112**,** 1503-9.

KAWABATA, H., YANG, R., HIRAMA, T., VUONG, P. T., KAWANO, S., GOMBART, A. F. & KOEFFLER, H. P. 1999. Molecular cloning of transferrin receptor 2. A new member of the transferrin receptor-like family. *J Biol Chem,* 274**,** 20826-32.

KAWABATA, M., IMAMURA, T. & MIYAZONO, K. 1998. Signal transduction by bone morphogenetic proteins. *Cytokine Growth Factor Rev,* 9**,** 49-61.

KELLEY, R., REN, R., PI, X., WU, Y., MORENO, I., WILLIS, M., MOSER, M., ROSS, M., PODKOWA, M., ATTISANO, L. & PATTERSON, C. 2009. A concentration-dependent endocytic trap and sink mechanism converts Bmper from an activator to an inhibitor of Bmp signaling. *J Cell Biol,* 184**,** 597-609.

KONG, W. N., CHANG, Y. Z., WANG, S. M., ZHAI, X. L., SHANG, J. X., LI, L. X. & DUAN, X. L. 2008. Effect of erythropoietin on hepcidin, DMT1 with IRE, and hephaestin gene expression in duodenum of rats. *J Gastroenterol,* 43**,** 136-43.

KOORTS, A. M. & VILJOEN, M. 2007. Ferritin and ferritin isoforms I: Structure-function relationships, synthesis, degradation and secretion. *Arch Physiol Biochem,* 113**,** 30-54.

KRAUSE, A., NEITZ, S., MAGERT, H. J., SCHULZ, A., FORSSMANN, W. G., SCHULZ-KNAPPE, P. & ADERMANN, K. 2000. LEAP-1, a novel highly disulfide-bonded human peptide, exhibits antimicrobial activity. *FEBS Lett,* 480**,** 147-50.

KRIJT, J., FUJIKURA, Y., SEFC, L., VOKURKA, M., HLOBENOVA, T. & NECAS, E. 2010. Hepcidin downregulation by repeated bleeding is not mediated by soluble hemojuvelin. *Physiol Res,* 59**,** 53-9.

KRIJT, J., VOKURKA, M., CHANG, K. T. & NECAS, E. 2004. Expression of Rgmc, the murine ortholog of hemojuvelin gene, is modulated by development and inflammation, but not by iron status or erythropoietin. *Blood,* 104**,** 4308-10.

LAKHAL, S., SCHODEL, J., TOWNSEND, A. R., PUGH, C. W., RATCLIFFE, P. J. & MOLE, D. R. 2011. Regulation of type II transmembrane serine proteinase TMPRSS6 by hypoxia-inducible factors: new link between hypoxia signaling and iron homeostasis. *J Biol Chem,* 286**,** 4090-7.

LARRAIN, J., BACHILLER, D., LU, B., AGIUS, E., PICCOLO, S. & DE ROBERTIS, E. M. 2000. BMP-binding modules in chordin: a model for signalling regulation in the extracellular space. *Development,* 127**,** 821-30.

LARRAIN, J., OELGESCHLAGER, M., KETPURA, N. I., REVERSADE, B., ZAKIN, L. & DE ROBERTIS, E. M. 2001. Proteolytic cleavage of Chordin as a switch for the dual activities of Twisted gastrulation in BMP signaling. *Development,* 128**,** 4439-47.

LATUNDE-DADA, G. O., MCKIE, A. T. & SIMPSON, R. J. 2006. Animal models with enhanced erythropoiesis and iron absorption. *Biochim Biophys Acta,* 1762**,** 414-23.

LATUNDE-DADA, G. O., XIANG, L., SIMPSON, R. J. & MCKIE, A. T. 2011. Duodenal cytochrome b (Cybrd 1) and HIF-2alpha expression during acute hypoxic exposure in mice. *Eur J Nutr,* 50**,** 699-704.

LAVAUTE, T., SMITH, S., COOPERMAN, S., IWAI, K., LAND, W., MEYRON-HOLTZ, E., DRAKE, S. K., MILLER, G., ABU-ASAB, M., TSOKOS, M., SWITZER, R., 3RD, GRINBERG, A., LOVE, P., TRESSER, N. & ROUAULT, T. A. 2001. Targeted deletion of the gene encoding iron regulatory protein-2 causes misregulation of iron metabolism and neurodegenerative disease in mice. *Nat Genet,* 27**,** 209-14.

LEBRON, J. A., WEST, A. P., JR. & BJORKMAN, P. J. 1999. The hemochromatosis protein HFE competes with transferrin for binding to the transferrin receptor. *J Mol Biol,* 294**,** 239-45.

LEDENT, V., PAQUET, O. & VERVOORT, M. 2002. Phylogenetic analysis of the human basic helix-loop-helix proteins. *Genome Biol,* 3**,** RESEARCH0030.

LEE, P., PENG, H., GELBART, T. & BEUTLER, E. 2004. The IL-6- and lipopolysaccharide-induced transcription of hepcidin in HFE-, transferrin receptor 2-, and beta 2-microglobulin-deficient hepatocytes. *Proc Natl Acad Sci U S A,* 101**,** 9263-5.

LEE, P. L., GELBART, T., WEST, C., HALLORAN, C. & BEUTLER, E. 1998. The human Nramp2 gene: characterization of the gene structure, alternative splicing, promoter region and polymorphisms. *Blood Cells Mol Dis,* 24**,** 199-215.

LEVY, J. E., JIN, O., FUJIWARA, Y., KUO, F. & ANDREWS, N. C. 1999. Transferrin receptor is necessary for development of erythrocytes and the nervous system. *Nat Genet,* 21**,** 396-9.

LIEU, P. T., HEISKALA, M., PETERSON, P. A. & YANG, Y. 2001. The roles of iron in health and disease. *Mol Aspects Med,* 22**,** 1-87.

LIN, L., VALORE, E. V., NEMETH, E., GOODNOUGH, J. B., GABAYAN, V. & GANZ, T. 2007. Iron transferrin regulates hepcidin synthesis in primary hepatocyte culture through hemojuvelin and BMP2/4. *Blood,* 110**,** 2182-9.

LIVAK, K. J. & SCHMITTGEN, T. D. 2001. Analysis of relative gene expression data using real-time quantitative PCR and the 2(-Delta Delta C(T)) Method. *Methods,* 25**,** 402-8.

LYNN, F. C., SANCHEZ, L., GOMIS, R., GERMAN, M. S. & GASA, R. 2008. Identification of the bHLH factor Math6 as a novel component of the embryonic pancreas transcriptional network. *PLoS One,* 3**,** e2430.

MARSHALL, C. J., KINNON, C. & THRASHER, A. J. 2000. Polarized expression of bone morphogenetic protein-4 in the human aorta-gonad-mesonephros region. *Blood,* 96**,** 1591-3.

MASARATANA, P., LATUNDE-DADA, G. O., PATEL, N., SIMPSON, R. J., VAULONT, S. & MCKIE, A. T. 2012. Iron metabolism in hepcidin1 knockout mice in response to phenylhydrazine-induced hemolysis. *Blood Cells Mol Dis*.

MASSAGUE, J., SEOANE, J. & WOTTON, D. 2005. Smad transcription factors. *Genes Dev,* 19**,** 2783-810.

MASSARI, M. E. & MURRE, C. 2000. Helix-loop-helix proteins: regulators of transcription in eucaryotic organisms. *Mol Cell Biol,* 20**,** 429-40.

MASTROGIANNAKI, M., MATAK, P., KEITH, B., SIMON, M. C., VAULONT, S. & PEYSSONNAUX, C. 2009. HIF-2alpha, but not HIF-1alpha, promotes iron absorption in mice. *J Clin Invest,* 119**,** 1159-66.

MATAK, P., CHASTON, T. B., CHUNG, B., SRAI, S. K., MCKIE, A. T. & SHARP, P. A. 2009. Activated macrophages induce hepcidin expression in HuH7 hepatoma cells. *Haematologica,* 94**,** 773-80.

MAXSON, J. E., ENNS, C. A. & ZHANG, A. S. 2009. Processing of hemojuvelin requires retrograde trafficking to the Golgi in HepG2 cells. *Blood,* 113**,** 1786-93.

MCKIE, A. T., BARROW, D., LATUNDE-DADA, G. O., ROLFS, A., SAGER, G., MUDALY, E., MUDALY, M., RICHARDSON, C., BARLOW, D., BOMFORD, A., PETERS, T. J., RAJA, K. B., SHIRALI, S., HEDIGER, M. A., FARZANEH, F. & SIMPSON, R. J. 2001. An iron-regulated ferric reductase associated with the absorption of dietary iron. *Science,* 291**,** 1755-9.

MCKIE, A. T., MARCIANI, P., ROLFS, A., BRENNAN, K., WEHR, K., BARROW, D., MIRET, S., BOMFORD, A., PETERS, T. J., FARZANEH, F., HEDIGER, M. A., HENTZE, M. W. & SIMPSON, R. J. 2000. A novel duodenal iron-regulated transporter, IREG1, implicated in the basolateral transfer of iron to the circulation. *Mol Cell,* 5**,** 299-309.

MEYNARD, D., KAUTZ, L., DARNAUD, V., CANONNE-HERGAUX, F., COPPIN, H. & ROTH, M. P. 2009. Lack of the bone morphogenetic protein BMP6 induces massive iron overload. *Nat Genet,* 41**,** 478-81.

MEYRON-HOLTZ, E. G., GHOSH, M. C., IWAI, K., LAVAUTE, T., BRAZZOLOTTO, X., BERGER, U. V., LAND, W., OLLIVIERRE-WILSON, H., GRINBERG, A., LOVE, P. & ROUAULT, T. A. 2004. Genetic ablations of iron regulatory proteins 1 and 2 reveal why iron regulatory protein 2 dominates iron homeostasis. *EMBO J,* 23**,** 386-95.

MITRY, R. R., HUGHES, R. D., AW, M. M., TERRY, C., MIELI-VERGANI, G., GIRLANDA, R., MUIESAN, P., RELA, M., HEATON, N. D. & DHAWAN, A. 2003. Human hepatocyte isolation and relationship of cell viability to early graft function. *Cell Transplant,* 12**,** 69-74.

MIYAZONO, K., KAMIYA, Y. & MORIKAWA, M. 2010. Bone morphogenetic protein receptors and signal transduction. *J Biochem,* 147**,** 35-51.

MLECZKO-SANECKA, K., CASANOVAS, G., RAGAB, A., BREITKOPF, K., MULLER, A., BOUTROS, M., DOOLEY, S., HENTZE, M. W. & MUCKENTHALER, M. U. 2010. SMAD7 controls iron metabolism as a potent inhibitor of hepcidin expression. *Blood,* 115**,** 2657-65.

MORENO-MIRALLES, I., REN, R., MOSER, M., HARTNETT, M. E. & PATTERSON, C. 2011. Bone morphogenetic protein endothelial cell precursor-derived regulator regulates retinal angiogenesis in vivo in a mouse model of oxygen-induced retinopathy. *Arterioscler Thromb Vasc Biol,* 31**,** 2216-22.

MOSER, M., BINDER, O., WU, Y., AITSEBAOMO, J., REN, R., BODE, C., BAUTCH, V. L., CONLON, F. L. & PATTERSON, C. 2003. BMPER, a novel endothelial cell

precursor-derived protein, antagonizes bone morphogenetic protein signaling and endothelial cell differentiation. *Mol Cell Biol,* 23**,** 5664-79.

MOSER, M., YU, Q., BODE, C., XIONG, J. W. & PATTERSON, C. 2007. BMPER is a conserved regulator of hematopoietic and vascular development in zebrafish. *J Mol Cell Cardiol,* 43**,** 243-53.

NAKAYAMA, K. 2009. Cellular signal transduction of the hypoxia response. *J Biochem,* 146**,** 757-65.

NAUGHTON, B. A., MOORE, E., BUSH, M. E., LAPIN, D. M. & DORNFEST, B. S. 1989. Hemostatic alterations associated with phenylhydrazine-induced anemia in the rat. *J Med,* 20**,** 305-30.

NEMETH, E., PREZA, G. C., JUNG, C. L., KAPLAN, J., WARING, A. J. & GANZ, T. 2006. The N-terminus of hepcidin is essential for its interaction with ferroportin: structure-function study. *Blood,* 107**,** 328-33.

NEMETH, E., RIVERA, S., GABAYAN, V., KELLER, C., TAUDORF, S., PEDERSEN, B. K. & GANZ, T. 2004a. IL-6 mediates hypoferremia of inflammation by inducing the synthesis of the iron regulatory hormone hepcidin. *J Clin Invest,* 113**,** 1271-6.

NEMETH, E., TUTTLE, M. S., POWELSON, J., VAUGHN, M. B., DONOVAN, A., WARD, D. M., GANZ, T. & KAPLAN, J. 2004b. Hepcidin regulates cellular iron efflux by binding to ferroportin and inducing its internalization. *Science,* 306**,** 2090-3.

NEMETH, E., VALORE, E. V., TERRITO, M., SCHILLER, G., LICHTENSTEIN, A. & GANZ, T. 2003. Hepcidin, a putative mediator of anemia of inflammation, is a type II acute-phase protein. *Blood,* 101**,** 2461-3.

NICOLAS, G., BENNOUN, M., DEVAUX, I., BEAUMONT, C., GRANDCHAMP, B., KAHN, A. & VAULONT, S. 2001a. Lack of hepcidin gene expression and severe tissue iron overload in upstream stimulatory factor 2 (USF2) knockout mice. *Proc.Natl.Acad.Sci.U.S.A,* 98**,** 8780-8785.

NICOLAS, G., BENNOUN, M., DEVAUX, I., BEAUMONT, C., GRANDCHAMP, B., KAHN, A. & VAULONT, S. 2001b. Lack of hepcidin gene expression and severe tissue iron overload in upstream stimulatory factor 2 (USF2) knockout mice. *Proc Natl Acad Sci U S A,* 98**,** 8780-5.

NICOLAS, G., BENNOUN, M., PORTEU, A., MATIVET, S., BEAUMONT, C., GRANDCHAMP, B., SIRITO, M., SAWADOGO, M., KAHN, A. & VAULONT, S. 2002a. Severe iron deficiency anemia in transgenic mice expressing liver hepcidin. *Proc Natl Acad Sci U S A,* 99**,** 4596-601.

NICOLAS, G., CHAUVET, C., VIATTE, L., DANAN, J. L., BIGARD, X., DEVAUX, I., BEAUMONT, C., KAHN, A. & VAULONT, S. 2002b. The gene encoding the iron regulatory peptide hepcidin is regulated by anemia, hypoxia, and inflammation. *J Clin Invest,* 110**,** 1037-44.

OHGAMI, R. S., CAMPAGNA, D. R., MCDONALD, A. & FLEMING, M. D. 2006. The Steap proteins are metalloreductases. *Blood,* 108**,** 1388-94.

ORIGA, R., GALANELLO, R., GANZ, T., GIAGU, N., MACCIONI, L., FAA, G. & NEMETH, E. 2007. Liver iron concentrations and urinary hepcidin in beta-thalassemia. *Haematologica,* 92**,** 583-8.

PAK, M., LOPEZ, M. A., GABAYAN, V., GANZ, T. & RIVERA, S. 2006. Suppression of hepcidin during anemia requires erythropoietic activity. *Blood,* 108**,** 3730-5.

PAPANIKOLAOU, G., SAMUELS, M. E., LUDWIG, E. H., MACDONALD, M. L., FRANCHINI, P. L., DUBE, M. P., ANDRES, L., MACFARLANE, J., SAKELLAROPOULOS, N., POLITOU, M., NEMETH, E., THOMPSON, J.,

RISLER, J. K., ZABOROWSKA, C., BABAKAIFF, R., RADOMSKI, C. C., PAPE, T. D., DAVIDAS, O., CHRISTAKIS, J., BRISSOT, P., LOCKITCH, G., GANZ, T., HAYDEN, M. R. & GOLDBERG, Y. P. 2004. Mutations in HFE2 cause iron overload in chromosome 1q-linked juvenile hemochromatosis. *Nat Genet,* 36**,** 77-82.

PARK, C. H., VALORE, E. V., WARING, A. J. & GANZ, T. 2001. Hepcidin, a urinary antimicrobial peptide synthesized in the liver. *J Biol Chem,* 276**,** 7806-10.

PEYSSONNAUX, C., ZINKERNAGEL, A. S., SCHUEPBACH, R. A., RANKIN, E., VAULONT, S., HAASE, V. H., NIZET, V. & JOHNSON, R. S. 2007. Regulation of iron homeostasis by the hypoxia-inducible transcription factors (HIFs). *J Clin Invest,* 117**,** 1926-32.

PIETRANGELO, A. 2006. Hereditary hemochromatosis. *Biochim Biophys Acta,* 1763**,** 700-10.

PIETRANGELO, A., DIERSSEN, U., VALLI, L., GARUTI, C., RUMP, A., CORRADINI, E., ERNST, M., KLEIN, C. & TRAUTWEIN, C. 2007. STAT3 is required for IL-6-gp130-dependent activation of hepcidin in vivo. *Gastroenterology,* 132**,** 294-300.

PIGEON, C., ILYIN, G., COURSELAUD, B., LEROYER, P., TURLIN, B., BRISSOT, P. & LOREAL, O. 2001. A new mouse liver-specific gene, encoding a protein homologous to human antimicrobial peptide hepcidin, is overexpressed during iron overload. *J Biol Chem,* 276**,** 7811-9.

PINTO, J. P., RIBEIRO, S., PONTES, H., THOWFEEQU, S., TOSH, D., CARVALHO, F. & PORTO, G. 2008. Erythropoietin mediates hepcidin expression in hepatocytes through EPOR signaling and regulation of C/EBPalpha. *Blood,* 111**,** 5727-33.

PONKA, P., BEAUMONT, C. & RICHARDSON, D. R. 1998. Function and regulation of transferrin and ferritin. *Semin Hematol,* 35**,** 35-54.

POSS, K. D. & TONEGAWA, S. 1997. Heme oxygenase 1 is required for mammalian iron reutilization. *Proc Natl Acad Sci U S A,* 94**,** 10919-24.

QIAO, B., SUGIANTO, P., FUNG, E., DEL-CASTILLO-RUEDA, A., MORAN-JIMENEZ, M. J., GANZ, T. & NEMETH, E. 2012. Hepcidin-induced endocytosis of ferroportin is dependent on ferroportin ubiquitination. *Cell Metab,* 15**,** 918-24.

QIU, A., JANSEN, M., SAKARIS, A., MIN, S. H., CHATTOPADHYAY, S., TSAI, E., SANDOVAL, C., ZHAO, R., AKABAS, M. H. & GOLDMAN, I. D. 2006. Identification of an intestinal folate transporter and the molecular basis for hereditary folate malabsorption. *Cell,* 127**,** 917-28.

RACHMILEWITZ, E. A., WEIZER-STERN, O., ADAMSKY, K., AMARIGLIO, N., RECHAVI, G., BREDA, L., RIVELLA, S. & CABANTCHIK, Z. I. 2005. Role of iron in inducing oxidative stress in thalassemia: Can it be prevented by inhibition of absorption and by antioxidants? *Ann N Y Acad Sci,* 1054**,** 118-23.

RAJA, K. B., SIMPSON, R. J. & PETERS, T. J. 1992. Investigation of a role for reduction in ferric iron uptake by mouse duodenum. *Biochim Biophys Acta,* 1135**,** 141-6.

RAJA, K. B., SIMPSON, R. J., PIPPARD, M. J. & PETERS, T. J. 1988. In vivo studies on the relationship between intestinal iron (Fe3+) absorption, hypoxia and erythropoiesis in the mouse. *Br J Haematol,* 68**,** 373-8.

RAMEY, G., DESCHEMIN, J. C. & VAULONT, S. 2009. Cross-talk between the mitogen activated protein kinase and bone morphogenetic protein/hemojuvelin pathways is required for the induction of hepcidin by holotransferrin in primary mouse hepatocytes. *Haematologica,* 94**,** 765-72.

RAMOS, E., KAUTZ, L., RODRIGUEZ, R., HANSEN, M., GABAYAN, V., GINZBURG, Y., ROTH, M. P., NEMETH, E. & GANZ, T. 2011. Evidence for distinct

pathways of hepcidin regulation by acute and chronic iron loading in mice. *Hepatology,* 53**,** 1333-41.

RAMSAY, A. J., HOOPER, J. D., FOLGUERAS, A. R., VELASCO, G. & LOPEZ-OTIN, C. 2009. Matriptase-2 (TMPRSS6): a proteolytic regulator of iron homeostasis. *Haematologica,* 94**,** 840-9.

RENTZSCH, F., ZHANG, J., KRAMER, C., SEBALD, W. & HAMMERSCHMIDT, M. 2006. Crossveinless 2 is an essential positive feedback regulator of Bmp signaling during zebrafish gastrulation. *Development,* 133**,** 801-11.

RIBATTI, D., NICO, B., SPINAZZI, R., VACCA, A. & NUSSDORFER, G. G. 2005. The role of adrenomedullin in angiogenesis. *Peptides,* 26**,** 1670-5.

RIEDEL, H. D., REMUS, A. J., FITSCHER, B. A. & STREMMEL, W. 1995. Characterization and partial purification of a ferrireductase from human duodenal microvillus membranes. *Biochem J,* 309 (Pt 3)**,** 745-8.

ROBB, A. & WESSLING-RESNICK, M. 2004. Regulation of transferrin receptor 2 protein levels by transferrin. *Blood,* 104**,** 4294-9.

RODRIGUEZ MARTINEZ, A., NIEMELA, O. & PARKKILA, S. 2004. Hepatic and extrahepatic expression of the new iron regulatory protein hemojuvelin. *Haematologica,* 89**,** 1441-5.

ROSS, M. D., MARTINKA, S., MUKHERJEE, A., SEDOR, J. R., VINSON, C. & BRUGGEMAN, L. A. 2006. Math6 expression during kidney development and altered expression in a mouse model of glomerulosclerosis. *Dev Dyn,* 235**,** 3102-9.

ROSS, S. L., TRAN, L., WINTERS, A., LEE, K. J., PLEWA, C., FOLTZ, I., KING, C., MIRANDA, L. P., ALLEN, J., BECKMAN, H., COOKE, K. S., MOODY, G., SASU, B. J., NEMETH, E., GANZ, T., MOLINEUX, G. & ARVEDSON, T. L. 2012. Molecular mechanism of hepcidin-mediated ferroportin internalization requires ferroportin lysines, not tyrosines or JAK-STAT. *Cell Metab,* 15**,** 905-17.

ROY, C. N., CUSTODIO, A. O., DE GRAAF, J., SCHNEIDER, S., AKPAN, I., MONTROSS, L. K., SANCHEZ, M., GAUDINO, A., HENTZE, M. W., ANDREWS, N. C. & MUCKENTHALER, M. U. 2004. An Hfe-dependent pathway mediates hyposideremia in response to lipopolysaccharide-induced inflammation in mice. *Nat Genet,* 36**,** 481-5.

SAMAD, T. A., REBBAPRAGADA, A., BELL, E., ZHANG, Y., SIDIS, Y., JEONG, S. J., CAMPAGNA, J. A., PERUSINI, S., FABRIZIO, D. A., SCHNEYER, A. L., LIN, H. Y., BRIVANLOU, A. H., ATTISANO, L. & WOOLF, C. J. 2005. DRAGON, a bone morphogenetic protein co-receptor. *J Biol Chem,* 280**,** 14122-9.

SASAI, Y., LU, B., STEINBEISSER, H., GEISSERT, D., GONT, L. K. & DE ROBERTIS, E. M. 1994. Xenopus chordin: a novel dorsalizing factor activated by organizer-specific homeobox genes. *Cell,* 79**,** 779-90.

SCHMIDT, P. J., ANDREWS, N. C. & FLEMING, M. D. 2010. Hepcidin induction by transgenic overexpression of Hfe does not require the Hfe cytoplasmic tail, but does require hemojuvelin. *Blood,* 116**,** 5679-87.

SCHMIDT, P. J., TORAN, P. T., GIANNETTI, A. M., BJORKMAN, P. J. & ANDREWS, N. C. 2008. The transferrin receptor modulates Hfe-dependent regulation of hepcidin expression. *Cell Metab,* 7**,** 205-14.

SEMENZA, G. L. & WANG, G. L. 1992. A nuclear factor induced by hypoxia via de novo protein synthesis binds to the human erythropoietin gene enhancer at a site required for transcriptional activation. *Mol Cell Biol,* 12**,** 5447-54.

SERPE, M., UMULIS, D., RALSTON, A., CHEN, J., OLSON, D. J., AVANESOV, A., OTHMER, H., O'CONNOR, M. B. & BLAIR, S. S. 2008. The BMP-binding protein Crossveinless 2 is a short-range, concentration-dependent, biphasic modulator of BMP signaling in Drosophila. *Dev Cell,* 14**,** 940-53.

SHAH, Y. M., MATSUBARA, T., ITO, S., YIM, S. H. & GONZALEZ, F. J. 2009. Intestinal hypoxia-inducible transcription factors are essential for iron absorption following iron deficiency. *Cell Metab,* 9**,** 152-64.

SHAYEGHI, M., LATUNDE-DADA, G. O., OAKHILL, J. S., LAFTAH, A. H., TAKEUCHI, K., HALLIDAY, N., KHAN, Y., WARLEY, A., MCCANN, F. E., HIDER, R. C., FRAZER, D. M., ANDERSON, G. J., VULPE, C. D., SIMPSON, R. J. & MCKIE, A. T. 2005. Identification of an intestinal heme transporter. *Cell,* 122**,** 789-801.

SILVESTRI, L., PAGANI, A. & CAMASCHELLA, C. 2008a. Furin-mediated release of soluble hemojuvelin: a new link between hypoxia and iron homeostasis. *Blood,* 111**,** 924-31.

SILVESTRI, L., PAGANI, A., NAI, A., DE DOMENICO, I., KAPLAN, J. & CAMASCHELLA, C. 2008b. The serine protease matriptase-2 (TMPRSS6) inhibits hepcidin activation by cleaving membrane hemojuvelin. *Cell Metab,* 8**,** 502-11.

SIMPSON, R. J., DEBNAM, E., BEAUMONT, N., BAHRAM, S., SCHUMANN, K. & SRAI, S. K. 2003. Duodenal mucosal reductase in wild-type and Hfe knockout mice on iron adequate, iron deficient, and iron rich feeding. *Gut,* 52**,** 510-3.

SIMPSON, R. J., LOMBARD, M., RAJA, K. B., THATCHER, R. & PETERS, T. J. 1991. Iron absorption by hypotransferrinaemic mice. *Br J Haematol,* 78**,** 565-70.

SIMPSON, R. J. & PETERS, T. J. 1990. Forms of soluble iron in mouse stomach and duodenal lumen: significance for mucosal uptake. *Br J Nutr,* 63**,** 79-89.

SMITH, P. M. 1969. Iron overload. *Postgrad Med J,* 45**,** 214-9.

STAUBLI, A. & BOELSTERLI, U. A. 1998. The labile iron pool in hepatocytes: prooxidant-induced increase in free iron precedes oxidative cell injury. *Am J Physiol,* 274**,** G1031-7.

STEINBICKER, A. U., BARTNIKAS, T. B., LOHMEYER, L. K., LEYTON, P., MAYEUR, C., KAO, S. M., PAPPAS, A. E., PETERSON, R. T., BLOCH, D. B., YU, P. B., FLEMING, M. D. & BLOCH, K. D. 2011. Perturbation of hepcidin expression by BMP type I receptor deletion induces iron overload in mice. *Blood,* 118**,** 4224-30.

SUBRAMANIAM, V. N., SUMMERVILLE, L. & WALLACE, D. F. 2002. Molecular and cellular characterization of transferrin receptor 2. *Cell Biochem Biophys,* 36**,** 235-9.

TANNO, T., BHANU, N. V., ONEAL, P. A., GOH, S. H., STAKER, P., LEE, Y. T., MORONEY, J. W., REED, C. H., LUBAN, N. L., WANG, R. H., ELING, T. E., CHILDS, R., GANZ, T., LEITMAN, S. F., FUCHAROEN, S. & MILLER, J. L. 2007. High levels of GDF15 in thalassemia suppress expression of the iron regulatory protein hepcidin. *Nat Med,* 13**,** 1096-101.

TANNO, T., PORAYETTE, P., SRIPICHAI, O., NOH, S. J., BYRNES, C., BHUPATIRAJU, A., LEE, Y. T., GOODNOUGH, J. B., HARANDI, O., GANZ, T., PAULSON, R. F. & MILLER, J. L. 2009. Identification of TWSG1 as a second novel erythroid regulator of hepcidin expression in murine and human cells. *Blood,* 114**,** 181-6.

TRENOR, C. C., 3RD, CAMPAGNA, D. R., SELLERS, V. M., ANDREWS, N. C. & FLEMING, M. D. 2000. The molecular defect in hypotransferrinemic mice. *Blood,* 96**,** 1113-8.

TRUKSA, J., PENG, H., LEE, P. & BEUTLER, E. 2006. Bone morphogenetic proteins 2, 4, and 9 stimulate murine hepcidin 1 expression independently of Hfe, transferrin receptor 2 (Tfr2), and IL-6. *Proc Natl Acad Sci U S A,* 103**,** 10289-93.

URIST, M. R. 1965. Bone: formation by autoinduction. *Science,* 150**,** 893-9.

UZEL, C. & CONRAD, M. E. 1998. Absorption of heme iron. *Semin Hematol,* 35**,** 27-34.

VALERA, E., ISAACS, M. J., KAWAKAMI, Y., IZPISUA BELMONTE, J. C. & CHOE, S. 2010. BMP-2/6 heterodimer is more effective than BMP-2 or BMP-6 homodimers as inductor of differentiation of human embryonic stem cells. *PLoS One,* 5**,** e11167.

VALORE, E. V. & GANZ, T. 2008. Posttranslational processing of hepcidin in human hepatocytes is mediated by the prohormone convertase furin. *Blood Cells Mol Dis,* 40**,** 132-8.

VELASCO, G., CAL, S., QUESADA, V., SANCHEZ, L. M. & LOPEZ-OTIN, C. 2002. Matriptase-2, a membrane-bound mosaic serine proteinase predominantly expressed in human liver and showing degrading activity against extracellular matrix proteins. *J Biol Chem,* 277**,** 37637-46.

VERGA FALZACAPPA, M. V., VUJIC SPASIC, M., KESSLER, R., STOLTE, J., HENTZE, M. W. & MUCKENTHALER, M. U. 2007. STAT3 mediates hepatic hepcidin expression and its inflammatory stimulation. *Blood,* 109**,** 353-8.

VOKURKA, M., KRIJT, J., SULC, K. & NECAS, E. 2006. Hepcidin mRNA levels in mouse liver respond to inhibition of erythropoiesis. *Physiol Res,* 55**,** 667-74.

VULPE, C. D., KUO, Y. M., MURPHY, T. L., COWLEY, L., ASKWITH, C., LIBINA, N., GITSCHIER, J. & ANDERSON, G. J. 1999. Hephaestin, a ceruloplasmin homologue implicated in intestinal iron transport, is defective in the sla mouse. *Nat Genet,* 21**,** 195-9.

WALLACE, D. F., SUMMERVILLE, L. & SUBRAMANIAM, V. N. 2007. Targeted disruption of the hepatic transferrin receptor 2 gene in mice leads to iron overload. *Gastroenterology,* 132**,** 301-10.

WANG, R. H., LI, C., XU, X., ZHENG, Y., XIAO, C., ZERFAS, P., COOPERMAN, S., ECKHAUS, M., ROUAULT, T., MISHRA, L. & DENG, C. X. 2005. A role of SMAD4 in iron metabolism through the positive regulation of hepcidin expression. *Cell Metab,* 2**,** 399-409.

WEISS, G. & GOODNOUGH, L. T. 2005. Anemia of chronic disease. *N Engl J Med,* 352**,** 1011-23.

WENGER, R. H. 2002. Cellular adaptation to hypoxia: O2-sensing protein hydroxylases, hypoxia-inducible transcription factors, and O2-regulated gene expression. *FASEB J,* 16**,** 1151-62.

WHITTLE, A. J., CAROBBIO, S., MARTINS, L., SLAWIK, M., HONDARES, E., VAZQUEZ, M. J., MORGAN, D., CSIKASZ, R. I., GALLEGO, R., RODRIGUEZ-CUENCA, S., DALE, M., VIRTUE, S., VILLARROYA, F., CANNON, B., RAHMOUNI, K., LOPEZ, M. & VIDAL-PUIG, A. 2012. BMP8B Increases Brown Adipose Tissue Thermogenesis through Both Central and Peripheral Actions. *Cell,* 149**,** 871-85.

WOZNEY, J. M. 2002. Overview of bone morphogenetic proteins. *Spine (Phila Pa 1976),* 27**,** S2-8.

WOZNEY, J. M., ROSEN, V., CELESTE, A. J., MITSOCK, L. M., WHITTERS, M. J., KRIZ, R. W., HEWICK, R. M. & WANG, E. A. 1988. Novel regulators of bone formation: molecular clones and activities. *Science,* 242**,** 1528-34.

WRIGHTING, D. M. & ANDREWS, N. C. 2006. Interleukin-6 induces hepcidin expression through STAT3. *Blood,* 108**,** 3204-9.

YANG, F., WANG, X., HAILE, D. J., PIANTADOSI, C. A. & GHIO, A. J. 2002. Iron increases expression of iron-export protein MTP1 in lung cells. *Am J Physiol Lung Cell Mol Physiol,* 283**,** L932-9.

YANOFF, L. B., MENZIE, C. M., DENKINGER, B., SEBRING, N. G., MCHUGH, T., REMALEY, A. T. & YANOVSKI, J. A. 2007. Inflammation and iron deficiency in the hypoferremia of obesity. *Int J Obes (Lond),* 31**,** 1412-9.

YAO, J., ZHOU, J., LIU, Q., LU, D., WANG, L., QIAO, X. & JIA, W. 2010. Atoh8, a bHLH transcription factor, is required for the development of retina and skeletal muscle in zebrafish. *PLoS One,* 5**,** e10945.

YING, Y., LIU, X. M., MARBLE, A., LAWSON, K. A. & ZHAO, G. Q. 2000. Requirement of Bmp8b for the generation of primordial germ cells in the mouse. *Mol Endocrinol,* 14**,** 1053-63.

YING, Y., QI, X. & ZHAO, G. Q. 2001. Induction of primordial germ cells from murine epiblasts by synergistic action of BMP4 and BMP8B signaling pathways. *Proc Natl Acad Sci U S A,* 98**,** 7858-62.

ZHANG, A. S., ANDERSON, S. A., MEYERS, K. R., HERNANDEZ, C., EISENSTEIN, R. S. & ENNS, C. A. 2007a. Evidence that inhibition of hemojuvelin shedding in response to iron is mediated through neogenin. *J Biol Chem,* 282**,** 12547-56.

ZHANG, A. S., GAO, J., KOEBERL, D. D. & ENNS, C. A. 2010a. The role of hepatocyte hemojuvelin in the regulation of bone morphogenic protein-6 and hepcidin expression in vivo. *J Biol Chem,* 285**,** 16416-23.

ZHANG, A. S., YANG, F., WANG, J., TSUKAMOTO, H. & ENNS, C. A. 2009a. Hemojuvelin-neogenin interaction is required for bone morphogenic protein-4-induced hepcidin expression. *J Biol Chem,* 284**,** 22580-9.

ZHANG, D. L., HUGHES, R. M., OLLIVIERRE-WILSON, H., GHOSH, M. C. & ROUAULT, T. A. 2009b. A ferroportin transcript that lacks an iron-responsive element enables duodenal and erythroid precursor cells to evade translational repression. *Cell Metab,* 9**,** 461-73.

ZHANG, J. L., HUANG, Y., QIU, L. Y., NICKEL, J. & SEBALD, W. 2007b. von Willebrand factor type C domain-containing proteins regulate bone morphogenetic protein signaling through different recognition mechanisms. *J Biol Chem,* 282**,** 20002-14.

ZHANG, J. L., PATTERSON, L. J., QIU, L. Y., GRAZIUSSI, D., SEBALD, W. & HAMMERSCHMIDT, M. 2010b. Binding between Crossveinless-2 and Chordin von Willebrand factor type C domains promotes BMP signaling by blocking Chordin activity. *PLoS One,* 5**,** e12846.

ZHAO, G. Q., DENG, K., LABOSKY, P. A., LIAW, L. & HOGAN, B. L. 1996. The gene encoding bone morphogenetic protein 8B is required for the initiation and maintenance of spermatogenesis in the mouse. *Genes Dev,* 10**,** 1657-69.

ZHAO, G. Q. & HOGAN, B. L. 1996. Evidence that mouse Bmp8a (Op2) and Bmp8b are duplicated genes that play a role in spermatogenesis and placental development. *Mech Dev,* 57**,** 159-68.

ZHAO, G. Q., LIAW, L. & HOGAN, B. L. 1998. Bone morphogenetic protein 8A plays a role in the maintenance of spermatogenesis and the integrity of the epididymis. *Development,* 125**,** 1103-12.

ZHOU, Q., HEINKE, J., VARGAS, A., WINNIK, S., KRAUSS, T., BODE, C., PATTERSON, C. & MOSER, M. 2007. ERK signaling is a central regulator for BMP-4 dependent capillary sprouting. *Cardiovasc Res,* 76**,** 390-9.

ZHOU, X. Y., TOMATSU, S., FLEMING, R. E., PARKKILA, S., WAHEED, A., JIANG, J., FEI, Y., BRUNT, E. M., RUDDY, D. A., PRASS, C. E., SCHATZMAN, R. C., O'NEILL, R., BRITTON, R. S., BACON, B. R. & SLY, W. S. 1998. HFE gene knockout produces mouse model of hereditary hemochromatosis. *Proc Natl Acad Sci U S A,* 95**,** 2492-7.

Appendices

Appendix 1: Common reagents

Formaldehyde RNA gel

10x MOPS: 0.2M MOPS

0.05 sodium acetate

0.01M EDTA

1% agarose gel for RNA electrophoresis: 10 mL 10xMPOS

82 mL distilled water

1 g agarose

8 mL formaldehyde

Ethidium bromide DNA gel

10x TBE: 1M Tris base

0.9M Boric acid

40 mL 0.5M EDTA

Made up to a final volume of 1 L

1% agarose gel if DNA electrophoresis: 1 g agarose

100 mL 1xTBE

1-2 μL ethidium bromide

List of primers used for real-time PCR in mouse studies

Gene	Accession number	Primer sequence (5′-3′)	Position of primer	Product size	Annealing temperature (ºC)
Actb	NM_007393.3	For: ctaaggccaaccgtgaaaag Rev: accagaggcatacagggaca	414 – 433 498 – 517	104	60
Adm	NM_009627.1	For: ttcgcagttccgaaagaagt Rev: ggtagctgctggatgcttgt	256 – 275 313 – 332	77	60
Atoh8	NM_153778.3	For: tcagcttctccgagtgtgtg Rev: tagcctgtggcaggtcact	1306 – 1325 1378 – 1396	91	60
Bmp2	NM_007553.2	For: cggactgcggtctcctaa Rev: ggggaagcagcaacactaga	134 – 151 184 – 203	70	60
Bmp4	NM_007554.2	For: gaggagtttccatcacgaaga Rev: gctctgccgaggagatca	782 – 802 886 – 903	122	60

List of primers used for real-time PCR in mouse studies (continued)

Gene	Accession number	Primer sequence (5′-3′)	Position of primer	Product size	Annealing temperature (ºC)
Bmp6	NM_007556.2	For: actgactagcgcgcagga Rev: tgtggggagaactccttgtc	805 – 822 881 – 900	96	60
Bmp8b	NM_007559.4	For: ctgtatgaactccaccaaccac Rev: tggggatgatatctggcttc	1197 – 1218 1248 – 1267	71	60
Bmper	NM_028472.1	For: tgtgcaagttcggtagcaag Rev: tgcagttgactgaggaccac	1464 – 1483 1504 – 1523	60	60
Chrd	NM_009893.2	For: tcactgcccacctccttg Rev: atcttttaccacgccctgag	1754 – 1771 1829 – 1848	95	60
Gdf15	NM_011819.2	For: gagctacggggtcgcttc Rev: gggaccccaatctcacct	189 – 206 301 – 318	130	60
Hamp	NM_032541.1	For: agaaagcagggcagacattg Rev: cactgggaattgttacagcatt	160 – 179 243 – 264	105	60

List of primers used for real-time PCR in mouse studies (continued)

Gene	Accession number	Primer sequence (5′-3′)	Position of primer	Product size	Annealing temperature (ºC)
Hfe2	NM_027126.4	For: gcttgacctcgggaaacat Rev: accggggactaggggact	129 – 147 240 – 257	129	60
Id1	NM_010495.2	For: gcgagatcagtgccttgg Rev: ctcctgaagggctggagtc	447 – 464 539 – 557	111	60
Nog	NM_008711.2	For: agacaaaccggtgccaac Rev: tgggccacttctctctgc	1 – 18 99 – 116	116	60
Rpl19	NM_001159483.1	For: ctcgttgccggaaaaaca Rev: tcatccaggtcaccttctca	230 – 247 318 – 337	108	60
Smad7	NM_001042660.1	For: acccccatcaccttagtcg Rev: gaaaatccattgggtatctgga	2172 – 2190 2225 – 2246	75	60
Trfr2	NM_015799.3	For: cagtaacatctttgcgtgcatc Rev: ggccccaatgacaacatagt	1367 – 1388 1411 – 1430	64	60

List of primers used for real-time PCR in mouse studies (continued)

Gene	Accession number	Primer sequence (5′-3′)	Position of primer	Product size	Annealing temperature (ºC)
Twsg1	NM_023053.2	For: ctgttcccagcaacaatgtc Rev: actgtgcacatgcgctctt	551 – 570 593 – 611	61	60
Vwf	NM_011708.3	For: gagaatgcagacccaccttt Rev: ggggacactctttgcactc	7292 – 7311 7333 – 7352	61	60
Vwce	NM_027913.1	For: cctgtgagttatgcgtctgc Rev: gtccacgcagtctgtcctct	1980 – 1999 2025 – 2044	65	60

List of primers used for real-time PCR in *in vitro* studies

Gene	Accession number	Primer sequence (5′-3′)	Position of primer	Product size	Annealing temperature (ºC)
ACTB	NM_001101.3	For: ccaaccgcgagaagatga Rev: ccagaggcgtacagggatag	425 – 442 502 – 521	97	60
ATOH8	NM_032827.6	For: gagggacgtgccaagaag Rev: cagtggtggccttggtct	1341 – 1358 1384 – 1401	61	60
BMP2	NM_001200.2	For: cagaccaccggttggaga Rev: cccactcgtttctggtagttct	1069 – 1086 1142 – 1163	95	60
BMP6	NM_001718.4	For: acatggtcatgagctttgtga Rev: actctttgtggtgtcgctga	816 – 836 871 – 890	75	60
BMPER	NM_133468.3	For: aagtgaccaccaaagcaggt Rev: gcgcagccatgacttctac	1505 – 1524 1555 – 1573	69	60

List of primers used for real-time PCR in *in vitro* studies (continued)

Gene	Accession number	Primer sequence (5′-3′)	Position of primer	Product size	Annealing temperature (ºC)
HAMP	NM_021175.2	For: ctgttttcccacaacagacg Rev: ttcgcctctggaacatgg	145 – 164 223 – 240	96	60
ID1	NM_002165.3	For: ccagaaccgcaaggtgag Rev: ggtccctgatgtagtcgatga	351 – 368 392 – 412	62	60
RPL19	NM_000981.3	For: gctctttcctttcgctgct Rev: cattggtctcattggggtct	32 – 50 134 – 153	122	60
SMAD 7	NM_001190821.1	For: cgatggattttctcaaaccaa Rev: aggggccagataattcgttc	931 – 951 997 – 1016	86	60

Appendix 3: Plasmid maps

pRL- TK renilla

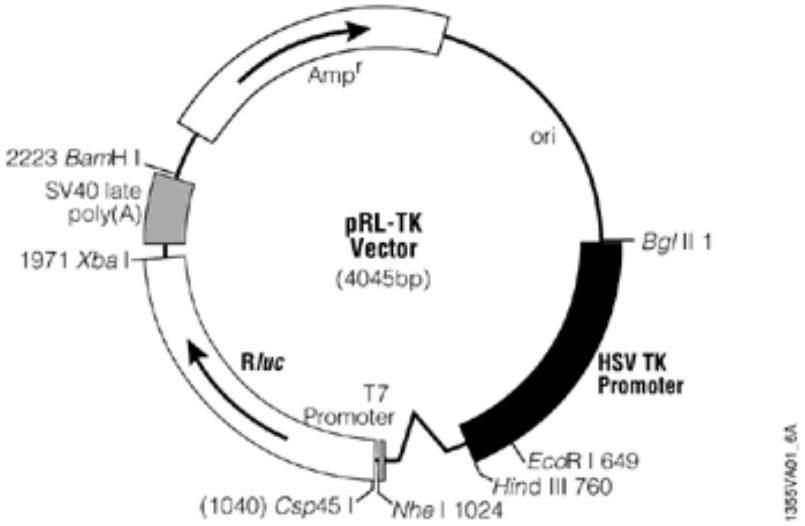

pGL3- Basic

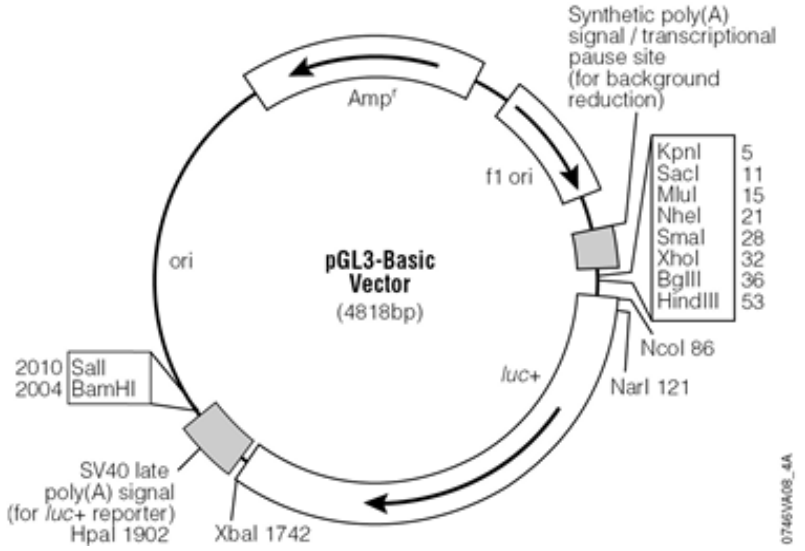

pCMV6-Entry vector (Myc-DDK tagged ORF clones)

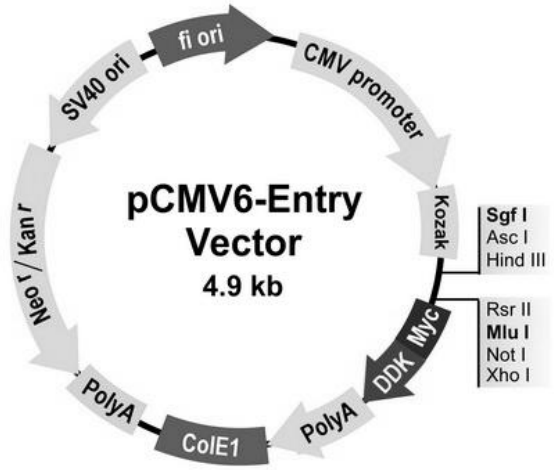

pSecTag2 (Bmper vector)

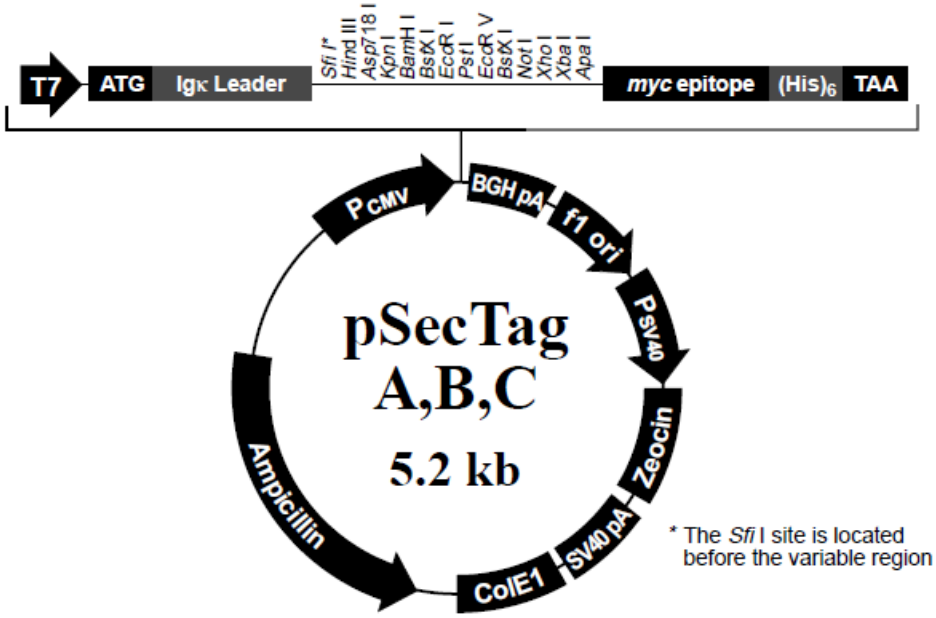

pCDNA3.1 (Matriptase-2/MASK/R774C)

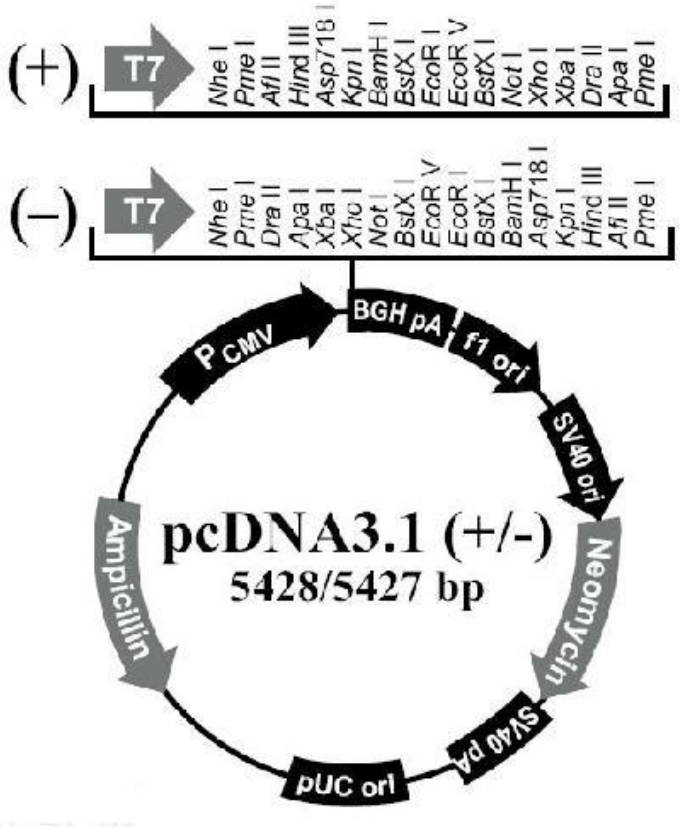

Publications

PATEL, N., MASARATANA, P., DIAZ-CASTRO, J., LATUNDE-DADA, G. O., QURESHI, A., LOCKYER, P., JACOB, M., ARNO, M., MATAK, P., MITRY, R. R., HUGHES, R. D., DHAWAN, A., PATTERSON, C., SIMPSON, R. J. & MCKIE, A. T. 2012. BMPER protein is a negative regulator of hepcidin and is up-regulated in hypotransferrinemic mice. *J Biol Chem,* 287**,** 4099-106.